

D-A049 000

FOREIGN TECHNOLOGY DIV WRIGHT-PATTERSON AFB OHIO
A WING IN AN UNSTEADY GAS FLOW. PART 2, (U)
SEP 77 S M BELOTSEKOVSKIY, B K SKRIPACH
FTD-ID(RS)T-1534-77-PT-2

F/G 1/3

UNCLASSIFIED

NL

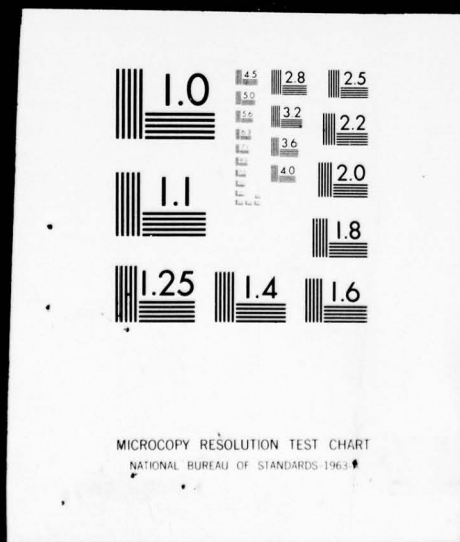
1 of 6

ADA048000



1 OF 6

ADAO49000



AD-A049000

FTD-ID(RS)T-1543-77
Part 2 of 3

(1)

FOREIGN TECHNOLOGY DIVISION



A WING IN AN UNSTEADY GAS FLOW

by

S. M. Belotserkovskiy, B. K. Skripach,
and V. G. Tabachnikov



Approved for public release;
distribution unlimited.

Table of Contents

U. S. Board on Geographic Names Transliteration System....	1v
Russian and English Trigonometric Functions.....	v
Preface.....	1
Part I. General Considerations.....	8
Chapter I. General Information.....	14
Chapter II. Aerodynamic Coefficients.....	29
Chapter III. Formulation of the Problem of the Unsteady Motion of Wing.....	118
Chapter IV. Basic Formula for the Potential of the Disturbed Velocities. Some Exact Solutions for the Wings of Arbitrary Platform.....	167
Chapter V. Common Properties of Linear Unsteady Problems. Similarity Parameters.....	198
Chapter VI. Duhamel Integral. Theorem of Momentum. Rational Method of Solution of Linear Unsteady Problems...	229
Chapter VII. Reciprocity Theorem and Its Corollaries.....	289
Chapter VIII. Experimental Determination of Unsteady Aerodynamic Wing Characteristics.....	337
Part II. Low Speeds (Incompressible Medium $M = 0$).....	410
Chapter IX. The Velocity Field of Oblique Horseshoe Vortex in an Incompressible Medium.....	415
Chapter X. Method of the Calculation of Aerodynamic Wing Characteristics with the Harmonic Dependences of the Kinematic Parameters on Time.....	438

Chapter XI. Method of the Calculation of Aerodynamic Wing Characteristics with the Arbitrary Dependences of the Kinematic Parameters on Time.....	467
Chapter XII. Method of the Calculation of Apparent Additional Masses of Wings of Arbitrary Planform.....	510
Chapter XIII. Some Point Solutions.....	555
Chapter XIV. Calculation of the Unsteady Wing Characteristics of Arbitrary Planform.....	604
Part III. High Subsonic Speeds ($0 < M < 1$). Introduction	689
Chapter XV. Method of the Calculation of the Coefficients of Aerodynamic Derivatives with $p^* \rightarrow 0$	695
Chapter XVI. The Velocity Field of Unsteady Discrete Vortex in a Compresses Medium.....	734
Chapter XVII. Method of the Calculation of Aerodynamic Wing Characteristics with Arbitrary Time Dependences.....	759
Chapter XVIII. Some Known Solutions.....	796
Chapter XIX. Calculation of the Unsteady Wing Characteristics of Arbitrary Planform.....	814
Part IV. Supersonic Speeds ($M > 1$). Introduction.....	855
Chapter XX. Numerical Method of the Calculation of Aerodynamic Wing Characteristics with Harmonic Time Dependences.....	861
Chapter XXI. Numerical Method of the Calculation of Aerodynamic Wing Characteristics with Arbitrary Time Dependences.....	917
Chapter XXII. Some Exact Solutions for Wings with Supersonic Edges with Harmonic Time Dependences.....	950
Chapter XXIII. Some Precise Solutions for Wings with Supersonic Edges with Arbitrary Time Dependences.....	1001
Chapter XXIV. Procedure of Calculation of the Aerodynamic Wing Characteristics of Arbitrary Planform.....	1023
Part V. Practical Applications. Introduction.....	1071
Chapter XXV. Special Features of the Practical Use of Duhamel Integral in Tasks of Aerodynamics.....	1077
Chapter XXVI. Approximation Method.....	1104

Chapter XXVII. Coefficients of the Aerodynamic Derivative and of Apparent Additional Masses.....	1145
Chapter XXVIII. Some Common Properties of Unsteady Characteristics. Effect of Planform, Numbers M and p^* on the Aerodynamic Derivatives of Wings.....	1240
Chapter XXIX. Effect of Planform, the Mach Numbers and Laws of Motion for Transient Functions.....	1300
Literature.....	1333
Principal Notations.....	1352
Index.....	1362

Page 277.

Chapter XII.

METHOD OF THE CALCULATION OF APPARENT ADDITIONAL MASSES OF WINGS OF ARBITRARY PLANFORM.

§1. Basic concepts of the numerical calculation method. Vortex/eddy model of wing. Selection of the position of bound vortexes and control points.

For calculation with the aid of the Duhamel integral of aerodynamic wing characteristics under the arbitrary laws of motion or during oscillations with finite Strouhal numbers p^* in the incompressible medium, besides transient functions, it is necessary to know the aerodynamic characteristics, which appear during noncirculating flow (see §§7-9 of chapter VI). Recall that the aerodynamic forces and moments which act on rigid body during noncirculating flow in the ideal incompressible medium, are expressed with the aid of apparent additional masses (see §9 of chapter II).

The noncirculating diagram of flow can be applied in the examination of the evolutions of wing on site, or for the approximate determination of aerodynamic forces and torque/moments with unsteady motion and the during strains of the strongly elongated bodies, including wings, in water or at small flight speeds in air.

For the calculation of noncirculatory flow about a wing as in the case of determining characteristics in the presence of circulation, let us replace wing with the vortex/eddy surface, which let us simulate further the system of discrete eddy/vortices [1.71]. Thus, the solution of this problem will be very similar to presented in chapter X. However, there are very essential differences. First with noncirculating streamlining, it is logical, there will not be free vortices after wing. This leads, in particular, to the fact that instead of chaplygina - Joukowski's hypothesis here we will have a condition about equality zero of total vorticity in each wing section. Due to this will change the method of the location of bound vortexes and control points on wing, i.e., the vortex/eddy model of wing.

Page 278.

And finally, for a noncirculating flow another form takes Joukowski's theorem "in small".

Let us examine at first the rigid wing of arbitrary planform, the accomplishing unsteady motion. The kinematic parameters of motion let us present in the form (2.45), namely (Fig. 12.1):

$$U = iU_1 + jU_2 + kU_3, \quad \Omega = iU_4 + jU_5 + kU_6. \quad (12.1)$$

As before let us simulate wing the system of the oblique bound vortexes. However, during noncirculating flow all wing edges (front/leading, rear and lateral) in a qualitative respect will be equal. Specifically, on all these edges the disturbed velocities, generally speaking, will go to infinity. Therefore the discrete bound vortexes must be arranged/located at certain distance from edges. Taking into account this observation, let us accept the following method of the separation of wing along axis Oz. The semirange of the wing is divided into $2N + 1$ equal parts, corresponding cut let us designate $\Delta l = l/2 (2N + 1)$. At a distance Δl from end chord, we rise from of the first band ($k = 1, p = 1$), width of each band between sections $k (p)$ and $k + 1 (p + 1)$ will be $2\Delta l$. Then the spread/scope of each bound vortex is equal to $2\Delta l$, therefore

$$\bar{l}_{kk+1} = \frac{2\Delta l}{b} = \frac{l}{b(2N+1)} = \zeta_k - \zeta_{k+1} \quad k = 1, 2, \dots, N. \quad (12.2)$$

Let us divide now yeachyu b_h into n of equal parts, middle of adjacent cuts b_h/n and b_{h+1}/n let us accept for the points, through which

it passes bound vortex. Hence easily we obtain formulas for determining middles $\Gamma_{\mu k k+1}$ eddy/vortices and the angles of their sweepback in the axes of the coordinates of Fig. 12.2:

$$\left. \begin{aligned} \xi_{\mu k+1}^{\mu k} &= \frac{1}{2} (\xi_{\mu k} + \xi_{\mu k+1}), & \zeta_{\mu k+1}^{\mu k} &= \frac{1}{2} (\zeta_{\mu k} + \zeta_{\mu k+1}), \\ \operatorname{tg} \chi_{\mu k+1}^{\mu k} &= \frac{\xi_{\mu k} - \xi_{\mu k+1}}{\zeta_{\mu k} - \zeta_{\mu k+1}}, \\ \xi_{\mu k+1} &= \xi_{0k+1} + \frac{b_{k+1}}{b} \frac{2\mu-1}{2n}, & \zeta_{\mu k+1} &= \zeta_{0k+1}, \\ \mu &= 1, 2, \dots, n; & k &= 1, 2, \dots, N. \end{aligned} \right\} \quad (12.3)$$

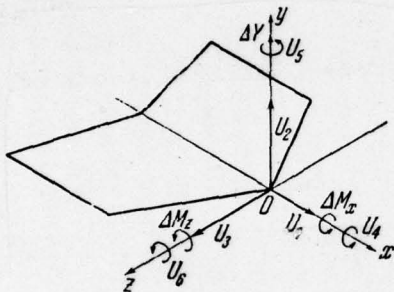


Fig. 12.1. System of the axes.

Page 279.

Here ξ_{0k}, ζ_{0k} — coordinates of leading wing edge in the k section.
Indices μ and k — positive integer numbers, the reading μ going from leading edge to rear, but k — from right to left.

Figure 12.2 in the form of an example depicts the vortex/eddy model of wing with direct/straight edges during noncirculating flow. In it it is undertaken by $N = 4$ and $n = 4$.

For a wing with the direct/straightedges of formula (12.3) they will be written in the form

$$\left. \begin{aligned} \xi_{\mu k+1}^{\mu k} &= \frac{2\mu-1}{2n} + \left[\operatorname{tg} \chi_0 - \frac{(4\mu-2)}{n} \frac{\eta-1}{\lambda(\eta+1)} \right] \xi_{\mu k+1}^{\mu k}, \\ \xi_{\mu k+1}^{\mu k} &= \frac{1}{2} (\xi_{\mu k} + \xi_{\mu k+1}), \\ \operatorname{tg} \chi_{\mu k+1}^{\mu k} &= \operatorname{tg} \chi_0 - \frac{4\mu-2}{n} \frac{\eta-1}{\lambda(\eta+1)}, \\ \mu &= 1, 2, \dots, n; \quad k = 1, 2, \dots, N. \end{aligned} \right\} \quad (12.4)$$

For the same reasons and for a circulation flow, control points one should arrange/locate so that they would lie/rest in the middle between eddy/vortices (crosses in Fig. 12.2). Let us arrange/locate them at the end of each cut b_{kk+1}/n , except the latter (count is conducted from leading edge to rear).

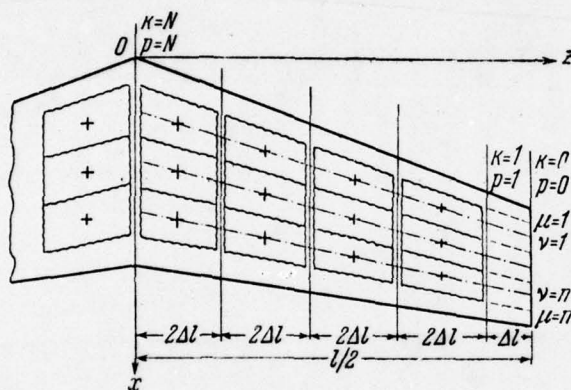


Fig. 12.2. Vortex/eddy model of wing during noncirculating flow.

Page 280.

For determining the coordinates of control points (indices v and p) they make the same sense, that μ and k) in the case of the wing of arbitrary planform we have the formulas

$$\left. \begin{aligned} \xi_{vp+1}^{vp} &= \frac{1}{2} (\xi_{vp} + \xi_{vp+1}), & \zeta_{vp+1}^{vp} &= \frac{1}{2} (\zeta_{vp} + \zeta_{vp+1}), \\ \xi_{vp+1} &= \xi_{0p+1} + \frac{b_{p+1}}{b} \frac{v}{n}, \\ v &= 1, 2, \dots, n-1; & p &= 1, 2, \dots, N. \end{aligned} \right\} \quad (12.5)$$

For wings with the direct/straight edges of the coordinate of control points they are located from the formulas

$$\left. \begin{aligned} \xi_{vp+1}^{vp} &= \frac{1}{2}(\xi_{vp} + \xi_{vp+1}), \\ \xi_{vp+1}^{vp} &= \frac{v}{n} + \left[\operatorname{tg} \chi_0 - 4 \frac{v}{n} \frac{\eta-1}{\lambda(\eta+1)} \right] \xi_{vp+1}^{vp}, \\ v &= 1, 2, \dots, n-1; \quad p = 1, 2, \dots, N. \end{aligned} \right\} \quad (12.6)$$

§2. Calculation of the circulations of bound vortexes during the motion of rigid wing.

On the basis of the described vortex/eddy model of wing, let us compose systems of equations for determining the intensity/strength of discrete eddy/vortices. During the calculation of the velocities in the control points of wing from vortex/eddy system we utilize the studied into §2 of chapter IX stationary oblique eddy/vortex with

free semi-infinite vortices. Let us note that wing vortex system (see Fig. 12.2) it is possible to present in the form of the locked vortex filaments, as this is shown in Fig. 12.3a, b in an example of one band. As earlier (see §3 of chapter XI), each locked vortex filament we consider as sum of two horseshoe vortices with equally contrasted/opposed circulations (Fig. 12.3c).

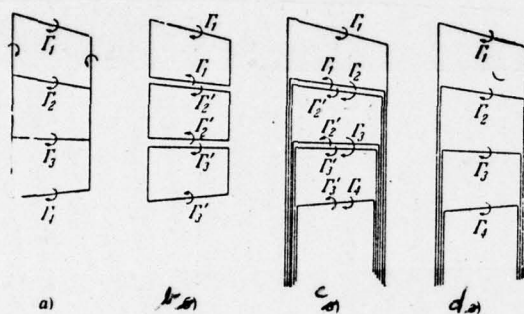


Fig. 12.3. To the determination of velocities from bound eddy/vortices.

Page 281.

If through one and the same points of wing they pass two bound vortexes, we unite them into one (Fig. 12.3d) with the circulation, equal to the sum of the circulations of the united eddy/vortices. Since during noncirculatory flow in each section the sum of the circulations of all bound vortexes is equal to zero, this leads to the fact that all free vortexes to the rear of wing average out and vortex/eddy captivities after wing will not be.

Let us examine the motion of the wing, with which $U_3 = U_5 = 0$, i.e., when motion it occurs without the angle of slip β and of angular yaw rate Ω_y . We will represent the circulation of eddy/vortices in the form

$$\Gamma_{\mu k k+1} = U_2 b \Gamma_{\mu k k+1}^{(2)} + U_4 b^2 \Gamma_{\mu k k+1}^{(4)} + U_6 b^2 \Gamma_{\mu k k+1}^{(6)}, \quad (12.7)$$

where $\Gamma_{\mu k k+1}^{(i)}$ - dimensionless functions, the time-independent, on which depend the only parameters U_i . The disturbed velocity, induced in control point $\xi_{vp+1}^{vp}, \zeta_{vp+1}^{vp}$, taking into account the parity of functions $\Gamma_{\mu k k+1}^{(2)}, \Gamma_{\mu k k+1}^{(6)}$ and the odd parity of functions $\Gamma_{\mu k k+1}^{(4)}$ on z will be written in the form

$$\begin{aligned} W_{vp+1} = & \frac{U_2}{4\pi} \sum_{k=1}^N \sum_{\mu=1}^n \Gamma_{\mu k k+1}^{(2)} (w_{vp+1}^{\mu k k+1} + \sigma w_{vp+1}^{\mu k k+1}) + \\ & + \frac{U_4 b}{4\pi} \sum_{k=1}^N \sum_{\mu=1}^n \Gamma_{\mu k k+1}^{(4)} (w_{vp+1}^{\mu k k+1} - \sigma w_{vp+1}^{\mu k k+1}) + \\ & + \frac{U_6 b}{4\pi} \sum_{k=1}^N \sum_{\mu=1}^n \Gamma_{\mu k k+1}^{(6)} (w_{vp+1}^{\mu k k+1} + \sigma w_{vp+1}^{\mu k k+1}). \quad (12.8) \end{aligned}$$

Dimensionless velocities $w_{vp+1}^{\mu k k+1}, \sigma w_{vp+1}^{\mu k k+1}$ are calculated from formulas (9.6) - (9.8) taking into account a change of the direction of the

axes for the arguments, indicated in the right side of the following relationship/ratios:

$$\left. \begin{aligned} w_{\mu\nu\rho\rho+1}^{\mu k k+1} &= w_{\mu}(\xi_{\nu\rho+1}^{\nu\rho} - \xi_{\mu k+1}^{\mu k}, \zeta_{\nu\rho+1}^{\nu\rho} - \zeta_{\mu k+1}^{\mu k}, l_{kk+1}, \operatorname{tg} \chi_{\mu k+1}^{\mu k}), \\ \sigma w_{\mu\nu\rho\rho+1}^{\mu k k+1} &= w_{\mu}(\xi_{\nu\rho+1}^{\nu\rho} - \xi_{\mu k+1}^{\mu k}, \zeta_{\nu\rho+1}^{\nu\rho} + \zeta_{\mu k+1}^{\mu k}, l_{kk+1}, -\operatorname{tg} \chi_{\mu k+1}^{\mu k}). \end{aligned} \right\} (12.9)$$

Boundary condition (3.56) about the nonpassage of wing in the adopted in this chapter designations for a rigid wing takes the form

$$\frac{W_y}{U_0} = \frac{U_z}{U_0} - \frac{U_{\phi b}}{U_0} \zeta - \frac{U_{\theta b}}{U_0} \xi. \quad (12.10)$$

By satisfying this boundary condition in all control points, we will obtain three independent systems from $(n - 1) N$ of linear algebraic equations with nN by unknown circulations each.

Page 282.

Missing N of equations for each system we will obtain from the condition of noncirculatory flow outside wing, for which they must be made the relationship/ratio

$$\sum_{\mu=1}^n \Gamma_{\mu k k+1}^{(i)} = 0, \quad i = 2, 4, 6; \quad k = 1, 2, \dots, N. \quad (12.11)$$

Thus, in the case of the forward motion of wing along axis Oy we have a system of equations

$$\left. \begin{aligned} \frac{1}{4\pi} \sum_{k=1}^N \sum_{\mu=1}^n \Gamma_{\mu k k+1}^{(2)} (w_{y\nu p p+1}^{\mu k k+1} + \sigma w_{y\nu p p+1}^{\mu k k+1}) &= 1, \\ p &= 1, 2, \dots, N; \quad \nu = 1, 2, \dots, n-1, \\ \sum_{\mu=1}^n \Gamma_{\mu k k+1}^{(2)} &= 0, \quad k = 1, 2, \dots, N. \end{aligned} \right\} \quad (12.12)$$

The second system corresponds to the rotation of wing relative to axis Ox:

$$\left. \begin{aligned} \frac{1}{4\pi} \sum_{k=1}^N \sum_{\mu=1}^n \Gamma_{\mu k k+1}^{(4)} (w_{y\nu p p+1}^{\mu k k+1} - \sigma w_{y\nu p p+1}^{\mu k k+1}) &= -\xi_{\nu p+1}^{\nu p}, \\ p &= 1, 2, \dots, N; \quad \nu = 1, 2, \dots, n-1, \\ \sum_{\mu=1}^n \Gamma_{\mu k k+1}^{(4)} &= 0, \quad k = 1, 2, \dots, N. \end{aligned} \right\} \quad (12.13)$$

And the third - to rotation around axis Oz:

$$\left. \begin{aligned} \frac{1}{4\pi} \sum_{k=1}^N \sum_{\mu=1}^n \Gamma_{\mu k k+1}^{(6)} (w_{y\nu p p+1}^{\mu k k+1} + \sigma w_{y\nu p p+1}^{\mu k k+1}) &= -\xi_{\nu p+1}^{\nu p}, \\ p &= 1, 2, \dots, N; \quad \nu = 1, 2, \dots, n-1, \\ \sum_{\mu=1}^n \Gamma_{\mu k k+1}^{(6)} &= 0, \quad k = 1, 2, \dots, N. \end{aligned} \right\} \quad (12.14)$$

§3. Calculation of aerodynamic loadings, forces and torque/moments during noncirculating flow.

On the basis of the circulations, obtained from the solution of the systems of equations indicated, let us find the aerodynamic loadings of wing, i.e., pressure difference on of its lower and upper surface. For this we will use Joukowski's theorem "in small" (3.48) during noncirculating flow.

Page 283.

Thus, we have

$$\frac{\Delta p}{\rho_{\infty}} = \frac{p_- - p_+}{\rho_{\infty}} = U_0 \gamma_z + \frac{\partial \Gamma_z}{\partial t}, \quad (12.15)$$

whereupon Γ_Σ (Fig. 12.4), in accordance with §4 of chapter II, it is determined by the relationship/ratio

$$\Gamma_\Sigma(x, z) = \int_{x_0}^x \gamma_z(x, z) dx. \quad (12.16)$$

Here x_0 is a coordinate of the leading wing edge, x - the coordinate of the point, at which is determined the unknown load.

Analogous to (with 12.7) let us present γ_z and Γ_Σ in the form

$$\left. \begin{aligned} \gamma_z &= U_2 \gamma_z^{(2)} + U_4 b \gamma_z^{(4)} + U_6 b \gamma_z^{(6)}, \\ \Gamma_\Sigma &= U_2 b \Gamma_\Sigma^{(2)} + U_4 b^2 \Gamma_\Sigma^{(4)} + U_6 b^2 \Gamma_\Sigma^{(6)}. \end{aligned} \right\} \quad (12.17)$$

Now expression (12.15) for a pressure difference can be written in the following form:

$$\begin{aligned} \frac{\Delta p}{\rho_\infty} &= U_0 (U_2 \gamma_z^{(2)} + U_4 b \gamma_z^{(4)} + U_6 b \gamma_z^{(6)}) + \\ &+ \frac{dU_2}{dt} b \Gamma_\Sigma^{(2)} + \frac{dU_4}{dt} b^2 \Gamma_\Sigma^{(4)} + \frac{dU_6}{dt} b^2 \Gamma_\Sigma^{(6)}. \end{aligned} \quad (12.18)$$

Let us consider that on cuts b_{kk+1}/n the intensity/strength of circulation γ_z is constant. Then

$$\left. \begin{aligned} \gamma_z^{(i)}(\xi_{\mu k+1}^{\mu k}, \zeta_{\mu k+1}^{\mu k}) &= n \frac{b}{b_{kk+1}} \Gamma_{\mu k k+1}^{(i)}, \\ \Gamma_\Sigma^{(i)}(\xi_{\mu k+1}^{\mu k}, \zeta_{\mu k+1}^{\mu k}) &= \sum_{\mu=1}^n \Gamma_{\mu k k+1}^{(i)} \end{aligned} \right\} \quad (12.19)$$

and for a pressure difference at point with coordinates $\xi_{\mu k+1}^{\mu k}, \zeta_{\mu k+1}^{\mu k}$

we obtain

$$\frac{\Delta p (\xi_{\mu k+1}^{\mu k}, \zeta_{\mu k+1}^{\mu k})}{\rho_{\infty}} = U_0 \frac{nb}{b_{kk+1}} (U_2 \Gamma_{\mu k k+1}^{(2)} + U_4 b \Gamma_{\mu k k+1}^{(4)} + U_6 b \Gamma_{\mu k k+1}^{(6)}) +$$

$$+ b \frac{dU_2}{dt} \sum_{\mu=1}^{\mu} \Gamma_{\mu k k+1}^{(2)} + b^2 \frac{dU_4}{dt} \sum_{\mu=1}^{\mu} \Gamma_{\mu k k+1}^{(4)} + b^2 \frac{dU_6}{dt} \sum_{\mu=1}^{\mu} \Gamma_{\mu k k+1}^{(6)}. \quad (12.20)$$

Loads at other points of wing are obtained by interpolation.

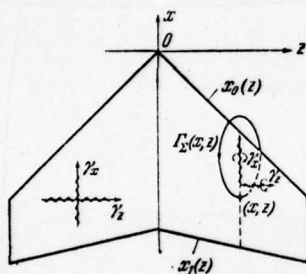


Fig. 12.4. To the determination of function

Page 284.

If wing planform is symmetrical relative to plane Oxy , then, obviously, flow pattern during motion at velocities U_2 and U_4 will be symmetrical, and therefore

$$\left. \begin{aligned} v_z^{(2)}(x, -z) &= v_z^{(2)}(x, z), & v_z^{(6)}(x, -z) &= v_z^{(6)}(x, z), \\ \Gamma_\Sigma^{(2)}(x, -z) &= \Gamma_\Sigma^{(2)}(x, z), & \Gamma_\Sigma^{(6)}(x, -z) &= \Gamma_\Sigma^{(6)}(x, z). \end{aligned} \right\} \quad (12.21)$$

During motion at velocity U_4 , the picture will be antisymmetric, therefore,

$$v_z^{(4)}(x, -z) = -v_z^{(4)}(x, z), \quad \Gamma_\Sigma^{(4)}(x, -z) = -\Gamma_\Sigma^{(4)}(x, z). \quad (12.22)$$

Aerodynamic loadings will possess by the same properties, i.e., will be symmetrical relative to plane Oxy during motions at velocities U_2 and U_4 and are antisymmetric during motion at velocity U_4 .

Let us find forces and the torque/moments, which act on wing, after decomposing them along the axes of body coordinate system (see Fig. 12.1). For their determination in chapter II are given formulas (2.2). Let us substitute into the right sides of these formulas expression (12.18) for Δp . Considering that the wing has symmetrical planform, taking into account relationship/ratics (12.21) and (12.11) we will obtain

$$\left. \begin{aligned}
 \frac{Y}{\rho_{\infty}} &= U_0 U_2 \int_{-l/2}^{l/2} \int_{x_0}^{x_1} \gamma_z^{(2)} dx dz - U_0 U_6 b \int_{-l/2}^{l/2} \int_{x_0}^{x_1} \gamma_z^{(6)} dx dz + \\
 &\quad + \frac{dU_2}{dt} b \int_{-l/2}^{l/2} \int_{x_0}^{x_1} \Gamma_{\Sigma}^{(2)} dx dz + \frac{dU_6}{dt} b^2 \int_{-l/2}^{l/2} \int_{x_0}^{x_1} \Gamma_{\Sigma}^{(6)} dx dz, \\
 \frac{M_x}{\rho_{\infty}} &= -U_0 U_4 b \int_{-l/2}^{l/2} \int_{x_0}^{x_1} \gamma_z^{(4)} z dx dz + \frac{dU_4}{dt} b^2 \int_{-l/2}^{l/2} \int_{x_0}^{x_1} \Gamma_{\Sigma}^{(4)} z dx dz, \\
 \frac{M_z}{\rho_{\infty}} &= U_0 U_2 \int_{-l/2}^{l/2} \int_{x_0}^{x_1} \gamma_z^{(2)} x dx dz + U_0 U_6 b \int_{-l/2}^{l/2} \int_{x_0}^{x_1} \gamma_z^{(6)} x dx dz + \\
 &\quad + \frac{dU_2}{dt} b \int_{-l/2}^{l/2} \int_{x_0}^{x_1} \Gamma_{\Sigma}^{(2)} x dx dz + \frac{dU_6}{dt} b^2 \int_{-l/2}^{l/2} \int_{x_0}^{x_1} \Gamma_{\Sigma}^{(6)} x dx dz.
 \end{aligned} \right\} \quad (12.23)$$

Comparing expressions (12.23) with (2.50), we find

$$\int_{-l/2}^{l/2} \int_{x_0}^{x_1} \gamma_z^{(i)} dx dz = 0, \quad i = 2, 4, 6. \quad (12.24)$$

Page 285.

This relationship/ratio escape/ensues directly from the condition of noncirculatory flow about a wing, as a result of which in each

section $z = \text{const}$ the total circulation of all eddy/vortices must be equal to zero, i.e.,

$$\int_{x_0}^{x_1} \gamma_z^{(i)} dx = 0, \quad i = 2, 4, 6. \quad (12.25)$$

For apparent additional masses λ_{22} , λ_{44} , λ_{66} and λ_{26} we have the following expressions through the circulations:

$$\frac{\lambda_{22}}{\rho_\infty} = -b \int_{-l/2}^{l/2} \int_{x_0}^{x_1} \Gamma_\Sigma^{(2)} dx dz, \quad \frac{\lambda_{22}}{\rho_\infty} = - \int_{-l/2}^{l/2} \int_{x_0}^{x_1} \gamma_z^{(2)} x dx dz, \quad (12.26)$$

$$\frac{\lambda_{44}}{\rho_\infty} = -b^2 \int_{-l/2}^{l/2} \int_{x_0}^{x_1} \Gamma_\Sigma^{(4)} z dx dz, \quad (12.27)$$

$$\frac{\lambda_{66}}{\rho_\infty} = -b^2 \int_{-l/2}^{l/2} \int_{x_0}^{x_1} \Gamma_\Sigma^{(6)} x dx dz, \quad (12.28)$$

$$\left. \begin{aligned} \frac{\lambda_{26}}{\rho_\infty} &= -b^2 \int_{-l/2}^{l/2} \int_{x_0}^{x_1} \Gamma_\Sigma^{(6)} dx dz, & \frac{\lambda_{26}}{\rho_\infty} &= -b \int_{-l/2}^{l/2} \int_{x_0}^{x_1} \Gamma_\Sigma^{(2)} x dx dz, \\ \frac{\lambda_{26}}{\rho_\infty} &= -b \int_{-l/2}^{l/2} \int_{x_0}^{x_1} \gamma_z^{(6)} x dx dz. \end{aligned} \right\} \quad (12.29)$$

During the calculation of the apparent additional masses of wing it

is more convenient than the wing are most conveniently utilized the following expressions:

$$\left. \begin{aligned} \lambda_{22} &= -\rho_{\infty} b \int_{-l/2}^{l/2} \int_{x_0}^{x_1} \Gamma_{\Sigma}^{(2)} dx dz, & \lambda_{44} &= -\rho_{\infty} b^2 \int_{-l/2}^{l/2} \int_{x_0}^{x_1} \Gamma_{\Sigma}^{(4)} z dx dz, \\ \lambda_{66} &= -\rho_{\infty} b^2 \int_{-l/2}^{l/2} \int_{x_0}^{x_1} \Gamma_{\Sigma}^{(6)} x dx dz, & \lambda_{26} &= -\rho_{\infty} b^2 \int_{-l/2}^{l/2} \int_{x_0}^{x_1} \Gamma_{\Sigma}^{(6)} dx dz. \end{aligned} \right\} \quad (12.30)$$

Let us introduce in formulas (2.55) the coefficients of apparent additional masses, then

$$\left. \begin{aligned} k_{22} &= -\frac{1}{S} \int_{-l/2}^{l/2} \int_{x_0}^{x_1} \Gamma_{\Sigma}^{(2)} dx dz, & k_{26} &= -\frac{1}{S} \int_{-l/2}^{l/2} \int_{x_0}^{x_1} \Gamma_{\Sigma}^{(6)} dx dz, \\ k_{44} &= -\frac{1}{Sb} \int_{-l/2}^{l/2} \int_{x_0}^{x_1} \Gamma_{\Sigma}^{(4)} z dx dz, & k_{66} &= -\frac{1}{Sb} \int_{-l/2}^{l/2} \int_{x_0}^{x_1} \Gamma_{\Sigma}^{(6)} x dx dz. \end{aligned} \right\} \quad (12.31)$$

Page 286.

We convert these formulas for the case, when continuous vorticity layer on wing is simulated by discrete eddy/vortices and integrals are replaced appropriate by sums. For circulations $\Gamma_{\Sigma}^{(l)}$ let us be relationship/ratio (12.19), namely:

$$\Gamma_{\Sigma \mu k k+1}^{(l)} = \sum_{\mu=1}^{\mu} \Gamma_{\mu k k+1}^{(l)}.$$

In this case the index μ with Γ_{Σ} means that the addition is conducted according to μ in section $\zeta_{k+1}^k = \text{const.}$ Let us note that as a result of (12.25)

$$\Gamma_{\Sigma_{kk+1}}^{(t)} = \sum_{\mu=1}^n \Gamma_{\mu k k+1}^{(t)} = 0. \quad (12.32)$$

Let us introduce the designations

$$\begin{aligned} R_{kk+1}^{(t)} &= -\frac{1}{n} \sum_{\mu=1}^{n-1} \sum_{\mu=1}^{\mu} \Gamma_{\Sigma_{\mu k k+1}}^{(t)} = \\ &= -\frac{1}{n} [\Gamma_{1kk+1}^{(t)} + (\Gamma_{1kk+1}^{(t)} + \Gamma_{2kk+1}^{(t)}) + \dots \\ &\quad \dots + (\Gamma_{1kk+1}^{(t)} + \Gamma_{2kk+1}^{(t)} + \dots + \Gamma_{n-1kk+1}^{(t)})], \\ \xi_{kk+1}^{(t)} &= -\frac{1}{n} \sum_{\mu=1}^{n-1} \sum_{\mu=1}^{\mu} \Gamma_{\Sigma_{\mu k k+1}}^{(t)} \xi_{\mu k+1}^{\mu} = \\ &= -\frac{1}{n} [\Gamma_{1kk+1}^{(t)} \xi_{1k+1}^{1k} + (\Gamma_{1kk+1}^{(t)} + \Gamma_{2kk+1}^{(t)}) \xi_{2k+1}^{2k} + \dots \\ &\quad \dots + (\Gamma_{1kk+1}^{(t)} + \Gamma_{2kk+1}^{(t)} + \dots + \Gamma_{n-1kk+1}^{(t)}) \xi_{n-1k+1}^{n-1k}], \end{aligned} \quad (12.33)$$

where the coordinate $\xi_{\mu k+1}^{\mu k}$, a subsequently and ζ_{k+1}^k they are determined by relationship/ratios (12.3). Then for the coefficients

of apparent additional masses we obtain the formulas

$$\left. \begin{aligned} k_{22} &= \frac{2lb}{(2N+1)S} \sum_{k=1}^N R_{kk+1}^{(2)} \frac{b_{kk+1}}{b}, & k_{26} &= \frac{2lb}{(2N+1)S} \sum_{k=1}^N R_{kk+1}^{(6)} \frac{b_{kk+1}}{b}, \\ k_{44} &= \frac{2lb}{(2N+1)S} \sum_{k=1}^N R_{kk+1}^{(4)} \frac{b_{kk+1}}{b} \zeta_{k+1}^k, & k_{66} &= \frac{2lb}{(2N+1)S} \sum_{k=1}^N L_{kk+1}^{(6)} \frac{b_{kk+1}}{b}. \end{aligned} \right\} \quad (12.34)$$

Forces and the torque/moments, which act in wing sections during noncirculating flow, we will obtain, by integrating chordwise aerodynamic loadings and the corresponding torque/moments.

Page 287.

From (12.18) we find

$$\begin{aligned}
 \frac{dY}{\rho_{\infty}} &= U_0 U_2 \int_{x_0}^{x_1} \gamma_z^{(2)} dx + U_0 U_4 b \int_{x_0}^{x_1} \gamma_z^{(4)} dx + U_0 U_6 b \int_{x_0}^{x_1} \gamma_z^{(6)} dx + \\
 &\quad + \frac{dU_2}{dt} b \int_{x_0}^{x_1} \Gamma_{\Sigma}^{(2)} dx + \frac{dU_4}{dt} b^2 \int_{x_0}^{x_1} \Gamma_{\Sigma}^{(4)} dx + \frac{dU_6}{dt} b^2 \int_{x_0}^{x_1} \Gamma_{\Sigma}^{(6)} dx, \\
 \frac{dM_x}{\rho_{\infty}} &= U_0 U_2 \int_{x_0}^{x_1} \gamma_z^{(2)} z dx + U_0 U_4 b \int_{x_0}^{x_1} \gamma_z^{(4)} z dx + U_0 U_6 b \int_{x_0}^{x_1} \gamma_z^{(6)} z dx + \\
 &\quad + \frac{dU_2}{dt} b \int_{x_0}^{x_1} \Gamma_{\Sigma}^{(2)} z dx + \frac{dU_4}{dt} b^2 \int_{x_0}^{x_1} \Gamma_{\Sigma}^{(4)} z dx + \frac{dU_6}{dt} b^2 \int_{x_0}^{x_1} \Gamma_{\Sigma}^{(6)} z dx, \\
 \frac{dM_z}{\rho_{\infty}} &= U_0 U_2 \int_{x_0}^{x_1} \gamma_z^{(2)} x dx + U_0 U_4 b \int_{x_0}^{x_1} \gamma_z^{(4)} x dx + U_0 U_6 b \int_{x_0}^{x_1} \gamma_z^{(6)} x dx + \\
 &\quad + \frac{dU_2}{dt} b \int_{x_0}^{x_1} \Gamma_{\Sigma}^{(2)} x dx + \frac{dU_4}{dt} b^2 \int_{x_0}^{x_1} \Gamma_{\Sigma}^{(4)} x dx + \frac{dU_6}{dt} b^2 \int_{x_0}^{x_1} \Gamma_{\Sigma}^{(6)} x dx.
 \end{aligned}
 \tag{12.35}$$

Let us characterize the unsteady motion of wing by dimensionless kinematic parameters (2.19), which are connected at velocities U_i by the relationships

$$\left. \begin{aligned} \frac{U_2}{U_0} &= -\alpha, & \frac{d(U_2/U_0)}{dt} \frac{b}{U_0} &= -\dot{\alpha}, & \frac{U_4 b}{U_0} &= \omega_x, \\ \frac{d(U_4 b/U_0)}{dt} \frac{b}{U_0} &= \dot{\omega}_x, & \frac{U_6 b}{U_0} &= \omega_z, & \frac{d(U_6 b/U_0)}{dt} \frac{b}{U_0} &= \dot{\omega}_z. \end{aligned} \right\} (12.36)$$

Let us introduce the coefficients of aerodynamic derivatives during noncirculatory flow. For a difference from the analogous coefficients during circulation flow, let us record/write them with index Δ before the coefficient:

$$\left. \begin{aligned} \frac{2 dY}{\rho_{\infty} U_0^2 b_{kk+1} dz} &= \Delta c'_y = \Delta c'_y{}^{\alpha} \alpha + \Delta c'_y{}^{\dot{\alpha}} \dot{\alpha} + \Delta c'_y{}^{\omega_x} \omega_x + \\ &\quad + \Delta c'_y{}^{\dot{\omega}_x} \dot{\omega}_x + \Delta c'_y{}^{\omega_z} \omega_z + \Delta c'_y{}^{\dot{\omega}_z} \dot{\omega}_z, \\ \frac{2 dM_x}{\rho_{\infty} U_0^2 b_{kk+1}^2 dz} &= \Delta m'_x = \Delta m'_x{}^{\alpha} \alpha + \Delta m'_x{}^{\dot{\alpha}} \dot{\alpha} + \\ &\quad + \Delta m'_x{}^{\omega_x} \omega_x + \Delta m'_x{}^{\dot{\omega}_x} \dot{\omega}_x + \Delta m'_x{}^{\omega_z} \omega_z + \Delta m'_x{}^{\dot{\omega}_z} \dot{\omega}_z, \\ \frac{2 dM_z}{\rho_{\infty} U_0^2 b_{kk+1}^2 dz} &= \Delta m'_z = \Delta m'_z{}^{\alpha} \alpha + \Delta m'_z{}^{\dot{\alpha}} \dot{\alpha} + \Delta m'_z{}^{\omega_x} \omega_x + \\ &\quad + \Delta m'_z{}^{\dot{\omega}_x} \dot{\omega}_x + \Delta m'_z{}^{\omega_z} \omega_z + \Delta m'_z{}^{\dot{\omega}_z} \dot{\omega}_z. \end{aligned} \right\} (12.37)$$

Page 288.

By comparing (12.35) and (12.37), we will obtain taking into account

(12.36)

$$\begin{aligned}
 \Delta c_y'^a &= -\frac{2}{b_{kk+1}} \int_{x_0}^{x_1} \gamma_z^{(2)} dx, & \Delta c_y'^{\omega x} &= \frac{2}{b_{kk+1}} \int_{x_0}^{x_1} \gamma_z^{(4)} dx, \\
 \Delta c_y'^{\omega z} &= \frac{2}{b_{kk+1}} \int_{x_0}^{x_1} \gamma_z^{(6)} dx, & \Delta c_y'^a &= -\frac{2}{b_{kk+1}} \int_{x_0}^{x_1} \Gamma_{\Sigma}^{(2)} dx, \\
 \Delta c_y'^{\omega x} &= \frac{2}{b_{kk+1}} \int_{x_0}^{x_1} \Gamma_{\Sigma}^{(4)} dx, & \Delta c_y'^{\omega z} &= \frac{2}{b_{kk+1}} \int_{x_0}^{x_1} \Gamma_{\Sigma}^{(6)} dx, \\
 \Delta m_x'^a &= -\frac{2}{b_{kk+1}^2} \int_{x_0}^{x_1} \gamma_z^{(2)} z dx, & \Delta m_x'^{\omega x} &= \frac{2}{b_{kk+1}^2} \int_{x_0}^{x_1} \gamma_z^{(4)} z dx, \\
 \Delta m_x'^{\omega z} &= \frac{2}{b_{kk+1}^2} \int_{x_0}^{x_1} \gamma_z^{(6)} z dx, & \Delta m_x'^a &= -\frac{2}{b_{kk+1}^2} \int_{x_0}^{x_1} \Gamma_{\Sigma}^{(2)} z dx, \\
 \Delta m_x'^{\omega x} &= \frac{2}{b_{kk+1}^2} \int_{x_0}^{x_1} \Gamma_{\Sigma}^{(4)} z dx, & \Delta m_x'^{\omega z} &= \frac{2}{b_{kk+1}^2} \int_{x_0}^{x_1} \Gamma_{\Sigma}^{(6)} z dx, \\
 \Delta m_z'^a &= -\frac{2}{b_{kk+1}^2} \int_{x_0}^{x_1} \gamma_z^{(2)} x dx, & \Delta m_z'^{\omega x} &= \frac{2}{b_{kk+1}^2} \int_{x_0}^{x_1} \gamma_z^{(4)} x dx, \\
 \Delta m_z'^{\omega z} &= \frac{2}{b_{kk+1}^2} \int_{x_0}^{x_1} \gamma_z^{(6)} x dx, & \Delta m_z'^a &= -\frac{2}{b_{kk+1}^2} \int_{x_0}^{x_1} \Gamma_{\Sigma}^{(2)} x dx, \\
 \Delta m_z'^{\omega x} &= \frac{2}{b_{kk+1}^2} \int_{x_0}^{x_1} \Gamma_{\Sigma}^{(4)} x dx, & \Delta m_z'^{\omega z} &= \frac{2}{b_{kk+1}^2} \int_{x_0}^{x_1} \Gamma_{\Sigma}^{(6)} x dx.
 \end{aligned} \tag{12.38}$$

During noncirculating flow in any section $z = \text{const}$ is satisfied condition (12.25); therefore

$$\left. \begin{aligned}
 \Delta c_y'^a &= \Delta c_y'^{\omega x} = \Delta c_y'^{\omega z} = 0, \\
 \Delta m_x'^a &= \Delta m_x'^{\omega x} = \Delta m_x'^{\omega z} = 0.
 \end{aligned} \right\} \tag{12.39}$$

Page 289.

For remaining conversion factors from integrals to sums gives

$$\left. \begin{aligned}
 \Delta c_y'^a &= -2R_{kk+1}^{(2)}, & \Delta c_y'^{\omega x} &= -2R_{kk+1}^{(4)}, & \Delta c_y'^{\omega z} &= -2R_{kk+1}^{(6)}, \\
 \Delta m_x'^a &= 2 \frac{b}{b_{kk+1}} \zeta_{k+1}^k R_{kk+1}^{(2)}, \\
 \Delta m_x'^{\omega x} &= -2 \frac{b}{b_{kk+1}} \zeta_{k+1}^k R_{kk+1}^{(4)}, \\
 \Delta m_x'^{\omega z} &= -2 \frac{b}{b_{kk+1}} \zeta_{k+1}^k R_{kk+1}^{(6)}, \\
 \Delta m_z'^a &= \frac{2b^2}{b_{kk+1}^2} \sum_{\mu=1}^n \Gamma_{\mu k k+1}^{(2)} \xi_{\mu k+1}^{\mu k}, \\
 \Delta m_z'^{\omega x} &= -\frac{2b^2}{b_{kk+1}^2} \sum_{\mu=1}^n \Gamma_{\mu k k+1}^{(4)} \xi_{\mu k+1}^{\mu k}, \\
 \Delta m_z'^{\omega z} &= -\frac{2b^2}{b_{kk+1}^2} \sum_{\mu=1}^n \Gamma_{\mu k k+1}^{(6)} \xi_{\mu k+1}^{\mu k}, & \Delta m_z'^a &= \frac{2b}{b_{kk+1}} L_{kk+1}^{(2)}, \\
 \Delta m_z'^{\omega x} &= -\frac{2b}{b_{kk+1}} L_{kk+1}^{(4)}, & \Delta m_z'^{\omega z} &= -\frac{2b}{b_{kk+1}} L_{kk+1}^{(6)}.
 \end{aligned} \right\} (12.40)$$

§4. Some relationship/ratios, utilized for testing the calculations.

As can be seen from (12.26) - (12.29), the same apparent additional masses can be determined through circulations by different formulas. This fact makes it possible to produce mutual testing the results of the calculations. However, let us point out that the group of formulas (12.26) even two formulas (12.29) are identities and during numerical calculations cannot serve as the means of control. Let us show that

$$\frac{b}{b_{kk+1}} \sum_{\mu=1}^n \Gamma_{\mu kk+1}^{(l)} \xi_{\mu k+1}^{\mu k} = R_{kk+1}^{(l)}. \quad (12.41)$$

Actually, coordinate $\xi_{\mu k+1}^{\mu k}$ discrete eddy/vortex $\Gamma_{\mu kk+1}^{(l)}$ can be written in the form

$$\xi_{\mu k+1}^{\mu k} = \frac{1}{2} \left[\left(x_1 - \frac{b_{kk+1}}{2n} \right) - \frac{b_{kk+1}}{n} (n - \mu) \right],$$

where x_1 is a coordinate of trailing edge.

Page 290.

The left side of expression (12.41) let us write as follows:

$$\begin{aligned} \frac{b}{b_{kk+1}} \sum_{\mu=1}^n \Gamma_{\mu kk+1}^{(l)} \xi_{\mu k+1}^{\mu k} &= \\ &= \frac{1}{b_{kk+1}} \left(x_1 - \frac{b_{kk+1}}{2n} \right) \sum_{\mu=1}^n \Gamma_{\mu kk+1}^{(l)} - \frac{1}{n} \sum_{\mu=1}^n (n - \mu) \Gamma_{\mu kk+1}^{(l)}. \end{aligned}$$

The first term on the right side of this equality equal to zero as a result of condition (12.11), and second term equally

$$\begin{aligned}
 -\frac{1}{n} \sum_{\mu=1}^n (n-\mu) \Gamma_{\mu k k+1}^{(i)} &= -\frac{1}{n} [(n-1) \Gamma_{1 k k+1}^{(i)} + (n-2) \Gamma_{2 k k+1}^{(i)} + \dots \\
 &\quad \dots + 2 \Gamma_{n-2 k k+1}^{(i)} + \Gamma_{n-1 k k+1}^{(i)} + 0 \Gamma_{n k k+1}^{(i)}] = \\
 &= -\frac{1}{n} [\Gamma_{1 k k+1}^{(i)} + (\Gamma_{1 k k+1}^{(i)} + \Gamma_{2 k k+1}^{(i)}) + \dots \\
 &\quad \dots + (\Gamma_{1 k k+1}^{(i)} + \Gamma_{2 k k+1}^{(i)} + \dots + \Gamma_{n-1 k k+1}^{(i)})] = R_{k k+1}^{(i)},
 \end{aligned}$$

that also proves affirmation (12.41).

On the basis (12.41) and (12.40) we consist that during noncirculating flow for the coefficients aerodynamic derivative distributed and of composite force and torque/moments they occur of the relationship/ratio

$$\begin{aligned}
 \frac{b}{b_{k k+1}} \Delta c_y^{q_i} &= \Delta m_z^{q_i}, \quad \Delta c_y^{q_i} = \Delta m_z^{q_i} \\
 (q_1 &= \alpha, \quad q_2 = \omega_x, \quad q_3 = \omega_z).
 \end{aligned} \tag{12.42}$$

From (12.29) we have

$$b \int_{-l/2}^{l/2} \int_{x_0}^{x_1} \Gamma_{\Sigma}^{(6)} dx dz = \int_{-l/2}^{l/2} \int_{x_0}^{x_1} \Gamma_{\Sigma}^{(2)} x dx dz.$$

By transfer/converting in this equality to sums and by utilizing designations (12.33), we will obtain

$$\sum_{k=1}^N R_{kk+1}^{(6)} = \sum_{k=1}^N L_{kk+1}^{(2)}. \quad (12.43)$$

This relationship/ratio makes it possible to produce mutual testing the calculations, produced respectively during the motion of wing at velocities U_2 and U_6 .

§5. Calculation of aerodynamic loadings, caused by the strain of wing surface, during noncirculating flow.

Let us examine now the extra loads, caused by the strain of wing surface. To each law of strain correspond their aerodynamic loadings; therefore to here inexpediently introduce the coefficients of apparent additional masses, but simpler directly to determine increment loads and the corresponding to them values of coefficients $\Delta c_y, \Delta m_x, \Delta m_z$.

Boundary condition about nonpassage (3.56) during the strains of wing takes the form in coordinate system of Fig. 12.2

$$\frac{W_y}{U_0} = \frac{\partial f_\delta(\xi, \zeta)}{\partial \xi} \delta(\tau) + f_\delta(\xi, \zeta) \dot{\delta}(\tau), \quad (12.44)$$

$$\tau = \frac{U_0 t}{b}.$$

Let us break boundary condition and entire task for two, solved formally independently:

$$\left. \begin{aligned} \frac{W_y}{U_0} &= \frac{W_{y1}}{U_0} + \frac{W_{y2}}{U_0}, \\ \frac{W_{y1}}{U_0} &= \frac{\partial f_\delta(\xi, \zeta)}{\partial \xi} \delta(\tau), \quad \frac{W_{y2}}{U_0} = f_\delta(\xi, \zeta) \dot{\delta}(\tau). \end{aligned} \right\} \quad (12.45)$$

As for a rigid wing, we utilize the vortex/eddy model, described in §1 this chapter, but boundary conditions let us satisfy at the same control points. The unknown circulation of the discrete bound vortexes let us present in the form

$$\Gamma_{+\mu k k+1} = U_0 b [\Gamma_{\mu k k+1}^\delta \delta(\tau) + \Gamma_{\mu k k+1}^{\dot{\delta}} \dot{\delta}(\tau)]. \quad (12.46)$$

For the determination of unknown values $\Gamma_{\mu k k+1}^\delta$ and $\Gamma_{\mu k k+1}^{\dot{\delta}}$ by the method, completely analogous described for a rigid wing, we compose

and solve the independently following two systems of the algebraic equations:

$$\left. \begin{aligned} \frac{1}{4\pi} \sum_{k=1}^N \sum_{\mu=1}^n \Gamma_{\mu k k+1}^{\delta} (w_{y^{\nu p p+1}}^{\mu k k+1} \pm \sigma w_{y^{\nu p p+1}}^{\mu k k+1}) &= \frac{\partial f_{\delta}}{\partial \xi} \Big|_{\xi = \xi_{\nu p+1}^{\nu p}, \zeta = \zeta_{\nu p+1}^{\nu p}}, \\ \nu &= 1, 2, \dots, n-1; \quad p = 1, 2, \dots, N, \end{aligned} \right\} \quad (12.47)$$

$$\left. \begin{aligned} \sum_{\mu=1}^n \Gamma_{\mu k k+1}^{\delta} &= 0, \quad k = 1, 2, \dots, N; \\ \frac{1}{4\pi} \sum_{k=1}^N \sum_{\mu=1}^n \Gamma_{\mu k k+1}^{\delta} (w_{y^{\nu p p+1}}^{\mu k k+1} \pm \sigma w_{y^{\nu p p+1}}^{\mu k k+1}) &= f_{\delta}(\xi_{\nu p+1}^{\nu p}, \zeta_{\nu p+1}^{\nu p}), \\ \nu &= 1, 2, \dots, n-1; \quad p = 1, 2, \dots, N, \\ \sum_{\mu=1}^n \Gamma_{\mu k k+1}^{\delta} &= 0, \quad k = 1, 2, \dots, N. \end{aligned} \right\} \quad (12.48)$$

Page 292.

Here sign "+" in brackets it is taken with deformations symmetrical on spread/scope, and "-" with antisymmetric.

Aerodynamic loadings on wing, we determine according to Joukowski's theorem (12.15). Values γ_z and Γ_z let us present,

analogous to (with 12.46), in the dependences

$$\gamma_z(\tau) = U_0 [\gamma_z^\delta(\tau) + \gamma_z^{\delta\dot{}}(\tau)], \quad \Gamma_\Sigma(\tau) = U_0 b [\Gamma_\Sigma^\delta(\tau) + \Gamma_\Sigma^{\delta\dot{}}(\tau)].$$

Taking into account that $d/dt = (U_0/b)(d/d\tau)$, and by utilizing (12.19), we will obtain from (12.15)

$$\begin{aligned} \Delta\bar{p} = \frac{2\Delta p}{\rho_\infty U_0^2} = 2 \frac{nb}{b_{kk+1}} \Gamma_{\mu kk+1}^\delta \delta + 2 \frac{nb}{b_{kk+1}} \Gamma_{\mu kk+1}^{\delta\dot{}} \dot{\delta} + \\ + \frac{d\delta}{d\tau} 2 \sum_{\mu=1}^n \Gamma_{\mu kk+1}^\delta + \frac{d\dot{\delta}}{d\tau} 2 \sum_{\mu=1}^n \Gamma_{\mu kk+1}^{\delta\dot{}}. \end{aligned} \quad (12.49)$$

For a dimensionless load $\Delta\bar{p}$ we can, on the basis of (12.49), write

$$\left. \begin{aligned} \Delta\bar{p} &= \Delta\bar{p}_1 + \Delta\bar{p}_2, \\ \Delta\bar{p}_1 &= \Delta p_1^\delta \delta + \Delta p_1^{\delta\dot{}} \dot{\delta}, \quad \Delta\bar{p}_2 = \Delta p_2^\delta \delta + \Delta p_2^{\delta\dot{}} \dot{\delta}, \end{aligned} \right\} \quad (12.50)$$

where

$$\left. \begin{aligned} \Delta p_1^\delta &= 2 \frac{nb}{b_{kk+1}} \Gamma_{\mu kk+1}^\delta, & \Delta p_1^{\delta\dot{}} &= 2 \sum_{\mu=1}^n \Gamma_{\mu kk+1}^{\delta\dot{}} \\ \Delta p_2^\delta &= 2 \frac{nb}{b_{kk+1}} \Gamma_{\mu kk+1}^\delta, & \Delta p_2^{\delta\dot{}} &= 2 \sum_{\mu=1}^n \Gamma_{\mu kk+1}^{\delta\dot{}} \end{aligned} \right\} \quad (12.51)$$

The relationship/ratios, analogous (12.50), can be written for any total and distributed aerodynamic characteristics:

$$\left. \begin{aligned} \Delta c &= \Delta c_1 + \Delta c_2, \\ \Delta c_1 &= \Delta c_1^\delta \delta + \Delta c_1^{\delta\dot{}} \dot{\delta}, & \Delta c_2 &= \Delta c_2^\delta \delta + \Delta c_2^{\delta\dot{}} \dot{\delta}. \end{aligned} \right\} \quad (12.52)$$

Let us introduce the force coefficients and torque/moments of sections wing to the formulas

$$\Delta c'_y = \frac{2 \Delta Y'}{\rho_\infty U_0^2 b_{kk+1}}, \quad \Delta m'_x = \frac{2 \Delta M'_x}{\rho_\infty U_0^2 b_{kk+1}^2}, \quad \Delta m'_z = \frac{2 \Delta M'_z}{\rho_\infty U_0^2 b_{kk+1}^2}. \quad (12.53)$$

Page 293.

Analogous to (with 12.33) let us designate

$$\begin{aligned} R_{kk+1}^\delta &= -\frac{1}{n} \sum_{\mu=1}^{n-1} \sum_{\mu=1}^{\mu} \Gamma_{\mu kk+1}^\delta, & R_{kk+1}^\delta &= -\frac{1}{n} \sum_{\mu=1}^{n-1} \sum_{\mu=1}^{\mu} \Gamma_{\mu \mu k+1}^\delta, \\ L_{kk+1}^\delta &= -\frac{1}{n} \sum_{\mu=1}^{n-1} \xi_{\mu k+1}^{\mu k} \sum_{\mu=1}^{\mu} \Gamma_{\mu k k+1}^\delta, & L_{kk+1}^\delta &= -\frac{1}{n} \sum_{\mu=1}^{n-1} \xi_{\mu k+1}^{\mu k} \sum_{\mu=1}^{\mu} \Gamma_{\mu \mu k+1}^\delta, \end{aligned} \quad (12.54)$$

then for the characteristics of wing sections taking into account (12.41) we will have

$$\begin{aligned} \Delta c'_{y1}^\delta &= \Delta c'_{y2}^\delta = \Delta m'_{x1}^\delta = \Delta m'_{x2}^\delta = 0, \\ \Delta c'_{y1}^\delta &= -2 R_{kk+1}^\delta, \quad \Delta c'_{y2}^\delta = -2 R_{kk+1}^\delta, \\ \Delta m'_{x1}^\delta &= -2 \frac{b}{b_{kk+1}} \xi_{k+1}^k R_{kk+1}^\delta, \quad \Delta m'_{x2}^\delta = -2 \frac{b}{b_{kk+1}} \xi_{k+1}^k R_{kk+1}^\delta, \\ \Delta m'_{z1}^\delta &= -2 \frac{b^2}{b_{kk+1}^2} \sum_{\mu=1}^n \Gamma_{\mu k k+1}^\delta \xi_{\mu k+1}^{\mu k} = \frac{b}{b_{kk+1}} \Delta c'_{y1}^\delta, \\ \Delta m'_{z2}^\delta &= -2 \frac{b^2}{b_{kk+1}^2} \sum_{\mu=1}^n \Gamma_{\mu k k+1}^\delta \xi_{\mu k+1}^{\mu k} = \frac{b}{b_{kk+1}} \Delta c'_{y2}^\delta, \\ \Delta m'_{z1}^\delta &= -2 \frac{b}{b_{kk+1}} L_{kk+1}^\delta, \quad \Delta m'_{z2}^\delta = -2 \frac{b}{b_{kk+1}} L_{kk+1}^\delta. \end{aligned} \quad (12.55)$$

Composite force and torque/moments we will obtain, by integrating the characteristics of sections by the wingspan.

Page 294.

By accepting as significant dimensions the root chord b of wing and its area S , we will obtain for the aerodynamic coefficients of entire wing the following formulas:

during the symmetrical strains

$$\begin{aligned}
 \Delta c_{y1}^\delta &= \Delta c_{y2}^\delta = \Delta m_{x1}^\delta = \Delta m_{x2}^\delta = \Delta m_{x1}^\delta = \Delta m_{x2}^\delta = 0, \\
 \Delta c_{y1}^\delta &= -\frac{4lb}{(2N+1)S} \sum_{k=1}^N R_{kk+1}^\delta \frac{b_{kk+1}}{b}, \\
 \Delta c_{y2}^\delta &= -\frac{4lb}{(2N+1)S} \sum_{k=1}^N R_{kk+1}^\delta \frac{b_{kk+1}}{b}, \\
 \Delta m_{z1}^\delta &= -\frac{4lb}{(2N+1)S} \sum_{k=1}^N \sum_{\mu=1}^n \Gamma_{\mu kk+1}^\delta \xi_{\mu k+1}^{\mu k} = \\
 &= -\frac{4lb}{(2N+1)S} \sum_{k=1}^N R_{kk+1}^\delta \frac{b_{kk+1}}{b} = \Delta c_{y1}^\delta,
 \end{aligned} \quad (12.56)$$

$$\begin{aligned}
 \Delta m_{z2}^{\delta} &= -\frac{4lb}{(2N+1)S} \sum_{k=1}^N \sum_{\mu=1}^n \Gamma_{\mu kk+1}^{\delta} \xi_{\mu k+1}^{\mu k} = \\
 &= -\frac{4lb}{(2N+1)S} \sum_{k=1}^N R_{kk+1}^{\delta} \frac{b_{kk+1}}{b} = \Delta c_{y2}^{\delta}, \\
 \Delta m_{z1}^{\delta} &= -\frac{4lb}{(2N+1)S} \sum_{k=1}^N L_{kk+1}^{\delta} \frac{b_{kk+1}}{b}, \\
 m_{z2}^{\delta} &= -\frac{4lb}{(2N+1)S} \sum_{k=1}^N L_{kk+1}^{\delta} \frac{b_{kk+1}}{b};
 \end{aligned}
 \tag{12.56}$$

with the antisymmetric deformations

$$\begin{aligned}
 \Delta c_{y1}^{\delta} &= \Delta c_{y2}^{\delta} = \Delta m_{x1}^{\delta} = \Delta m_{x2}^{\delta} = 0, \\
 \Delta c_{y1}^{\delta} &= \Delta c_{y2}^{\delta} = \Delta m_{z1}^{\delta} = \Delta m_{z2}^{\delta} = \Delta m_{x2}^{\delta} = \Delta m_{z2}^{\delta} = 0, \\
 \Delta m_{x1}^{\delta} &= -\frac{4lb}{(2N+1)S} \sum_{k=1}^N R_{kk+1}^{\delta} \xi_{k+1}^k \frac{b_{kk+1}}{b}, \\
 \Delta m_{x2}^{\delta} &= -\frac{4lb}{(2N+1)S} \sum_{k=1}^N R_{kk+1}^{\delta} \xi_{k+1}^k \frac{b_{kk+1}}{b}.
 \end{aligned}
 \tag{12.57}$$

§6. Special feature/peculiarities of the application/use of a Duhamel integral in the tasks of the strains of wing with $M = 0$.

The transient functions of aerodynamic loadings, which correspond to deformations of wing surface in the incompressible medium, have with $\tau = 0$ special feature/peculiarity. If we for the calculation aerodynamically of characteristics with the arbitrary dependences of strains on time or for determining the coefficients of aerodynamic derivatives utilize Duhamel integral, these special feature/peculiarities must be isolated. In chapter II was done the isolation/liberation of special feature/peculiarities in the case of the motion of rigid wing. Let us show now, as this is made during strains.

Page 295.

The reaction of wing $c_\delta(\tau)$ under the arbitrary law of strain $f_\delta(\xi, \zeta, \tau)$ let us present in the form of two reactions:

$$c_\delta(\xi, \zeta, \tau) = c_\delta^{(1)}(\xi, \zeta, \tau) + c_\delta^{(2)}(\xi, \zeta, \tau), \quad (12.58)$$

where $c_\delta^{(1)}$ it corresponds to member $\frac{\partial f_\delta(\xi, \zeta)}{\partial \xi} \delta(\tau)$ under boundary

conditions, and $c_{\delta}^{(2)}$ — to member $f_{\delta}(\xi, \zeta) \frac{d\delta}{d\tau}$. Then according to (6.6), (6.33), (6.34) for determining them we have

$$\left. \begin{aligned} c_{\delta}^{(1)}(\xi, \zeta, \tau) &= \delta(0) \left[\frac{c_1(\tau)}{\delta^*} \right] + \int_0^{\tau-\varepsilon} \frac{d\delta}{d\tau_1} \left[\frac{c_1(\tau-\tau_1)}{\delta^*} \right] d\tau_1 + \\ &\quad + \lim_{\varepsilon \rightarrow 0} \int_{\tau-\varepsilon}^{\tau} \frac{d\delta}{d\tau_1} \left[\frac{c_1(\tau-\tau_1)}{\delta^*} \right] d\tau_1, \\ c_{\delta}^{(2)}(\xi, \zeta, \tau) &= \frac{d\delta}{d\tau} \Big|_{\tau=0} \left[\frac{c_2(\tau)}{\delta^*} \right] + \int_0^{\tau-\varepsilon} \frac{d^2\delta}{d\tau_1^2} \left[\frac{c_2(\tau-\tau_1)}{\delta^*} \right] d\tau_1 + \\ &\quad + \lim_{\varepsilon \rightarrow 0} \int_{\tau-\varepsilon}^{\tau} \frac{d^2\delta}{d\tau_1^2} \left[\frac{c_2(\tau-\tau_1)}{\delta^*} \right] d\tau_1. \end{aligned} \right\} \quad (12.59)$$

Here $\left[\frac{c_1(\tau)}{\delta^*} \right]$ and $\left[\frac{c_2(\tau)}{\delta^*} \right]$ are the transient functions, found at the stepped law of a change in $\delta(\tau)/\delta^*$ and $\dot{\delta}(\tau)/\dot{\delta}^*$ by the methods, presented in chapter XI. As earlier (see §5 of chapter VI), the step function of change $\delta(\tau)/\delta^*$, $\dot{\delta}(\tau)/\dot{\delta}^*$ we consider as limit with $\varepsilon \rightarrow 0$ of law (see Fig. 6.3)

$$\frac{\delta(\tau)}{\delta^*} = \frac{\dot{\delta}(\tau)}{\dot{\delta}^*} = \begin{cases} 0 & \text{при } \tau < 0, \\ \tau/\varepsilon & \text{при } 0 \leq \tau \leq \varepsilon, \\ 1 & \text{при } \tau > \varepsilon. \end{cases} \quad (12.60)$$

Key: (1). with.

In time interval $0 \leq \tau \leq \varepsilon$ we consider flow around of the wing noncirculating. Then in accordance with (12.52) and (12.60) transient functions $\left[\frac{c_1(\tau - \tau_1)}{\delta^*} \right]$ and $\left[\frac{c_2(\tau - \tau_1)}{\dot{\delta}^*} \right]$ with $0 \leq \tau - \tau_1 \leq \varepsilon$ are equal to

$$\left. \begin{aligned} \left[\frac{c_1(\tau - \tau_1)}{\delta^*} \right] &= \frac{\Delta c_1^\delta}{\varepsilon} (\tau - \tau_1) + \frac{\Delta c_1^\delta}{\varepsilon}, \\ \left[\frac{c_2(\tau - \tau_1)}{\dot{\delta}^*} \right] &= \frac{\Delta c_2^\delta}{\varepsilon} (\tau - \tau_1) + \frac{\Delta c_2^\delta}{\varepsilon}. \end{aligned} \right\} \quad (12.61)$$

Page 296.

By substituting (12.61) in (12.59) and by taking into account (6.36), we will obtain

$$\left. \begin{aligned} \lim_{\varepsilon \rightarrow 0} \frac{\Delta c_1^\delta}{\varepsilon} \int_{\tau-\varepsilon}^{\tau} \frac{d\delta}{d\tau_1} (\tau - \tau_1) d\tau_1 &= 0, \\ \lim_{\varepsilon \rightarrow 0} \frac{\Delta c_1^\delta}{\varepsilon} \int_{\tau-\varepsilon}^{\tau} \frac{d\delta}{d\tau_1} d\tau_1 &= \Delta c_1^\delta \frac{d\delta}{d\tau}, \\ \lim_{\varepsilon \rightarrow 0} \frac{\Delta c_2^\delta}{\varepsilon} \int_{\tau-\varepsilon}^{\tau} \frac{d^2\delta}{d\tau_1^2} (\tau - \tau_1) d\tau_1 &= 0, \\ \lim_{\varepsilon \rightarrow 0} \frac{\Delta c_2^\delta}{\varepsilon} \int_{\tau-\varepsilon}^{\tau} \frac{d^2\delta}{d\tau_1^2} d\tau_1 &= \Delta c_2^\delta \frac{d^2\delta}{d\tau^2}. \end{aligned} \right\} \quad (12.62)$$

Thus, finally we have

$$\left. \begin{aligned} c_\delta^{(2)}(\xi, \zeta, \tau) &= \delta(0) \left[\frac{c_1(\tau)}{\delta^*} \right] + \int_0^\tau \frac{d\delta}{d\tau_1} \left[\frac{c_1(\tau - \tau_1)}{\delta^*} \right] d\tau_1 + \Delta c_1^\delta \frac{d\delta}{d\tau}, \\ c_\delta^{(2)}(\xi, \zeta, \tau) &= \frac{d\delta}{d\tau} \Big|_{\tau=0} \left[\frac{c_2(\tau)}{\delta^*} \right] + \\ &\quad + \int_0^\tau \frac{d^2\delta}{d\tau_1^2} \left[\frac{c_2(\tau - \tau_1)}{\delta^*} \right] d\tau_1 + \Delta c_2^\delta \frac{d^2\delta}{d\tau^2}, \\ c_\delta(\xi, \zeta, \tau) &= c_\delta^{(1)}(\xi, \zeta, \tau) + c_\delta^{(2)}(\xi, \zeta, \tau), \\ c &= c_p, \quad m_x, \quad m_z, \quad \Delta p. \end{aligned} \right\} \quad (12.63)$$

In these formulas is integrated the only regular part of the transient functions.

Let us derive formulas for the calculation of the coefficients of aerodynamic derivatives in the incompressible medium with the harmonic dependences of the deformation of wing on time.

Let us present according to (7.27) the coefficients of aerodynamic derivatives in the form

$$\left. \begin{aligned} c &= c_1 + c_2, & c_1 &= c_1^0 \delta + c_1^1 \dot{\delta}, & c_2 &= c_2^0 \delta + c_2^1 \dot{\delta}, \\ c &= c^0 \delta + c^1 \dot{\delta}, & c^0 &= c_1^0 - p^* c_2^0, & c^1 &= c_1^1 + c_2^1. \end{aligned} \right\} \quad (12.64)$$

Page 297.

For determining the coefficients of aerodynamic derivatives we have formulas (6.54), which in this case will be written in the form

$$\left. \begin{aligned} c_1^0(p^*) &= p^* \int_0^\infty \left[\frac{c_1(\tau)}{\delta^*} \right] \sin p^* \tau d\tau + p^* \lim_{\varepsilon \rightarrow 0} \int_0^\varepsilon \left[\frac{c_1(\tau)}{\delta^*} \right] \sin p^* \tau d\tau, \\ c_1^0(p^*) &= \int_0^\infty \left[\frac{c_1(\tau)}{\delta^*} \right] \cos p^* \tau d\tau + \lim_{\varepsilon \rightarrow 0} \int_0^\varepsilon \left[\frac{c_1(\tau)}{\delta^*} \right] \cos p^* \tau d\tau, \\ c_2^0(p^*) &= p^* \int_0^\infty \left[\frac{c_2(\tau)}{\delta^*} \right] \sin p^* \tau d\tau + p^* \lim_{\varepsilon \rightarrow 0} \int_0^\varepsilon \left[\frac{c_2(\tau)}{\delta^*} \right] \sin p^* \tau d\tau, \\ c_2^0(p^*) &= \int_0^\infty \left[\frac{c_2(\tau)}{\delta^*} \right] \cos p^* \tau d\tau + \lim_{\varepsilon \rightarrow 0} \int_0^\varepsilon \left[\frac{c_2(\tau)}{\delta^*} \right] \cos p^* \tau d\tau. \end{aligned} \right\} \quad (12.65)$$

In this case we consider that in the first members of right sides (12.65) of special feature/peculiarity of of subintegral functions are excluded, and in the second members the transient functions correspond to noncirculating flow. Then on section $0 \leq \tau \leq \varepsilon$ we have

$$\left. \begin{aligned} \left[\frac{c_1(\tau)}{\delta^*} \right] &= \frac{\Delta c_1^\delta}{\varepsilon} \tau + \frac{\Delta c_1^\delta}{\varepsilon}, \\ \left[\frac{c_2(\tau)}{\delta^*} \right] &= \frac{\Delta c_2^\delta}{\varepsilon} \tau + \frac{\Delta c_2^\delta}{\varepsilon}. \end{aligned} \right\} \quad (12.66)$$

By substituting the value (12.66) in the appropriate integrals of right sides (12.65), we will obtain taking into account (6.38)

$$\left. \begin{aligned} \lim_{\varepsilon \rightarrow 0} \frac{\Delta c_1^\delta}{\varepsilon} \int_0^\varepsilon \tau \sin p^* \tau d\tau &= 0, & \lim_{\varepsilon \rightarrow 0} \frac{\Delta c_1^\delta}{\varepsilon} \int_0^\varepsilon \sin p^* \tau d\tau &= 0, \\ \lim_{\varepsilon \rightarrow 0} \frac{\Delta c_1^\delta}{\varepsilon} \int_0^\varepsilon \tau \cos p^* \tau d\tau &= 0, & \lim_{\varepsilon \rightarrow 0} \frac{\Delta c_1^\delta}{\varepsilon} \int_0^\varepsilon \cos p^* \tau d\tau &= \Delta c_1^\delta, \\ \lim_{\varepsilon \rightarrow 0} \frac{\Delta c_2^\delta}{\varepsilon} \int_0^\varepsilon \tau \sin p^* \tau d\tau &= 0, & \lim_{\varepsilon \rightarrow 0} \frac{\Delta c_2^\delta}{\varepsilon} \int_0^\varepsilon \sin p^* \tau d\tau &= 0, \\ \lim_{\varepsilon \rightarrow 0} \frac{\Delta c_2^\delta}{\varepsilon} \int_0^\varepsilon \tau \cos p^* \tau d\tau &= 0, & \lim_{\varepsilon \rightarrow 0} \frac{\Delta c_2^\delta}{\varepsilon} \int_0^\varepsilon \cos p^* \tau d\tau &= \Delta c_2^\delta. \end{aligned} \right\} \quad (12.67)$$

Page 298.

In summation, for the coefficients aerodynamic derivative total

Characteristic, by taking into account (12.56), let us have: during the symmetrical strains of the wing

$$\begin{aligned}
 m_{x1}^{\delta} &= m_{x1}^{\delta} = m_{x2}^{\delta} = m_{x2}^{\delta} = 0, \\
 c_{y1}^{\delta}(p^*) &= p^* \int_0^{\infty} \left[\frac{c_{y1}(\tau)}{\delta^*} \right] \sin p^* \tau d\tau, \\
 c_{y1}^{\delta}(p^*) &= \int_0^{\infty} \left[\frac{c_{y1}(\tau)}{\delta^*} \right] \cos p^* \tau d\tau + \Delta c_{y1}^{\delta}, \\
 c_{y2}^{\delta}(p^*) &= p^* \int_0^{\infty} \left[\frac{c_{y2}(\tau)}{\delta^*} \right] \sin p^* \tau d\tau, \\
 c_{y2}^{\delta}(p^*) &= \int_0^{\infty} \left[\frac{c_{y2}(\tau)}{\delta^*} \right] \cos p^* \tau d\tau + \Delta c_{y2}^{\delta}, \\
 m_{z1}^{\delta}(p^*) &= p^* \int_0^{\infty} \left[\frac{m_{z1}(\tau)}{\delta^*} \right] \sin p^* \tau d\tau, \\
 m_{z1}^{\delta}(p^*) &= \int_0^{\infty} \left[\frac{m_{z1}(\tau)}{\delta^*} \right] \cos p^* \tau d\tau + \Delta m_{z1}^{\delta}, \\
 m_{z2}^{\delta}(p^*) &= p^* \int_0^{\infty} \left[\frac{m_{z2}(\tau)}{\delta^*} \right] \sin p^* \tau d\tau, \\
 m_{z2}^{\delta}(p^*) &= \int_0^{\infty} \left[\frac{m_{z2}(\tau)}{\delta^*} \right] \cos p^* \tau d\tau + \Delta m_{z2}^{\delta};
 \end{aligned} \tag{12.68}$$

during the antisymmetric strains

$$\left. \begin{aligned}
 c_{y1}^{\delta} &= c_{y1}^{\delta} = c_{y2}^{\delta} = c_{y2}^{\delta} = 0, \\
 m_{z1}^{\delta} &= m_{z1}^{\delta} = m_{z2}^{\delta} = m_{z2}^{\delta} = 0, \\
 m_{x1}^{\delta}(p^*) &= p^* \int_0^{\infty} \left[\frac{m_{x1}(\tau)}{\delta^*} \right] \sin p^* \tau d\tau, \\
 m_{x1}^{\delta}(p^*) &= \int_0^{\infty} \left[\frac{m_{x1}(\tau)}{\delta^*} \right] \cos p^* \tau d\tau + \Delta m_{x1}^{\delta}, \\
 m_{x2}^{\delta}(p^*) &= p^* \int_0^{\infty} \left[\frac{m_{x2}(\tau)}{\delta^*} \right] \sin p^* \tau d\tau, \\
 m_{x2}^{\delta}(p^*) &= \int_0^{\infty} \left[\frac{m_{x2}(\tau)}{\delta^*} \right] \cos p^* \tau d\tau + \Delta m_{x2}^{\delta}.
 \end{aligned} \right\} \quad (12.69)$$

Page 299.

Chapter XIII.

Some Point Solutions.

§1. Infinite-span wing. Coefficients of aerodynamic derivatives.

Solution of the problem of the harmonic oscillations of the plate of infinite elongation ($\lambda = \infty$) in the incompressible medium is given in works [1.7], [2.5]. Is represented, however, it is advisable to give the detailed derivation of fundamental principles, after examining this question from the positions of the method, used in chapter X. For integral equations are obtained the exact solutions in the locked form for two limiting values of Strouhal number ($p^* \rightarrow 0$ and $p^* \rightarrow \infty$). For the arbitrary values of p^* are given the results of the numerical calculations of the aerodynamic derivatives of the intensity of bound vorticity layer $\gamma^a, \dot{\gamma}^a, \gamma^{\omega z}, \dot{\gamma}^{\omega z}$.

Let us determine the disturbed speed, induced by carrying layer in the arbitrary point of infinite-span wing. Let us place plate in plane Oxz the rectangular coordinate system whose beginning is located in the middle of wing chord. The positive axis Ox coincides

with the direction of speed U_0 (Fig. 13.1). Wing let us replace with the connected carrying vorticity layer whose intensity changes in time according to the harmonic law

$$\gamma_+(x, t) = U_0 \gamma(x) \sin pt, \quad (13.1)$$

where $\gamma(x)$ is dimensionless intensity of layer, U_0 is the average speed of flow, p - angular frequency.



Fig. 13.1. Determination of the disturbed speed w_y .

Page 300.

The elementary strip of vorticity layer AA induces in point P (x_0) the speed

$$du_y = - \frac{\gamma_+(x, t) dx}{2\pi(x_0 - x)}. \quad (13.2)$$

From this strip of the vortex/eddy connected layer due to its transiency flows the taken away by flow vortex sheet, linear intensity of which at a distance x_1 (calculated off this strip) at torque/moment t is equal to

$$\gamma(x_1, t) = - \frac{1}{U_0} \frac{d}{dt_1} [\gamma_+(x_1, t_1) dx_1], \quad (13.3)$$

where $t_1 = t - x_1/U_0$.

The elementary strip of vortex sheet BB at point P (x_0) induces the speed

$$dv_y = - \frac{\gamma(x_1, t_1) dx_1}{2\pi(x_0 - x - x_1)}. \quad (13.4)$$

We present the total speed induced by the examined vortex/eddy system (layer + film), in the form

$$W_y = \frac{U_0}{2\pi} (w_y^{(1)} \sin pt + w_y^{(2)} \cos pt). \quad (13.5)$$

Dimensionless speeds $w_y^{(1)}, w_y^{(2)}$ taking into account relationship/ratios (13.1) - (13.4) will be equal to

$$w_y^{(1)} = u_y + v_{y1}, \quad w_y^{(2)} = v_{y2},$$

where

$$\left. \begin{aligned} u_y &= - \int_{-1/2}^{1/2} \frac{\gamma(\xi)}{\xi_0 - \xi} d\xi, \\ v_{y1} &= \int_{-1/2}^{1/2} \gamma(\xi) d\xi p^* \int_0^\infty \frac{\sin p^* \xi_1}{(\xi_0 - \xi) - \xi_1} d\xi_1, \\ v_{y2} &= \int_{-1/2}^{1/2} \gamma(\xi) d\xi p^* \int_0^\infty \frac{\cos p^* \xi_1}{(\xi_0 - \xi) - \xi_1} d\xi_1, \\ \xi &= \frac{x}{b}, \quad \xi_0 = \frac{x_0}{b}, \quad \xi_1 = \frac{x_1}{b}, \quad p^* = \frac{pb}{U_0}. \end{aligned} \right\} \quad (13.6)$$

Page 301.

If the intensity of the connected vorticity layer changes in time according to the law

$$\gamma_+(x, t) = \gamma(x) U_0 \cos pt, \quad (13.7)$$

that total velocity (in the adopted designations) will be expressed by the formula

$$W_y = \frac{U_0}{2\pi} (w_y^{(1)} \cos pt - w_y^{(2)} \sin pt). \quad (13.8)$$

Let us compose integral equations for the flow-field analysis of

infinite-span wing. The plane-parallel unsteady motion of this wing is characterized by the following by the dimensionless kinematic parameters:

$$\alpha = \alpha(t), \quad \omega_z = \frac{\Omega_z(t) b}{U_0}, \quad \dot{\alpha} = \frac{d\alpha}{dt} \frac{b}{U_0}, \quad \dot{\omega}_z = \frac{d\Omega_z}{dt} \frac{b^2}{U_0^2}. \quad (13.9)$$

In this case the condition of even flow will be written in the form

$$\frac{W_y}{U_0} = -\alpha - \omega_z \xi_0, \quad (13.10)$$

where $\xi_0 = x_0/b$ - the relative coordinate of the point at which is satisfied boundary condition.

With the harmonic dependence of the kinematic parameters on the time:

$$\alpha = \alpha^* \cos p^* \tau, \quad \omega_z = \omega_z^* \cos p^* \tau, \quad (13.11)$$

boundary condition (3.56) assumes the form

$$\frac{W_y}{U_0} = -\alpha^* \cos p^* \tau - \xi_0 \omega_z^* \cos p^* \tau. \quad (13.12)$$

Let us present the dimensionless intensity of the connected vorticity layer in the form

$$\gamma(x) = \gamma^a \alpha + \gamma^{\dot{\alpha}} \dot{\alpha} + \gamma^{\omega_z} \omega_z + \gamma^{\dot{\omega}_z} \dot{\omega}_z \quad (13.13)$$

and substitute here the values of kinematic parameters (13.9) and (13.11):

$$\gamma(x) = \alpha^* (\gamma^a \cos p^* \tau - p^* \gamma^a \sin p^* \tau) + \omega_z^* (\gamma^{\omega z} \cos p^* \tau - p^* \gamma^{\omega z} \sin p^* \tau). \quad (13.14)$$

The total velocity, induced in point $P(x_0)$ by components γ^a , $\gamma^{\omega z}$, $\gamma^{\omega z}$ the connected vorticity layer, taking into account (13.5) and (13.8) we will obtain in the form

$$\begin{aligned} \frac{W_y}{U_0} = & \frac{1}{2\pi} \alpha^* [\omega_y^{(1)} \gamma^a \cos p^* \tau - \omega_y^{(2)} \gamma^a \sin p^* \tau - p^* \omega_y^{(1)} \gamma^a \sin p^* \tau - \\ & - p^* \omega_y^{(2)} \gamma^a \cos p^* \tau] + \frac{1}{2\pi} \omega_z^* [\omega_y^{(1)} \gamma^{\omega z} \cos p^* \tau - \omega_y^{(2)} \gamma^{\omega z} \sin p^* \tau - \\ & - p^* \omega_y^{(1)} \gamma^{\omega z} \sin p^* \tau - p^* \omega_y^{(2)} \gamma^{\omega z} \cos p^* \tau]. \quad (13.15) \end{aligned}$$

Page 302.

The comparison of the obtained expression with boundary condition (13.12) gives two systems of integral equations.

In α -problem they take the form

$$\left. \begin{aligned} & \int_{-1/2}^{1/2} \gamma^a d\xi p^* \int_0^\infty \frac{\cos p^* \xi_1}{(\xi_0 - \xi) - \xi_1} d\xi_1 - p^* \int_{-1/2}^{1/2} \frac{\gamma^a}{\xi_0 - \xi} d\xi + \\ & + p^* \int_{-1/2}^{1/2} \gamma^a d\xi p^* \int_0^\infty \frac{\sin p^* \xi_1}{(\xi_0 - \xi) - \xi_1} d\xi_1 = 0, \\ & \int_{-1/2}^{1/2} \frac{\gamma^a}{\xi_0 - \xi} d\xi - \int_{-1/2}^{1/2} \gamma^a d\xi p^* \int_0^\infty \frac{\sin p^* \xi_1}{(\xi_0 - \xi) - \xi_1} d\xi_1 + \\ & + p^* \int_{-1/2}^{1/2} \gamma^a d\xi p^* \int_0^\infty \frac{\cos p^* \xi_1}{(\xi_0 - \xi) - \xi_1} d\xi_1 = 2\pi. \end{aligned} \right\} \quad (13.16)$$

In the ω_z -problem

$$\left. \begin{aligned} & \int_{-1/2}^{1/2} \gamma^{\omega_z} d\xi p^* \int_0^\infty \frac{\cos p^* \xi_1}{(\xi_0 - \xi) - \xi_1} d\xi_1 - p^* \int_{-1/2}^{1/2} \frac{\gamma^{\omega_z}}{\xi_0 - \xi} d\xi + \\ & + p^* \int_{-1/2}^{1/2} \gamma^{\omega_z} d\xi p^* \int_0^\infty \frac{\sin p^* \xi_1}{(\xi_0 - \xi) - \xi_1} d\xi_1 = 0, \\ & \int_{-1/2}^{1/2} \frac{\gamma^{\omega_z}}{\xi_0 - \xi} d\xi - \int_{-1/2}^{1/2} \gamma^{\omega_z} d\xi p^* \int_0^\infty \frac{\sin p^* \xi_1}{(\xi_0 - \xi) - \xi_1} d\xi_1 + \\ & + p^* \int_{-1/2}^{1/2} \gamma^{\omega_z} d\xi p^* \int_0^\infty \frac{\cos p^* \xi_1}{(\xi_0 - \xi) - \xi_1} d\xi_1 = 2\pi\xi_0. \end{aligned} \right\} \quad (13.17)$$

Is given below the exact solution of these systems for two limiting cases:

1. Very low values of Strouhal number ($p^* \rightarrow 0$).

With $p^* \rightarrow 0$ the first equations of systems (13.16) and (13.17) become identical, but the second substantially are simplified, taking the following form:

$$\int_{-1/2}^{1/2} \frac{\gamma^a}{\xi_0 - \xi} d\xi = 2\pi, \quad \int_{-1/2}^{1/2} \frac{\gamma^{\omega_z}}{\xi_0 - \xi} d\xi = 2\pi\xi_0. \quad (13.18)$$

Page 303.

The solution to these equations are the functions

$$\gamma^a = \gamma_0^a \sqrt{\frac{1/2 - \xi}{1/2 + \xi}}, \quad \gamma^{\omega z} = \gamma_0^{\omega z} \sqrt{\frac{1}{4} - \xi^2}, \quad (13.19)$$

that it is checked direct formulation:

$$\gamma_0^a \int_{-1/2}^{1/2} \sqrt{\frac{1/2 - \xi}{1/2 + \xi}} \frac{d\xi}{\xi_0 - \xi} = 2\pi.$$

Set/assuming $\xi = (1/2) \cos \theta$ and considering that

$$\int_0^\pi \frac{\cos n\theta}{\cos \varphi - \cos \theta} = \pi \frac{\sin n\varphi}{\sin \varphi} \quad (n = 0, 1, 2, \dots), \quad (13.20)$$

let us have $\gamma_0^a = 2$. Analogously we will obtain $\gamma_0^{\omega z} \pi \xi_0 = 2\pi \xi_0$ or $\gamma_0^{\omega z} = 2$.

Thus, with $\rho \rightarrow 0$ the solution to integral equations (13.16) and (13.17) are the functions

$$\gamma^a = 2 \sqrt{\frac{1/2 - \xi}{1/2 + \xi}}, \quad \gamma^{\omega z} = 2 \sqrt{\frac{1}{4} - \xi^2}. \quad (13.21)$$

It is easy to ascertain that the functions γ^a and $\gamma^{\omega z}$ will be equal minus of infinity.

For the section of the wing of unit length from (3.39) we have

$$c_y = 2 \int_{-1/2}^{1/2} \gamma(\xi) d\xi, \quad m_z = 2 \int_{-1/2}^{1/2} \gamma(\xi) \xi d\xi. \quad (13.22)$$

Taking into account (13.13) and representing the lift coefficients and pitching moment c_y and m_z in the form

$$\left. \begin{aligned} c_y &= c_y^a \alpha + c_y^{\dot{\alpha}} \dot{\alpha} + c_y^{\omega_z} \omega_z + c_y^{\dot{\omega}_z} \dot{\omega}_z, \\ m_z &= m_z^a \alpha + m_z^{\dot{\alpha}} \dot{\alpha} + m_z^{\omega_z} \omega_z + m_z^{\dot{\omega}_z} \dot{\omega}_z, \end{aligned} \right\} \quad (13.23)$$

we will obtain

$$\left. \begin{aligned} c_y^a &= 2\pi, & c_y^{\omega_z} &= \frac{\pi}{2}, \\ m_z^a &= \frac{\pi}{2}, & m_z^{\dot{\omega}_z} &= 0. \end{aligned} \right\} \quad (13.24)$$

Corresponding coefficients in by points in the case $p^* \rightarrow 0$ would minus of infinity.

2. Very large values of Strouhal number ($p^* \rightarrow \infty$).

Page 304.

We convert some integrals in systems (13.16) and (13.17). If function $\gamma^a(\xi)$ turns into zero on leading wing edge, then, by following Ye. M. Moiseyev, it is possible to demonstrate that

$$\begin{aligned}
& p^{*2} \int_{-1/2}^{1/2} \gamma^a d\xi \int_0^\infty \frac{\cos p^* \xi_1}{(\xi_0 - \xi) - \xi_1} d\xi_1 = -\pi \sin p^* \left(\xi_0 + \frac{1}{2} \right) \left[\frac{d\gamma^a}{d\xi} \right]_{\xi = -1/2} + \\
& + \int_{-1/2}^{1/2} \frac{d\gamma^a}{\xi_0 - \xi} d\xi - \pi \int_{-1/2}^{\xi_0} \sin(\xi_0 - \xi) \frac{d^2 \gamma^a}{d\xi^2} d\xi - \\
& - \int_{-1/2}^{\xi_0} \frac{d\gamma^a}{d\xi} d\xi \int_{(\xi_0 - \xi)}^\infty \frac{\cos p^* [(\xi_0 - \xi) - \tau]}{\tau^2} d\tau + \\
& + \int_{\xi_0}^{1/2} \frac{d\gamma^a}{d\xi} d\xi \int_{-(\xi_0 - \xi)}^\infty \frac{\cos p^* [(\xi_0 - \xi) + \tau]}{\tau^2} d\tau, \\
& \int_{-1/2}^{1/2} \gamma^a d\xi p^* \int_0^\infty \frac{\sin p^* \xi_1}{(\xi_0 - \xi) - \xi_1} d\xi_1 = -\pi \sin p^* \left(\xi_0 + \frac{1}{2} \right) \gamma^a \left(-\frac{1}{2} \right) + \\
& + \int_{-1/2}^{1/2} \frac{\gamma^a}{\xi_0 - \xi} d\xi - \pi \int_{-1/2}^{\xi_0} \sin p^* (\xi_0 - \xi) \frac{d\gamma^a}{d\xi} d\xi - \\
& - \int_{-1/2}^{\xi_0} \gamma^a d\xi \int_{(\xi_0 - \xi)}^\infty \frac{\cos p^* [(\xi_0 - \xi) - \tau]}{\tau^2} d\tau + \\
& + \int_{\xi_0}^{1/2} \gamma^a d\xi \int_{-(\xi_0 - \xi)}^\infty \frac{\cos p^* [(\xi_0 - \xi) + \tau]}{\tau^2} d\tau; \\
& \tau = \frac{U_0 t}{b}.
\end{aligned}$$

(13.25)

Let us divide first equation (13.16) into parameter p^* . Since (13.25) it is related also to the third integral of first equation (13.16), the system of integral equations is converted to the form

$$\left. \begin{aligned} & \int_{-1/2}^{1/2} \gamma^a d\xi \int_0^\infty \frac{\cos p^* \xi_1}{(\xi_0 - \xi) - \xi_1} d\xi_1 - \pi \sin p^* \left(\xi_0 + \frac{1}{2} \right) \gamma^a \left(-\frac{1}{2} \right) - \\ & - \pi \int_{-1/2}^{1/2} \sin p^* (\xi_0 - \xi) \frac{d\gamma^a}{d\xi} d\xi - \int_{-1/2}^{\xi_0} \gamma^a d\xi \int_{(\xi_0 - \xi)}^\infty \frac{\cos p^* [(\xi_0 - \xi) - \tau]}{\tau^2} d\tau + \\ & + \int_{\xi_0}^{1/2} \gamma^a d\xi \int_{-(\xi_0 - \xi)}^\infty \frac{\cos p^* [(\xi_0 - \xi) + \tau]}{\tau^2} d\tau = 0, \\ & \pi \sin p^* \left(\xi_0 + \frac{1}{2} \right) \gamma^a \left(-\frac{1}{2} \right) + \pi \int_{-1/2}^{\xi_0} \sin p^* (\xi_0 - \xi) \frac{d\gamma^a}{d\xi} d\xi - \\ & - \pi \sin p^* \left(\xi_0 + \frac{1}{2} \right) \left[\frac{d\gamma^a}{d\xi} \right]_{\xi = -1/2} + \int_{-1/2}^{\xi_0} \gamma^a d\xi \int_{-(\xi_0 - \xi)}^\infty \frac{\cos p^* [(\xi_0 - \xi) - \tau]}{\tau^2} d\tau - \\ & - \int_{\xi_0}^{+1/2} \gamma^a d\xi \int_{-(\xi_0 - \xi)}^\infty \frac{\cos p^* [(\xi_0 - \xi) + \tau]}{\tau^2} d\tau + \int_{-1/2}^{1/2} \frac{d\gamma^a}{d\xi} d\xi - \\ & - \pi \int_{-1/2}^{\xi_0} \sin p^* (\xi_0 - \xi) \frac{d^2 \gamma^a}{d\xi^2} d\xi - \int_{-1/2}^{1/2} \frac{d\gamma^a}{d\xi} d\xi \int_{(\xi_0 - \xi)}^\infty \frac{\cos p^* [(\xi_0 - \xi) - \tau]}{\tau^2} d\tau + \\ & + \int_{\xi_0}^{1/2} \frac{d\gamma^a}{d\xi} d\xi \int_{-(\xi_0 - \xi)}^\infty \frac{\cos p^* [(\xi_0 - \xi) + \tau]}{\tau^2} d\tau = 2\pi. \end{aligned} \right\} \quad (13.26)$$

Page 305.

If one considers that on the basis of riemann's lemma [1.93]

$$\left. \begin{aligned} & \lim_{p^* \rightarrow \infty} \int_m^\infty g(\tau) \sin p^* \tau d\tau = 0, \\ & \lim_{p^* \rightarrow \infty} \int_m^\infty g(\tau) \cos p^* \tau d\tau = 0, \end{aligned} \right\} \quad (13.27)$$

where $g(\tau)$ - the continuous integrated function, the first equation of system (13.26) during passage to the limit $p^* \rightarrow \infty$ will become identity, and the second it will take the form

$$\pi \sin p^* \left(\xi_0 + \frac{1}{2} \right) \left[\gamma^a - \frac{d\gamma^a}{d\xi} \right]_{\xi=-1/2} + \int_{-1/2}^{1/2} \frac{d\gamma^a}{d\xi} \frac{d\xi}{\xi_0 - \xi} = 2\pi. \quad (13.28)$$

Since the obtained expression is identity, are obvious the conditions, superimposed for the existence of exact solution with $p^* \rightarrow \infty$:

$$\int_{-1/2}^{1/2} \frac{d\gamma^a}{d\xi} \frac{d\xi}{\xi_0 - \xi} = 2\pi, \quad \left[\gamma^a - \frac{d\gamma^a}{d\xi} \right]_{\xi=-1/2} = 0. \quad (13.29)$$

Page 306.

The solution to first equation (13.29) is the function

$$\gamma^a = \gamma_0^a \sqrt{\frac{1}{4} - \xi^2}, \quad (13.30)$$

that it is proven by substitution. Is really/actually

$$-\gamma_0^a \int_{-1/2}^{1/2} \frac{\xi}{\sqrt{\frac{1}{4} - \xi^2}} \frac{d\xi}{\xi_0 - \xi} = 2\pi,$$

set/assuming $\xi = \frac{1}{2} \cos \theta$ and taking into account (13.20), we will obtain $\gamma_0^a = 2$.

Second equation (13.29) satisfies the function

$$\gamma^a = \gamma_0^a \sqrt{\frac{1/2 - \xi}{1/2 + \xi}}. \quad (13.31)$$

Representing this expression in the form

$$\gamma^a = \gamma_0^a \frac{1/2 - \xi}{\sqrt{1/4 - \xi^2}}$$

and considering the equality of the denominators of functions γ^a $d\gamma^a/d\xi$,
and Λ from second equation (13.29) we will obtain

$$\left[\gamma_0^a \left(\frac{1}{2} - \xi \right) + 2\xi \right]_{\xi = -1/2} = 0,$$

whence $\gamma_0^a = 1$.

Thus, the solution of the system of integral equalizations (13.16) with $p^* \rightarrow \infty$ are the functions

$$\gamma^a = \sqrt{\frac{1/2 - \xi}{1/2 + \xi}}, \quad \gamma^{\dot{a}} = 2 \sqrt{\frac{1}{4} - \xi^2}. \quad (13.32)$$

Analogously is obtained the solution of system (13.17):

$$\gamma^{\omega z} = 2 \sqrt{\frac{1}{4} - \xi^2} - \frac{1}{4} \sqrt{\frac{1/2 - \xi}{1/2 + \xi}}, \quad \gamma^{\dot{\omega} z} = \xi \sqrt{\frac{1}{4} - \xi^2}. \quad (13.33)$$

The coefficients of aerodynamic derivatives, obtained by the appropriate integration of loads (13.22), will be

$$\left. \begin{aligned} c_y^a &= \pi, & c_y^{\dot{a}} &= \frac{\pi}{2}, & m_z^a &= \frac{\pi}{4}, & m_z^{\dot{a}} &= 0, \\ c_y^{\omega z} &= \frac{\pi}{4}, & c_y^{\dot{\omega} z} &= 0, & m_z^{\omega z} &= -\frac{\pi}{16}, & m_z^{\dot{\omega} z} &= -\frac{\pi}{64}. \end{aligned} \right\} \quad (13.34)$$

From (13.24) and (13.34) it is evident that for the plate of the

final elongation are fulfilled the consequences of reciprocity theorem, namely:

$$c_{y+}^{\omega_z} = m_{z-}^{\alpha}, \quad c_{y+}^{\dot{\omega}_z} = m_{z-}^{\dot{\alpha}}.$$

The given results it is possible, in particular, to give this interpretation. In the case of the motion, characterized by the parameters $\alpha = \text{const}$ and $\omega_z = \text{const}$ (i.e. with $p^* = 0$) for centering $\bar{x}_T = 0.50$, the effect of flow to infinite-span wing is reduced to two forces.

Page 307.

One of them, Y_1 , proportional α , is applied at a distance $x_{\alpha} = 0.25b$ from leading wing edge, and the second, Y_2 , proportional to ω_z , is applied at a distance $x_{\omega_z} = 0.50b$ from leading edge. One should note that the amount of force Y_2 and coordinate \bar{x}_{ω_z} depend on centering \bar{x}_T . At the same time force Y_1 and coordinate \bar{x}_{α} , characterizing the position of aerodynamic center of profile relative to leading edge/nose during the forward/progressive steady motion, from \bar{x}_T do not depend.

For an infinite-span wing are given the coefficients aerodynamic derivatives in all range of a change in Strouhal number p^* . Some materials of these calculations for $\bar{x}_T = 0.50$ are given in Fig.

13.2-13.4 [1.7]. Table 13.1 gives the numerical values of the coefficients of aerodynamic force derivative depending on Strouhal number for a plate with $\lambda = \infty$ and by centering $\bar{x}_T = 0.25$. This centering is selected because for it the coefficients of aerodynamic moment derivative do not depend on the number of Strouhal. Are given below precise values of coefficients of aerodynamic moment derivative for this same centering ($\bar{x}_T = 0.25$) with any Strouhal numbers:

$$m_z^a = 0, \quad m_z^{\dot{a}} = -\frac{\pi}{8}, \quad m_z^{\omega z} = -\frac{\pi}{8}, \quad m_z^{\dot{\omega} z} = -\frac{3\pi}{64}. \quad (13.35)$$

Passage from one centering to another is conducted on the basis of the formulas of recalculation (2.73).

Table 13.1.

ρ^*	c_y^a	$c_y^{\dot{a}}$	$c_y^{\omega z}$	$c_y^{\dot{\omega} z}$	ρ^*	c_y^a	$c_y^{\dot{a}}$	$c_y^{\omega z}$	$c_y^{\dot{\omega} z}$
0	2π	$-\infty$	π	$-\infty$	0,72	4,015	+0,0794	2,008	-0,3530
0,04	6,055	-10,232	3,028	-5,514	0,76	3,969	0,1828	1,985	-0,3013
0,08	5,823	-7,540	2,911	-4,153	0,80	3,927	0,2749	1,964	-0,2553
0,12	5,593	-5,896	2,797	-3,341	0,84	3,887	0,3583	1,944	-0,2136
0,16	5,406	-4,728	2,703	-2,757	0,88	3,852	0,4341	1,926	-0,1756
0,20	5,228	-3,842	2,614	-2,314	0,92	3,818	0,5033	1,909	-0,1410
0,24	5,066	-3,144	2,533	-1,965	0,96	3,786	0,5661	1,893	-0,1096
0,28	4,922	-2,578	2,461	-1,682	1,00	3,757	0,6239	1,878	-0,0807
0,32	4,793	-2,111	2,396	-1,448	1,20	3,637	0,8493	1,818	0,0319
0,36	4,676	-1,723	2,338	-1,254	1,40	3,549	1,004	1,774	0,1091
0,40	4,572	-1,392	2,286	-1,089	1,60	3,482	1,113	1,741	0,1639
0,44	4,477	-1,110	2,238	-0,9475	1,80	3,430	1,195	1,715	0,2046
0,48	4,391	-0,8666	2,196	-0,8260	2,0	3,389	1,256	1,695	0,2352
0,52	4,313	-0,6549	2,157	-0,7202	3,0	3,274	1,417	1,637	0,3156
0,56	4,242	-0,4701	2,121	-0,6278	4,0	3,223	1,480	1,612	0,3474
0,60	4,178	-0,3068	2,089	-0,5461	5,0	3,196	1,511	1,598	0,3650
0,64	4,119	-0,1630	2,060	-0,4742	10	3,157	1,555	1,578	0,3850
0,68	4,065	-0,0351	2,032	-0,4103	∞	π	$\pi/2$	$\pi/2$	$\pi/8$

Page 308.

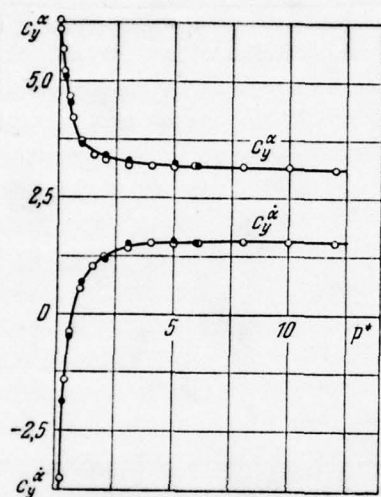


Fig. 13.2.

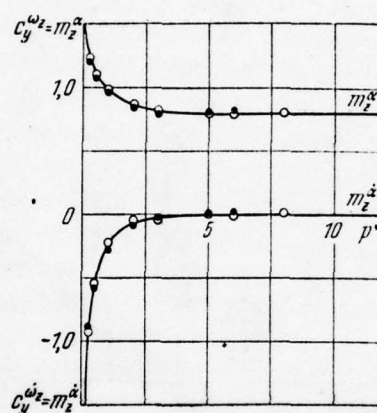


Fig. 13.3.

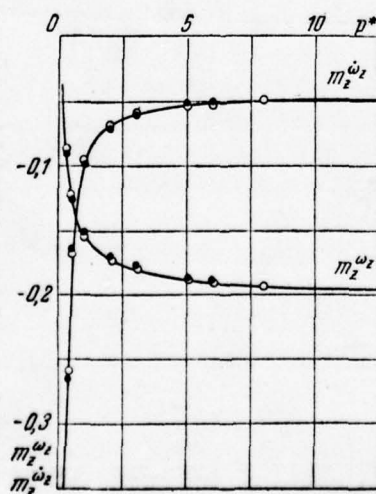


Fig. 13.4.

Page 308. Fig. 13.2. Comparison of precise (curves) and numerical (point) calculations of wing $\lambda = \infty$. White points are the calculation with the aid of Duhamel integral, black points are numerical calculations.

Fig. 13.3. Comparison of precise (curves) and numerical (point) calculations of wing $\lambda = \infty$. White points are the calculation with the aid of Duhamel integral, black points are numerical calculations.

Fig. 13.4. Comparison of precise (curves) and numerical (point) calculations of wing $\lambda = \infty$. White points are the calculation with the aid of Duhamel integral, black points are numerical calculations.

Page 309.

§2. Infinite-span wing. Coefficients of apparent additional masses.

During noncirculating flow around of the wing of the ideal incompressible fluid the aerodynamic influence of flow to this wing can be determined with the aid of the so-called coefficients of apparent additional masses (see §9 of chapter II). The coefficients

indicated are necessary, in particular, for the calculation of aerodynamic wing characteristics with the aid of Duhamel integral. The numerical solution of the problem of the determination of the coefficients of the apparent additional masses of the rigid and wings of arbitrary planform being deformed can be realized by methods, presented in chapter XII. For a fine/thin infinite-span wing (plate) it is possible to indicate precise values of coefficients of the apparent additional masses, designed relative to the middle of wing chord ($\bar{x}_T = 0,50$):

$$k_{22} = \frac{\pi}{4}, \quad k_{26} = 0, \quad k_{66} = \frac{\pi}{128}. \quad (13.36)$$

The coefficients of apparent additional masses for other centering are recounted by formulas (2.93).

§3. Infinite-span wings. Effect of harmonic gust.

Let the vertical gust $W_{y\Delta}$ in fixed coordinate system be assigned in the form

$$\dot{W}_{y\Delta}(x^*) = W_{y\Delta}^* e^{-i \frac{px^*}{U_0}}. \quad (13.37)$$

Then in the movable system of axes, connected with wing, we have

$$\frac{W_{y\Delta}(x, t)}{U_0} = w_{y\Delta}^* e^{ip \left(t + \frac{x}{U_0} \right)}, \quad w_{y\Delta}^* = \frac{W_{y\Delta}^*}{U_0}. \quad (13.38)$$

Seures [2.9] obtained the following exact expressions for lift of Y and pitching moment M_z per unit of the length of the wingspan with elongation $\lambda = -$, the being subject to the influence harmonic gust:

$$Y = \pi \rho_\infty \frac{U_0^2}{2} b w_{y\Delta}^* e^{ip^*t} \varphi(p^*), \quad M_z = b \left(\bar{x}_T - \frac{1}{4} \right) Y. \quad (13.39)$$

Here $\varphi(p^*)$ is the function of Seures, which corresponds to the case, when the beginning of the connected with wing system is located on the middle of wing ($\bar{x}_T = 0,50$).

Page 310.

Introducing the kinematic parameters of the gust

$$\Delta = \Delta^* e^{ip^*t}, \quad \dot{\Delta} = \frac{d\Delta}{dt} \frac{b}{U_0} = ip^* \Delta, \quad (\Delta^* = w_{y\Delta}^*) \quad (13.40)$$

and the coefficients of aerodynamic derivatives, caused by the gust:

$$c_y = c_y^{\Delta} \Delta + c_y^{\dot{\Delta}} \dot{\Delta}, \quad m_z = m_z^{\Delta} \Delta + m_z^{\dot{\Delta}} \dot{\Delta}, \quad (13.41)$$

we will obtain expressions for derivatives through the real and imaginary part of the function of Seures:

$$\left. \begin{aligned} c_y^{\Delta} &= 2\pi \operatorname{Re} \varphi(p^*), & c_y^{\dot{\Delta}} &= \frac{2\pi}{p^*} \operatorname{Im} \varphi(p^*), \\ m_z^{\Delta} &= \left(x_0 - \frac{1}{4}\right) c_y^{\Delta}, & m_z^{\dot{\Delta}} &= \left(x_0 - \frac{1}{4}\right) c_y^{\dot{\Delta}}. \end{aligned} \right\} \quad (13.42)$$

These relationship/ratios are obtained with centering $\bar{x}_T = 0.50$; recalculation for other centering is conducted on the basis of formulas (2.82). Hence it follows that the position of foci $\bar{x}_A = 0.25$, $\bar{x}_{\dot{A}} = 0.25$ do not depend on Strouhal number.

Figure 13.5 gives the obtained by formulas (13.42) coefficients of aerodynamic derivatives of lift c_y^{Δ} and $c_y^{\dot{\Delta}}$ with harmonic gust depending on Strouhal number for the position of the beginning of the axes in the leading edge/nose of wing ($\bar{x}_T = 0$). The numerical values of these ^{derivatives with different p^* for} ~~a~~ movable system of axes with beginning in the wing leading edge are given in table 13.2. Countdown is conducted so that with $t = 0$ beginning of movable and fixed coordinate systems they coincide.

The coefficients of aerodynamic moment derivatives m_z^{Δ} and $m_z^{\dot{\Delta}}$ are determined from relationship/ratios (13.42). The corresponding net force is applied at point, which is located at a distance of $1/4$ chords from leading wing edge.

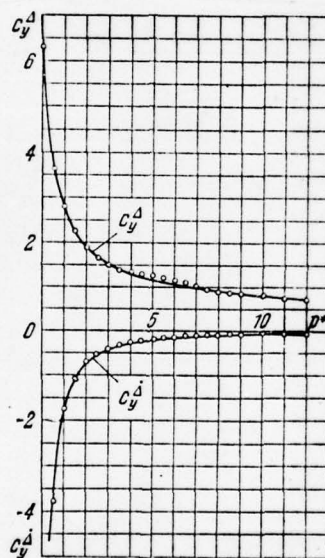


Fig. 13.5. Coefficients of aerodynamic derivatives under the influence of harmonic gust on wing $\lambda = \infty$. Curves are exact solution, points are the calculation with the aid of Duhamel integral.

Page 311.

With $p^* \rightarrow 0$, as it was shown earlier [see formulas (5.56)], the coefficients of aerodynamic derivatives with harmonic gust are connected with the coefficients of the aerodynamic derivatives of the harmonically oscillating wing by the relationship/ratios

$$c_y^{\Delta} = c_y^{\alpha}, \quad c_y^{\dot{\Delta}} = c_y^{\dot{\alpha}} - c_y^{\omega_z},$$

therefore with $p^* \rightarrow 0$ also we have for centering $\bar{x}_T = 0$

$$c_y^{\Delta} = 2\pi, \quad c_y^{\dot{\Delta}} = -\infty.$$

§4. Infinite-span wing. Instantaneous change in the angle of attack.

In [1.7] are brought the results of precise calculations of the lift coefficients and pitching moment, carried out by Wagner for an infinite-span wing, the angle of attack of which changes instantly. In this case the law of a change in the angle of attack in dimensionless time will take the form

$$\frac{\alpha}{\alpha^*} = \begin{cases} 0 & \text{при } \tau < 0, \\ 1 & \text{при } \tau \geq 0 \end{cases}$$

Key: (1). with.

(α^* - the amplitude value of angle of attack). Relationship/ratios for aerodynamic coefficients (transient functions) in this case are represented in the form

$$\left[\frac{c_y}{\alpha^*} \right] = 2\pi\Phi(\tau), \quad \left[\frac{m_z}{\alpha^*} \right] = \frac{\pi}{2}\Phi(\tau), \quad (13.43)$$

where $\Phi(\tau)$ - the function of Wagner.

Table 13.2.

p^*	c_y^{Δ}	c_y^{Δ}	p^*	c_y^{Δ}	c_y^{Δ}
0	2π	$-\infty$	2,8	1,6020	-0,4819
0,04	6,0401	-14,8039	3,2	1,4835	-0,4085
0,08	5,7734	-11,8492	3,6	1,3932	-0,3375
0,12	5,5089	-10,3129	4,0	1,3169	-0,2923
0,16	5,2889	-8,7015	5,0	1,1705	-0,2126
0,20	5,0299	-7,7005	6,0	1,0595	-0,1627
0,40	4,1233	-4,6544	7,0	1,0198	-0,1303
0,60	3,5115	-3,1914	8,0	0,9118	-0,1283
0,80	3,0793	-2,3517	9,0	0,8519	-0,1213
1,0	2,7624	-1,8240	10	0,8135	-0,0771
1,2	2,5130	-1,4639	12	0,7350	-0,0588
1,4	2,3204	-1,2088	14	0,6757	-0,0571
1,6	2,1619	-1,0197	16	0,6310	-0,0383
1,8	2,0281	-0,8749	18	0,6017	-0,0344
2,0	1,9188	-0,7617	20	0,5772	-0,0217
2,4	1,7404	-0,5943	∞	0	0

Table 13.3.

Page 312.

Figures 13.6, 13.7 give dependences on dimensionless time τ the lift coefficients and the pitching moment of the plate of infinite elongation during instantaneous stepped variation in the angle of attack. Lift coefficient in the first torque/moment reaches infinite value, instantly it falls to value $[c_y/\alpha^*] = \pi$ and then gradually with $\tau \rightarrow \infty$ it approaches its stationary value equal to $[c_y/\alpha^*] = 2\pi$. Position of initial small time interval in this case is changed from $\bar{x}_F = 0.5$ to $\bar{x}_F = 0.25$ (counting from leading wing edge). Numerical values $[c_y/\alpha^*]$ the dependence that τ are given in table 13.3.

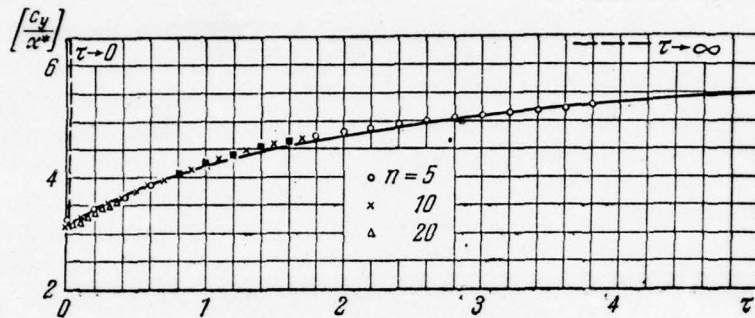


Fig. 13.6. Wing $\lambda = \infty$. Instantaneous change in the angle of attack in stepped law. Curve is exact solution, points are a numerical calculation.

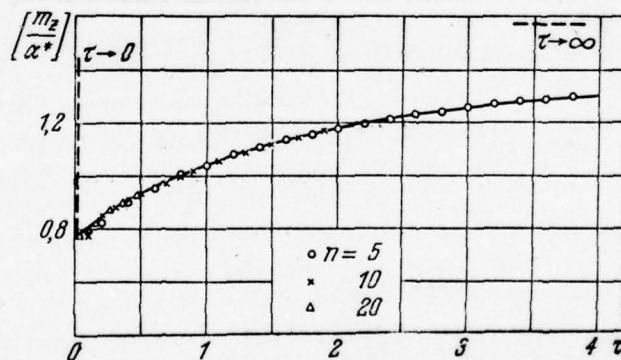


Fig. 13.7. Wing $\lambda = \infty$. Instantaneous change in the angle of attack in stepped law ($\bar{x}_T=0.5$). Curve is exact solution, points are a numerical calculation.

Page 313.

580

Table 13.3.

τ	$\left[\frac{c_y}{a^*} \right]$	τ	$\left[\frac{c_y}{a^*} \right]$	τ	$\left[\frac{c_y}{a^*} \right]$
0	$\left\{ \begin{array}{l} \infty \\ \pi \end{array} \right.$	2,75	5,0328	5,5	5,5625
0,25	3,4909	3,0	5,1051	6,0	5,6178
0,50	3,7737	3,25	5,1711	7,5	5,7479
0,75	4,0074	3,5	5,2308	10	5,8848
1,0	4,2053	3,75	5,2854	12,5	5,9697
1,25	4,3744	4,0	5,3351	15	6,0262
1,50	4,5208	4,25	5,3809	20	6,0960
2,0	4,7620	4,5	5,4230	25	6,1368
2,25	4,8632	4,75	5,4620	50	6,2141
2,5	4,9524	5,0	5,4978	∞	2π

§5. Infinite-span wing. Gradual entrance into gust.

In [1.7] are carried out the results of precise calculations of the aerodynamic coefficients of the plate of infinite elongation, by the entering gradual the step gust. Formulas for the lift coefficients and pitching moment take the form

$$\left[\frac{c_y}{w_{y\Delta}} \right] = 2\pi F(\tau), \quad \left[\frac{m_z}{w_{y\Delta}} \right] = \frac{\pi}{2} F(\tau), \quad (13.44)$$

where $F(\tau)$ - the function of Cussner.

Table 13.8.

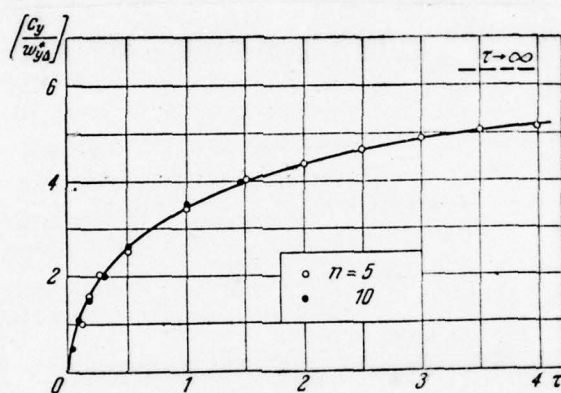


Fig. 13.8. Wing $\lambda = \infty$. Gradual entrance into step gust. Curve is exact solution, points are a numerical calculation.

Page 314.

Figure 13.8 gives the dependence of the transient function of lift coefficient of dimensionless time, whereupon $[c_y / w_{y\Delta}^*]_{\tau \rightarrow 0} = 0$ and $[c_y / w_{y\Delta}^*]_{\tau \rightarrow \infty} \rightarrow 2\pi$. The dependence of the transient function of the coefficient of pitching moment $[m_z / w_{y\Delta}^*]$ of τ is given in Fig. 13.9. The position of focus in this case will be constant ($\bar{x}_{w_{y\Delta}} = 0,25$). The

numerical values of the transient function of lift coefficient $[c_y/w_{y\Delta}]$ for entire range $0 \leq \tau \leq \infty$ are given in table 13.4.

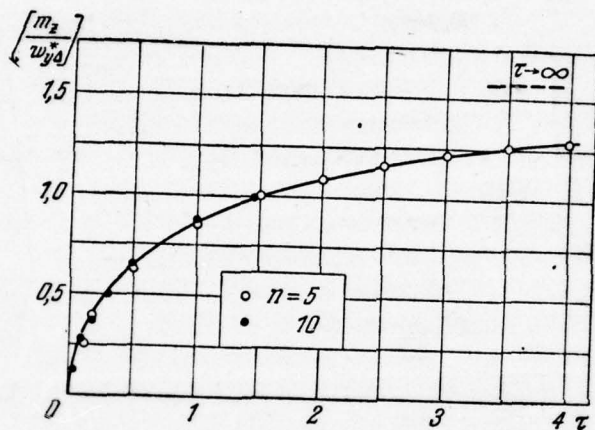


Fig. 13.9. Wing $\lambda = \infty$. Gradual entrance into step gust ($\bar{x}_T = 0.5$). Curve is exact solution, points are a numerical calculation.

Table 13.4.

τ	$\left[\frac{c_y}{w_{y\Delta}} \right]$	τ	$\left[\frac{c_y}{w_{y\Delta}} \right]$	τ	$\left[\frac{c_y}{w_{y\Delta}} \right]$	τ	$\left[\frac{c_y}{w_{y\Delta}} \right]$
0	0	0,55	2,7263	1,50	3,9905	4,25	5,2282
0,050	0,8872	0,60	2,8274	1,75	4,1921	4,50	5,2829
0,10	1,2472	0,65	2,9223	2,0	4,3637	4,75	5,3332
0,15	1,5117	0,70	3,0122	2,25	4,5126	5,00	5,3841
0,20	1,7316	0,75	3,0964	2,50	4,6420	6,00	5,5298
0,25	1,9384	0,80	3,1768	2,75	4,7564	8,00	5,7284
0,30	2,0885	0,85	3,2528	3,00	4,8575	10,50	5,8742
0,35	2,2393	0,90	3,3257	3,25	4,9480	13,00	5,9627
0,40	2,3757	0,95	3,3948	3,50	5,0291	20,50	6,0934
0,45	2,5020	1,00	3,4608	3,75	5,1019	50,50	6,2141
0,50	2,6182	1,25	3,7517	4,00	5,1679	∞	2π

§ 6. Infinite-span wing with control. Coefficients of aerodynamic derivatives.

For an infinite-span wing ($\lambda = \infty$) with the oscillating according to harmonic law control there is exact solution of δ -problem, obtained by Theodorsen [2.5] and Cussner [2.12].

If we the angle of deflection of control present in the form

$$\delta = \delta^* \cos pt, \quad (13.45)$$

that as a result of data processing of Theodorsen and Cussner it is possible to write the following expressions for the coefficients of aerodynamic derivatives $c_{y1}^{\delta p}, c_{y1}^{\delta}, c_{y2}^{\delta p}, c_{y2}^{\delta}, m_{z1}^{\delta p}, m_{z1}^{\delta}, m_{z2}^{\delta p}, m_{z2}^{\delta}$, determining the effectiveness of wing high-lift device:

$$\left. \begin{aligned} c_{y1}^{\delta p} &= 2\bar{\Phi}_1 \bar{F}, & c_{y1}^{\delta} &= \frac{\bar{\Phi}_3}{2} + \frac{2\bar{\Phi}_1}{p^*} \bar{G}, \\ c_{y2}^{\delta p} &= \frac{\bar{\Phi}_2}{2} \bar{F}, & c_{y2}^{\delta} &= \frac{\bar{\Phi}_4}{8} + \frac{\bar{\Phi}_2}{2p^*} \bar{G}, \\ m_{z1}^{\delta p} &= -\frac{\bar{\Phi}_5}{2}, & m_{z1}^{\delta} &= -\frac{\bar{\Phi}_6}{16}, \\ m_{z2}^{\delta p} &= -\frac{\bar{\Phi}_6}{16}, & m_{z2}^{\delta} &= -\frac{\bar{\Phi}_7}{32}. \end{aligned} \right\} \quad (13.46)$$

The total coefficients of aerodynamic derivatives $c_y^{\delta p}, c_y^{\delta}, m_z^{\delta p}, m_z^{\delta}$

according to (7.27) are determined the following relationships:

$$\left. \begin{aligned} c_y^{\delta p} &= c_{y1}^{\delta p} - p^2 c_{y2}^{\delta p}, & c_y^{\delta p} &= c_{y1}^{\delta p} + c_{y2}^{\delta p}, \\ m_z^{\delta p} &= m_{z1}^{\delta p} - p^2 m_{z2}^{\delta p}, & m_z^{\delta p} &= m_{z1}^{\delta p} + m_{z2}^{\delta p}. \end{aligned} \right\} \quad (13.47)$$

Recall that the coefficients with index 1 in expressions (13.46) are related to δ -problem 1, and with index 2 - to δ -problem 2 (see §2 of chapter V). The moment derivative coefficients m_i are undertaken for centering $\bar{x}_T = 0.25$. Functions $\bar{\Phi}_i(\varphi)$ are tabulated by Cussner, φ - certain parameter, connected with the relative chord of control $\bar{b}_p = b_p/b$ by relationship/ratio $\cos \varphi = 1 - 2\bar{b}_p$. Values \bar{F} and \bar{G} depending only that Strouhal number form the function of Theodorsen

$$\bar{C}(p^*) = \bar{F}(p^*) + i\bar{G}(p^*) = \frac{H_1^{(2)}(p^*)}{H_1^{(2)}(p^*) + iH_0^{(2)}(p^*)}. \quad (13.48)$$

Page 316.

In the last/latter expression of value $H_n^{(k)}$ they are the functions of Hankel and are also tabulated.

By formulas (13.46) were calculated the values of the corresponding derivatives depending on Strouhal number ($p^* = 0 - \infty$) and of relative chord of control ($\bar{b}_p = 0,1 + 1,0$). The results of these calculations with $\bar{x}_T = 0.25$ are represented in Fig. 13.10-13.14.

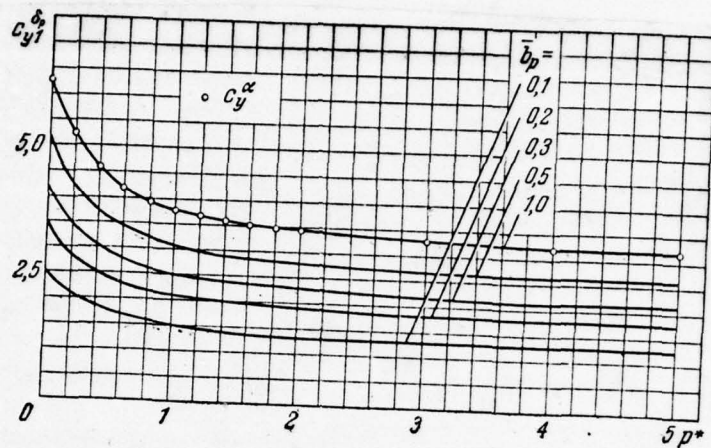


Fig. 13.10. Wing $\lambda = -$ with control.

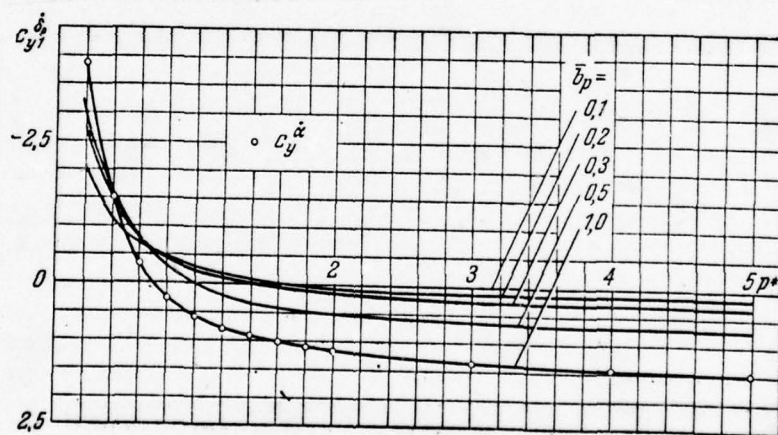


Fig. 13.11. Wing $\lambda = -$ with control.

Page 317.

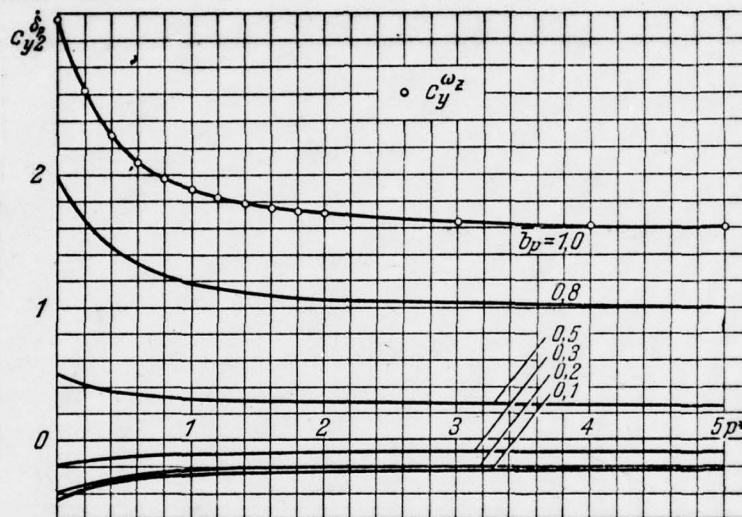


Fig. 13.12.

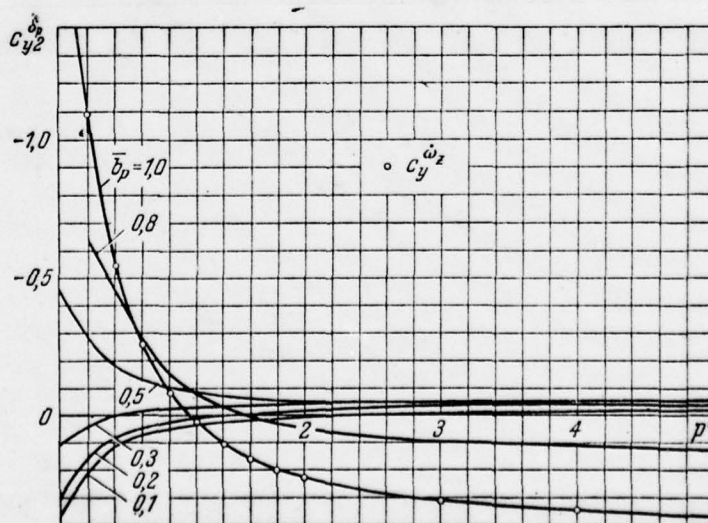


Fig. 13.13.

Fig. 13.12. Wing $\lambda = \infty$ with control ($\bar{x}_T = 0.25$).

Fig. 13.13. Wing $\lambda = \infty$ with control ($\bar{x}_T = 0.25$).

Page 318.

In Fig. 13.14 for $\bar{b}_p = 1$ are plotted the points, obtained from exact solution for an airfoil/profile (see these tables 13.1). As one would expect, equalities (7.97) and (7.98) here are satisfied.

§7. The rectangular wing of very small elongation. Coefficients of aerodynamic derivatives.

The problem of the harmonic oscillations of the rectangular wing of very small elongation ($\lambda \rightarrow 0$) with very small Strouhal number ($\rho^* \rightarrow 0$) can be solved accurately. Here, along with continuous vorticity layer, one should introduce the discrete connected vortex lines.

Let us examine the cut of direct/straight vortex line ($-i/2, i/2$), intensity/strength of which $\dot{\Gamma}_+(z, t_0)$. The origin of coordinates is

arranged to the middle of the spread/scope of eddy/vortex, then the induced with this vorticity by ~~Bio~~ - Savart's formula is equal in the axes of Fig. 9.2 [1.29]

$$U_y(x_0, z_0, t_0) = -\frac{x_0}{4\pi} \int_{-l/2}^{l/2} \frac{\Gamma_+(z, t_0) dz}{[x_0^2 + (z_0 - z)^2]^{3/2}}. \quad (13.49)$$

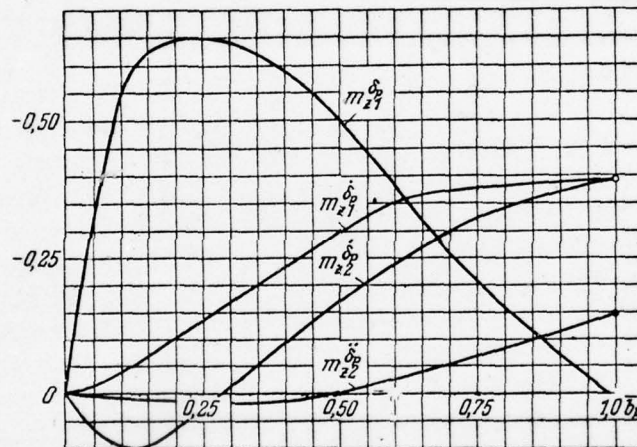


Fig. 13.14. Wing $\lambda = \infty$ with control ($\bar{x}_T = 0.25$). Points are exact solution with $\bar{b}_p = 1$.

From the basic vortex line due to a change in its

intensity/strength in time will move away the film of free vortices with the axes, parallel to axes Oz and Ox. Velocity from transverse free vortices will be

$$V'_y = -\frac{1}{4\pi} \int_{-l/2}^{l/2} \int_0^\infty \frac{\gamma_z(x, z, t_0)(x_0 - x)}{[(x_0 - x)^2 + (z_0 - z)^2]^{3/2}} dx dz, \quad (13.50)$$

and

from longitudinal free vortices

$$V''_y = \frac{1}{4\pi} \int_{-l/2}^{l/2} \int_0^\infty \frac{\gamma_x(x, z, t_0)(z_0 - z)}{[(x_0 - x)^2 + (z_0 - z)^2]^{3/2}} dx dz. \quad (13.51)$$

For a total velocity we have the expression

$$W_y = U_y + V'_y + V''_y.$$

In the case of harmonic time dependence

$$\Gamma_+(z, t_0) = \Gamma_+(z) \sin pt_0 \quad (13.52)$$

for transverse free eddy/vortex can be written

$$\begin{aligned} \gamma_{z+}(x, z, t_0) &= -\frac{1}{U_0} \Gamma_+(z) p \cos p \left(t_0 - \frac{x}{U_0} \right) = \\ &= -\frac{p \Gamma_+(z)}{U_0} \left(\cos pt_0 \cos \frac{px}{U_0} + \sin pt_0 \sin \frac{px}{U_0} \right), \end{aligned} \quad (13.53)$$

since

$$\gamma_{z+}(x, z, t_0) = -\frac{1}{U_0} \left[\frac{d\Gamma_+(z, t_1)}{dt_1} \right]_{t_1=t_0-\frac{x}{U_0}}.$$

For transverse free vortex we have

$$\begin{aligned} \gamma_{x+}(x, z, t_0) &= -\left[\frac{d\Gamma_+(z)}{dz} \sin p \left(t_0 - \frac{x}{U_0} \right) \right] = \\ &= -\frac{d\Gamma_+(z)}{dz} \left(\sin pt_0 \cos \frac{px}{U_0} - \cos pt_0 \sin \frac{px}{U_0} \right), \end{aligned} \quad (13.54)$$

since

$$\gamma_{x+}(x, z, t_0) = - \left[\frac{d\Gamma_+(z, t_1)}{dz} \right]_{t_1=t_0-\frac{x}{U_0}}.$$

Page 320.

Substituting expressions (13.52) - (13.54) respectively in (13.49) - (13.51) and bearing in mind that the total velocity

$$W_{y*} = W_{y*}^{(1)} \sin pt_0 + W_{y*}^{(2)} \cos pt_0,$$

we will obtain

$$\begin{aligned}
 W_{y^*}^{(1)} = & -\frac{x_0}{4\pi} \int_{-l/2}^{l/2} \frac{\Gamma_+(z) dz}{[x_0^2 + (z_0 - z)^2]^{3/2}} + \\
 & + \frac{p}{4\pi U_0} \int_{-l/2}^{l/2} \int_0^\infty \frac{\Gamma_+(z) (x_0 - x) \sin p \frac{x}{U_0} dx dz}{[(x_0 - x)^2 + (z_0 - z)^2]^{3/2}} - \\
 & - \frac{1}{4\pi} \int_{-l/2}^{l/2} \int_0^\infty \frac{\frac{d\Gamma_+}{dz} (z_0 - z) \cos \frac{px}{U_0} dx dz}{[(x_0 - x)^2 + (z_0 - z)^2]^{3/2}} = I_1 + I_2 + I_3, \\
 W_{y^*}^{(2)} = & \frac{p}{4\pi U_0} \int_{-l/2}^{l/2} \int_0^\infty \frac{\Gamma_+(z) (x_0 - x) \cos \frac{px}{U_0} dx dz}{[(x_0 - x)^2 + (z_0 - z)^2]^{3/2}} + \\
 & + \frac{1}{4\pi} \int_{-l/2}^{l/2} \int_0^\infty \frac{\frac{d\Gamma_+}{dz} (z_0 - z) \sin \frac{px}{U_0} dx dz}{[(x_0 - x)^2 + (z_0 - z)^2]^{3/2}} = I_4 + I_5.
 \end{aligned} \tag{13.55}$$

If $\Gamma_+(z, t) = \Gamma_+(z) \cos pt_0$, then

$$W_{y^*} = W_{y^*}^{(1)} \cos pt_0 - W_{y^*}^{(2)} \sin pt_0.$$

It is possible to show that with $\lambda \rightarrow 0$ I_1, I_2, I_4 vanish, I_3 - for value $\frac{W_{y^*}^{(1)}}{U_0}$ (13.57), and I_5 for $\frac{W_{y^*}^{(2)}}{U_0}$ (13.58). After introducing the dimensionless coordinates

$$\xi = \frac{x}{b}, \quad \xi_0 = \frac{x_0}{b}, \quad \bar{z} = \frac{2z}{l}, \quad \bar{z}_0 = \frac{2z_0}{l}, \quad (13.56)$$

we will obtain for the direct/straight discrete eddy/vortices

$$\frac{W_{y*}^{(1)}}{U_0} = \begin{cases} -\frac{1}{2\pi} \int_{-1}^1 \frac{\frac{d\Gamma}{d\bar{z}} d\bar{z}}{\bar{z}_0 - \bar{z}} & \text{при } \xi_0 > 0, \\ 0 & \text{при } \xi_0 < 0, \end{cases} \quad (13.57)$$

$$\frac{W_{y*}^{(2)}}{U_0} = \begin{cases} \frac{\rho^* \xi_0}{2\pi} \int_{-1}^1 \frac{\frac{d\Gamma}{d\bar{z}} d\bar{z}}{\bar{z}_0 - \bar{z}} & \text{при } \xi_0 > 0, \\ 0 & \text{при } \xi_0 < 0. \end{cases} \quad (13.58)$$

Key: (1). with.

Page 321.

Let us examine the now continuous vorticity layer on wing surface. Intensity of this layer

$$\gamma_{z+}(x, z, t_0) = \gamma_{z+}(x, z) \sin pt_0,$$

whereupon $\gamma_{z+}(x, z) \rightarrow 0$ with $\lambda \rightarrow 0$. The solution of problem with $\lambda \rightarrow 0$ let us search for, by representing $\gamma_{z+}(x, z)$ in the form of the product of two functions, one of which depends on ξ , and the second - on \bar{z} :

$$\gamma_+(\bar{x}, \bar{z}) = U_0 \frac{l}{2} \bar{\Gamma}(\bar{z}) X(\xi) \frac{1}{b}. \quad (13.59)$$

In order to find velocities from continuous eddy/vortices, let us examine in section $x = \text{const}$ the vortex/eddy band dx with circulation $\gamma(x, z) dx$ and corresponding free vortices. The velocities from this vortex/eddy system in the point ξ_0, \bar{z}_0 will be

$$dW_y^{(1)} = X(\xi) \frac{dx}{b} W_{y*}^{(1)}(\xi_0 - \xi, \bar{z}_0),$$

$$dW_y^{(2)} = X(\xi) \frac{dx}{b} W_{y*}^{(2)}(\xi_0 - \xi, \bar{z}_0),$$

whence

$$\left. \begin{aligned} W_y^{(1)}(\xi_0, \bar{z}_0) &= \int_{-1/2}^{1/2} X(\xi) W_{y*}^{(1)}(\xi_0 - \xi, \bar{z}_0) d\xi, \\ W_y^{(2)}(\xi_0, \bar{z}_0) &= \int_{-1/2}^{1/2} X(\xi) W_{y*}^{(2)}(\xi_0 - \xi, \bar{z}_0) d\xi. \end{aligned} \right\} \quad (13.60)$$

In these formulas are used designations (13.56).

With $\lambda \rightarrow 0$ in expressions (13.57), (13.58) it is necessary ξ_0 to estimate on $\xi_0 - \xi$. Since with $\xi_0 - \xi < 0$, i.e. with $\xi_0 < \xi$, $W_{y*}^{(1)} = W_{y*}^{(2)} = 0$,

with $\lambda \rightarrow 0$ integration in formulas (13.60) will be conducted not from $-1/2$ to $1/2$, but from $-1/2$ to ξ_0 . As a result for the distributed vorticity layer let us have

$$\frac{W_y^{(1)}}{U_0} = -\frac{1}{2\pi} \int_{-1/2}^{\xi_0} X(\xi) \int_{-1}^1 \frac{d\bar{\Gamma}}{d\bar{z}} \frac{d\bar{z}}{\bar{z}_0 - \bar{z}} d\xi, \quad (13.61)$$

$$\frac{W_y^{(2)}}{U_0} = \frac{p}{2\pi} \int_{-1/2}^{\xi_0} X(\xi) (\xi_0 - \xi) \int_{-1}^1 \frac{d\bar{\Gamma}}{d\bar{z}} \frac{d\bar{z}}{\bar{z}_0 - \bar{z}} d\xi. \quad (13.62)$$

Let us replace wing with the system of discrete vortex lines with coordinates ξ_μ and continuous bound vorticity layer.

Page 322.

The intensity/strength of the circulations of direct/straight vortex line Γ and of the connected vorticity layer γ let us write in the form

$$\left. \begin{aligned} \Gamma_+ &= U_0 \frac{l}{2} \left(\Gamma^a \alpha + \Gamma^{\dot{a}} \dot{\alpha} + \Gamma^{\omega} \omega_z + \Gamma^{\dot{\omega}} \dot{\omega}_z + \Gamma^{\omega} \omega_x + \Gamma^{\dot{\omega}} \dot{\omega}_x \right), \\ \gamma_+ &= U_0 \left(\gamma^a \alpha + \gamma^{\dot{a}} \dot{\alpha} + \gamma^{\omega} \omega_z + \gamma^{\dot{\omega}} \dot{\omega}_z + \gamma^{\omega} \omega_x + \gamma^{\dot{\omega}} \dot{\omega}_x \right), \end{aligned} \right\} \quad (13.63)$$

whereupon

$$\gamma^{q_l}(\xi, \bar{z}) = \frac{\lambda}{2} \bar{\Gamma}^{q_l}(\bar{z}) X^{q_l}(\xi), \quad \gamma^{q_l}(\xi, \bar{z}) = \frac{\lambda}{2} \bar{\Gamma}^{q_l}(\bar{z}) X^{q_l}(\xi). \quad (13.64)$$

It is not difficult to show that the bound vortexes have the elliptical law of circulation distribution according to spread/scope. Therefore for discrete eddy/vortices we can write:

in the symmetrical case

$$\Gamma^{q_i} = \Gamma_*^{q_i} \sqrt{1 - \bar{z}^2}, \quad (13.65)$$

in antisymmetric

$$\Gamma^{q_i} = \bar{z} \Gamma_*^{q_i} \sqrt{1 - \bar{z}^2}. \quad (13.66)$$

For the distributed vorticity layer in the symmetrical case

$$\bar{\Gamma}^{q_i}(\bar{z}) = \sqrt{1 - \bar{z}^2}, \quad (13.67)$$

in antisymmetric

$$\bar{\Gamma}^{q_i}(\bar{z}) = \bar{z} \sqrt{1 - \bar{z}^2}. \quad (13.68)$$

Let us calculate the values of velocities W_y/U_0 under the law of circulation distribution indicated for $|\bar{z}_0| \leq 1$. Set/assuming $\bar{z} = -\cos \theta$, $\bar{z}_0 = -\cos \theta_0$)

and keeping in mind formula (13.20), we will obtain for the arranged/located on the axis Oz discrete eddy/vortex in the symmetrical case

$$\frac{W_y^{(1)}}{U_0} = -\frac{\Gamma_*}{2}, \quad \frac{W_y^{(2)}}{U_0} = \frac{\rho \dot{\epsilon}_0}{2} \Gamma. \quad (13.69)$$

and in antisymmetric

$$\frac{W_y^{(1)}}{U_0} = -\bar{z}_0 \Gamma, \quad \frac{W_y^{(2)}}{U_0} = \rho^* \xi_0 \bar{z}_0 \Gamma. \quad (13.70)$$

For the distributed vorticity layer in the symmetrical case

$$\frac{W_y^{(1)}}{U_0} = -\frac{1}{2} \int_{-1/2}^{\xi_0} X(\xi) d\xi, \quad \frac{W_y^{(2)}}{U_0} = \frac{\rho^*}{2} \int_{-1/2}^{\xi_0} X(\xi) (\xi_0 - \xi) d\xi \quad (13.71)$$

and in antisymmetric

$$\frac{W_y^{(1)}}{U_0} = -\bar{z}_0 \int_{-1/2}^{\xi_0} X(\xi) d\xi, \quad \frac{W_y^{(2)}}{U_0} = \bar{z}_0 \rho^* \int_{-1/2}^{\xi_0} X(\xi_0 - \xi) d\xi. \quad (13.72)$$

Page 323.

Let us note that the discrete bound vortex cannot be located anywhere, besides leading edge. If it was arranged/located somewhere on the wing between leading and trailing edges, then the induced velocities in this place would have a discontinuity/interruption, what probably then since boundary conditions (3.56) were continuous. On the strength of Chaplygina - Joukowski's hypothesis there cannot be discrete eddy/vortex, also, on trailing wing edge because during any finite wing aspect ratio λ here the intensity of vorticity layer

must be equal to zero.

Higher vortex/eddy system indicated will induce on wing the velocity

$$\left. \begin{aligned} \frac{W_y}{U_0} &= \sum_{i=1}^3 \left\{ \left[\left(w_{yq_i}^{(1)} - p^* w_{yq_i}^{(2)} \right) + \left(w_{yq_i}^{(1)} - p^* w_{yq_i}^{(2)} \right) \right] q_i^* \cos p^* \tau_0 + \right. \\ &\quad \left. + \left[\left(w_{yq_i}^{(2)} + p^* w_{yq_i}^{(1)} \right) + \left(w_{yq_i}^{(2)} + p^* w_{yq_i}^{(1)} \right) \right] q_i^* \sin p^* \tau_0 \right\}, \\ w_y^{(1)} &= \frac{W_y^{(1)}}{U_0}, \quad w_y^{(2)} = \frac{W_y^{(2)}}{U_0}, \end{aligned} \right\} \quad (13.73)$$

where $w_{yq_i}^{(1)}, w_{yq_i}^{(2)}$ they are determined from formulas (13.57) and (13.58) with after exchange in them Γ on $\Gamma^a, \Gamma^{\omega_z}, \Gamma^{\omega_x}, \dots$ and $w_{yq_i}^{(1)}, w_{yq_i}^{(2)}$ from formulas (13.61) and (13.62) during the corresponding replacement of x on $X^a, X^{\omega_z}, X^{\omega_x}, \dots$. We will write condition (3.56) in the form

$$\frac{W_y}{U_0} = -\alpha \cos pt_0 - \xi_0 \omega_z \cos pt_0 - z_0 \frac{\lambda}{2} \omega_x \cos pt_0. \quad (13.74)$$

Then systems (13.73) we obtain in the following form:

for the α -problem

$$\left. \begin{aligned} (w_{ya}^{(1)} + w_{ya}^{(1)}) - p^* (w_{ya}^{(2)} + w_{ya}^{(2)}) &= -1, \\ (w_{ya}^{(2)} + w_{ya}^{(2)}) + p^* (w_{ya}^{(1)} + w_{ya}^{(1)}) &= 0, \end{aligned} \right\} \quad (13.75)$$

for the ω_z -Problem

$$\left. \begin{aligned} (w_{y\omega_z}^{(1)} + w_{y\omega_z}^{(1)}) - p^* (w_{y\omega_z}^{(2)} + w_{y\omega_z}^{(2)}) &= -\xi_{0z} \\ (w_{y\omega_z}^{(2)} + w_{y\omega_z}^{(2)}) + p^* (w_{y\omega_z}^{(1)} + w_{y\omega_z}^{(1)}) &= 0. \end{aligned} \right\} \quad (13.76)$$

for the ω_x -Problem

$$\left. \begin{aligned} (w_{y\omega_x}^{(1)} + w_{y\omega_x}^{(1)}) - p^* (w_{y\omega_x}^{(2)} + w_{y\omega_x}^{(2)}) &= -\frac{\lambda}{2} \bar{z}_0 \\ (w_{y\omega_x}^{(2)} + w_{y\omega_x}^{(2)}) + p^* (w_{y\omega_x}^{(1)} + w_{y\omega_x}^{(1)}) &= 0. \end{aligned} \right\} \quad (13.77)$$

Page 324.

By substituting in (13.75) - (13.77) the values of velocities from (13.69) - (13.72), we will obtain, for example, for the equations of system (13.75)

$$\left. \begin{aligned} \left(\frac{1}{2} + \xi_0\right) \Gamma_*^a + \int_{-1/2}^{\xi_0} X^a (\xi_0 - \xi) d\xi - \Gamma_*^a - \int_{-1/2}^{\xi_0} X^a d\xi &= 0, \\ \Gamma_*^a + \int_{-1/2}^{\xi_0} X^a d\xi + p^* \left(\frac{1}{2} + \xi_0\right) \Gamma_*^a + p^* \int_{-1/2}^{\xi_0} X^a (\xi_0 - \xi) d\xi &= 2. \end{aligned} \right\} \quad (13.78)$$

With $p^* \rightarrow 0$ we have

$$\left. \begin{aligned} \Gamma_*^a + \int_{-1/2}^{\xi_0} X^a d\xi &= 2, \\ \left(\frac{1}{2} + \xi_0\right) \Gamma_*^a + \int_{-1/2}^{\xi_0} X^a (\xi_0 - \xi) d\xi - \Gamma_*^a - \int_{-1/2}^{\xi_0} X^a d\xi &= 0. \end{aligned} \right\} \quad (13.79)$$

Solution of this system:

$$X^a = 0, \quad \Gamma_*^a = 2, \quad X^a = 2, \quad \Gamma_*^a = 0. \quad (13.80)$$

For the equations of system (13.76) we have with $p^* \rightarrow 0$

$$\left. \begin{aligned} \Gamma_z^{\omega} + \int_{-1/2}^{\xi_0} X^{\omega_z} d\xi &= 2\xi_0, \\ \Gamma_z^{\omega} \left(\frac{1}{2} + \xi_0 \right) - \Gamma_z^{\omega} + \int_{-1/2}^{\xi_0} X^{\omega_z} (\xi_0 - \xi) d\xi - \int_{-1/2}^{\xi_0} X^{\omega_z} d\xi &= 0. \end{aligned} \right\} \quad (13.81)$$

Solution of this system:

$$X^{\omega_z} = 2, \quad \Gamma_z^{\omega} = -1, \quad X^{\omega_z} = 2\xi_0, \quad \Gamma_z^{\omega} = 0. \quad (13.82)$$

It is analogous for the equations of system (13.77) with $p^* \rightarrow 0$

$$\left. \begin{aligned} \Gamma_x^{\omega} + \int_{-1/2}^{\xi_0} X^{\omega_x} d\xi &= \frac{\lambda}{2}, \\ \left(\frac{1}{2} + \xi_0 \right) \Gamma_x^{\omega} - \Gamma_x^{\omega} + \int_{-1/2}^{\xi_0} X^{\omega_x} (\xi_0 - \xi) d\xi - \int_{-1/2}^{\xi_0} X^{\omega_x} d\xi &= 0. \end{aligned} \right\} \quad (13.83)$$

Solution of this system:

$$X^{\omega_x} = 0, \quad \Gamma_x^{\omega} = \frac{\lambda}{2}, \quad X^{\omega_x} = \frac{\lambda}{2}, \quad \Gamma_x^{\omega} = 0. \quad (13.84)$$

Page 325.

N. Ye

Let us present the Joukowski theorem "in small" for unsteady motion in the following form:

$$\Delta p = p_- - p_+ = \rho_{\infty} U_0 v_{z+} = \frac{\rho_{\infty} U_0^2}{2} \frac{l}{b} \sum_{l=1}^3 (\bar{\Gamma}^{q_l} X^{q_l} q_l + \bar{\Gamma}^{q_l} X^{q_l} \dot{q}_l).$$

Bearing in mind that from vorticity layer and the discrete

eddy/vortex

$$\begin{aligned}
 Y &= c_y \rho_\infty \frac{U_0^2}{2} S = \int_{-l/2}^{l/2} \int_{-b/2}^{b/2} \Delta p \, dx \, dz + \rho_\infty U_0 \int_{-l/2}^{l/2} \Gamma_+(z) \, dz, \\
 M_z &= m_z \rho_\infty \frac{U_0^2}{2} S b = - \int_{-l/2}^{l/2} \int_{-b/2}^{b/2} \Delta p \, x \, dx \, dz - \rho_\infty U_0 \int_{-l/2}^{l/2} \Gamma_+(z) \, x_* \, dz, \\
 M_x &= m_x \rho_\infty \frac{U_0^2}{2} S l = - \int_{-l/2}^{l/2} \int_{-b/2}^{b/2} \Delta p \, z \, dx \, dz - \rho_\infty U_0 \int_{-l/2}^{l/2} \Gamma_+(z) \, z \, dz.
 \end{aligned}$$

Taking into account representation (13.63) - (13.68) and the equality

$$\int_{-1}^1 \sqrt{1-\bar{z}^2} \, d\bar{z} = \frac{\pi}{4}, \quad \int_{-1}^1 \bar{z} \sqrt{1-\bar{z}^2} \, d\bar{z} = 0, \quad \int_{-1}^1 \bar{z}^2 \sqrt{1-\bar{z}^2} \, d\bar{z} = \frac{\pi}{8},$$

we will obtain

$$\left. \begin{aligned}
 Y &= \rho_\infty \frac{U_0^2}{2} S \frac{\pi \lambda}{4} \left[\left(q_i \int_{-1/2}^{1/2} X^{q_i} d\xi + \dot{q}_i \int_{-1/2}^{1/2} X^{q_i} d\xi \right) + (\Gamma_*^{q_i} q_i + \Gamma_*^{q_i} \dot{q}_i) \right], \\
 M_z &= - \rho_\infty \frac{U_0^2}{2} S b \frac{\pi \lambda}{4} \left[\left(q_i \int_{-1/2}^{1/2} X^{q_i \xi} d\xi + \dot{q}_i \int_{-1/2}^{1/2} X^{q_i \xi} d\xi \right) + \right. \\
 &\quad \left. + \xi_* (\Gamma_*^{q_i} q_i + \Gamma_*^{q_i} \dot{q}_i) \right], \\
 M_x &= - \rho_\infty \frac{U_0^2}{2} S l \frac{\pi \lambda}{32} \left[\omega_x \int_{-1/2}^{1/2} X^{\omega_x} d\xi + \dot{\omega}_x \int_{-1/2}^{1/2} X^{\omega_x} d\xi + \right. \\
 &\quad \left. + \omega_x \Gamma_*^{\omega_x} + \dot{\omega}_x \Gamma_*^{\omega_x} \right],
 \end{aligned} \right\} \quad i = 1, 3;$$

(13.85)

ξ_* - the coordinates of discrete eddy/vortex, $q_1 = \alpha$, $q_2 = \omega_x$, $q_3 = \omega_z$.
Substituting in (13.85) values X and Γ_* from (13.80), (13.82), (13.84) and taking into account that $\xi_* = -1/2$, we will obtain formulas for the coefficients of the aerodynamic derivatives, designed relative to the rotational axis, passing through the middle of wing chord ($\bar{x}_T = 0,50$):

$$\left. \begin{aligned} c_y^a &= \frac{\pi\lambda}{2}, & c_y^{\dot{a}} &= \frac{\pi\lambda}{2}, & c_y^{\omega_z} &= \frac{\pi\lambda}{4}, & c_y^{\dot{\omega}_z} &= 0, \\ m_z^a &= \frac{\pi\lambda}{4}, & m_z^{\dot{a}} &= 0, & m_z^{\omega_z} &= -\frac{\pi\lambda}{8}, \\ m_z^{\omega_z} &= -\frac{\pi\lambda}{24}, & m_{x1}^{\omega_{x1}} &= -\frac{\pi\lambda}{32}, & m_{x1}^{\dot{\omega}_{x1}} &= -\frac{\pi}{16}. \end{aligned} \right\} \quad (13.86)$$

Coefficients $m_{x1}^{\omega_{x1}}$, $m_{x1}^{\dot{\omega}_{x1}}$ are obtained when $\omega_{x1} = \Omega_x l / 2U_0$, $\dot{\omega}_{x1} = \frac{d\Omega_x}{dt} \frac{l^2}{4U_0^2}$, the moment of roll is referred to the span of wing l . From the given formulas it is evident that and for the rectangular wing is extremely small elongation ($\bar{x}_T = 0,50$) are valid the consequences of reciprocity theorem:

$$c_{y+}^{\omega_z} = m_{z-}^a, \quad c_{y-}^{\omega_z} = m_{z+}^a, \quad c_{y+}^{\dot{\omega}_z} = m_{z-}^{\dot{a}}, \quad c_{y-}^{\dot{\omega}_z} = m_{z+}^{\dot{a}}.$$

§8. The rectangular wing of very small elongation. Transient functions.

Is interesting to find transient functions $[c(\tau)/q_i^*]$ for the rectangular wing of extremely small elongation. Let us point out the indirect way of the determination of the transient function of this

AD-A049 000

FOREIGN TECHNOLOGY DIV WRIGHT-PATTERSON AFB OHIO
A WING IN AN UNSTEADY GAS FLOW. PART 2, (U)
SEP 77 S M BELOTSEKOVSKIY, B K SKRIPACH
FTD-ID(RS)T-1534-77-PT-2

F/G 1/3

UNCLASSIFIED

NL

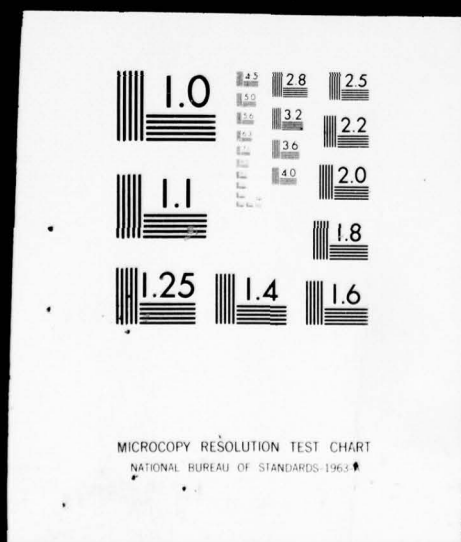
2 OF 6

ADA049000



2 OF 6

ADA049000



wing. Let us write for a lift coefficient communication/connection of transient function $[c_y(\tau)/\alpha^*]$ and the coefficient of aerodynamic derivative with point c^q with $\rho^* \rightarrow 0$ (theorem of momentum, chapter VI):

$$\int_0^\infty \left\{ \left[\frac{c_y(\tau)}{\alpha^*} \right] - \left[\frac{c_y(\infty)}{\alpha^*} \right] \right\} d\tau = c_y^a \Big|_{\rho^* \rightarrow 0} - 2k_{22}. \quad (13.87)$$

For the wing of very small elongation ($\lambda \rightarrow 0$), the coefficient $c_y^a \Big|_{\rho^* \rightarrow 0} = \pi\lambda/2$, and the coefficient of bound mass k_{22} in the range of small wing aspect ratios linearly depends on λ , so that $k_{22} = A\lambda$.

Page 327.

Therefore in the case of the passage to the limit to of wing $\lambda \rightarrow 0$

$$\int_0^\infty \left\{ \left[\frac{c_y(\tau)}{\alpha^*} \right] - \left[\frac{c_y(\infty)}{\alpha^*} \right] \right\} d\tau \rightarrow 0$$

and, therefore,

$$\left\{ \left[\frac{c_y(\tau)}{\alpha^*} \right] - \left[\frac{c_y(\infty)}{\alpha^*} \right] \right\} \rightarrow 0.$$

Thus, for the wing in question the regular part of the transient function of lift coefficient $[c_y(\tau)/\alpha^*]$ during an instantaneous change in the angle of attack will be

$$\left[\frac{c_y(\tau)}{\alpha^*} \right] \rightarrow \frac{\pi\lambda}{2}. \quad (13.88)$$

Analogously it is possible to demonstrate that

$$\left. \begin{aligned} \left[\frac{m_z(\tau)}{\alpha^*} \right] &\rightarrow \frac{\pi\lambda}{4}, & \left[\frac{m_{x1}(\tau)}{\omega_{x1}^*} \right] &\rightarrow -\frac{\pi\lambda}{32}, \\ \left[\frac{c_y(\tau)}{\omega_z^*} \right] &\rightarrow \frac{\pi\lambda}{4}, & \left[\frac{m_z(\tau)}{\omega_z^*} \right] &\rightarrow -\frac{\pi\lambda}{8}. \end{aligned} \right\} \quad (13.89)$$

Transient functions $[c_y(\tau)/\omega_z^*]$, $[m_z(\tau)/\alpha^*]$, $[m_z(\tau)/\omega_z^*]$ are extracted here for centering $\bar{x}_T = 0.50$. For the gradual entrance of this wing into gust with the same centering to analogously preceding/previous let us have

$$\left[\frac{c_y(\tau)}{\omega_{y\Delta}^*} \right] \rightarrow \frac{\pi\lambda}{2}, \quad \left[\frac{m_z(\tau)}{\omega_{y\Delta}^*} \right] \rightarrow \frac{\pi\lambda}{4}. \quad (13.90)$$

Page 328.

Chapter XIV.

CALCULATION OF THE UNSTEADY WING CHARACTERISTICS OF ARBITRARY PLANFORM.

§1. Special feature/peculiarities of calculation procedure.

During the calculation of aerodynamic wing characteristics by the methods, presented in chapters of X-XII, it is necessary to observe a series of conditions. Specifically, this is related to Chaplygin - Joukowski's hypothesis about the finiteness of velocities on trailing wing edge. Since the last/latter point on the wing, where is satisfied boundary condition about the evenness of flow, is located nearer to tail than any eddy/vortex, during the unlimited increase in the number of eddy/vortices ($n \rightarrow \infty$) the designed disturbed velocities on tail they will vanish. The sums, which replaced integrals, within limit will give the principal values of

integrals in Cauchy's sense, since all the calculation points lie/rest in the middle between adjacent eddy/vortices. The numerical values of circulation and loads make it possible to answer the question, is provided the execution by the taken diagram of Chaplygina - Joukowski's hypothesis. If circulation turns into zero on trailing wing edge, then by this most the hypothesis indicated is satisfied, whereupon this must be fulfilled with the arbitrary dependence of the kinematic parameters on time, including harmonic oscillations.

For a noncirculating flow, as is known, instead of Chaplygin - Joukowski's hypothesis must be satisfied the condition about equality zero of the total intensity of eddy/vortices in each wing section. This gives, in particular, to conclusion about the absence of free vortices after wing, in consequence of which changes the method of the location of bound vortexes and calculation points on wing. It is known that on leading wing edge is a special feature/peculiarity. Furthermore, if along wing chord are fractures, for example, for a wing with flap or aileron, then in point of rupture some of the distributed loads also have a special feature/peculiarity. It is interesting to check, how numerical a calculation method for a wing with flap reflects the picture indicated.

Page 329.

The large role in the final adjustment of the numerical calculation methods play the investigations of procedural nature. It is very important to ensure this identification of the parameters, which determine the accuracy of the calculation in order to obtain the results of the calculations with the necessary for a practice accuracy. There are different methods of the control of the numerical data, obtained from the calculation, that make it possible with the aid of special systematic investigations to establish/install the reliability of these data and to provide the necessary accuracy.

Before enumerating some methods of this control, let us note that as a result of the analysis of numerical calculations in digital computers it was establish/installated that the systems of the algebraic equations, determining the circulations of bound vortexes, are very stable. This is explained by the facts that the cell/elements of the principal diagonal of matrix/dies in terms of absolute value considerably more remaining elements, since maximum velocity produces the eddy/vortex, directly beyond which is located the calculation point.

The results of numerical calculations are compared usually with the existing exact solutions, for example, for an infinite-span wing

($\lambda = \infty$) and for the rectangular wing of very small elongation ($\lambda \rightarrow 0$). In this case is examined the circulation flow about the wings indicated with the arbitrary dependences of the kinematic parameters on time, including harmonic dependences, and also the noncirculation flow. Thus is conducted the comparison of precise and numerical data for transient functions, coefficients of aerodynamic derivative and apparent additional masses in connection with to rigid wing and the deforming wing, for example to airfoil with flap.

Another method of control is it is the systematic investigation of the practical convergence of numerical solution with an increase in the number of eddy/vortices n chordwise of wing and N along semirange on each connected vortex line. The greater the value of n and by N , the higher the accuracy of the conducted numerical calculations. In order to virtually determine the necessary values of n and N , one should establish/install, from which values of n and N the results of the calculations practically cease to depend on the number of eddy/vortices.

As is known (see Chapter VII), reciprocity theorem establish/installs communication/connection between aerodynamic characteristics in straight line and that which was turned the flows, when forward velocity U_0 is replaced by reverse/inverse. Within the framework of the linear theory of the consequence of reciprocity

theorem they are precise. By utilizing known corollaries of this, it is possible to conduct the control of data, obtained from numerical calculations.

Page 330.

For this is made the calculation of the aerodynamic characteristics of the direct/straight and reverse/inverse wings of any planform and compare the appropriate characteristics.

Everything said is related to the total characteristics - the coefficients of aerodynamic derivatives and to transient functions. There is broad a class of the virtually interesting problems, in which it is necessary to know, which aerodynamic effect accompanies one strain or the other of wing, for example the deflection of flap or aileron. The direct method of the determination of the total aerodynamic loadings in this case is complex. The calculations can be highly simplified, if them are conducted on the basis of the consequences of reciprocity theorem. The comparison of two methods of the calculation makes it possible also to control the used numerical methods.

If we examine the arbitrary motion of wing, then both of the physical content of problem and from its mathematical setting it

follows that during an infinite increase in dimensionless time ($\tau \rightarrow \infty$), when concludes transient process, we come to the steady-state values of the corresponding derivatives without points. In the problem of harmonic oscillations they are obtained with $p \rightarrow 0$; therefore the numerical values of transient functions at large values τ can be monitored those which were obtained from another numerical calculation by the coefficients of aerodynamic derivatives with very small Strouhal number ($p \rightarrow 0$). For an infinite-span wing are exact solutions with $p \rightarrow 0$; therefore with them it is possible to make a comparison of the value of the transient function, determined at large τ of numerical calculation, since occurs the equality

$$c^{q_i}|_{p \rightarrow 0} = \left[\frac{c}{q_i} \right]_{\tau \rightarrow \infty},$$

where $\left[\frac{c}{q_i} \right]$ is a transient function of the coefficient of aerodynamic force or torque/moment. Earlier it was shown (chapter VI), that there is communication/connection between momentum/impulse/pulse $I \left[\frac{c}{q_i} \right]$ of transient function and the coefficients of aerodynamic derivatives with points (c^{q_i}) with $p \rightarrow 0$. Momentum/impulse/pulse from transient function $I \left[\frac{c}{q_i} \right]$ can be written in the form

$$I \left[\frac{c}{q_i} \right] = \int_0^{\infty} \left\{ \left[\frac{c(\tau)}{q_i} \right] - \left[\frac{c(\infty)}{q_i} \right] \right\} d\tau.$$

In this case above communication/connection indicated can be represented in the following form:

$$c^{q_i}|_{p^* \rightarrow 0} = 2k_{q_i} + I \left[\frac{c}{q_i} \right],$$

where k_{q_i} is a coefficient of apparent additional mass. Hence it is apparent that, besides the control of the behavior of transient functions at their limit points ($\tau \rightarrow 0$ and $\tau \rightarrow \infty$), it is possible to integral control the behavior of the dependence of transient function in all range of change τ .

The values of the coefficients of aerodynamic derivatives with points with very small Strouhal number ($p^* \rightarrow 0$) are obtained independent of the calculation of transient functions, whereupon the last/latter calculations are more complex. The application/use of a theorem of momentum permits implementation of a cross check of each numerical data, numerical calculations of aerodynamic wing characteristics with arbitrary Strouhal numbers it is possible to control with the aid of the dependence, obtained by the calculation of Duhamel integral and which relates the coefficient of aerodynamic derivative $c^{q_i}(p^*)$ with the appropriate transient function $\left[\frac{c(\tau)}{q_i} \right]$ and the coefficient of apparent additional mass k_{q_i} (chapter VI). The indicated communication/connection has important practical value,

since it makes it possible by this way to obtain the coefficients of aerodynamic derivatives over a wide range of Strouhal numbers. Frequently it is simpler to determine transient functions than the coefficients of aerodynamic derivatives depending on Strouhal number. Not randomly so little carried out numerical calculations regarding dependences $c^q_i(p')$ by direct method.

Thus, control of numerical calculations with the aid of Duhamel integral can be sometimes carried out according to this diagram:

1. Direct/straight calculation of transient functions. Here the kinematic parameters are changed on stepped chaconne.

2. Direct/straight calculation for any law of change q_i in particular harmonic.

3. Calculation of aerodynamic wing characteristics under the same law, as in point/item 2, but with the aid of transient function and the integral of Duhamel. Comparison of these results with those which were obtained in point/item 2.

After above reception/procedures indicated is provided the necessary accuracy of numerical calculations, can be considered as them virtually precise data of linear theory.

Page 332.

The comparison of these data with reliable data of experiment makes it possible to reveal/detect/expose the correctness of the diagram of phenomenon, placed as the basis of linear theory, and also to explain the ways of its refinement.

As can be seen from chapter VIII, monitoring of the reliability of the obtained from experiment results for unsteady characteristics represents also very complex problem. Therefore the systematic comparison of experimental and calculated data is good means of cross check. Comparison is done for stationary and unsteady characteristics during harmonic oscillations and with arbitrary time dependences. The study of the structure of the flow about the model makes it possible to rate/estimate the field of application of a linear theory. In connection with this it is necessary to keep in mind that during the unsteady motion of wing the separating mode/conditions of flow can be observed, also, at such angles of attack, with which in the case of steady motion is obtained the even flow. Experimental research on separating phenomena is very complicated, since the character of breakaways is determined by all similarity criteria and the simulation of phenomenon here becomes very difficult. Unfortunately,

in experiment not it is always easy to reveal/detect a change of the structure of the flow about the model in the process of oscillations. as one of the possible sign/criteria of this can serve the powerful Reynolds number effect on the coefficients of aerodynamic derivative. It should be noted that on the oscillating models of the phenomenon of breakaway frequently they do not lead to the disturbance/breakdown of the linear dependence of aerodynamic loadings on the kinematic parameters. This can be explained by the facts that during position tests the passage, for example, from one value of angle of attack to another is completed during very large time interval and the character of the flow about the model manages to be changed together with change α . On the contrary, during oscillations with sufficiently high frequency and small amplitude on model is realized certain average/mean virtually the constant/invariable in time structure of flow, that also leads to the linear dependences of aerodynamic forces and torque/moments on the kinematic parameters.

§2. Chaplygin - Joukowski's hypothesis. Distributed characteristics.

The numerical calculations of circulations conducted make it possible to establish that the taken calculation procedure provides the execution of Chaplygina - Joukowski's hypothesis on trailing wing

edges.

Let us examine the at first harmonically oscillating wing of infinite elongation ($\lambda = \infty$).

Page 333.

For it there is exact solution, which determines the circulations of bound vortexes, in particular their intensity γ , caused by motions with the angle of attack $\alpha(\gamma^\alpha)$ and of angular velocity $\omega_z(\gamma^{\omega_z})$ with $p \rightarrow 0$. For the wing indicated with $\bar{x}_T = 0$ was produced the numerical calculation of circulations with the different number of bound vortexes chordwise of wing ($n = 5, 16, 30$). As show given data (Fig. 14.1 and 14.2), there is a tendency of reduction to zero appropriate circulation on trailing wing edge ($\xi = x/b = 1.0$). This especially is noticeable with a large quantity of undertaken chordwise of wing eddy/vortices ($n = 30$). Numerical calculation for an infinite-span wing coincides well with exact solution virtually on an entire wing chord. Analogous curves for circulations $\gamma^\alpha, \gamma^{\dot{\alpha}}, \gamma^{\omega_z}, \gamma^{\dot{\omega}_z}$ are given in Fig. 14.3-14.6, whereupon circulations γ^{q_i} are calculated with centering $\bar{x}_T = 0.5$, therefore inversion γ^{q_i} into zero it occurs at the point $\xi = 0.5$, which now corresponds to trailing edge. Numerical calculations make it possible also to judge how is fulfilled the hypothesis indicated, also, for aperiodic motion. Figure 14.7-14.9

depicts the picture of a change in the intensity of vorticity layer chordwise of delta wing ($\lambda = 2.31$) for the law of a change in the angle, depicted on Fig. 14.7, and the different torque/moments of dimensionless time and three wing sections: $\bar{z} = 0; 0,50; 0,83$. Zdes6 bezrazmerna4 koordinata $x'/b' = 0$ correspond to the wing leading edge, $x'/b' = 1$ - to trailing edge. The character of the given curves testifies to the tendency of reduction to zero appropriate circulation on trailing wing edge.

An abrupt change in the boundary condition on surface of wing usually leads to the appearance of special feature/peculiarities in the distributed characteristics. As an example that serves the case of the deviation of control surface of certain angle δ (r) at the zero angle of attack of wing. Data given in Fig. 14.10 for the plate of infinite span ($\bar{b}_p = 0,25$), show that the special feature/peculiarities, which occur during the deflection of control, automatically recover by the taken calculation procedure. In points of rupture the coefficient of aerodynamic derived load without point (p^{δ_p}) has logarithmic special feature/peculiarity [2.52]. These special feature/peculiarities are observed on the wings of the final elongation, including complex planform. Figure 14.11 gives the results of the calculations for the wing of aircraft "Concorde" with the control, arrange/located into parts of the span of this wing. The coefficients aerodynamic derivative loads with points p^{δ_p} above

special feature/peculiarity indicated do not have. This is connected with the fact that the right sides of boundary condition (3.56) contain the function $f_0(\tau)$, which is changed continuously, and function $\partial f_0 / \partial \xi$ suffers discontinuity/interruption on control.

Page 334.

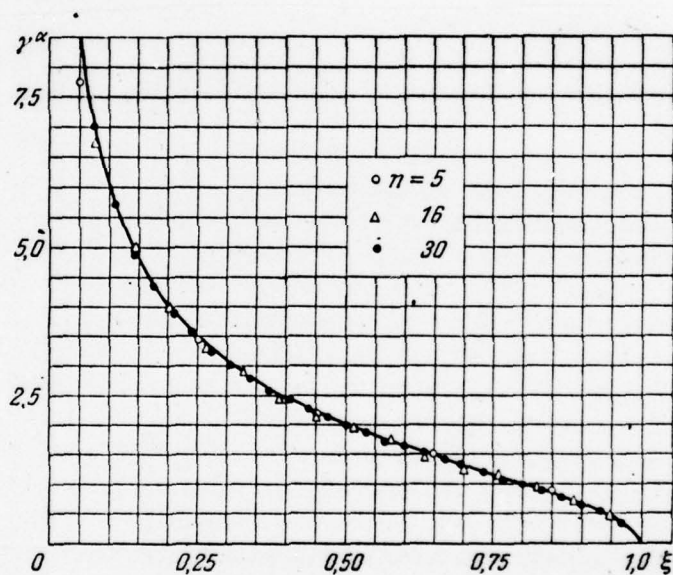


Fig. 14.1. Comparison of precise and numerical calculations of wing λ
 = -. Unbroken curve is exact solution, points are a numerical calculation.

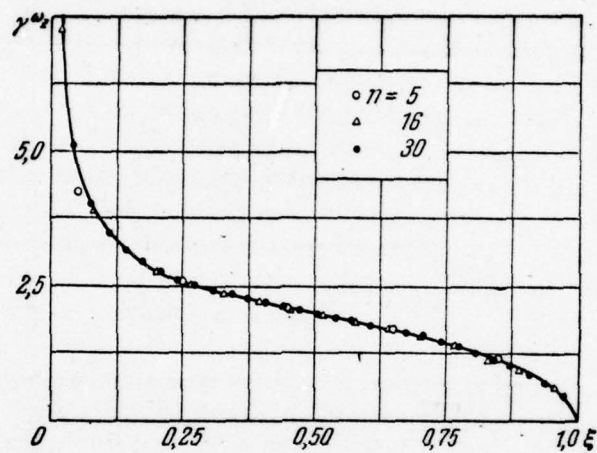


Fig. 14.2. Comparison of precise and numerical calculations of wing λ
 $= \lambda(\bar{x}_T=0)$. Unbroken curve is exact solution, points are a numerical
 calculation.

Page 335.

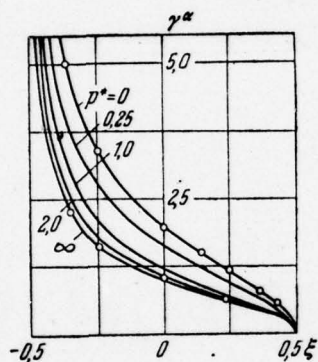


Fig. 14.3.

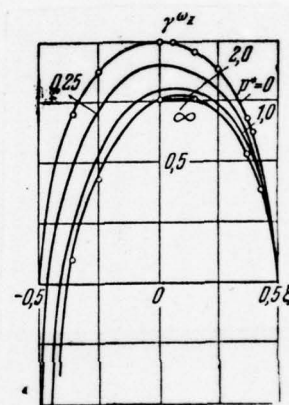


Fig. 14.4.

Fig. 14.3. Comparison of precise and numerical calculations of wing λ = -. Curves are a numerical calculation, points are exact solution.

Fig. 14.4. Comparison of the precise and numerical calculations of wing λ = - ($\lambda_1 = 0$). Curves are a numerical calculation, points are exact solution.

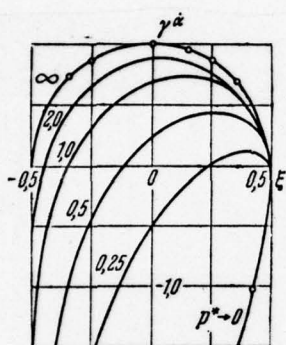


Fig. 14.5

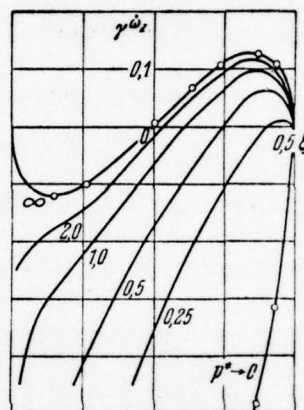


Fig. 14.6.

Fig. 14.5. Comparison of precise and numerical calculations of wing λ
 $= - (\bar{x}_T = 0.5)$. Curves are a numerical calculation, points are exact
 solution.

Fig. 14.6. Comparison of precise and numerical calculations of wing λ
 $= - (\bar{x}_T = 0.5)$. Curves are a numerical calculation, points are exact

solution.

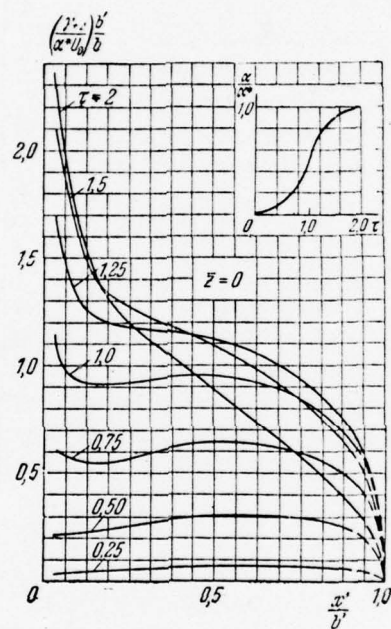


Fig. 14.7. Circulation control chordwise of delta wing $\lambda = 2.31$; $\bar{z} = 0$.

Page 336.

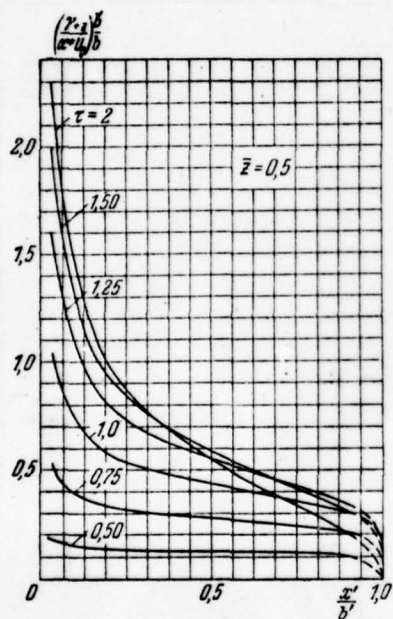


Fig. 14.8.

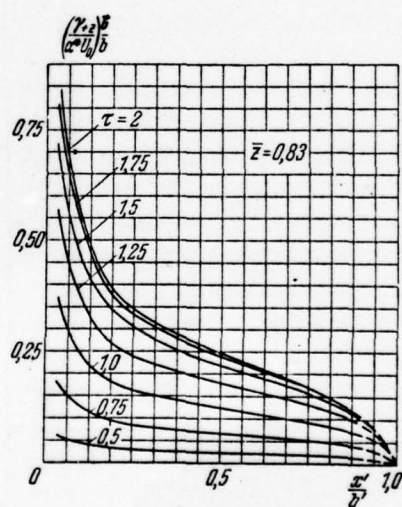


Fig. 14.9.

Fig. 14.8. Circulation control chordwise of delta wing $\lambda = 2.31$; $\bar{z} = 0.5$.

Fig. 14.9. Circulation control chordwise of delta wing $\lambda = 2.31$; $\bar{z} = 0.83$.

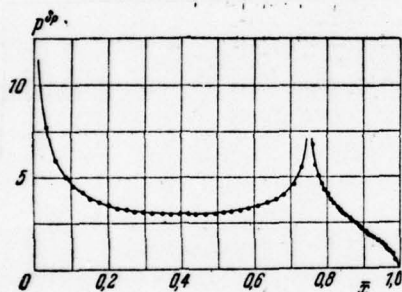


Fig. 14.10.

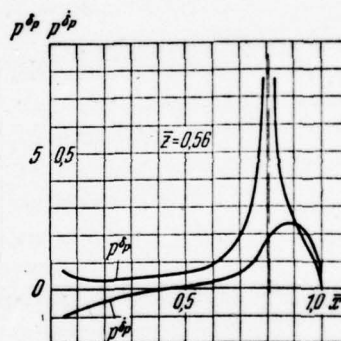


Fig. 14.11.

Fig. 14.10. Comparison of precise and numerical calculations of the plate of infinite span with control $(\bar{b}_p = 0.25)$. Curve is exact solution, points are numerical calculation, $n = 60$
 $(n_{\mu A} = 31, n_p = 29)$.

Fig. 14.11. Coefficients aerodynamic derivative loads of wing with aircraft control surface "Concorde".

Page 337.

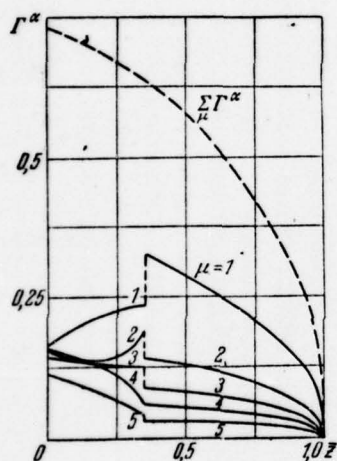


Fig. 14.12.

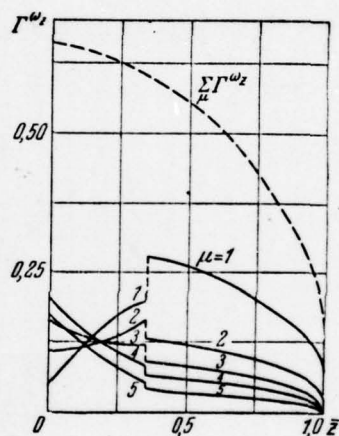


Fig. 14.13.

Fig. 14.12. Circulation control Γ^α in the spread/scope of the wing of aircraft F-111.

Fig. 14.13. Circulation control Γ^{ω_z} in the spread/scope of the wing of

aircraft F-111 ($\dot{x}_T=0$).

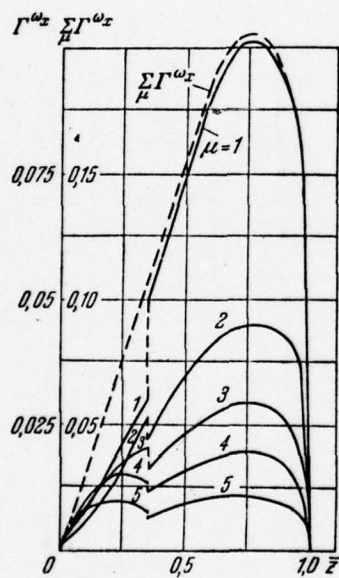


Fig. 14.14.

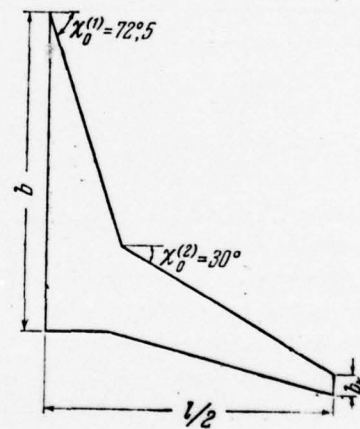


Fig. 14.15.

Fig. 14.14. Circulation control of r^{ω_x} in the spread/scope of the

wing of aircraft F-111.

Fig. 14.15. Schematic of the wing of aircraft F-111.

Page 338.

The developed numerical calculation method is valid for the wings of arbitrary planform, including for the wings, which have fractures on leading and trailing edges. The law of the load distribution or circulations according to the span of such wings can have a series of special feature/peculiarities. The method of discrete eddy/vortices makes it possible to consider these special feature/peculiarities, without being given previously their form. In this case it is necessary only so to arrange/locate eddy/vortices, in order to section $z = \text{const}$, in which occur the fractures of edges, they were undertaken beyond the boundaries of oblique eddy/vortices. In Fig. 14.12-14.14 are given results of the numerical calculations of circulations $\Gamma^a, \Gamma^{\omega_2}$ and Γ^{ω_1} for the wing of complex planform for aircraft F-111 with sweep angles on leading edge $\chi_0^{(1)} = 72^\circ, 5'$, $\chi_0^{(2)} = 30^\circ$ and elongation $\lambda = 6.43$ (Fig. 14.15).

From the presented materials it follows that in the sections, which correspond to the fracture of leading wing edge, is observed

the discontinuity/interruption of the circulations of vortex lines, whereupon the total circulation of the wing in question on its spread/scope is changed continuously. From the common/general/total theorems of mechanics it follows that from wing cannot converge the infinite fine/thin vortex lines of the final intensity, since they would cause in Trefftz's plane the infinite in value kinetic energy of liquid. This would lead to infinite wing drag, which is physically impossible.

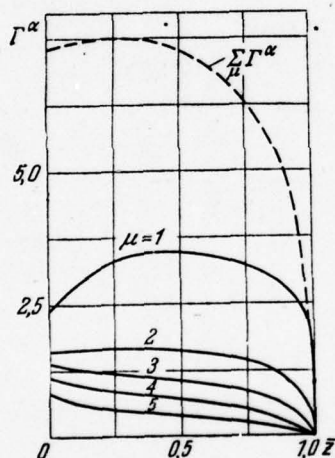


Fig. 14.16.

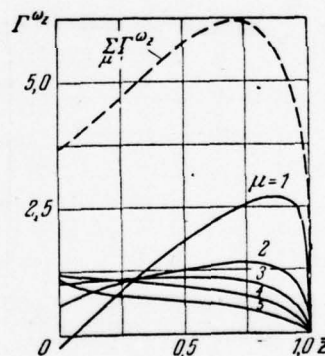


Fig. 14.17.

Fig. 14.16. Dimensionless circulation $r^α$ on the spread/scope of sweptback wing $λ = 2.5$, $χ_0 = 60^\circ$, $η = 2$.

Fig. 14.17. Dimensionless circulation $r^{ω_z}$ on the spread/scope of sweptback wing $λ = 2.5$, $χ_0 = 60^\circ$, $η = 2$.

Page 339.

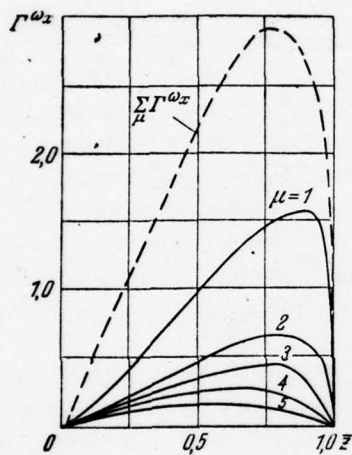


Fig. 14.18

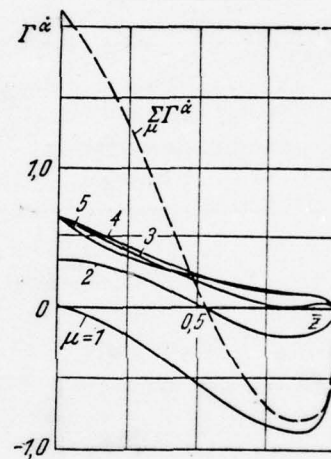


Fig. 14.19.

Fig. 14.18. Dimensionless circulation $\Gamma\omega_x$ on the spread/scope of sweptback wing $\lambda = 2.5$, $\chi_0 = 60^\circ$, $\eta = 2$.

Fig. 14.19. Dimensionless circulation $\Gamma\alpha$ on the spread/scope of sweptback wing $\lambda = 2.5$, $\chi_0 = 60^\circ$, $\eta = 2$.

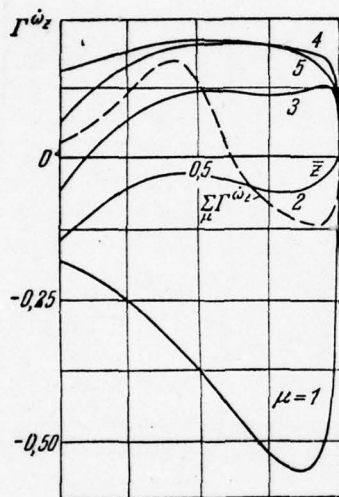


Fig. 14.20.

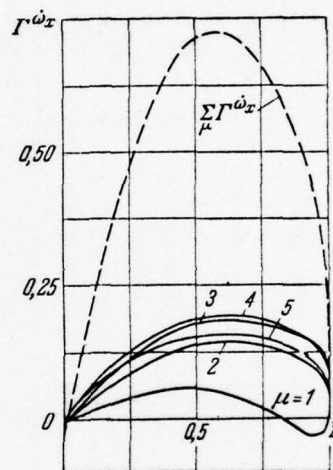


Fig. 14.21.

Fig. 14.20. Dimensionless circulation $\Gamma\omega_z$ on the spread/scope of sweptback wing $\lambda = 2.5$, $\chi_0 = 60^\circ$, $\eta = 2$ ($\bar{x}_T = 0$).

Fig. 14.21. Dimensionless circulation $\Gamma^{\omega x}$ on the spread/scope of sweptback wing $\lambda = 2,5$, $\alpha = 60^\circ$, $\eta = 2$.

Page 340.

For a wing with constant sweepback ($\lambda = 2,5$; $\alpha_0 = 60^\circ$, $\eta = 2$) subsequent the dimensionless quantities of circulations $\Gamma^a, \Gamma^{\omega z}, \Gamma^{\omega y}, \Gamma^a, \Gamma^{\omega z}, \Gamma^{\omega x}$. For this wing the circulation of each vortex line μ , just as total circulation $\sum_{\mu} \Gamma^{\omega i}$, is continuous on entire span of wing and does not have, as one would expect, fractures (Fig. 14.16-14.21). Dimensionless circulations $\Gamma^{(2)}, \Gamma^{(4)}, \Gamma^{(6)}$ along the spread/scope of rectangular wing $\lambda = 1.0$ (Fig. 14.22), obtained for a noncirculating flow, are also continuous and do not have fractures (Fig. 14.23-14.25).

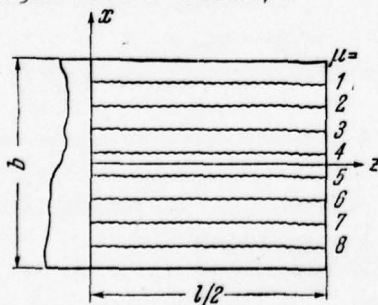


Fig. 14.22.

Fig. 14.22. To the determination of circulations of rectangular wing $\lambda = 1$.

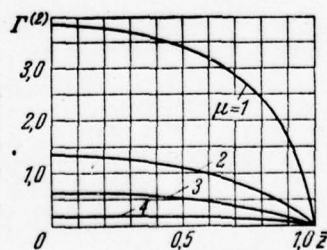


Fig. 14.23.

Fig. 14.23. Dimensionless circulations $\Gamma^{(2)}$ rectangular wing $\lambda = 1.0$.

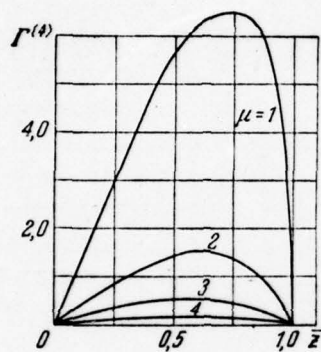


Fig. 14.24

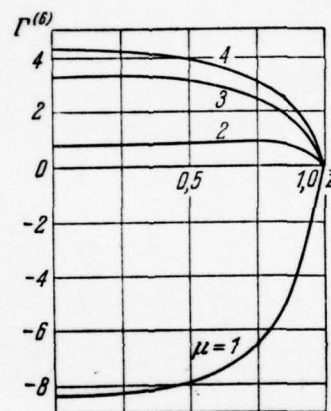


Fig. 14.25.

Fig. 14.24. Dimensionless circulation $\Gamma^{(4)}$ rectangular wing $\lambda = 1.0$.

Fig. 14.25. Dimensionless circulation $\Gamma^{(6)}$ rectangular wing $\lambda = 1.0$ ($\bar{x}_T = 0$).

Page 341.

Attention is drawn to the sufficiently complex law of a circulation control of discrete vortices in the wingspan in the majority of the given here examples. Therefore it is difficult, using, for example, the method of the expansion of circulations in a series, to fit the approaching law of its change with the limited number of terms of expansion.

§3. Comparison of numerical calculations with exact solutions.

During the final adjustment of the rational procedure of numerical calculations the results of the latter are compared with the available exact solutions for the wings infinite and very small elongations. Let us examine at first infinite-span wing. Employing the presented in the preceding/previous chapter procedure are produced numerical calculations for different Strouhal numbers p^* . Higher Fig. 14.3-14.6 depicts the laws of a change in the intensities of bound vortices $\gamma^a, \gamma^b, \gamma^{\omega z}, \gamma^{\omega z}$ along wing chord for determined

Strouhal numbers ($p^* = 0 - 2$). On these diagrams are plotted/applied the points for two cases: $p^* \rightarrow 0$ and $p^* \rightarrow \infty$, obtained from exact solution (13.21), (13.32) and (13.33). As we see, numerical calculation in these cases coincides sufficiently well with exact solution. The total coefficients of the aerodynamic derivatives of plate $\lambda = \infty$ depending on Strouhal number for harmonic oscillations and an harmonic gust are given in the preceding/previous chapter in Fig. 13.2-13.5. Along with exact solutions are plotted/applied the results of numerical calculations. As for distributed loads, the results of the numerical calculation of the total coefficients will agree well with exact solutions in all range of Strouhal numbers p^* .

For the wings of the final elongation numerical calculations are compared with exact solutions for the rectangular wings of very small elongations (13.86) in the extreme case of $p^* \rightarrow 0$ (dotted curves in Fig. 14.26-14.33). The carried out comparison it indicates the completely satisfactory coincidence of the coefficients of aerodynamic derivatives for small wing aspect ratios ($\lambda \approx 0.25-0.50$).

For wings with an instantaneous change in the angle of attack or the upon gradual entrance into step gust also it is possible to conduct the control of numerical calculation, by comparing it with exact solution. In this case for an infinite-span wing the comparison produces for entire range of a change in the dimensionless time τ ,

and for finite-span wings - only for a limiting case $r \rightarrow \infty$,
utilizing asymptotic equalities of the form

$$\left[\frac{c}{q_l} \right]_{r \rightarrow \infty} = c^{q_l} |_{p^* \rightarrow 0}.$$

Page 342.

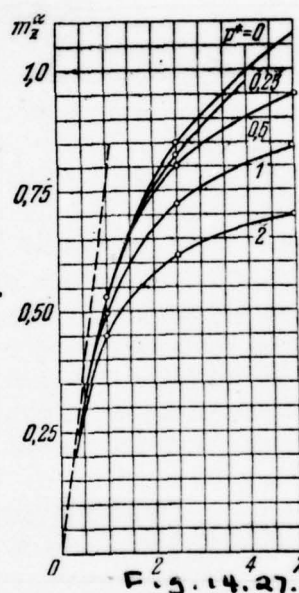
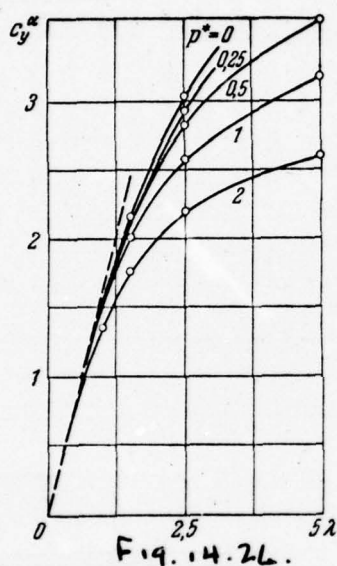


Fig. 14.26. The effect of Strouhal number on the derivative c_y^{α} of rectangular wings; unbroken curves are a numerical calculation, dotted curve is exact solution, points are the calculation according to Duhamel integral.

Fig. 14.27. The effect of Strouhal number on the derivative m_z^{α} of rectangular wings; unbroken curves are a numerical calculation, dotted curve is exact solution, points are the calculation according to Duhamel integral ($\bar{x}_T = 0$).

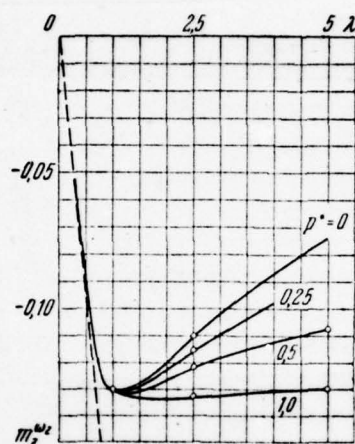


Fig. 14.28. The effect of Strouhal number on the derivative $m_z^{\omega_z}$ of rectangular wings; unbroken curves are a numerical calculation, dotted curve is exact solution, points are the calculation according to Duhamel integral ($\bar{x}_T = 0$).

Page 343.

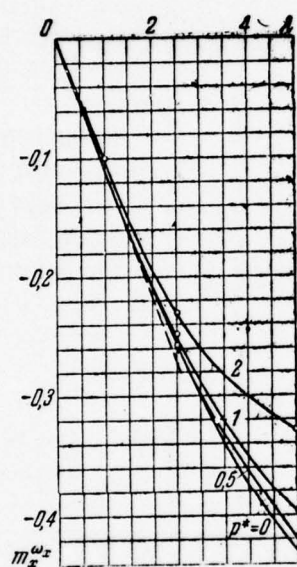


Figure 14.29

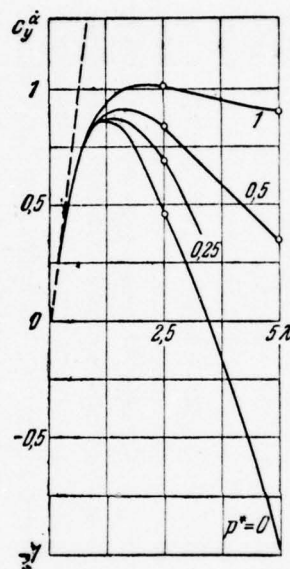


Figure 14.30

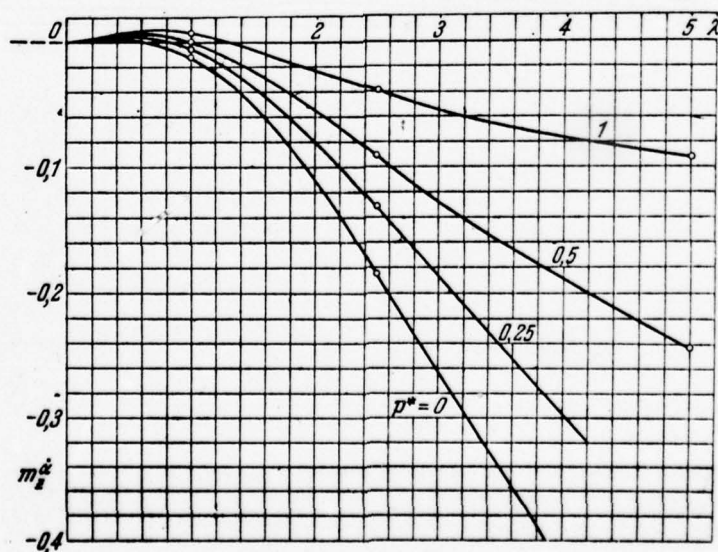


Figure 14.31

Fig. 14.29. The effect of Strouhal number on the derivative $m_x^{\omega x}$ of rectangular wings; unbroken curves are a numerical calculation, dotted curve is exact solution, points are the calculation according to Duhamel integral.

Fig. 14.30. The effect of Strouhal number on the derivative $c_y^{\dot{\alpha}}$ of rectangular wings; unbroken curves are a numerical calculation, dotted curve is exact solution, points are the calculation according to Duhamel integral.

Fig. 14.31. The effect of Strouhal number on the derivative $m_z^{\dot{\alpha}}$ of rectangular wings; unbroken curves are a numerical calculation, dotted curve is exact solution, points are the calculation according to Duhamel integral ($\dot{x}_T=0$).

Page 344.

As they show data given for a plate $\lambda = \infty$ (see Fig. 13.6-13.9), numerical calculations coincide well with precise in all investigated range τ . Furthermore, is observed tendency toward the coincidence of the numerical values of transient functions with very large τ with the data of asymptotic equalities.

For an infinite-span wing is carried out the comparison of numerical calculation with exact solution during noncirculating flow. As it will be shown below (see Fig. 14.51), the coefficients of apparent additional masses k_{22} and k_{66} , obtained from numerical calculations with the large number of bound vortexes, will agree sufficiently well with the appropriate exact solution.

§4. Investigation of the practical convergence of solution with an increase in the number of bound vortexes.

one of the methods of the control of numerical calculations is the investigation of the practical convergence of numerical solution with change in the number of bound vortexes n along chord and N on semirange.

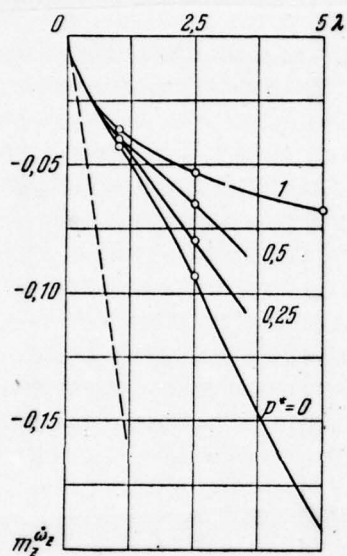


Fig. 14.32.

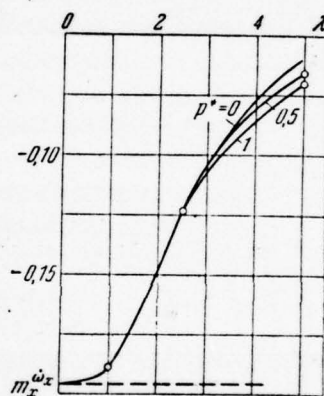


Fig. 14.33.

Fig. 14.32. The effect of Strouhal number on the derivative $m_z \dot{\omega}_z$ of

rectangular wings; unbroken curves are a numerical calculation, dotted curve is exact solution, points are the calculation according to Duhamel integral ($\dot{x}_T=0$).

Fig. 14.33. The effect of Strouhal number on derivative $m_x^{\dot{\omega}x}$ rectangular wings; unbroken curves are a numerical calculation, dotted curve is exact solution, points are the calculation according to Duhamel integral.

Page 345.

For an infinite-span wing, designed on presented in chapter X to procedure, is made a evaluation of the effect of the selected number of bound vortexes on the coefficient of aerodynamic derivative c_y^a for each assigned value of Strouhal number. From the given diagram (Fig. 14.34) it is evident that with small Strouhal numbers ($p^* < 1$) the network, which consists of 6-8 bound vortexes, already gives virtually sufficiently precise characteristics. However, the greater Strouhal number, the by the large quantity of vortex lines necessary to replace vorticity layer in order to obtain reliable results. So, with $p^* = 2.0$ acceptable results gives the scheme which consists of 20 bound vortexes.

For the wings of the final elongation the analysis of the convergence of numerical solution is carried out by Ye. M. Moiseyev with the aid of the curves, arguments of which are the values of a quantity of eddy/vortices chordwise n ($N = \text{const}$) and semirange N ($n = \text{const}$). As already previously it was indicated, here n and N - integers; therefore the given below curves bear conditional character. Analysis is carried out in examples of the wings of small and great lengthenings - two direct/straight and two swept ($\bar{x}_T = 0,5$). The geometric parameters of the investigated wings are given in table 14.1.

Figure 14.35-14.42 depicts to the dependence of unsteady aerodynamic characteristics c_y^{qi} and m_z^{qi} on n and N with $p \rightarrow 0$, which make it possible to judge the selection of the rational vortex/eddy schematic of wing. As show the given materials, and also these works [1.29], for determining the coefficients of aerodynamic derivatives usually it is sufficient to take the vortex/eddy schematic of wing with the number of eddy/vortices $n = 6-8$ and $N = 12-15$.

During investigations in the final adjustment of the numerical methods of the calculation of the different types of aperiodic motion is used the same approach, which was used for harmonic oscillations.

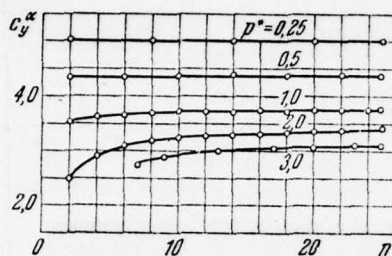


Fig. 14.34. Effect of the number of eddy/vortices on the derivative c_y^α of wing $\lambda = \infty$.

Table 14.1.

(1) Крыло	λ	χ_0	η
1	1,0	0	1,0
2	1,5	60°	5,0
3	5,0	45°	2,0
4	5,0	0	1,0

Key: (1). Wing.

Page 346.

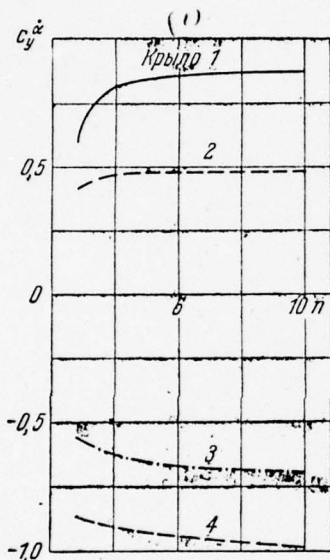


Figure 14.35

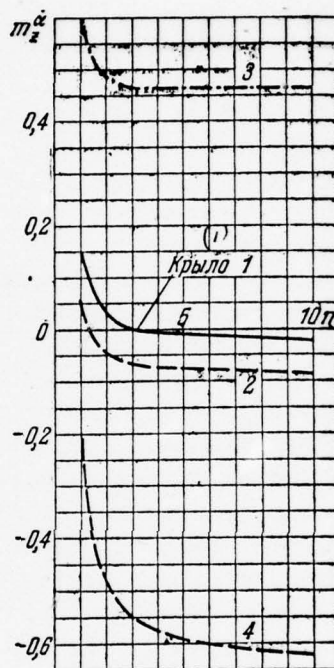


Figure 14.36

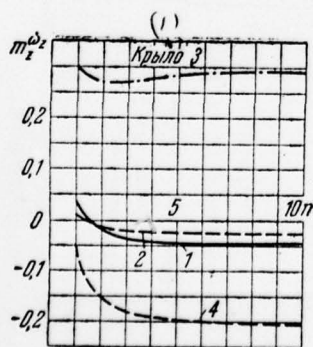


Figure 14.37

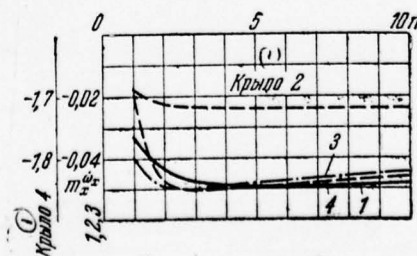


Figure 14.38

Fig. 14.35. Effect of the number of vortex lines n on derivative $c_y^{\dot{\alpha}}$.

Key: (1). Wing.

Fig. 14.36. Effect of the number of vortex lines n on derivative $m_z^{\dot{\alpha}}$.

Key: (1). Wing.

Fig. 14.37. Effect of the number of vortex lines n on derivative $m_z^{\dot{\omega}_z}$.

Key: (1). Wing.

Fig. 14.38. Effect of the number of vortex lines n on derivative $m_x^{\dot{\omega}_x}$.

Key: (1). Wing.

Page 347.

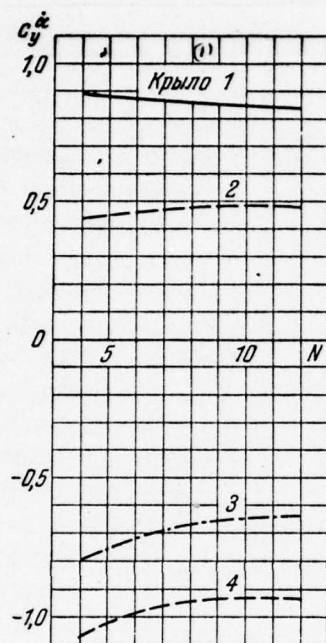


Figure 14.39

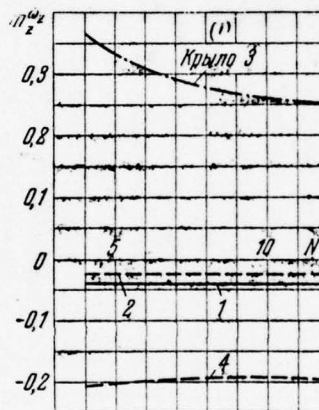


Figure 14.41

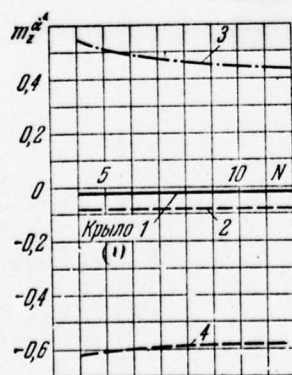


Figure 14.40

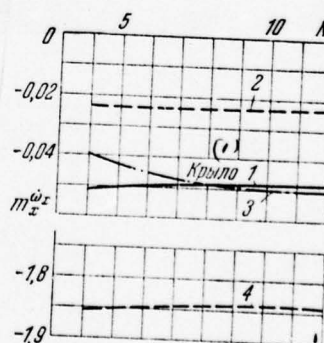


Figure 14.42

Fig. 14.39. Effect of the number of bands N on derivative c_y^{α} .

Key: (1). Wing.

Fig. 14.40. Effect of the number of bands N on derivative $m_z^{\dot{\alpha}}$.

Key: (1). Wing.

Fig. 14.41. Effect of the number of bands N on derivative $m_z^{\dot{\omega}_z}$.

Key: (1). Wing.

Fig. 14.42. Effect of the number of bands N on derivative $m_x^{\dot{\omega}_x}$.

Key: (1). Wing.

Page 348.

For an infinite-span wing according to the method, presented in chapter XI, is made a evaluation of the effect of the number of bound vortexes n on aerodynamic wing characteristics, in this case were undertaken three values: n = 5, 10, 20.

Above (see Fig. 13.6-13.9) were given the dependences of the transient functions of lift and pitching moment of dimensionless time τ with a stepped variation in α/α^* (Figs. 13.6, 13.7) and the upon gradual entrance (Figs. 13.8, 13.9) into step gust. Points answer numerical calculations; unbroken curve corresponds to exact solution, dotted line - to the limiting value of the corresponding transient function with $\tau \rightarrow \infty$, i.e., to the corresponding coefficient of aerodynamic derivative with $p^* \rightarrow 0$. From the preceding information it is evident that it suffices to simulate wing 5-10 by eddy/vortices chordwise in order to obtain the reliable solutions, which coincide on all range τ with precise. This is correct for two basic mode/conditions of an aperiodic motion: an instantaneous change in the kinematic parameters and gradual entrance of wing into stepped gust.

The effect of the number of the bound vortexes, which simulate finite-span wing both on the chord (n) and on semirange (N) to the coefficients of lift and pitching moment it is shown in Fig. 14.43-14.46.

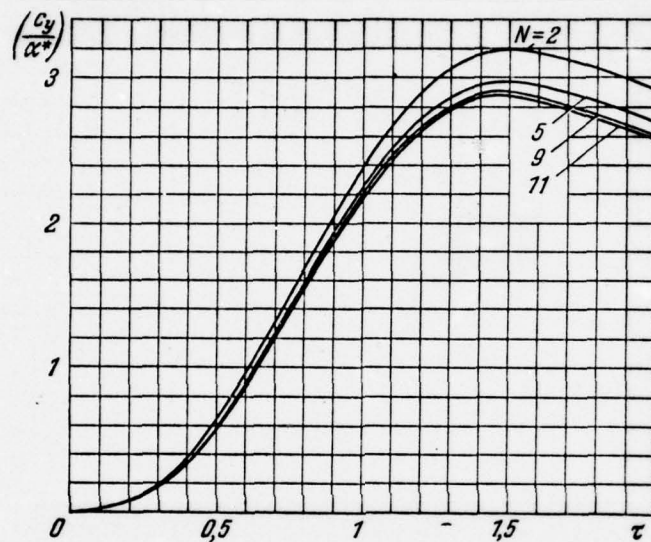


Fig. 14.43. Effect of the number of bound vortexes N on the lift of rectangular wing $\lambda = 2.31$ with $n = 5$.

Page 349.

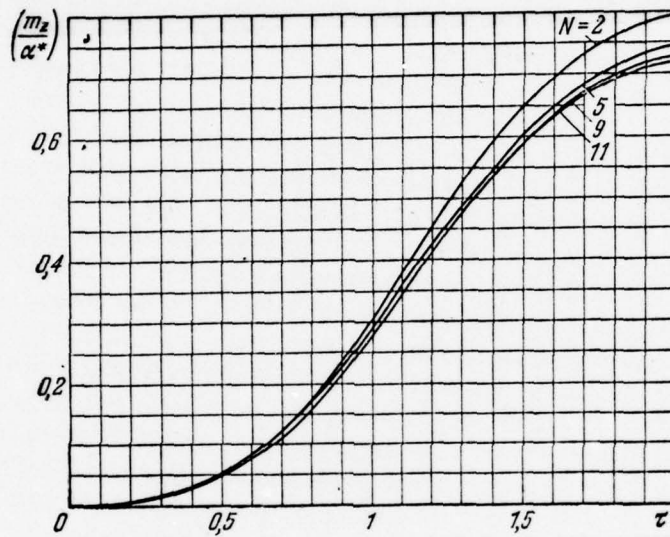


Figure 14.44

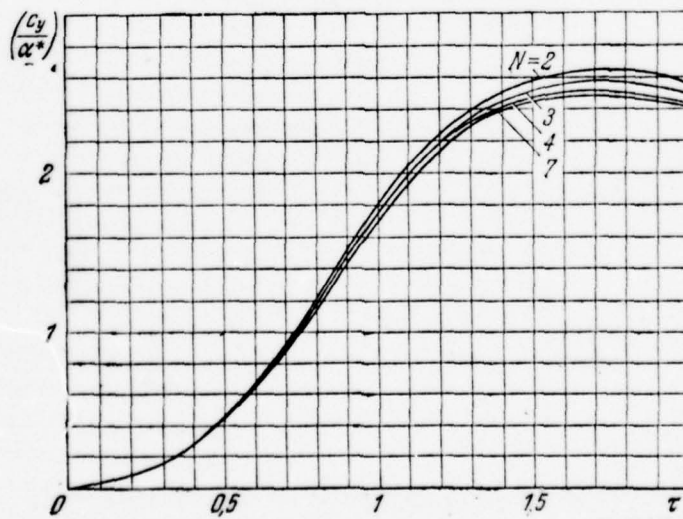


Figure 14.45

Fig. 14.44. Effect of the number of bound vortexes N on the pitching moment of rectangular wing $\lambda=2.31$ with $n = 5$ ($\bar{x}_T=0.5$).

Fig. 14.45. Effect of the number of bound vortexes N on the lift of delta wing $\lambda=2.31$ with $n = 5$.

Page 350.

Are here examined two wings with lengthening $\lambda = 2.31$: rectangular and triangular, whereupon for constant value of $n = 5$ it is undertaken by $N = 2, 5, 9, 11$; during a change in number n undertaken by $N = 6$. These investigations are carried out in an example of the smooth law of a change in the kinematic parameters in dimensionless time τ (see Fig. 14.7). As can be seen from the graphs, with a fixed number of vortices along the chord $n = 5$ number of eddy/vortices on the semirange of wing can be in practical calculations taken as equal to $N = 10-12$. The effect of number n noticeably manifests itself only at low values τ and n . The number of eddy/vortices of order $n = 6-10$ is sufficient for obtaining reliable results.

Aerodynamic characteristics during a stepped variation in the kinematic parameters in time are examined in an example of

rectangular and delta wings with lengthenings $\lambda = 2.5$ ($\bar{x}_T = 0$). Figure 14.47-14-50 depicts to the dependence of transient functions of dimensionless time τ for an instantaneous and gradual entrance into gust. For a rectangular wing the total number of bound vortices is undertaken $nN = 40$ ($n = 5, N = 8$) and $nN = 56$ ($n = 7, N = 8$); for delta wing $nN = 35$ and $nN = 60$. Dotted line carried out limiting cases $\tau \rightarrow \infty$. Thus, independent of the law of a change in the kinematic parameters in time the practical convergence of the results of numerical calculation can be reached by the replacement of the vorticity layer of wing approximately sixty by bound vortices.

Investigations in the development of the rational circuit of the calculation of the coefficients of apparent additional masses are carried out by E. P. Kapustina for the wings of different planform on the basis of the method, presented in chapter XII. Let us examine at first infinite-span wing ($\lambda = \infty$). Figure 14.51 shows the effect of the number of eddy/vortices $m = nN$, by which is simulated the plate, to the coefficients of apparent additional masses k_{22} and $k_{\bullet\bullet}$ ($\bar{x}_T = 0.5$). From the preceding information it is evident that effect m is substantial only for the small number of eddy/vortices, whereupon for $m \rightarrow \infty$ numerical calculations coincide with exact solution. For the wings of the final lengthening the effect of the total number of eddy/vortices nN , by which is simulated the semirange of wing, it is shown for the rectangular and delta wings of different lengthening in Fig. 14.52-14.55.

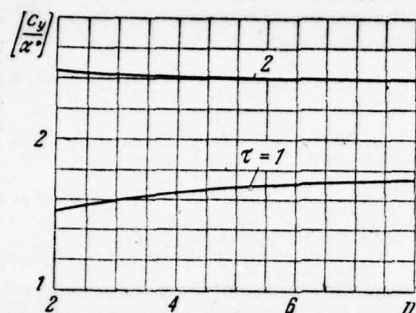


Fig. 14.46. Effect of the number of bound vortices n on the lift of delta wing $\lambda = 2.31$ with $N = 6$.

Page 351.

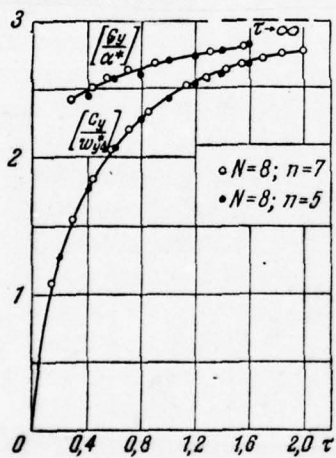


Figure 14.47

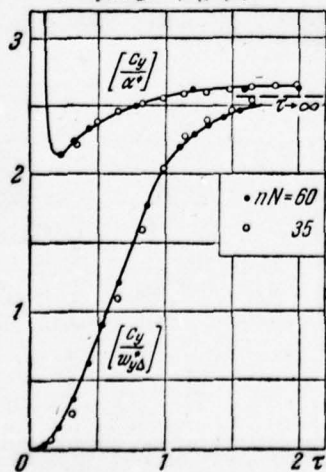


Figure 14.49

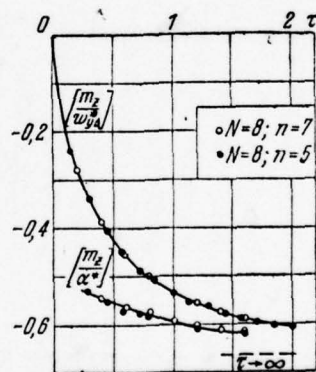


Figure 14.48

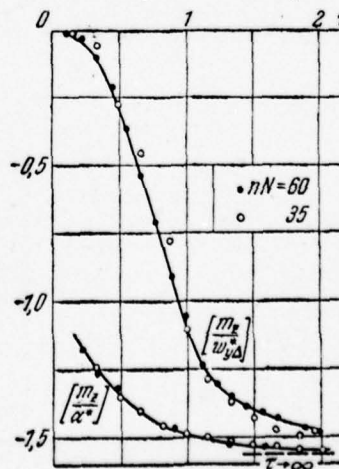


Figure 14.50

Fig. 14.47. Effect of the number of bound vortexes on the lift of rectangular wing $\lambda = 2.5$.

Fig. 14.48. Effect of the number of bound vortexes on the pitching moment of rectangular wing $\lambda = 2.5$ ($\bar{x}_T=0$).

Fig. 14.49. Effect of the number of bound vortexes on the lift of delta wing $\lambda = 2.5$.

Fig. 14.50. Effect of the number of bound vortexes on the pitching moment of delta wing $\lambda = 2.5$ ($\bar{x}_T=0$).

Page 352.

Centering was taken on the middle of root chord ($\bar{x}_T = 0.5$). The dot-dash straight line in Fig. 14.52, carried out from the origin of coordinates, corresponds to the wing of very small lengthening ($\lambda \rightarrow 0$).

Let us note one special feature/peculiarity, which must be born in mind during vorticity distribution on the fine/thin wing, when are calculated its apparent additional masses. If during the circulation flow about the direction, parallel to the spread/scope and wing

chord, were not equivalent and the character of the flow about the leading, trailing and the flank edges qualitatively it was distinguished, then in the case being investigated there will be different picture: all wing edges qualitatively flow themselves equally, of each of the edges, generally speaking, are formed infinite evacuation/rarefactions, etc. Therefore, when are examined, for example, forward/progressive oscillations (k_{22}) of square wing along axis Oy , perpendicular to wing plane, all sides are located under identical conditions and logical to take the identical number of bound vortexes both chordwise and on spread/scope. It is possible that during asymmetric motions even of square wing will be reveal/detect/exposed the need for in one direction taking a larger quantity of eddy/vortices, than on another. ; however, even, here we will not obtain the qualitative difference in the flow about the wing edges, as this is observed during circulation flow, i.e., during the calculation of the coefficients of aerodynamic derivatives.

The given materials show that the total number of eddy/vortices 60-100 usually provides practical convergence of numerical solution and obtaining reliable data on the coefficients of apparent additional masses.

In conclusion let us give the results of the investigation of the effect of the number of separations n chordwise of the wing of

very great lengthening ($\lambda = \infty$) with the being deflect/diverted control surface. The numerical calculations of transient functions for the δ -problem were performed with three numbers: $n = 8, 16, 32$ (Fig 14.56, 14.57).

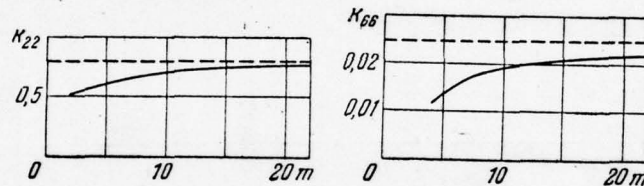


Fig. 14.51. The effect of the total number of eddy/vortices m on the coefficients of the apparent additional masses of wing $\lambda = \infty$; unbroken curves are numerical calculations, dotted line is exact solution.

Page 353.

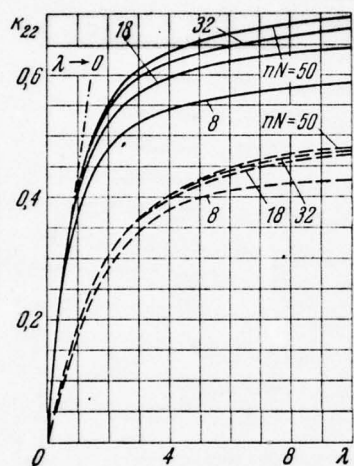


Figure 14.52.

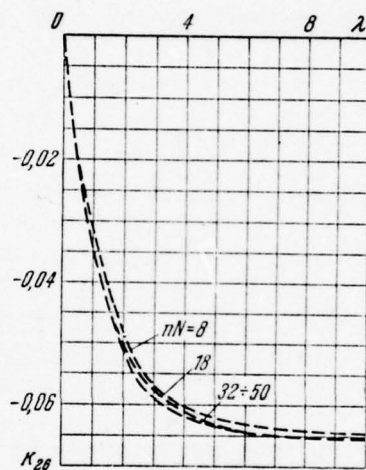


Figure 14.53.

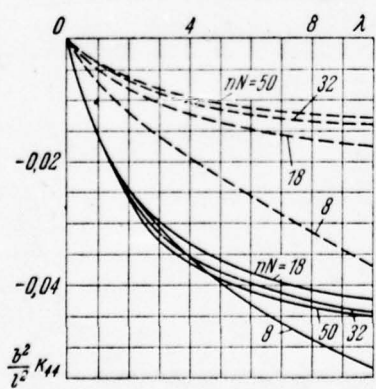


Figure 14.54.

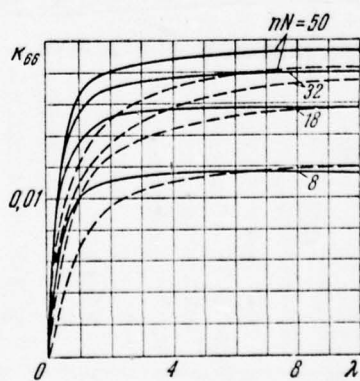


Figure 14.55.

Fig. 14.52. The effect of the number of eddy/vortices nN on the coefficient of apparent additional mass k_{22} ; unbroken curves are rectangular wing, dotted line is triangular.

Fig. 14.53. Effect of the number of eddy/vortices nN on the coefficient of apparent additional mass k_{26} for a delta wing. For rectangular wing $k_{26} = 0$.

Fig. 14.54. The effect of the number of eddy/vortices nN on the coefficient of apparent additional mass k_{44} ; unbroken curves are rectangular wing, dotted line is triangular.

14.55. The effect of the number of eddy/vortices nN on the coefficient of apparent additional mass k_{66} ; unbroken curves are rectangular wing, dotted line is triangular.

Page 354.

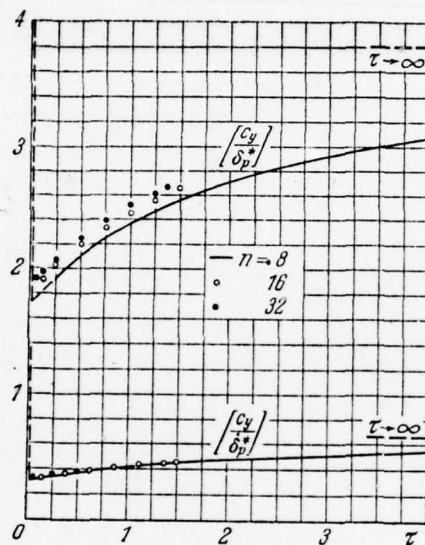


Figure 14.56.

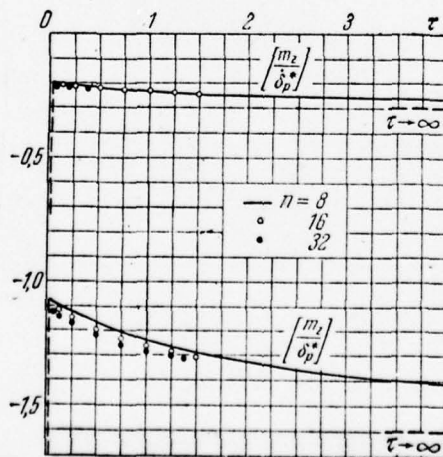


Figure 14.57.

Fig. 14.56. Effect of the number of eddy/vortices n on the transient function of airfoil lift $\lambda = -$ with control ($\bar{b}_p = 0.25$).

Fig. 14.57. Effect of the number of eddy/vortices nnn on the transient function of the pitching moment of wing $\lambda = -$ by control ($\bar{b}_p = 0.25, \bar{x}_T = 0$).

Page 355.

On these curve/graphs dotted line designated the limiting values of the corresponding transient functions ($r \rightarrow -$), obtained from the known solution of Simpson [2.44]. From the given materials it follows that with $n > 30$ numerical calculations reflect sufficiently well the real picture of phenomenon.

§5. Checking of numerical calculations with the aid of reciprocity theorem.

The reciprocity theorem and all consequences, which escape/ensue from it, as is known, are precise within the framework of linear theory (chapter VII). Is carried out below the control of the

aerodynamic characteristics, obtained by numerical calculations, with the aid of the consequences of reciprocity theorem.

With centering $\bar{x}_T = 0,5$ for the wings of any lengthenings, in particular, they occur of the equality

$$c_{y+}^{\omega_z} = m_{z-}^a, \quad c_{y+}^{\dot{\omega}_z} = m_{z-}^{\dot{a}}. \quad (14.1)$$

These relationship/ratios for rectangular wings (among other things for the wings of very small and infinite lengthening) are fulfilled with any n and N accurately; therefore they cannot serve as the method of the control of numerical calculations. Figure 14.58-14.61 gives the results of the numerical calculations, made for the direct/straight ($\chi_1 = 0$) and reverse/inverse ($\chi_0 = 0$) delta wings of different lengthening.

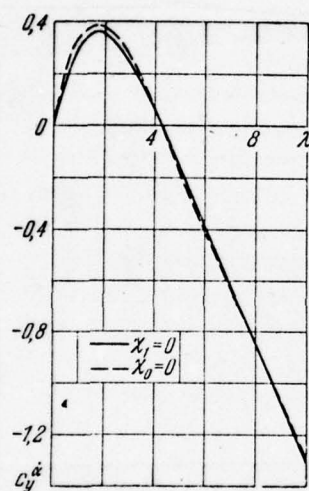


Fig. 14.58.

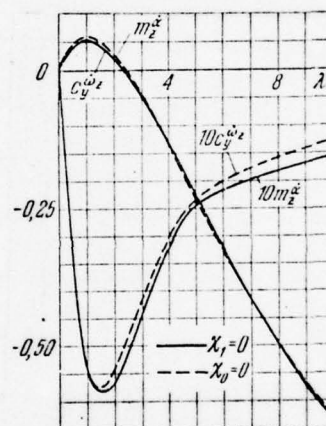


Fig. 14.59.

Fig. 14.58. Comparison of the calculations c_y^{α} for direct/straight and reverse/inverse delta wings.

Fig. 14.59. Comparison of the calculations $c_y^{\omega_z}$ and m_z^{α} for direct/straight and reverse/inverse delta wings ($\bar{x}_T = 0.5$).

356.

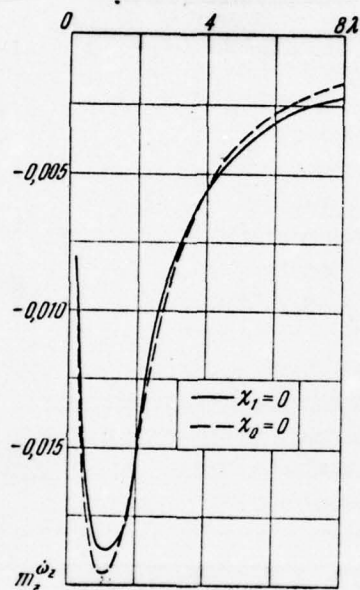


Figure 14.60.

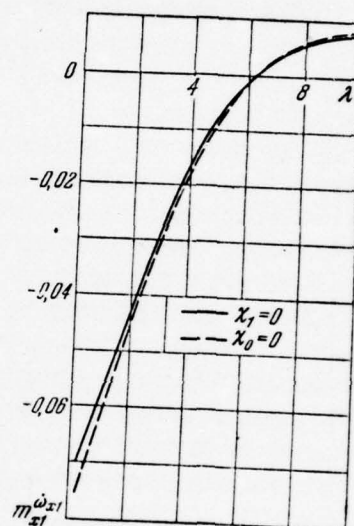


Figure 14.61.

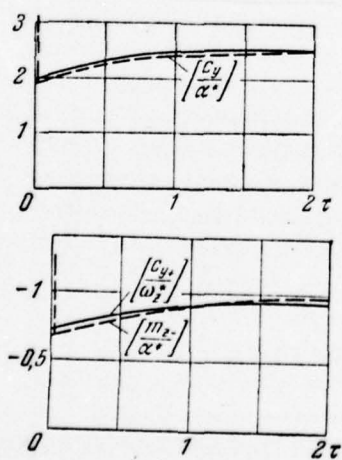


Figure 14.62

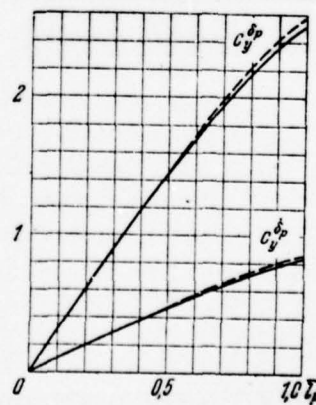


Figure 14.63.

Fig. 14.60. Comparison of the calculations $m_z^{\dot{\omega}_z}$ for direct/straight and reverse/inverse delta wings ($\bar{x}_T = 0.5$).

Fig. 14.61. Comparison of the calculations $m_{x1}^{\dot{\omega}_x}$ for direct/straight and reverse/inverse delta wings.

Fig. 14.62. Comparison of the calculations of the transient functions of straight line (unbroken curves) and reverse/inverse (dotted line) delta wings $\lambda = 2.5$ ($\bar{x}_T = 0$).

Fig. 14.63. Comparison of direct/straight calculation (unbroken curves) with the calculation according to the reciprocity theorem (dotted line) of rectangular wing $\lambda = 2.5$ with control ($\bar{\delta}_p = 0.5$).

Page 357.

In all investigated cases, and also on the basis of the results [1.29] is obtained sufficient accuracy of the made calculations. Let us note that all the given coefficients of the aerodynamic derivatives were calculated for the case, when for significant dimension is undertaken root wing chord, and reference point arranged on the middle of this chord.

Reciprocity theorem is valid not only during harmonic oscillations. With the arbitrary dependences of the kinematic parameters on time, in particular upon the entrance of wing into step gust, also occur precise equalities, which relate the total coefficients of direct/straight and reverse/inverse wings with any τ . Figure 14.62 gives the materials of the comparison of numerical calculations for a straight line and reverse/inverse delta wings ($\lambda = 2,5$) during a stepped variation in the angle of attack α . As we see, the coefficients of transient functions $[c_y/a']$ for direct/straight and inverse wings are equal. Is fulfilled also relationship/ratio $[c_y/\omega_z] = [m_z/a']$.

The use of a reciprocity theorem for wings with mechanization makes it possible to simplify the numerical calculations of such wings.

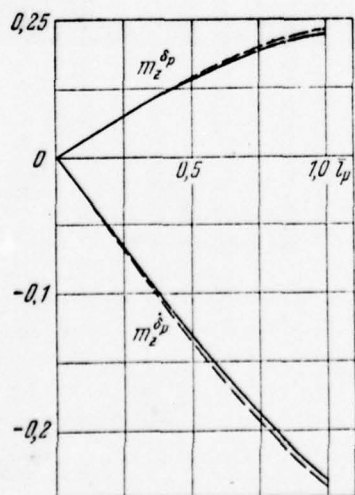


Figure 14.64.

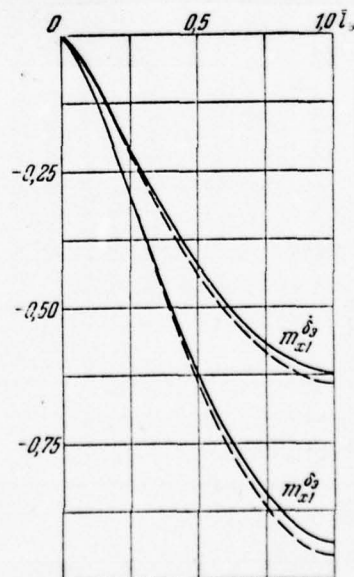


Figure 14.65.

Fig. 14.64. Comparison of direct/straight calculation (continuous curve) with the calculation according to the reciprocity theorem

(dotted line) of rectangular wing $\lambda = 2.5$ ($\bar{x}_T = 0.5$) with control ($\bar{b}_p = 0.5$).

14.65. Comparison of direct/straight calculation (unbroken curves) with the calculation according to the reciprocity theorem (dotted line) of rectangular wing $\lambda = 2.5$ with aileron ($\bar{b}_a = 0.5$).

Page 358.

Having circulation distribution according to the span of reverse/inverse wing, it is not difficult to obtain the total coefficients of the aerodynamic derivatives of straight wing with mechanization (chapter VII). As an example Fig. 14.63-14.65 gives the dependences of derivatives $c_y^{\delta_p}, c_y^{\delta_a}, m_z^{\delta_p}, m_z^{\delta_a}, m_{x1}^{\delta_p}, m_{x1}^{\delta_a}$ of the given spread/scope of control $\bar{l}_p = 2l_p/l$ and aileron $\bar{l}_a = 2l_a/l$ respectively. Examined rectangular wing ($\lambda = 2.5$) with relative chord of control $\bar{b}_p = 0.5$ (aileron $\bar{b}_a = 0.5$) for the case, when the origin of coordinates is located on the middle of wing chord. For above wing indicated with mechanization was carried out direct/straight calculation of derivatives, determining the effectiveness of this mechanization, and also the calculation according to reciprocity theorem. The agreement of two methods of the calculation in question turns out to be completely satisfactory.

§6. Checking of the calculations with the aid of the theorem of momentum and Duhamel integral.

As has already been indicated, the application/use of a theorem of momentum makes it possible to integral control the behavior of transient function in all range of change τ . As an example is carried out the comparison of derivatives c_y^a , obtained from direct/straight numerical calculation also according to theorem of momentum. Figure 14.66 gives dependence $c_y^a = f(\lambda)$ for the rectangular wings of different lengthening ($\lambda = 0.5-5.0$). The given comparison shows the completely satisfactory coincidence of each data. The use of a Duhamel integral makes it possible mutually to control the accuracy of the numerical calculations of transient functions $[c(\tau)/q_i^*]$, and also the coefficients of aerodynamic derivatives $c^{ai}(p^*)$. Therefore in many instances along with exact solutions are given the results of the numerical calculations of the coefficients of aerodynamic derivatives depending on Strouhal number for a plate ($\lambda = \infty$) (see Fig. 13.2-13.5) and for the rectangular wings of different lengthening (see Fig. 14.26-14.33). There are plotted/applied the points, obtained by the calculation according to Duhamel integral. As initial data here served the corresponding transient functions.

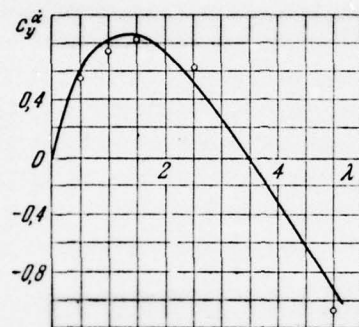


Fig. 14.66. The comparison of numerical calculation (is curve) with the calculation according to the theorem of momentum (point) of rectangular wings.

Page 359.

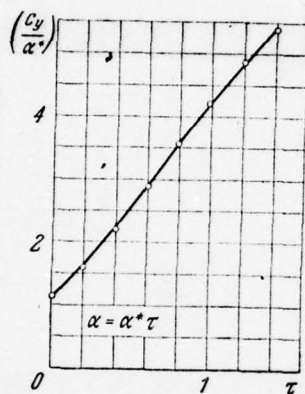


Figure 14.67.

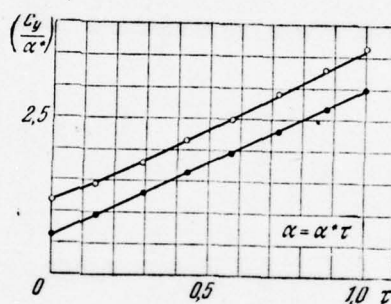


Figure 14.68.

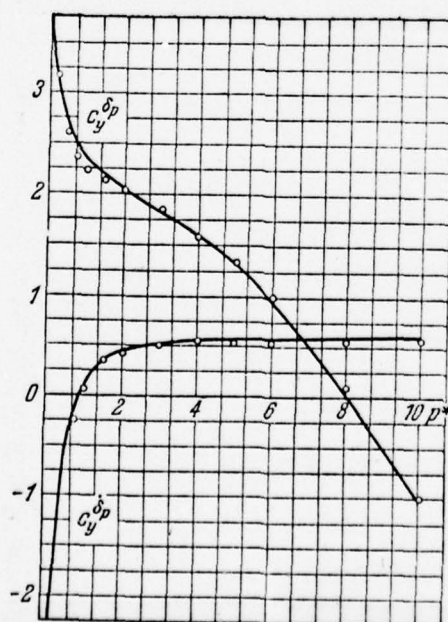


Figure 14.69.

Fig. 14.67. The comparison of numerical calculation (is curve) with the calculation according to Duhamel integral (point) for a wing $\lambda = -$.

Fig. 14.68. The comparison of numerical calculation (curves) with the calculation according to Duhamel integral (points: white are rectangular wing, black are triangular).

Fig. 14.69. Comparison of exact solution (curves) with the calculation according to Duhamel integral (point) for a wing $\lambda = -$ with control ($\delta_p = 0.25$).

Page 360.

By knowing the reaction of wing to stepped perturbation, with the aid of transient function and Duhamel integral it is possible, as was indicated above, to pass to the arbitrary law of a change in the kinematic parameters. For an example Fig. 14.67, 14.68 give the results of the direct/straight numerical calculation of function (c_y/α^*) for the case, when the angle of attack of wing changes according to linear law $\alpha = \alpha^* \tau$. On these curve/graphs are plotted/applied the points, obtained from the calculation with the use of transient function $[c_y/\alpha^*]$ and Duhamel integral. Are examined three wings:

plate $\lambda = \infty$ (Fig. 14.67), rectangular and delta wings with lengthening $\lambda = 2.5$ (Fig. 14.68). Given data show that the direct/straight numerical calculation of transient function (c_y/α^*) for the law of the growth/build-up of gust being investigated completely satisfactorily coincides with the calculation according to Duhamel integral.

Exact solution of δ -problem for an airfoil/profile with control in the incompressible medium is given by Theodorsen and Kussner [2.5], [2.12]. Having for this case transient functions (see Fig. 14.56, 14.57), it is possible with the help of Duhamel integral to find numerically coefficients of aerodynamic derivatives $c_y^{\delta p}$, $c_z^{\delta p}$, $m_z^{\delta p}$, $m_z^{\delta p}$ in all range of Strouhal numbers ($p^* = 0 - \infty$). The results of such a calculation ($\bar{b}_p = 0.25$) and its comparison with the exact solution indicated given in Fig. 14.69 and 14.70.

87. Comparison of experimental and calculated data.

Experimental data on stationary wing characteristics are sufficiently numerous, which creates known difficulty in reasonable selection and the analysis of this material.

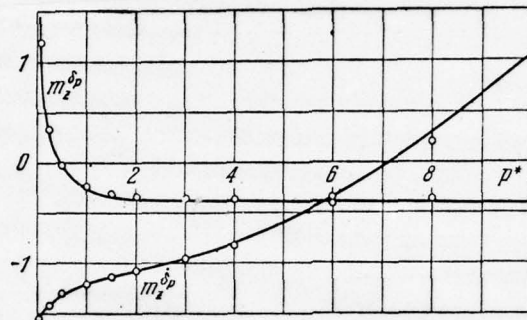


Fig. 14.70. Comparison of exact solution (curves) with the calculation according to Duhamel integral (point) for a wing $\lambda = \infty$ with control ($\delta_p = 0.25$, $\bar{x}_T = 0$).

Page 361.

Even greater difficulties from this viewpoint appear during the comparison of experimental and theoretical data for unsteady characteristics, since hardly ever known test conditions, the complete data on models, the accuracy and the recurrence of the

obtained results and so forth / however, after taking the large number of the most reliable experimental data and after comparing them with calculated, it is possible to conduct the cross check of those and other materials, or to derive conclusion of the authenticity of the basic condition/positions of theory and field of its application/use.

The comparison of experimental and theoretical data for small harmonic oscillations rigid wings (amplitude $\alpha^* = 3-5^\circ$) was carried out for the following total aerodynamic characteristics: the derived c_y^a (Fig. 14.71), dimensionless coordinate of the focus \bar{x}_P (Fig. 14.72), of derivative $m_{\dot{\alpha}}^{(0)}$, determining roll damping of wing (Fig. 14.73), and also for the combination of derivatives $m_z^{\omega_z} + m_z^{\dot{\alpha}}$, by that determining the longitudinal attenuation of wing during rotary oscillations (Fig. 14.74).

The procedure of the experimental determination of the coefficients of aerodynamic derivatives is described in chapter VIII, . each point on curve/graphs (Fig. 14.71-14.74) corresponds to the determined wing; therefore this diagram is related to dozens wings of different planform. The nearer lie/rest the plotted points to straight line, the the coincidence of calculation and experimental data.

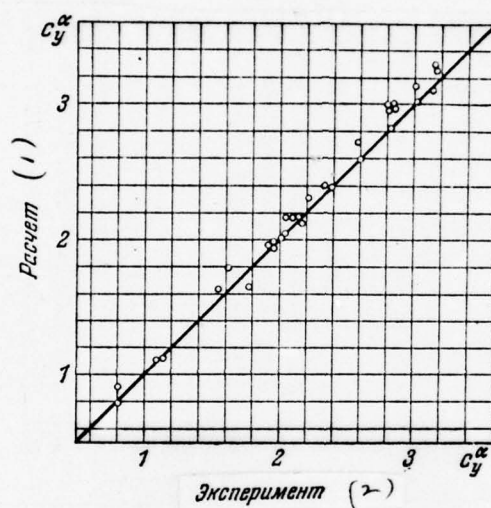


Fig. 14.71. Comparison of calculated and experimental data for different wings, $\alpha_0 = 0$.

Key: (1). Calculation. (2). Experiment.

Page 362.

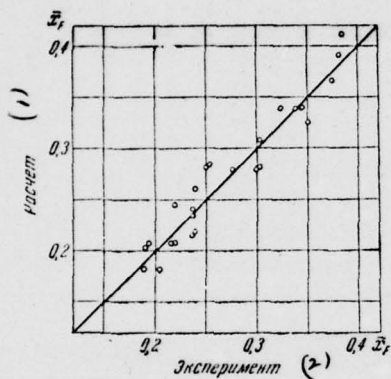


Fig. 14.72.

Fig. 14.72. Comparison of calculation and experimental data for different wings, $\alpha_0 = 0$.

Key: (1). Calculation. (2). Experiment.

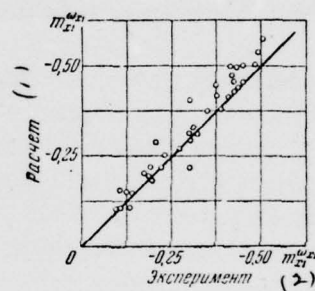


Fig. 14.73.

Fig. 14.73. Comparison of calculated and experimental data for different wings, $\alpha_0 = 0$.

Key: (1). Calculation. (2). Experiment.

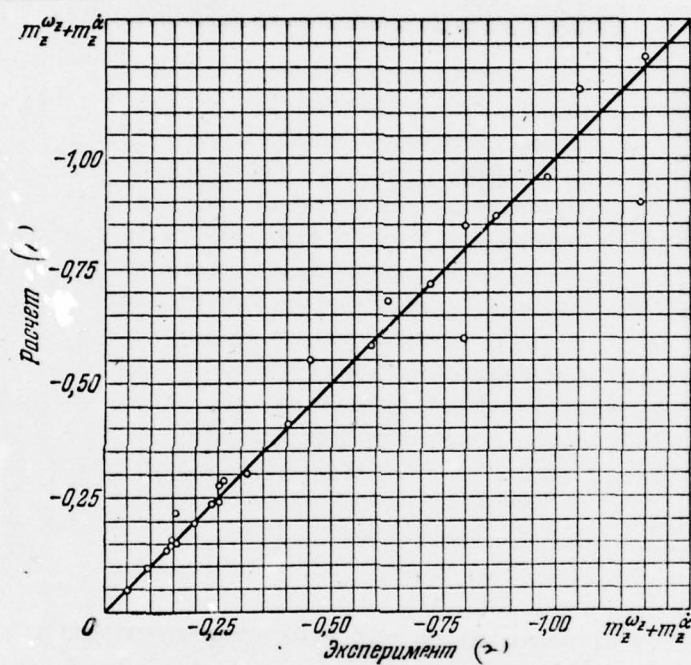


Fig. 14.74. Comparison of calculated and experimental data for

different wings, $\alpha_0 = 0$.

Key: (1). Calculation. (2). Experiment.

Page 363.

Best of all converge these data for the lift effectiveness of wing - here the scatter of points smallest. Larger scatter is observed for moment characteristics - they are determined with smaller accuracy; however, the conformity of the calculation with experiment can be considered sufficiently satisfactory. The given materials can be used for the approximate determination of the field of the applicability of linear theory [169] and [1.72].

During harmonic rolls the best coincidence of experimental and calculated data is obtained for fine/thin wings at small mean incidences α_0 . From an increase in the thickness of the wing profile and mean incidence α_0 the experimental data all more diverge from linear theory due to the redistribution of loads in end wing sections. Of delta wings occur the disruption/separations and incidence/drop of the lift effectiveness of end sections, while of rectangular low-aspect-ratio wings - an increase in the load at end/leads in comparison with the data of linear theory. Better/best

coincidence of the calculation with experiment is observed for delta wings. This is explained by the facts that the secondary forces, occurring on the tips of delta wing, due to the low value of end chords play smaller role than of rectangular wing (Fig. 14.75).

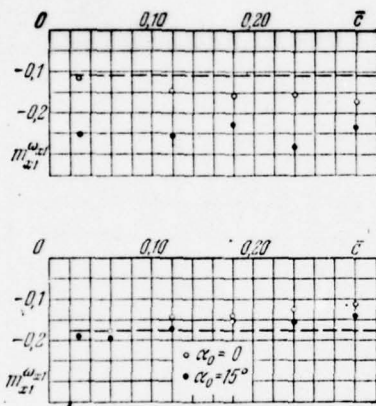


Fig. 14.75

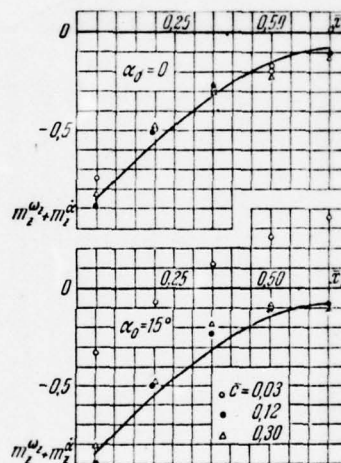


Fig 14.76.

Fig. 14.75. Comparison of calculated and experimental data for rectangular ($\lambda = 1.0$, the upper curve/graph) and triangular ($\lambda = 2.31$, lower curve/graph) wings. Points are an experiment, dotted line

is linear theory.

Fig. 14.76. Comparison of the calculated (curves) and experimental data (point) for a rectangular wing $\lambda = 1.0$.

Page 364.

Of the wings of very small lengthenings with the contractions, close to unity, in actuality end wing sections are loaded more than it gives linear theory, and the experimental values of coefficient m_{x1}^{ω} more theoretical.

The given in Fig. 14.76 data for combination $m_z^{\omega} + m_z^{\alpha}$ testify to a good coincidence of theory with experiment for the wings of the average/mean thickness in considerable range α_0 , and also for fine/thin wings at zero angle of attack ($\alpha_0 = 0$). In these cases the wings flow themselves smoothly in all modes of oscillations. The greatest disagreement of experimental and theoretical data is observed for fine/thin wings at the large values of mean incidence ($\alpha_0 = 15^\circ$); on stern heaviness of these wings are obtained even the mode/conditions of auto-oscillations. This is connected with the fact that in the forward section of the fine/thin wing is sufficiently considerable flow separation. The studies of the structure of flow

around of the wing showed that the area of disruption/separation on suction side of wing during oscillations is changed on angles of attack. Figure 14.77 shows greatest and smallest to the area of disruption/separation on fine/thin and thick rectangular wings ($\lambda = 1$) during the fluctuations of relatively mean incidence $\alpha_0 = 15^\circ$ with amplitude $\alpha^* = 5^\circ$. The data of experiment for very thick wings ($\bar{z} = 0.3$) weakly depend on mean incidence and are sufficiently close to the results of linear theory. The greatest disagreement of theory with experiment is observed on bow heavinesses. This is explained by the small area of disruption/separation for thick wings; this region is arranged/located in trailing section of wing and little is changed on angles of attack.

Thus, the conducted investigations of the total coefficients of aerodynamic derivatives and structure of the flow around of the wing of flow showed that for the incompressible fluid most essential is the hypothesis of smooth flow about the oscillating wing.

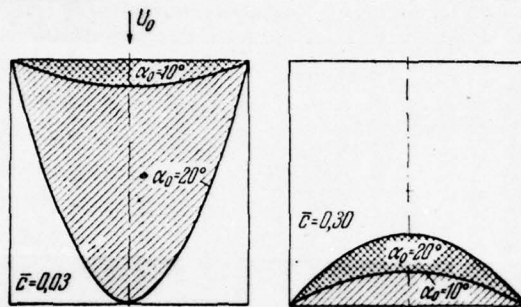


Fig. 14.77. Areas of disruption/separation on rectangular wing $\lambda = 1.0$.

Page 365.

If it is fulfilled, then theory gives the results, close to experimental, otherwise (presence of flow separation) is observed the disagreement of experimental and calculated data.

In contrast to the harmonic oscillations, for which there is a

sufficiently large quantity of experimental data, experiments for the different types of aperiodic motion are conducted very rarely. This is explained by the serious technical difficulties, connected from of this type by experiments.

In chapter VIII is described the method of the measurement of instantaneous pressures and subsequent determination of aerodynamic forces and torque/moments. According to the method indicated was tested rigid rectangular wing with lengthening $\lambda = 1.0$ and fine/thin symmetrical airfoil/profiles with thickness ratio $\bar{t} = 0.06$. Figure 14.78 depicts the law of a change in the angle of attack during the rotation of this wing, there are plotted/applied experimental points for the lift coefficients (c_y/α^*) and of pitching moment (m_z/α^*) depending on dimensionless time τ . Calculated curves are obtained on the basis of the methods of linear theory, presented in chapter XI. The given writing of the law of motion $\alpha(\tau)/\alpha^*$ will coincide with value (c_y/α^*), the designed in stability hypothesis. Therefore its difference from actual values ($c_y(\tau)/\alpha^*$) gives error during the calculation of this characteristic according to stability hypothesis.

Let us examine experimental data during noncirculating flow. The apparent additional masses are determined from experiment by the different methods, which are connected with the study of the oscillations of bodies on the spot in continuous medium (air, water

etc.) and in vacuum. Description of these methods is partially given in chapter VIII and in [1.47].

Is carried out below the comparison of some calculation data with the experimental, obtained different authors during the sufficiently prolonged period of time (1930-1950). Figure 14.79 gives given data on the apparent additional masses λ_{22} of the rectangular wings of different lengthenings. The values indicated are referred to the apparent additional mass of the wing of very great lengthening ($\lambda = \infty$); therefore during an increase in the lengthening this relation approaches unity.

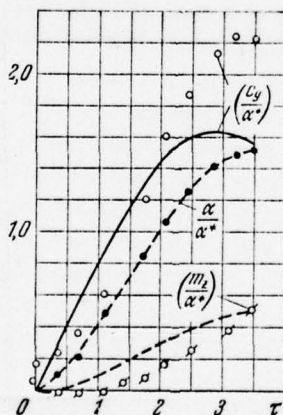


Fig. 14.78. Comparison of calculation (curves) and experimental (point) data for the rectangular wing, which accomplishes rotation relative to axis Oz , $\bar{x}_T = 0.5$.

Page 366.

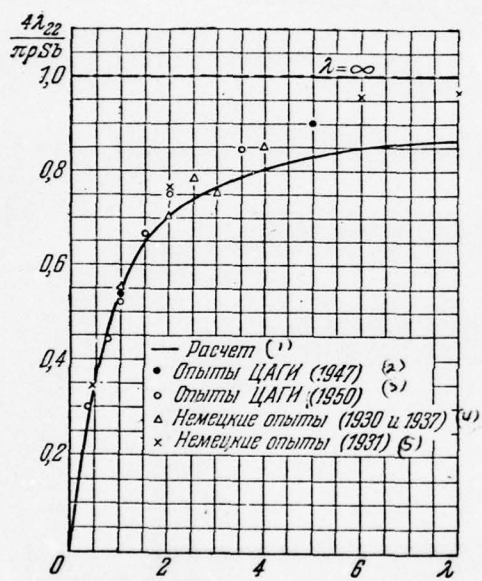


Figure 14.79.

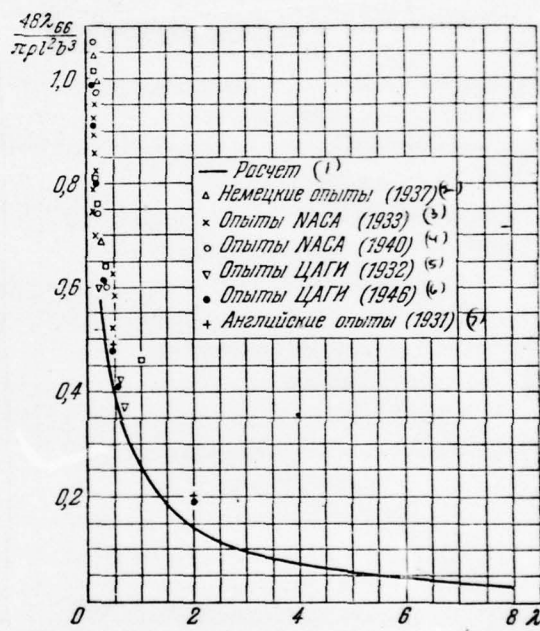


Figure 14.80.

Fig. 14.79. Comparison of calculated and experimental data for the

apparent additional masses λ_{22} of rectangular wings.

Key: (1). Calculation. (2). Experiments of TsAGI [ЦАГИ - Central Institute of Aerohydrodynamics im. N. Ye Zhukovskiy (1947)]. (3). Experiments of TsAGI (1950). (4). Nemeckie opyty (1930 and 1937). (5). German experiments (1931).

Fig. 14.80. Comparison of calculated and experimental data for the apparent additional masses λ_{66} of rectangular wings ($\bar{x}_T = 0.5$).

Key: (1). Calculation. (2). German experiments. (3). Experiments of NASA. (4). Experiments of NASA. (5). Experiments of TsAGI. (6). Experiments of TsAGI. (7). English experiments.

Page 367.

In [1.47] are contained the experimental data, which characterize the torque/moment M_z , which acts on rectangular plate, when it completes rotary oscillations relative to axis Oz . In Fig. 14.80 are compared experimental and calculated data on the dimensionless coefficient, examined [1/47] and proportional to value, k_{66} . For sweptback wings without contraction ($\eta = 1$) with lengthening $\lambda = 1$ is carried out the

comparison of the calculation with experiment for the apparent additional mass λ_{22} (Fig. 14.81). In this case the comparison is conducted for the relation $\lambda_{22}(\alpha_0)/\lambda_{22}(0)$ depending on sweep angle α_0 .

As can be seen from the given materials, in spite of the sufficiently complex phenomenon, which is in actuality, and the sufficiently simple diagram, which is accepted as basis during calculations of the coefficients of apparent additional masses, conformity between experimental and calculated data as a whole satisfactory.

Above was carried out the comparison of experimental and calculated data for a rigid wing with circulation and noncirculation flow. Let us examine the theoretical and experimental values of aerodynamic characteristics for different wings with control. Figure 14.82 schematically depicts the rectangular, swept and delta wings of the lengthenings $\lambda = 2.1$, for which R. A. Zasolov and N. N. Fominoy obtained experimental data. The geometric parameters of the investigated models are given in table 14.2.

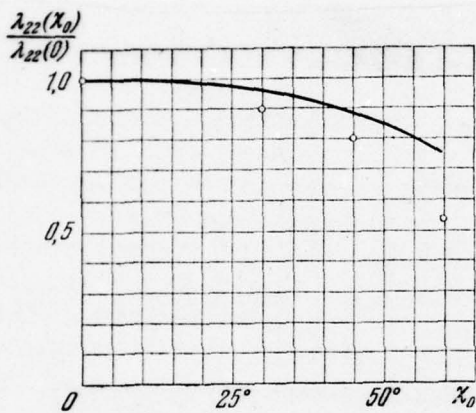


Figure 14.81.

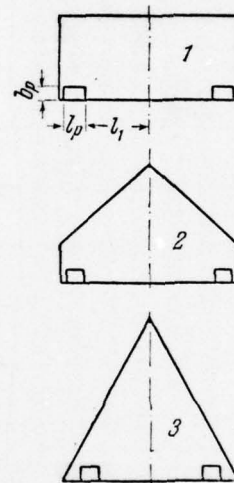


Figure 14.82.

Fig. 14.81. The comparison of calculation (is curve) and experimental (point) data for apparent additional masses λ_{22} sweptback wings.

Fig. 14.82. Diagram of the investigated wings.

Page 368.

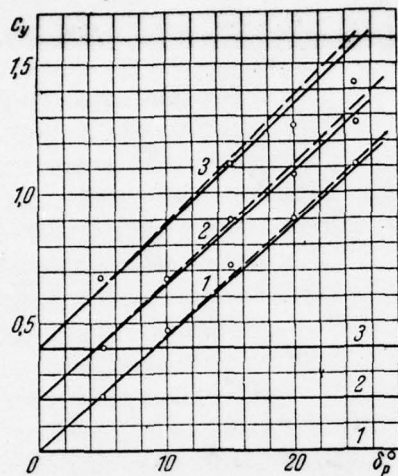


Figure 14.83.

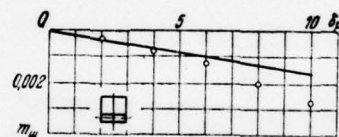
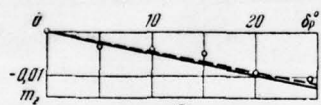
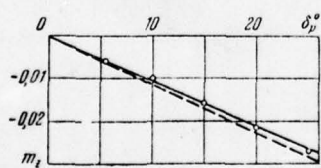


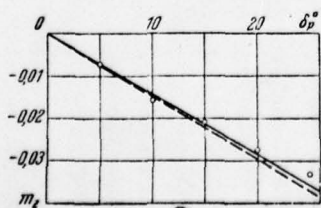
Figure 14.85.



(1)

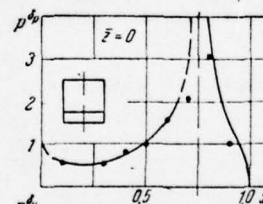


(2)

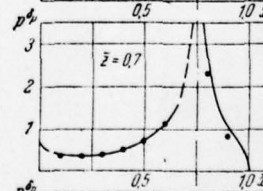


(3)

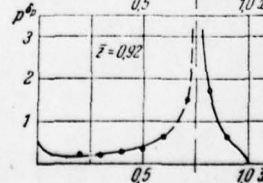
Figure 14.84.



$\bar{z} = 0$



$\bar{z} = 0.7$



$\bar{z} = 0.92$

Figure 14.86.

Fig. 14.83. The comparison of calculation (curves) and experimental (point) data for wings with control; unbroken curves are direct/straight calculation, dotted line - according to reciprocity theorem.

Fig. 14.84. The comparison of calculation (curves) and experimental (point) data for wings with control; unbroken curves are direct/straight calculation, dotted line - according to reciprocity theorem, $x_T = 0.5$.

Fig. 14.85. The comparison of calculation (is curve) and experimental (point) data for a wing with control.

Fig. 14.86. Comparison of calculation (curves) and experimental (point) data for a rectangular wing $\lambda = 1$.

Page 369.

The results of the comparison of experimental and calculation data for the wings indicated in the form dependences $c_y(\delta_p)$, $m_z(\delta_p)$ are given in Fig. 14.83, 14.84. Numerical calculations are carried out by direct method also according to reciprocity theorem. As is evident, the selected vortex/eddy diagram provides obtaining reliable

calculation data. In Fig. 14.85 and 14.86 is conducted the comparison of calculation and experimental data on the fine/thinner characteristics: hinge-moment coefficients (m_m) and the distributed characteristics (aerodynamic derivative load $p^{\delta p}$). The values indicated were determined for the wing of lengthening $\lambda = 1$ with control $b_p = 0,25$. As is known, the distributed characteristics they have peculiarities on the axis of control (theoretically they turn here into infinity). The given materials attest to the fact that the network, based on the replacement of wing by discrete eddy/vortices, makes it possible to determine with sufficient accuracy and these characteristics.

Table 14.2.

(1) Крыло	η	b_p/b	$2l_p/l$	$2l_1/b$
1	1	0,217	0,238	0,705
2	3	0,142	0,238	0,705
3	∞	0,106	0,238	0,546

Key: (1). Wing.

Page 370.

Part III.

High subsonic speeds ($0 < M < 1$)

Introduction.

The most difficult among unsteady problems airfoil theory is the problem of the flow-field analysis of wing at high subsonic speeds ($0 < M < 1$). This is connected with the fact that, unlike the incompressible medium, here the disturbance/perturbations are spread at the final velocity. Therefore it is necessary to consider the delay of the disturbance/perturbations, which come in into the point in question from any cell/element of wing or vortex sheet. But if at supersonic speeds, where also occurs the delay of disturbance/perturbations, the latter are spread only downstream within Mach cone, then here they they reach any point of space. Therefore, for example, entire/all vortex sheet, which is formed after wing, any moment of time affects flow around of the wing. This

fact substantially complicates the solution of problem as compared with the cases $M=0$ (incompressible medium) and $M>1$ (supersonic flow). Without being stopped on detailed survey/coverage of all investigations in the problem (it is contained in [1.7] in question, [1.9], [2.53]), let us note here only the state of question, most characteristic of the published works, or briefly let us pause at the ideas of those methods which are set forth by authors in this monograph.

The problem of the harmonic oscillations of the airfoil/profile, which accomplishes forward motion at constant velocity, obtained most complete solution. Unlike incompressible medium, here it is impossible to obtain solution in the locked form. Therefore they were utilized two methods of its determination. one of them, proposed by Reisner [2.25], Haskind [1.46], Timman [2.34], utilizes transformations of differential equations for the velocity potentials or accelerations to elliptical coordinates and resolution of solution in infinite series in Mathieu functions. The results of the calculations for an airfoil/profile are contained in a series of works, most complete of them in [2.35].

Page 371.

Numerical calculations according to this method are very bulky, since

solution is represented in the form of infinite series, and the number of terms whose calculation is necessary for providing a sufficient accuracy, changes over wide limits depending on the Mach numbers and Strouhal. Therefore for the flow-field analysis of wings of the final spread/scope the method indicated propagation did not receive. The second method, utilized with those or other changes in the large number of works, is based on the numerical solution of the singular integrodifferential equations, which relate normal velocity on wing with the intensity of the distribution of the special feature/peculiarities (connected vorticity layer, dipoles), which replace wing. First it was proposed for Possio's infinite plate [2.6] and somewhat an improved form was used for the performance calculation of the oscillating plate of infinite span [2.11]. Subsequently by the works of a series of the researchers this method was developed in the case of finite-span wings. In it is examined the continuous distribution of special feature/peculiarities on wing and it is conducted the approximation of the sufficiently complex nucleus of equation. Then, assuming that the special feature/peculiarity of leading wing edge is retained the same as of airfoil/profile, they are assigned by the law of a change in the intensity of special feature/peculiarities chordwise and spread/scope. The coefficients of the expansion indicated determine, satisfying or boundary conditions at several points of wing surface [2.38], [2.42], [2.43], [2.49], or to the integral relationship/ratios, derived from variation

principles [2.51]. This approach makes it possible to calculate the unsteady characteristics of the harmonically oscillating wings of a comparatively simple planform, then not only with very small Strouhal numbers ($p^* \rightarrow 0$), but also with final, although those which were limited.

The common/general/total and complex unsteady problems are those, in which are studied the arbitrary time dependences. When are investigated steady-state oscillations of wing, time finally it is possible to exclude from examination. Here dependences on time play the significant role, for example, in the process of the calculation it is necessary to find vortex/eddy wing wake. Therefore plane-parallel problem becomes three-dimensional, and three-dimensional/space, that corresponds to finite-span wing, four-dimensional. Some numerical solutions, constructed for the aperiodically driving in subsonic flow plate of infinite span, are given in works [2.23], [2.26], [2.36]. The transient functions of aerodynamic loadings can be determined by the coefficients of aerodynamic derivatives with the aid of Fourier integral [2.29]. However, this path requires the knowledge of aerodynamic characteristics over a wide range of Strouhal numbers (strictly speaking, with $0 \leq p^* \leq \infty$).

It should be noted that the determination of aerodynamic characteristics above methods indicated requires for each new Strouhal number of the complete solution to boundary-value problem.

Into III parts of the present monograph for a problem of the harmonic aperiodic motions of wings at subsonic speeds are developed the numerical methods, presented for the incompressible medium in part II. They are based on the replacement of the continuous layer, which simulates wing, discrete by special feature/peculiarities (oblique horseshoe vortices) [1.29]. Here it is not necessary to make supplementary assumptions about the character of a circulation control chordwise and spread/scope. This, in particular, makes it possible to calculate flow around of the wings not only idle time, but also complex planform (wings of the variable geometry, with curvilinear edges so forth). With harmonic time dependences, the film of free vortices, which bypass from those which were connected, stretches to infinity. In the particular case of harmonic oscillations with small Strouhal numbers ($p \rightarrow 0$) the problem is reduced to the solution of the problem of the harmonic oscillations of the converted wing in incompressible medium [1.79].

During aperiodic motions the continuous processes are replaced

stepped. At the determined (calculated) moments of time occurs an abrupt circulation control of bound vortexes and from them they converge free vortices [1.85]. Since in the compressed medium of disturbance/perturbation are spread with the final velocity, here necessary to examine entire process of formation/education and removal/drift of free vortices, but not only those positions, which correspond to the calculated moments of time as in the incompressible fluid. One should note the published recently interesting investigations of V. Ye. Baskin in the theory of eddy/vortices [1.83], [1.89].

Page 373.

Chapter XV.

Method of the calculation of the coefficients of aerodynamic derivatives with $p \rightarrow 0$.

§1. Basic transformation. The geometric parameters of the converted wing.

If flight speed U_0 is low as compared with the speed of sound, then the medium, in which moves the body, it is possible to consider incompressible with $p \rightarrow 0$. This escape/ensues from the fact that the compressibility of the medium virtually will not be exhibited, if the disturbed pressures p' , caused by the motion of body, are very small in comparison with pressure in the undisturbed medium p_∞ , i.e. $p'/p_\infty \ll 1$. Noting the density of undisturbed flow by index ∞ , we can write

$$\frac{\rho_\infty U_0^2}{2p_\infty} = \frac{\kappa}{2} M^2,$$

consequently,

$$\frac{p'}{p_\infty} = \frac{\kappa}{2} \bar{p} M^2, \quad (15.1)$$

where $\bar{p} = 2p'/\rho_\infty U_0^2$ - pressure coefficient. This coefficient in essence depends on the coordinate of the point, at which it is determined, the form of body and its position in flow. Coefficient \bar{p} comparatively barely depends on M at subsonic speeds; therefore increase M for the assigned wing always will lead to an increase $|p'/p_\infty|$. Furthermore, with an increase in the thickness of body and its angle of attack at those which were fix/recorded M the maximum value of the absolute value \bar{p} will grow/rise, value $|p'/p_\infty|_{\max}$ - increase, the compressibility effect of the medium will be exhibited with smaller numbers M . Thus, the compressibility effect of the medium it manifests itself the more powerful, the greater the number M the incident flow and the more powerful the disturbance/perturbation, produced by body with small numbers M .

Page 374.

Within the framework of linear theory the account of the compressibility effect of the medium in certain cases of the unsteady motion of wing can be produced, by reducing the problem to flow of the incompressible fluid about other certain wing. Further it will be shown, that in the case of the motion of wing as rigid body and the strains of its surface along harmonic laws with Strouhal number,

which vanishes, it is possible in the incompressible fluid to fit this lifting surface and such motions, that the solution of problem for it will satisfy all conditions of problem in gas.

Let us examine the fine/thin slightly bent/curved lifting surface being deformed, which moves forward/progressively at average speed U_0 and accomplishing in this case small harmonic rotary and forward/progressive oscillations. Let us take standard rectangular system of coordinates connected with lifting surface (Fig. 15.1). Its beginning let us place on the leading edge/nose of root chord, plane Oxz is consistent with the plane of lifting surface, axis Ox is directed forward, axis Oz - to the right along spread/scope, axis Oy - upward. Instead of the motion of wing in the physical space of the compressible gas, let us examine the motion of the converted wing in the fictitious (auxiliary) space, filled by the incompressible fluid. The coordinates of fictitious space x_M, y_M, z_M are connected with the coordinates of the physical space by the formulas

$$x = kx_M, \quad y = y_M, \quad z = z_M, \quad b = kb_M, \quad k = \sqrt{1 - M^2}. \quad (15.2)$$

Let us introduce the dimensionless coordinates

$$\left. \begin{aligned} \xi &= \frac{x}{b}, & \eta &= \frac{y}{b}, & \zeta &= \frac{z}{b}; \\ \xi_M &= \frac{x_M}{b_M}, & \eta_M &= \frac{y_M}{b_M}, & \zeta_M &= \frac{z_M}{b_M}, \end{aligned} \right\} \quad (15.3)$$

for which of (15.2) we have the obvious relationship/ratios

D-A049 000

FOREIGN TECHNOLOGY DIV WRIGHT-PATTERSON AFB OHIO

F70 173

A WING IN AN UNSTEADY GAS FLOW. PART 2, (U)

SEP 77 S M BELOTSEKOVSKIY, B K SKRIPACH

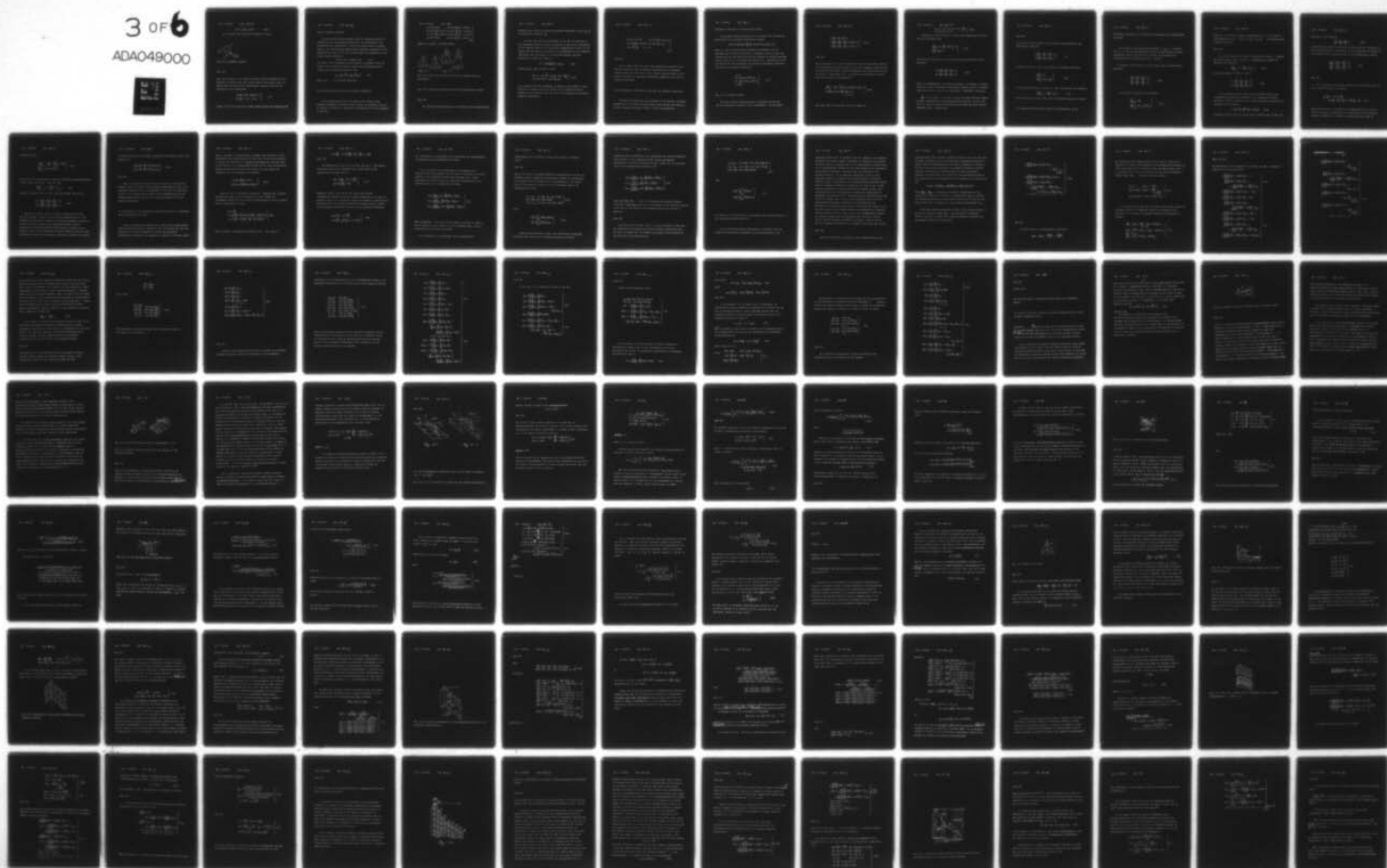
FTD-ID(RS)T-1534-77-PT-2

NL

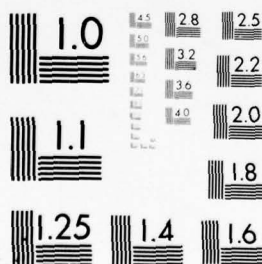
UNCLASSIFIED

3 of 6

ADA049000



ADA049000



$$\xi_M = \xi, \quad \eta_M = k\eta, \quad \zeta_M = k\zeta. \quad (15.4)$$

Let us change wing planform according to (15.2).

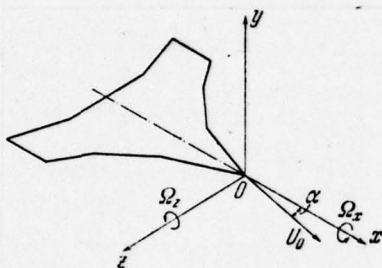


Fig. 15.1. Coordinate system.

Page 375.

Then for the wing of the complex planform, which is assigned by the equations of leading edge and current chord in the form (1.10), we obtain that the form of the corresponding converted wing will be determined by the dependences

$$\left. \begin{aligned} \xi_{0M}(\zeta_M) &= \frac{1}{k} \xi_0(\zeta), \quad \bar{b}'_M(\zeta_M) = \bar{b}'(\zeta); \\ b'_M &= \frac{b'_M}{b_M}, \quad b' = \frac{b'}{b}, \quad b_M = \frac{b}{k}. \end{aligned} \right\} \quad (15.5)$$

Figure 15.2 in the form of an example shows initial and converted the

wings of complex planform.

For wings with direct/straight edges the planform usually is assigned by the dimensionless parameters: the lengthening λ , by reverse/inverse contraction $\bar{\eta}$ and by the sweep angle of leading edge χ_0 . The corresponding dimensionless geometric parameters of the converted wing (Fig. 15.3) are connected with the parameters of the initial wing as follows:

$$\lambda_M = k\lambda, \quad \bar{\eta}_M = \bar{\eta}, \quad \lambda_M \operatorname{tg} \chi_{0M} = \lambda \operatorname{tg} \chi_0. \quad (15.6)$$

The strain of the converted lifting surface is connected with the strain of the calculated lifting surface by relationship/ratios (15.4), and its equation takes the form

$$\eta_M = f_0\left(\xi_M, \frac{\zeta_M}{k}\right) + f_\delta\left(\xi_M, \frac{\zeta_M}{k}\right)\delta_M(t), \quad (15.7)$$

where f_0, f_δ - the assigned functions.

§2. Relationship/ratios between kinematic parameters.

Let us study motion and the strains of the initial wing, kinematic parameters of which (2.19), (2.20), in accordance with §2 of chapter V, without the limitation of generality it can be assigned in the form

$$\left. \begin{aligned}
 q_1 = \alpha(t) &= \alpha^* \cos pt, & \dot{q}_1 = \dot{\alpha}(t) &= \frac{d\alpha}{dt} \frac{b}{U_0} = -p^* \alpha^* \sin pt, \\
 q_2 = \omega_x(t) &= \frac{\Omega_x b}{U_0} = \omega_x^* \cos pt, & \dot{q}_2 = \dot{\omega}_x(t) &= \frac{d\omega_x}{dt} \frac{b}{U_0} = -p^* \omega_x^* \sin pt, \\
 q_3 = \omega_z(t) &= \frac{\Omega_z b}{U_0} = \omega_z^* \cos pt, & \dot{q}_3 = \dot{\omega}_z(t) &= \frac{d\omega_z}{dt} \frac{b}{U_0} = -p^* \omega_z^* \sin pt, \\
 q_4 = \delta(t) &= \delta^* \cos pt, & \dot{q}_4 = \dot{\delta}(t) &= \frac{d\delta}{dt} \frac{b}{U_0} = -p^* \delta^* \sin pt,
 \end{aligned} \right\} \quad (15.8)$$

where $p^* = pb/U_0$ - Strouhal number.

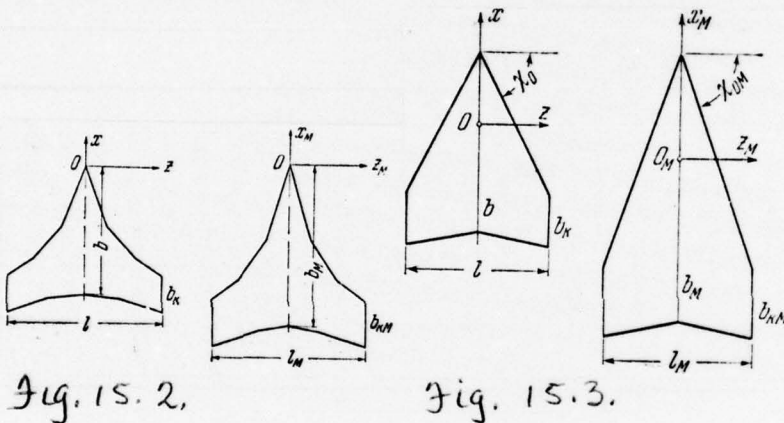


Fig. 15.2. Basic and converted the wings of complex form and plan/layout.

Fig. 15.3. Basic and converted wings with direct/straight edges.

The average forward velocity of the motion of the converted wing

designate U_{0M} , a angle of attack and angular velocities - by α_M , Ω_{xM} , Ω_{zM} , the parameter of strain $-\delta_M$.

In order that from the calculation of the wing in question in the compressed medium it would be possible to pass on the calculation of the converted wing in the fictitious incompressible fluid, let us assume that the motion of the latter is subordinated to the following conditions. The wing moves in the disturbed medium, vertical velocities of which are equal to

$$V_y = -U_{0M} M^2 \sum_{i=1}^4 (\xi_M B_{iM} - E_{iM}) \dot{q}_{iM}. \quad (15.9)$$

Values B_{iM} , E_{iM} make following sense:

$$\left. \begin{aligned} B_{1M} &= -1, \quad B_{2M} = \frac{\zeta_M}{k}, \quad B_{3M} = \xi_M, \quad B_{4M} = -\frac{\partial f_\delta}{\partial \xi_M}; \\ E_{1M} &= E_{2M} = E_{3M} = 0, \quad E_{4M} = f_\delta(\xi_M, \zeta_M). \end{aligned} \right\} \quad (15.10)$$

Let us assume that the parameters q_{iM} change in the course of time according to harmonic law. The motion of the converted lifting surface let us determine with the aid of the following dimensionless kinematic parameters:

$$\left. \begin{aligned}
 q_{1M} &= \alpha_M = \alpha_M^* \cos p_M t, & q_{2M} &= \Omega_{xM} k \frac{b_M}{U_{0M}} = \omega_{xM}^* \cos p_M t, \\
 q_{3M} &= \Omega_{zM} \frac{b_M}{U_{0M}} = \omega_{zM}^* \cos p_M t, & q_{4M} &= \delta_M(t) = \delta_M^* \cos p_M t, \\
 \dot{q}_{iM} &= \frac{dq_{iM}}{dt} \frac{b_M}{U_{0M}}, & i &= 1, 2, 3, 4.
 \end{aligned} \right\} \quad (15.11)$$

Page 377.

Let us look, which form must take differential equations for a velocity potential and the boundary conditions on the converted lifting surface in order that on the initial lifting surface in the flow of gas would be satisfied differential equation (3.30) and all boundary conditions.

§3. Transformation differential equations and boundary conditions.

As shown in chapter III, the potential of the absolute disturbed velocities of the initial lifting surface must satisfy wave equation (3.30), boundary conditions (3.56'), (3.57) and chaplygina -

Joukowski's condition on trailing edge (3.72).

Is expressed velocity potential in the form (5.11) through the coefficients of aerodynamic derivatives, namely:

$$\varphi(\xi, \zeta, t) = U_0 b \left\{ \varphi_0(\xi, \zeta) + \sum_{i=1}^4 [\varphi^{q_i}(\xi, \zeta) q_i(t) + \varphi^{\dot{q}_i}(\xi, \zeta) \dot{q}_i(t)] \right\}, \quad (15.12)$$

where q_i are the dimensionless kinematic parameters. For the determination of velocity potential, following [1.79], we will use formulation that was applied during the solution of unsteady problems [1.9]. [2.28]. Let us introduce functions $\psi^{q_i}, \psi^{\dot{q}_i}$, connected with the coefficients of the aerodynamic derivatives of potential velocities (15.12) by the following equalities

$$\left. \begin{aligned} \varphi_0 &= \psi_0, \\ \varphi^{q_i} &= \psi^{q_i} \cos \omega \xi + \frac{p^*}{k^2} \psi^{\dot{q}_i} \sin \omega \xi, \\ \varphi^{\dot{q}_i} &= \frac{1}{k^2} \psi^{q_i} \cos \omega \xi - \frac{1}{p^*} \psi^{\dot{q}_i} \sin \omega \xi, \\ \omega &= \frac{M^2}{k^2} p^*. \end{aligned} \right\} \quad (15.13)$$

Here p^* is Strouhal number.

With the selected representation of potential (15.12) and (15.13) differential equation (3.30) decomposes to the following:

$$\left. \begin{aligned} k^2 \frac{\partial^2 \psi_0}{\partial \xi^2} + \frac{\partial^2 \psi_0}{\partial \eta^2} + \frac{\partial^2 \psi_0}{\partial \xi^2} &= 0, \\ k^2 \frac{\partial^2 \psi^{q_i}}{\partial \xi^2} + \frac{\partial^2 \psi^{q_i}}{\partial \eta^2} + \frac{\partial^2 \psi^{q_i}}{\partial \xi^2} + \rho^* \frac{M^2}{k^2} \psi^{q_i} &= 0, \\ k^2 \frac{\partial^2 \psi^{q_i}}{\partial \xi^2} + \frac{\partial^2 \psi^{q_i}}{\partial \eta^2} + \frac{\partial^2 \psi^{q_i}}{\partial \xi^2} + \rho^* \frac{M^2}{k^2} \psi^{q_i} &= 0. \end{aligned} \right\} \quad (15.14)$$

Page 378.

Let us designate by Σ the projection of wing on plane Oxz , and by Σ_i - the projection of vortex sheet. Let us find boundary conditions for the functions ψ^{q_i} and ψ^{q_l} . Transfer/converting in (3.56') with the aid of (15.13) to functions ψ^{q_i}, ψ^{q_l} , we obtain the conditions, by which they must satisfy on wing surface Σ :

$$\left. \begin{aligned} \left[\frac{\partial \psi_0}{\partial \eta} \right]_{\Sigma} &= - \frac{\partial f_0}{\partial \xi}, \quad \left[\frac{\partial \psi^{q_l}}{\partial \eta} \cos \omega \xi + \frac{\rho^*}{k^2} \frac{\partial \psi^{q_l}}{\partial \eta} \sin \omega \xi \right]_{\Sigma} = B_i, \\ \left[\frac{1}{k^2} \frac{\partial \psi^{q_l}}{\partial \eta} \cos \omega \xi - \frac{1}{\rho^*} \frac{\partial \psi^{q_l}}{\partial \eta} \sin \omega \xi \right]_{\Sigma} &= E_i, \\ i &= 1, 2, 3, 4. \end{aligned} \right\} \quad (15.15)$$

The right sides of equations (15.15) is equal to

$$\left. \begin{aligned} B_1 = -1, \quad B_2 = -\zeta, \quad B_3 = \xi, \quad B_4 = -\frac{\partial f_0}{\partial \xi}; \\ E_1 = E_2 = E_3 = 0, \quad E_4 = f_0. \end{aligned} \right\} \quad (15.16)$$

Condition on vortex sheet Σ_1 (3.57) after substitution (15.13) takes the following form:

$$\left. \begin{aligned} \left[\frac{\partial \psi_0}{\partial \xi} \right]_{\Sigma_1} &= 0, \quad \left[\frac{\partial \psi^{q_i}}{\partial \xi} + \frac{p^2}{k^4} \psi^{q_i} \right]_{\Sigma_1} = 0, \\ \left[\frac{\partial \psi^{q_i}}{\partial \xi} - \psi^{q_i} \right]_{\Sigma_1} &= 0. \end{aligned} \right\} \quad (15.17)$$

Conditions at infinity far from wing and vortex sheet will be the following:

$$\left. \begin{aligned} \psi^{q_i} = \frac{\partial \psi^{q_i}}{\partial \xi} = \frac{\partial \psi^{q_i}}{\partial \eta} = \frac{\partial \psi^{q_i}}{\partial \zeta} &= 0, \\ \psi^{q_i} = \frac{\partial \psi^{q_i}}{\partial \xi} = \frac{\partial \psi^{q_i}}{\partial \eta} = \frac{\partial \psi^{q_i}}{\partial \zeta} &= 0. \end{aligned} \right\} \quad (15.18)$$

Thus, the determination of velocity potential ϕ is reduced to finding functions ψ^{q_i}, ψ^{q_i} , satisfying differential equations (15.14), boundary conditions (15.15), (15.18) and Chaplygina - Joukowski's condition.

One of the basic is the case of flow with small Strouhal numbers ($p \rightarrow 0$). Set/assuming in relationship/ratios (15.14), (15.15), and (15.17) $p \rightarrow 0$, we obtain the conditions, by which they must satisfy function ψ^{q_i}, ψ^{q_i} in this case.

Page 379.

In an entire area outside $(\Sigma + \Sigma_1)$ they are the solutions to the differential equations

$$\left. \begin{aligned} k^2 \frac{\partial^2 \psi^{q_i}}{\partial \xi^2} + \frac{\partial^2 \psi^{q_i}}{\partial \eta^2} + \frac{\partial^2 \psi^{q_i}}{\partial \zeta^2} &= 0, \\ k^2 \frac{\partial^2 \psi^{\dot{q}_i}}{\partial \xi^2} + \frac{\partial^2 \psi^{\dot{q}_i}}{\partial \eta^2} + \frac{\partial^2 \psi^{\dot{q}_i}}{\partial \zeta^2} &= 0. \end{aligned} \right\} \quad (15.19)$$

On wing (in area Σ) must be satisfied the boundary conditions

$$\left. \begin{aligned} \left[\frac{\partial \psi^{q_i}}{\partial \eta} \right]_{\Sigma} &= B_i, \\ \left[\frac{\partial \psi^{\dot{q}_i}}{\partial \eta} \right]_{\Sigma} &= k^2 E_i + \xi M^2 B_i. \end{aligned} \right\} \quad (15.20)$$

On vortex/eddy direction (in area Σ_1) must be fulfilled the condition

$$\left[\frac{\partial \psi^{q_i}}{\partial \xi} \right]_{\Sigma_1} = 0, \quad \left[\frac{\partial \psi^{\dot{q}_i}}{\partial \xi} - \psi^{q_i} \right]_{\Sigma_1} = 0. \quad (15.21)$$

Far from wing and vortex sheet must be fulfilled equalities (15.18).

§4. Communication/connection between the coefficients of the

aerodynamic derivatives of potential in compressed and incompressible the media.

Let us pass to new alternating/variable x_M, y_M, z_M , connected with x, y, z to relationship/ratios (15.2). By introducing relative coordinates (15.3), with the aid of (15.4) let us produce the transformation of conditions (15.19) - (15.21).

Everywhere outside wing and vortex sheet must be fulfilled the equations

$$\left. \begin{aligned} \frac{\partial^2 \psi^{q_i}}{\partial \xi_M^2} + \frac{\partial^2 \psi^{q_i}}{\partial \eta_M^2} + \frac{\partial^2 \psi^{q_i}}{\partial \zeta_M^2} &= 0, \\ \frac{\partial^2 \psi^{\dot{q}_i}}{\partial \xi_M^2} + \frac{\partial^2 \psi^{\dot{q}_i}}{\partial \eta_M^2} + \frac{\partial^2 \psi^{\dot{q}_i}}{\partial \zeta_M^2} &= 0. \end{aligned} \right\} \quad (15.22)$$

On Σ_M must be observed the conditions

$$\left. \begin{aligned} \frac{\partial \psi^{q_i}}{\partial \eta_M} \Big|_{\Sigma_M} &= \frac{B_{iM}}{k}, \\ \frac{\partial \psi^{\dot{q}_i}}{\partial \eta_M} \Big|_{\Sigma_M} &= k E_{iM} + \xi_M \frac{M^2}{k} B_{iM}, \end{aligned} \right\} \quad (15.23)$$

where Σ_M - the area, to which transfer/converts Σ as a result of transformations (15.2) - (15.4). Values B_{iM} , E_{iM} are determined by equalities (15.10).

Page 380.

On Σ_{iM} the regions into which is converted the area Σ_i , occupied with vortex sheet, during passage to variables ξ_M , η_M , ζ_M must be fulfilled the condition

$$\left. \frac{\partial \psi^{q_i}}{\partial \xi_M} \right|_{\Sigma_{iM}} = 0, \quad \left[\frac{\partial \psi^{q_i}}{\partial \xi_M} - \psi^{q_i} \right]_{\Sigma_{iM}} = 0. \quad (15.24)$$

From relationships (15.18) we obtain

$$\left. \begin{aligned} \psi^{q_i} &= \frac{\partial \psi^{q_i}}{\partial \xi_M} = \frac{\partial \psi^{q_i}}{\partial \eta_M} = \frac{\partial \psi^{q_i}}{\partial \zeta_M} = 0, \\ \psi^{q_i} &= \frac{\partial \psi^{q_i}}{\partial \xi_M} = \frac{\partial \psi^{q_i}}{\partial \eta_M} = \frac{\partial \psi^{q_i}}{\partial \zeta_M} = 0. \end{aligned} \right\} \quad (15.25)$$

Let us examine now the motion of the converted wing in the incompressible medium. The potential of the absolute disturbed velocities θ with an accuracy to the small second-order quantities is expressed by the formula

$$\theta = kb_M U_{0M} \left[\theta_0 + \sum_{i=1}^4 (\theta^{q_{iM}} q_{iM} + \theta^{q_{iM}} \dot{q}_{iM}) \right]. \quad (15.26)$$

Everywhere outside wing and vortex sheet potential must satisfy the

equation of the continuity

$$\frac{\partial^2 \theta}{\partial x_M^2} + \frac{\partial^2 \theta}{\partial y_M^2} + \frac{\partial^2 \theta}{\partial z_M^2} = 0. \quad (15.27)$$

By substituting (15.26) in (15.27), we will obtain the equations, by which must satisfy the coefficients of the aerodynamic derivatives of the potential of the converted wing in the incompressible medium:

$$\left. \begin{aligned} \frac{\partial^2 \theta^{qIM}}{\partial \xi_M^2} + \frac{\partial^2 \theta^{qIM}}{\partial \eta_M^2} + \frac{\partial^2 \theta^{qIM}}{\partial \zeta_M^2} &= 0, \\ \frac{\partial^2 \theta^{qIM}}{\partial \xi_M^2} + \frac{\partial^2 \theta^{qIM}}{\partial \eta_M^2} + \frac{\partial^2 \theta^{qIM}}{\partial \zeta_M^2} &= 0. \end{aligned} \right\} \quad (15.28)$$

Page 381.

Let us examine now boundary condition on the converted wing. It is possible to write as follows:

$$\begin{aligned} \frac{1}{U_{0M}} \frac{\partial \theta}{\partial y_M} &= -\alpha_M - \Omega_{xM} \frac{z_M}{U_{0M}} + \\ &+ \Omega_{zM} \frac{x_M}{U_{0M}} - \frac{\partial f_0}{\partial \xi_M} - \frac{\partial f_\delta}{\partial \xi_M} \delta_M + f_\delta \frac{d\delta_M}{dt} \frac{b_M}{U_{0M}} - \frac{V_y}{U_{0M}}. \end{aligned} \quad (15.29)$$

This equality must be fulfilled on Σ_M . Substituting in it (15.9) - (15.11), (15.26) and equalizing the coefficients in the identical kinematic parameters, we obtain the conditions, which must be

fulfilled on Σ_M :

$$\left. \begin{aligned} \frac{\partial \theta_0}{\partial \eta_M} \Big|_{\Sigma_M} &= - \frac{\partial f_0}{\partial \xi_M}, \quad \frac{\partial \theta^{q_{IM}}}{\partial \eta_M} \Big|_{\Sigma_M} = \frac{B_{IM}}{k}, \\ \frac{\partial \theta^{q_{IM}}}{\partial \eta_M} \Big|_{\Sigma_M} &= k E_{IM} + \xi_M \frac{M^2}{k} B_{IM}. \end{aligned} \right\} \quad (15.30)$$

In the area of vortex sheet Σ_{IM} must be fulfilled relationship/ratios (3.57), which with $\rho_M^* \rightarrow 0$ take the form

$$\frac{\partial \theta^{q_{IM}}}{\partial \xi_M} \Big|_{\Sigma_{IM}} = 0, \quad \left[\frac{\partial \theta^{q_{IM}}}{\partial \xi_M} - \theta^{q_i} \right]_{\Sigma_{IM}} = 0. \quad (15.31)$$

Finally, conditions far from wing and vortex sheet they will be

$$\left. \begin{aligned} \theta^{q_{IM}} = \frac{\partial \theta^{q_{IM}}}{\partial \xi_M} = \frac{\partial \theta^{q_{IM}}}{\partial \eta_M} = \frac{\partial \theta^{q_{IM}}}{\partial \zeta_M} = 0, \\ \theta^{q_{IM}} = \frac{\partial \theta^{q_{IM}}}{\partial \xi_M} = \frac{\partial \theta^{q_{IM}}}{\partial \eta_M} = \frac{\partial \theta^{q_{IM}}}{\partial \zeta_M} = 0. \end{aligned} \right\} \quad (15.32)$$

Comparing (15.22), (15.23), (15.24), (15.25) with (15.28), (15.30), (15.31), (15.32), we find that the functions ψ^{q_i} , ψ^{q_i} , the determining aerodynamic derivatives of velocity potential during the motion of lifting surface in the compressed medium, and the aerodynamic derivatives $\theta^{q_{IM}}$, $\theta^{q_{IM}}$ of the velocity potential of the converted wing in the incompressible medium satisfy one and the same differential equations and boundary conditions. Therefore the values

of these functions at the points, connected by conditions (15.4), are equal, i.e.,

$$\left. \begin{aligned} \psi^{q_i} \left(\xi_M, \frac{\eta_M}{k}, \frac{\zeta_M}{k} \right) &= \theta^{q_{iM}} (\xi_M, \eta_M, \zeta_M), \\ \psi^{\dot{q}_i} \left(\xi_M, \frac{\eta_M}{k}, \frac{\zeta_M}{k} \right) &= \theta^{\dot{q}_{iM}} (\xi_M, \eta_M, \zeta_M). \end{aligned} \right\} \quad (15.33)$$

Page 382.

Thus, the problem of motion and the strains of wing with the harmonic laws of a change of the kinematic parameters in time in the compressed medium at $p^* \rightarrow 0$ is equivalent in the sense of equalities (15.33) to the problem of the motion of the converted wing in the incompressible medium, but with the changed according to (15.29) boundary conditions.

§5. Coefficients of the aerodynamic derivatives of load in compressed and incompressible the media.

During the solution of problem for a wing in the incompressible medium velocity potential θ usually do not find (chapter X, part II), calculating the only circulation the loads and aerodynamic coefficients. Therefore it is expedient to obtain the formulas, which

make it possible to complete direct passage from these data to the appropriate wing characteristics in gas flow. Let us write according to (2.24) the coefficient of load $\Delta\bar{p}_M = 2\Delta p_M/\rho_\infty U_{0M}^2$ on the converted wing in the space of the incompressible medium and the same coefficient $\Delta\bar{p} = 2\Delta p/\rho_\infty U_0^2$ on the initial wing in the flow of the gas through the coefficient of the aerodynamic derivatives:

$$\left. \begin{aligned} \Delta\bar{p} &= \Delta\bar{p}_0 + \sum_{i=1}^4 (p^{q_i} q_i + p^{q_i} \dot{q}_i), \\ \Delta\bar{p}_M &= \Delta\bar{p}_{0M} + \sum_{i=1}^4 (\bar{p}_M^{q_{iM}} q_{iM} + \bar{p}_M^{q_{iM}} \dot{q}_{iM}). \end{aligned} \right\} \quad (15.34)$$

With the aid of the Cauchy integral of - Lagrange were obtained expressions (3.21) for the derivatives of load through the aerodynamic derivatives of potential. Substituting in (3.21) values φ^{q_i} and $\varphi^{\dot{q}_i}$ from (5.13), we find

$$\left. \begin{aligned} \Delta\bar{p}_0 &= 4 \frac{\partial \psi_0}{\partial \xi}, \\ p^{q_i} &= 4 \left\{ \left[\frac{\partial \psi^{q_i}}{\partial \xi} + \frac{p^{*2}}{k^4} \psi^{q_i} \right] \cos \omega \xi + \left[\frac{\partial \psi^{\dot{q}_i}}{\partial \xi} - \psi^{q_i} \right] \frac{p^*}{k^2} \sin \omega \xi \right\}, \\ p^{\dot{q}_i} &= 4 \left\{ \left[\frac{\partial \psi^{q_i}}{\partial \xi} - \psi^{q_i} \right] \frac{\cos \omega \xi}{k^2} - \left[\frac{\partial \psi^{\dot{q}_i}}{\partial \xi} + \frac{p^{*2}}{k^4} \psi^{\dot{q}_i} \right] \frac{\sin \omega \xi}{p^*} \right\}. \end{aligned} \right\} \quad (15.35)$$

With $p^* \rightarrow 0 (\omega \rightarrow 0)$ aerodynamic derivatives $p^{q_i}, p^{\dot{q}_i}$ are equal to

$$p^{q_l} = 4 \frac{\partial \psi^{q_l}}{\partial \xi}, \quad p^{q_l} = \frac{4}{k^2} \left(\frac{\partial \psi^{q_l}}{\partial \xi} - \psi^{q_l} \right) - 4\xi \frac{M^2}{k^2} p^{q_l}. \quad (15.36)$$

Page 383.

Analogously from (3.21) we find that with $p_M^* \rightarrow 0$ aerodynamic derivative loads on the converted wing, which moves in the incompressible medium, will be

$$\left. \begin{aligned} \Delta \bar{p}_{0M} &= 4k \frac{\partial \theta_0}{\partial \xi_M}, \quad \bar{p}^{q_{IM}} = 4k \frac{\partial \theta^{q_{IM}}}{\partial \xi_M}, \\ \bar{p}_M^{q_{IM}} &= 4k \left(\frac{\partial \theta^{q_{IM}}}{\partial \xi_M} - \theta^{q_{IM}} \right). \end{aligned} \right\} \quad (15.37)$$

Comparing (15.36) with (15.37) and taking into account communication/connection (15.33) between potentials, it is easy to establish that at the appropriate points that which is compressed and incompressible of the media, connected by equality (15.4), between the aerodynamic derivatives of loads is the following dependence:

$$\left. \begin{aligned} \Delta \bar{p}_0 &= \frac{\Delta \bar{p}_{0M}}{k}, \quad p^{q_l} = \frac{\bar{p}_M^{q_{IM}}}{k}, \\ p^{q_l} &= \frac{\bar{p}_M^{q_{IM}}}{k^3} - \xi_M \frac{M^2}{k^3} \bar{p}_M^{q_{IM}}, \quad k = \sqrt{1 - M^2}. \end{aligned} \right\} \quad (15.38)$$

§6. Coefficients of aerodynamic force derivative and torque/moments in compressed and incompressible the media.

Let us introduce the coefficients of aerodynamic force derivative and torque/moments for the case of the motion of lifting surface in the compressed medium along formulas (2.1), (2.24). Analogously let us determine the appropriate coefficients of the converted wing in the incompressible medium:

$$\left. \begin{aligned} \bar{c}_{yM} &= \frac{2Y_M}{\rho_\infty U_{0M}^2 S_M} = \bar{c}_{y0M} + \sum_{i=1}^4 (\bar{c}_{yM}^{q_{iM}} q_{iM} + \bar{c}_{yM}^{\dot{q}_{iM}} \dot{q}_{iM}), \\ \bar{m}_{xM} &= \frac{2M_{xM}}{\rho_\infty U_{0M}^2 S_M b_M} = \sum_{i=1}^4 (\bar{m}_{xM}^{q_{iM}} q_{iM} + \bar{m}_{xM}^{\dot{q}_{iM}} \dot{q}_{iM}), \\ \bar{m}_{zM} &= \frac{2M_{zM}}{\rho_\infty U_{0M}^2 S_M b_M} = \bar{m}_{z0M} + \sum_{i=1}^4 (\bar{m}_{zM}^{q_{iM}} q_{iM} + \bar{m}_{zM}^{\dot{q}_{iM}} \dot{q}_{iM}), \end{aligned} \right\} (15.39)$$

where Y_M, M_{zM}, M_{xM} - lift, the pitching moment (relative to axis z_M) and the moment of roll, which act on the converted wing, S_M, b_M - respectively its area and root chord.

The coefficients of aerodynamic force derivative and

torque/moments are calculated through load factors in formulas (2.25).

Page 384.

Taking into account that $kb_M = b$, $kS_M = S$ and representation (15.39), we establish/install communication/connection between the coefficients of aerodynamic force derivative and torque/moments of the initial wing in the compressed medium and of the converted wing in the incompressible medium:

$$\left. \begin{aligned} kc_{y_0} &= \bar{c}_{y0M}, & kc_y^{q_i} &= \bar{c}_{yM}^{q_i}, & k^3 c_y^{q_i} &= \bar{c}_{yM}^{q_i} - M^2 \bar{m}_{zM}^{q_i}, \\ k^2 m_x^{q_i} &= \bar{m}_{xM}^{q_i}, & k^4 m_x^{q_i} &= \bar{m}_{xM}^{q_i} - M^2 \bar{I}_{xzM}^{q_i}, \\ km_{z0} &= \bar{m}_{z0M}, & km_z^{q_i} &= \bar{m}_{zM}^{q_i}, & k^3 m_z^{q_i} &= \bar{m}_{zM}^{q_i} - M^2 \bar{I}_{zzM}^{q_i}, \end{aligned} \right\} \quad (15.40)$$

where

$$\left. \begin{aligned} \bar{I}_{xzM}^{q_i} &= \frac{b_M^2}{S_M} \int \int_{\Sigma_M} \bar{p}_M^{q_i} \xi_M \zeta_M d\xi_M d\zeta_M, \\ \bar{I}_{zzM}^{q_i} &= \frac{b_M^2}{S_M} \int \int_{\Sigma_M} \bar{p}_M^{q_i} \xi_M^2 d\xi_M d\zeta_M. \end{aligned} \right\} \quad (15.41)$$

Communication/connection between the coefficients aerodynamic derivative wing sections is establish/installed as follows.

Expressing lift coefficients, the longitudinal and rolling moments of wing sections in the compressed medium through aerodynamic derivatives, we obtain relationship/ratios (2.24). For the converted wing in the incompressible medium we have

$$\left. \begin{aligned} \bar{c}'_{yM} &= \frac{2 dY_M}{\rho_\infty U_{0M}^2 b_M' dz_M} = \bar{c}'_{y0M} + \sum_{i=1}^4 (\bar{c}'_{yM}{}^{q_{iM}} q_{iM} + \bar{c}'_{yM}{}^{\dot{q}_{iM}} \dot{q}_{iM}), \\ \bar{m}'_{xM} &= \frac{2 dM_{xM}}{\rho_\infty U_{0M}^2 b_M'^2 dz_M} = \sum_{i=1}^4 (\bar{m}'_{xM}{}^{q_{iM}} q_{iM} + \bar{m}'_{xM}{}^{\dot{q}_{iM}} \dot{q}_{iM}), \\ \bar{m}'_{zM} &= \frac{2 dM_{zM}}{\rho_\infty U_{0M}^2 b_M'^2 dz_M} = \bar{m}'_{z0M} + \sum_{i=1}^4 (\bar{m}'_{zM}{}^{q_{iM}} q_{iM} + \bar{m}'_{zM}{}^{\dot{q}_{iM}} \dot{q}_{iM}), \end{aligned} \right\} (15.42)$$

where dY_M , dM_{xM} , dM_{zM} - lift, the transverse and pitching moments (relative to axis Oz_M), which act in the section of the converted wing, b_M' - the value of the chord of the converted wing in the section in question.

Page 385.

With the aid of (15.38), (15.5) it is not difficult to show that the coefficients aerodynamic derivative sections, equidistant from the plane of symmetries, for which $z = z_M$, $k\zeta = \zeta_M$, $kb_M' = b'$, are connected by the following relationship/ratios:

$$\left. \begin{aligned}
 kc'_{y0} &= \tilde{c}'_{y0M}, & kc'^q_{yi} &= \tilde{c}'^q_{yiM}, & k^3c'^q_{yi} &= \tilde{c}'^q_{yiM} - M^2 \frac{b'_M}{b_M} \tilde{m}'^q_{ziM}, \\
 km'_{z0} &= \tilde{m}'_{z0M}, & km'^q_{zi} &= \tilde{m}'^q_{ziM}, & k^3m'^q_{zi} &= \tilde{m}'^q_{ziM} - M^2 \tilde{m}'^q_{zzM}, \\
 k^2m'^q_{xi} &= \tilde{m}'^q_{xiM}, & k^4m'^q_{xi} &= \tilde{m}'^q_{xiM} - M^2 \tilde{m}'^q_{xzM}.
 \end{aligned} \right\} \quad (15.43)$$

Here

$$\left. \begin{aligned}
 \tilde{m}'^q_{zzM} &= \frac{b_M^2}{b'^2_M} \int_{\xi_{0M}}^{\xi_{1M}} \tilde{\rho}^q_{iM} \xi_M^2 d\xi_M, \\
 \tilde{m}'^q_{xzM} &= \frac{b_M^2}{b'^2_M} \int_{\xi_{0M}}^{\xi_{1M}} \tilde{\rho}^q_{iM} \xi_M \xi_M d\xi_M.
 \end{aligned} \right\} \quad (15.44)$$

§7. Method of the calculation of aerodynamic wing characteristics in the compressed medium with $p^* \rightarrow 0$.

In the preceding/previous paragraphs it was shown, that the problem of determining aerodynamic wing characteristics in the

compressed medium with the harmonic laws of a change in the kinematic parameters at Strouhal number, vanishing, is reduced to the problem of motion along the harmonic laws of the geometrically converted wing in the incompressible medium, but with the changed by the determined form boundary conditions. Therefore with $p^* \rightarrow 0$ we come to the following method of the performance calculation of wing in the compressed medium. Is examined the lifting surface of arbitrary planform, which accomplishes in the compressed medium harmonic motion with the kinematic parameters, assigned in the form (2.19), (2.20). Boundary conditions on wing are assigned by formula (3.56'). The target/purpose of the calculation is finding the coefficients of aerodynamic derivatives c^{q_i} , c^{q_i} , determining wing characteristics. The effect of harmonic gust on wing is not examined, since with $p^* \rightarrow 0$ corresponding aerodynamic derivatives are expressed as the derivatives of the wing, which moves as solid body (§5 chapter of V). In order to find these characteristics, is introduced the converted lifting surface (see Fig. 15.2, 15.3) in the incompressible medium. Its geometric parameters are determined with the aid of (15.5), (15.6), and the kinematic parameters of motion - with the aid of (15.11). Boundary conditions on the converted wing take form (15.29).

Page 386.

During the solution of problem for the converted wing in the

incompressible medium velocity potential θ they do not find, but they calculate circulations and the coefficients aerodynamic derivative loads, forces, torque/moments in the method, presented in chapter X. For this let us replace wing with the system of discrete transient vortices. The position of bound vortexes on wing is selected according to indications §1 of chapter X. The intensity/strength of the circulation of each eddy/vortex let us present in the form of the sum

$$\bar{\Gamma}_{+M\mu k k-1} = U_{\infty} b_M \left[\bar{\Gamma}_{0M\mu k k-1} + \sum_{i=1}^4 \left(\bar{\Gamma}_{M\mu k k-1}^{q_{iM}} q_{iM} + \bar{\Gamma}_{M\mu k k-1}^{\dot{q}_{iM}} \dot{q}_{iM} \right) \right], \quad (15.45)$$

where $\bar{\Gamma}_{M\mu k k-1}^{q_{iM}}$, $\bar{\Gamma}_{M\mu k k-1}^{\dot{q}_{iM}}$ - aerodynamic derivative circulations. As has already been indicated in chapter X, differential equation (15.28) and boundary conditions on vortex sheet (15.31) and far from it and wing (15.32) will be fulfilled at any values of circulation $\bar{\Gamma}_{+M\mu k k-1}$.

Satisfying boundary conditions (15.29) at the control points of wing whose coordinates ξ_{Mvp-1}^{vp} , ζ_{Mvp-1}^{vp} are determined by formulas (10.11), (10.12), we obtain the following systems of equations for aerodynamic derivative circulations:

$$\begin{aligned}
& \frac{1}{4\pi} \sum_{k=1}^N \sum_{\mu=1}^n (\omega_{y\nu\rho\rho-1}^{\mu k k-1} \pm \sigma \omega_{y\nu\rho\rho-1}^{\mu k k-1}) \bar{\Gamma}_{0M\mu k k-1} = \\
& \qquad \qquad \qquad = - \frac{\partial f_0}{\partial \xi_M} \bigg|_{\substack{\xi_M = \xi_{M\nu\rho}^{vp} \\ \xi_M = \xi_{M\nu\rho-1}^{vp}}}, \\
& \frac{1}{4\pi} \sum_{k=1}^N \sum_{\mu=1}^n (\omega_{y\nu\rho\rho-1}^{\mu k k-1} \pm \sigma \omega_{y\nu\rho\rho-1}^{\mu k k-1}) \bar{\Gamma}_{M\mu k k-1}^{q_i} = B_{iM\nu\rho\rho-1}, \\
& \frac{1}{4\pi} \sum_{k=1}^N \sum_{\mu=1}^n (\omega_{y\nu\rho\rho-1}^{\mu k k-1} \pm \sigma \omega_{y\nu\rho\rho-1}^{\mu k k-1}) \bar{\Gamma}_{M\mu k k-1}^{q_i} = \\
& = - \frac{1}{4\pi} \sum_{k=1}^N \sum_{\mu=1}^n \left(\frac{\partial \omega_{y\nu\rho\rho-1}^{(2)\mu k k-1}}{\partial p^*} \pm \sigma \frac{\partial \omega_{y\nu\rho\rho-1}^{(2)\mu k k-1}}{\partial p^*} \right) \bar{\Gamma}_{M\mu k k-1}^{q_i} + \\
& \qquad \qquad \qquad + (1 - M^2) E_{iM\nu\rho\rho-1} + M^2 \xi_{M\nu\rho-1}^{vp} B_{iM\nu\rho\rho-1}; \\
& i = 1, 2, 3, 4; \quad \nu = 1, 2, \dots, n; \quad p = 1, 2, \dots, N.
\end{aligned} \tag{15.46}$$

Page 387.

In these systems the dimensionless velocities

$$\omega_{y\nu\rho\rho-1}^{\mu k k-1}, \quad \sigma \omega_{y\nu\rho\rho-1}^{\mu k k-1}, \quad \frac{\partial \omega_{y\nu\rho\rho-1}^{(2)\mu k k-1}}{\partial p^*}, \quad \sigma \frac{\partial \omega_{y\nu\rho\rho-1}^{(2)\mu k k-1}}{\partial p^*}$$

are calculated from formulas (9.6), (9.7), (9.8), (9.26) by the account of a change in the beginning of coordinates and direction of their axes; minus sign in brackets under sign $\sum \sum$ is taken with $i = 2$, and also with $i = 4$, if the strains of wing are antisymmetric. Values $B_{1M\nu pp-1}$, $E_{1M\nu pp-1}$ have the following values:

$$\left. \begin{aligned} B_{1M\nu pp-1} &= -1, & B_{2M\nu pp-1} &= -\frac{1}{k} \xi_{M\nu pp-1}^{\nu p}, \\ B_{3M\nu pp-1} &= \xi_{M\nu pp-1}^{\nu p}, & B_{4M\nu pp-1} &= -\frac{\partial f_\delta}{\partial \xi_M} \begin{vmatrix} \xi_M - \xi_{M\nu pp-1}^{\nu p} \\ \xi_M - \xi_{M\nu pp-1}^{\nu p} \end{vmatrix}, \\ E_{1M} &= E_{2M} = E_{3M} = 0, & E_{4M\nu pp-1} &= f_\delta (\xi_{M\nu pp-1}^{\nu p}, \xi_{M\nu pp-1}^{\nu p}). \end{aligned} \right\} \quad (15.47)$$

It is easy to see that into the right sides of some systems of equations (15.46) the number M enters in an explicit form. Therefore let us present aerodynamic derivative circulations as follows:

$$\left. \begin{aligned} \bar{\Gamma}_{M\mu kk-1}^{q_{IM}} &= \Gamma_{M\mu kk-1}^{q_I}, & \bar{\Gamma}_{M\mu kk-1}^{q_{IM}} &= \Gamma_{M\mu kk-1}^{q_I} + M^2 \Delta \Gamma_{M\mu kk-1}^{q_I}, \\ q_I &= \alpha, \omega_i; \\ \bar{\Gamma}_{M\mu kk-1}^{\omega_{XM}} &= \frac{\Gamma_{M\mu kk-1}^{\omega_X}}{k}, & \bar{\Gamma}_{M\mu kk-1}^{\omega_{XM}} &= \frac{1}{k} (\Gamma_{M\mu kk-1}^{\omega_X} + M^2 \Delta \Gamma_{M\mu kk-1}^{\omega_X}); \\ \bar{\Gamma}_{M\mu kk-1}^{\delta_M} &= \Gamma_{M\mu kk-1}^{\delta}, \\ \bar{\Gamma}_{M\mu kk-1}^{\delta_M} &= \Gamma_{M\mu kk-1}^{\delta} + k^2 \Delta_1 \Gamma_{M\mu kk-1}^{\delta} + M^2 \Delta_2 \Gamma_{M\mu kk-1}^{\delta}. \end{aligned} \right\} \quad (15.48)$$

Pages 388-389.

By substituting these expressions in (15.46), we come to systems of equations for the circulations

$$\begin{aligned} \frac{1}{4\pi} \sum_{k=1}^N \sum_{\mu=1}^n (w_{y\nu\rho\rho-1}^{\mu k k-1} + \sigma w_{y\nu\rho\rho-1}^{\mu k k-1}) \Gamma_{M\mu k k-1}^a &= -1, \\ \sum_{k=1}^N \sum_{\mu=1}^n (w_{y\nu\rho\rho-1}^{\mu k k-1} + \sigma w_{y\nu\rho\rho-1}^{\mu k k-1}) \Gamma_{M\mu k k-1}^a &= \\ &= - \sum_{k=1}^N \sum_{\mu=1}^n \left(\frac{\partial w_{y\nu\rho\rho-1}^{(2)\mu k k-1}}{\partial p^*} + \sigma \frac{\partial w_{y\nu\rho\rho-1}^{(2)\mu k k-1}}{\partial p^*} \right) \Gamma_{M\mu k k-1}^a, \end{aligned} \quad (15.49)$$

$$\begin{aligned} \frac{1}{4\pi} \sum_{k=1}^N \sum_{\mu=1}^n (w_{y\nu\rho\rho-1}^{\mu k k-1} + \sigma w_{y\nu\rho\rho-1}^{\mu k k-1}) \Delta \Gamma_{M\mu k k-1}^a &= -\xi_{M\nu\rho-1}^{\nu\rho}, \\ \frac{1}{4\pi} \sum_{k=1}^N \sum_{\mu=1}^n (w_{y\nu\rho\rho-1}^{\mu k k-1} + \sigma w_{y\nu\rho\rho-1}^{\mu k k-1}) \Gamma_{M\mu k k-1}^{\omega_z} &= \xi_{M\nu\rho-1}^{\nu\rho}, \\ \sum_{k=1}^N \sum_{\mu=1}^n (w_{y\nu\rho\rho-1}^{\mu k k-1} + \sigma w_{y\nu\rho\rho-1}^{\mu k k-1}) \Gamma_{M\mu k k-1}^{\omega_z} &= \\ &= - \sum_{k=1}^N \sum_{\mu=1}^n \left(\frac{\partial w_{y\nu\rho\rho-1}^{(2)\mu k k-1}}{\partial p^*} + \sigma \frac{\partial w_{y\nu\rho\rho-1}^{(2)\mu k k-1}}{\partial p^*} \right) \Gamma_{M\mu k k-1}^{\omega_z}, \end{aligned}$$

$$\begin{aligned} \frac{1}{4\pi} \sum_{k=1}^N \sum_{\mu=1}^n (w_{y\nu\rho\rho-1}^{\mu k k-1} + \sigma w_{y\nu\rho\rho-1}^{\mu k k-1}) \Delta \Gamma_{M\mu k k-1}^{\omega_z} &= (\xi_{M\nu\rho-1}^{\nu\rho})^2, \\ \frac{1}{4\pi} \sum_{k=1}^N \sum_{\mu=1}^n (w_{y\nu\rho\rho-1}^{\mu k k-1} - \sigma w_{y\nu\rho\rho-1}^{\mu k k-1}) \Gamma_{M\mu k k-1}^{\omega_x} &= -\xi_{M\nu\rho-1}^{\nu\rho}, \\ \sum_{k=1}^N \sum_{\mu=1}^n (w_{y\nu\rho\rho-1}^{\mu k k-1} - \sigma w_{y\nu\rho\rho-1}^{\mu k k-1}) \Gamma_{M\mu k k-1}^{\omega_x} &= \\ &= - \sum_{k=1}^N \sum_{\mu=1}^n \left(\frac{\partial w_{y\nu\rho\rho-1}^{(2)\mu k k-1}}{\partial p^*} - \sigma \frac{\partial w_{y\nu\rho\rho-1}^{(2)\mu k k-1}}{\partial p^*} \right) \Gamma_{M\mu k k-1}^{\omega_x}, \end{aligned} \quad (15.49)$$

$$\frac{1}{4\pi} \sum_{k=1}^N \sum_{\mu=1}^n (w_{y\nu\rho\rho-1}^{\mu k k-1} - \sigma w_{y\nu\rho\rho-1}^{\mu k k-1}) \Delta \Gamma_{M\mu k k-1}^{\omega_x} = -\xi_{M\nu\rho-1}^{\nu\rho} \xi_{M\nu\rho-1}^{\nu\rho},$$

$$\frac{1}{4\pi} \sum_{k=1}^N \sum_{\mu=1}^n (\omega_{y\nu\rho\rho-1}^{\mu k k-1} \pm \sigma \omega_{y\nu\rho\rho-1}^{\mu k k-1}) \Gamma_{M\mu k k-1}^{\delta} =$$

$$= - \frac{\partial f_{\delta}}{\partial \xi_M} \bigg|_{\substack{\xi_M = \xi_{M\nu\rho-1}^{\nu\rho} \\ \zeta_M = \zeta_{M\nu\rho-1}^{\nu\rho}}},$$

$$\sum_{k=1}^N \sum_{\mu=1}^n (\omega_{y\nu\rho\rho-1}^{\mu k k-1} \pm \sigma \omega_{y\nu\rho\rho-1}^{\mu k k-1}) \Gamma_{M\mu k k-1}^{\delta} =$$

$$= - \sum_{k=1}^N \sum_{\mu=1}^n \left(\frac{\partial \omega_{y\nu\rho\rho-1}^{\mu k k-1}}{\partial \rho^*} \pm \sigma \frac{\partial \omega_{y\nu\rho\rho-1}^{\mu k k-1}}{\partial \rho^*} \right) \Gamma_{M\mu k k-1}^{\delta},$$

$$\frac{1}{4\pi} \sum_{k=1}^N \sum_{\mu=1}^n (\omega_{y\nu\rho\rho-1}^{\mu k k-1} \pm \sigma \omega_{y\nu\rho\rho-1}^{\mu k k-1}) \Delta_1 \Gamma_{M\mu k k-1}^{\delta} =$$

$$= f_{\delta} (\xi_{M\nu\rho-1}^{\nu\rho}, \zeta_{M\nu\rho-1}^{\nu\rho}),$$

$$\frac{1}{4\pi} \sum_{k=1}^N \sum_{\mu=1}^n (\omega_{y\nu\rho\rho-1}^{\mu k k-1} \pm \sigma \omega_{y\nu\rho\rho-1}^{\mu k k-1}) \Delta_2 \Gamma_{M\mu k k-1}^{\delta} =$$

$$= - \xi_{M\nu\rho-1}^{\nu\rho} \frac{\partial f_{\delta}}{\partial \xi_M} \bigg|_{\substack{\xi_M = \xi_{M\nu\rho-1}^{\nu\rho} \\ \zeta_M = \zeta_{M\nu\rho-1}^{\nu\rho}}},$$

(15.49)

$$\frac{1}{4\pi} \sum_{k=1}^N \sum_{\mu=1}^n (\omega_{y\nu\rho\rho-1}^{\mu k k-1} \pm \sigma \omega_{y\nu\rho\rho-1}^{\mu k k-1}) \Gamma_{0M\mu k k-1} =$$

$$= - \frac{\partial f_0}{\partial \xi_M} \bigg|_{\substack{\xi_M = \xi_{M\nu\rho-1}^{\nu\rho} \\ \zeta_M = \zeta_{M\nu\rho-1}^{\nu\rho}}};$$

$$\nu = 1, 2, \dots, n; \quad \rho = 1, 2, \dots, N.$$

In the last/latter five systems of equations (15.49) the plus sign in brackets is taken during the symmetrical strain of wing and minus sign - with antisymmetric. It is evident that all systems are solved independently of each other, except systems relatively Γ^q_i (second, fifth, eighth and eleventh systems), which are solved after are found from the solution of the preceding/previous systems of circulation Γ^q_i . It is easy also to note that as compared with the case $M=0$ appear four new systems (third, sixth, ninth and thirteenth); however, system relatively $\Delta\Gamma^a$ with an accuracy to sign coincides with system for Γ^{ω}_z , whence it follows that

$$\Delta\Gamma^a_{M\mu k k-1} = -\Gamma^{\omega}_z_{M\mu k k-1}. \quad (15.50)$$

On the basis of obtained from solution to system (15.49) of the coefficients aerodynamic derivative circulations we determine, analogously presented into §6 of chapter X, distributed and the total loads on the converted wing and, utilizing relationship/ratios (15.38), (15.40), (15.43), coefficients of the aerodynamic derivatives of the initial wing in the compressed medium.

Page 390.

For example, for the coefficients of the derivatives of load of (10.39), (10.40) taking into account (15.38), (15.48) at the corresponding points of the initial and converted wing

$$\xi_{\mu k-1}^{\mu k} = \xi_{M\mu k-1}^{\mu k},$$

$$\zeta_{\mu k-1}^{\mu k} = \frac{1}{k} \zeta_{M\mu k-1}^{\mu k}$$

let us have

$$\left. \begin{aligned} k \Delta \bar{p}_0 &= \Delta \bar{p}_{0M}, \\ kp^a &= p_M^a, & k^3 p^a &= p_{1M}^a + M^2 p_{2M}^a, \\ k^2 p^{\omega x} &= p_M^{\omega x}, & k^4 p^{\omega x} &= p_{1M}^{\omega x} + M^2 p_{2M}^{\omega x}, \\ kp^{\omega z} &= p_M^{\omega z}, & k^3 p^{\omega z} &= p_{1M}^{\omega z} + M^2 p_{2M}^{\omega z}, \\ kp^\delta &= p_M^\delta, & k^3 p^\delta &= p_{1M}^\delta + M^2 p_{2M}^\delta. \end{aligned} \right\} \quad (15.51)$$

The aerodynamic derivatives $p_M^{q_i}$, $p_M^{q_i}$ for the converted wing are determined by the equalities

$$\begin{aligned}
 \Delta \bar{p}_{0M} &= 2n \frac{b_M}{b_{Mkk-1}} \Gamma_{0M\mu kk-1}, \\
 p_M^{q_i} &= 2n \frac{b_M}{b_{Mkk-1}} \Gamma_{M\mu kk-1}^{q_i}, \\
 p_{1M}^{\dot{q}_i} &= 2n \frac{b_M}{b_{Mkk-1}} \Gamma_{M\mu kk-1}^{\dot{q}_i}, \\
 p_{2M}^{\dot{q}_i} &= 2n \frac{b_M}{b_{Mkk-1}} \Delta \Gamma_{M\mu kk-1}^{\dot{q}_i} - \xi_M p_M^{q_i}, \\
 &\quad i = 1, 2, 3; \\
 p_M^\delta &= 2n \frac{b_M}{b_{Mkk-1}} \Gamma_{M\mu kk-1}^\delta, \\
 p_{1M}^\delta &= 2n \frac{b_M}{b_{Mkk-1}} (\Gamma_{M\mu kk-1}^\delta + \Delta_1 \Gamma_{M\mu kk-1}^\delta), \\
 p_{2M}^\delta &= 2n \frac{b_M}{b_{Mkk-1}} (\Delta_2 \Gamma_{M\mu kk-1}^\delta - \Delta_1 \Gamma_{M\mu kk-1}^\delta - \xi_{M\mu k} \Gamma_{M\mu kk-1}^\delta).
 \end{aligned}
 \tag{15.52}$$

Page 391.

Utilizing relationship/ratios (15.40), we obtain the following formulas for passage from the coefficients of the aerodynamic

derivatives of the converted wing in the incompressible medium to the aerodynamic derivatives of the initial wing in the compressed medium:

$$\left. \begin{aligned}
 kc_{y0} &= c_{y0M}, & km_{z0} &= m_{z0M}, \\
 kc_y^a &= c_{yM}^a, & k^3 c_y^a &= c_{y1M}^a + M^2 c_{y2M}^a, \\
 km_z^a &= m_{zM}^a, & k^3 m_z^a &= m_{z1M}^a + M^2 m_{z2M}^a, \\
 kc_y^{\omega_z} &= c_{yM}^{\omega_z}, & k^3 c_y^{\omega_z} &= c_{y1M}^{\omega_z} + M^2 c_{y2M}^{\omega_z}, \\
 km_z^{\omega_z} &= m_{zM}^{\omega_z}, & k^3 m_z^{\omega_z} &= m_{z1M}^{\omega_z} + M^2 m_{z2M}^{\omega_z}, \\
 k^2 m_x^{\omega_x} &= m_{xM}^{\omega_x}, & k^4 m_x^{\omega_x} &= (m_{xM}^{\omega_x})_1 + M^2 (m_{xM}^{\omega_x})_2, \\
 kc_y^\delta &= c_{yM}^\delta, & k^3 c_y^\delta &= c_{y1M}^\delta + M^2 c_{y2M}^\delta, \\
 km_z^\delta &= m_{zM}^\delta, & k^3 m_z^\delta &= m_{z1M}^\delta + M^2 m_{z2M}^\delta.
 \end{aligned} \right\} (15.53)$$

Here for significant dimension for the kinematic parameters and the torque/moments is undertaken the root chord b . In formulas (15.53) the coefficients with index M are determined from the obtained values of the aerodynamic derivatives of the circulation of the converted wing according to the formulas

$$\begin{aligned}
c_{y0M} &= 4 \frac{b_M^2}{S_M} \sum_{k=1}^N l_{Mkk-1} \sum_{\mu=1}^n \Gamma_{0M\mu kk-1}, \\
m_{z0M} &= 4 \frac{b_M^2}{S_M} \sum_{k=1}^N l_{Mkk-1} \sum_{\mu=1}^n \Gamma_{0M\mu kk-1} \xi_{M\mu k-1}^{\mu k}, \\
c_{y1M}^{q_i} &= 4 \frac{b_M^2}{S_M} \sum_{k=1}^N l_{Mkk-1} \sum_{\mu=1}^n \Gamma_{M\mu kk-1}^{q_i}, \\
c_{y1M}^{q_i} &= 4 \frac{b_M^2}{S_M} \sum_{k=1}^N l_{Mkk-1} \sum_{\mu=1}^n \Gamma_{M\mu kk-1}^{q_i}, \\
c_{y2M}^{q_i} &= 4 \frac{b_M^2}{S_M} \sum_{k=1}^N l_{Mkk-1} \sum_{\mu=1}^n \Delta \Gamma_{M\mu kk-1}^{q_i} - m_{z1M}^{q_i}, \\
m_{z1M}^{q_i} &= 4 \frac{b_M^2}{S_M} \sum_{k=1}^N l_{Mkk-1} \sum_{\mu=1}^n \Gamma_{M\mu kk-1}^{q_i} \xi_{M\mu k-1}^{\mu k}, \\
m_{z1M}^{q_i} &= 4 \frac{b_M^2}{S_M} \sum_{k=1}^N l_{Mkk-1} \sum_{\mu=1}^n \Gamma_{M\mu kk-1}^{q_i} \xi_{M\mu k-1}^{\mu k},
\end{aligned} \tag{15.54}$$

$$\begin{aligned}
m_{z2M}^{q_i} &= 4 \frac{b_M^2}{S_M} \left[\sum_{k=1}^N l_{Mkk-1} \sum_{\mu=1}^n \Delta \Gamma_{M\mu kk-1}^{q_i} \xi_{M\mu k-1}^{\mu k} - \right. \\
&\quad \left. - \sum_{k=1}^N l_{Mkk-1} \sum_{\mu=1}^n \Gamma_{M\mu kk-1}^{q_i} (\xi_{M\mu k-1}^{\mu k})^2 \right] - \\
&\quad - \frac{b_M^2}{3S_M} \sum_{k=1}^N l_{Mkk-1}^3 \sum_{\mu=1}^n \Gamma_{M\mu kk-1}^{q_i} \operatorname{tg}^2 \chi_{M\mu k-1}^{\mu k}, \\
&\quad j = 1, 3; \quad l_{Mkk-1} = \xi_{Mk} - \xi_{Mk-1}, \\
m_{xM}^{\omega_r} &= -4 \frac{b_M^2}{S_M} \sum_{k=1}^N l_{Mkk-1} \sum_{\mu=1}^n \Gamma_{M\mu kk-1}^{\omega_r} \xi_{M\mu k-1}^{\mu k}, \\
(m_{xM}^{\omega_r})_1 &= -4 \frac{b_M^2}{S_M} \sum_{k=1}^N l_{Mkk-1} \sum_{\mu=1}^n \Gamma_{M\mu kk-1}^{\omega_r} \xi_{M\mu k-1}^{\mu k}, \\
(m_{xM}^{\omega_r})_2 &= -4 \frac{b_M^2}{S_M} \left[\sum_{k=1}^N l_{Mkk-1} \sum_{\mu=1}^n \Delta \Gamma_{M\mu kk-1}^{\omega_r} \xi_{M\mu k-1}^{\mu k} - \right. \\
&\quad \left. - \sum_{k=1}^N l_{Mkk-1} \sum_{\mu=1}^n \Gamma_{M\mu kk-1}^{\omega_r} \xi_{M\mu k-1}^{\mu k} \xi_{M\mu k-1}^{\mu k} \right] - \\
&\quad - \frac{b_M^2}{3S_M} \sum_{k=1}^N l_{Mkk-1}^3 \sum_{\mu=1}^n \Gamma_{M\mu kk-1}^{\omega_r} \operatorname{tg} \chi_{M\mu k-1}^{\mu k}.
\end{aligned} \tag{15.54}$$

Page 392.

In the case of the symmetrical strain of the wing

$$\begin{aligned}
 c_{yM}^{\delta} &= 4 \frac{b_M^2}{S_M} \sum_{k=1}^N l_{Mkk-1} \sum_{\mu=1}^n \Gamma_{M\mu kk-1}^{\delta}, \\
 c_{y1M}^{\delta} &= 4 \frac{b_M^2}{S_M} \sum_{k=1}^N l_{Mkk-1} \sum_{\mu=1}^n (\Gamma_{M\mu kk-1}^{\delta} + \Delta_1 \Gamma_{M\mu kk-1}^{\delta}), \\
 c_{y2M}^{\delta} &= 4 \frac{b_M^2}{S_M} \sum_{k=1}^N l_{Mkk-1} \sum_{\mu=1}^n (\Delta_2 \Gamma_{M\mu kk-1}^{\delta} - \Delta_1 \Gamma_{M\mu kk-1}^{\delta} - \\
 &\quad - \xi_{M\mu k-1}^{\mu k} \Gamma_{M\mu kk-1}^{\delta}), \\
 m_{zM}^{\delta} &= 4 \frac{b_M^2}{S_M} \sum_{k=1}^N l_{Mkk-1} \sum_{\mu=1}^n \Gamma_{M\mu kk-1}^{\delta} \xi_{M\mu k-1}^{\mu k}, \\
 m_{z1M}^{\delta} &= 4 \frac{b_M^2}{S_M} \sum_{k=1}^N l_{Mkk-1} \sum_{\mu=1}^n (\Gamma_{M\mu kk-1}^{\delta} + \Delta_1 \Gamma_{M\mu kk-1}^{\delta}) \xi_{M\mu k-1}^{\mu k}, \\
 m_{z2M}^{\delta} &= 4 \frac{b_M^2}{S_M} \sum_{k=1}^N l_{Mkk-1} \sum_{\mu=1}^n \left[\Delta_2 \Gamma_{M\mu kk-1}^{\delta} \xi_{M\mu k-1}^{\mu k} - \right. \\
 &\quad \left. - \Delta_1 \Gamma_{M\mu kk-1}^{\delta} \xi_{M\mu k-1}^{\mu k} - \Gamma_{M\mu kk-1}^{\delta} (\xi_{M\mu k-1}^{\mu k})^2 - \right. \\
 &\quad \left. - \frac{\bar{l}_{Mkk-1}^2}{12} \Gamma_{M\mu kk-1}^{\delta} t g^2 \chi_{M\mu k-1}^{\mu k} \right].
 \end{aligned}
 \tag{15.55}$$

Page 393.

During the antisymmetric strain

$$\begin{aligned}
 c_{yM}^\delta &= c_{y1M}^\delta = c_{y2M}^\delta = m_{zM}^\delta = m_{z1M}^\delta = m_{z2M}^\delta = 0, \\
 k^2 m_x^\delta &= m_{xM}^\delta, \quad k^4 m_x^\delta = (m_{xM}^\delta)_1 + M^2 (m_{xM}^\delta)_2, \\
 m_{xM}^\delta &= -4 \frac{b_M^2}{S_M} \sum_{k=1}^N l_{Mkk-1} \sum_{\mu=1}^n \Gamma_{M\mu kk-1}^\delta \xi_{M\mu k-1}^{\mu k}, \\
 (m_{xM}^\delta)_1 &= -4 \frac{b_M^2}{S_M} \sum_{k=1}^N l_{Mkk-1} \sum_{\mu=1}^n (\Gamma_{M\mu kk-1}^\delta + \Delta_1 \Gamma_{M\mu kk-1}^\delta) \xi_{M\mu k-1}^{\mu k}, \\
 (m_{xM}^\delta)_2 &= -4 \frac{b_M^2}{S_M} \sum_{k=1}^N l_{Mkk-1} \sum_{\mu=1}^n \left[(\Delta_2 \Gamma_{M\mu kk-1}^\delta - \Delta_1 \Gamma_{M\mu kk-1}^\delta - \right. \\
 &\quad \left. - \xi_{M\mu k-1}^{\mu k} \Gamma_{M\mu kk-1}^\delta) \xi_{M\mu k-1}^{\mu k} - \frac{\tilde{l}_{Mkk-1}^3}{12} \Gamma_{M\mu kk-1}^\delta \operatorname{tg} \chi_{M\mu k-1}^{\mu k} \right].
 \end{aligned} \tag{15.56}$$

The coefficient of rolling moment, as noted in chapter II, frequently are related not to root wing chord b , but to its spread/scope **2**. Noting the appropriate coefficients of aerodynamic derivatives by index 1:

$$m_{x1M} = \frac{2M_{xM}}{\rho_\infty U_0^2 S_M l_M} = \sum_{i=1}^4 (m_{x1M}^{q_i} q_i + m_{x1M}^{\dot{q}_i} \dot{q}_i), \tag{15.57}$$

let us have

$$km_{x1}^{\delta} = m_{x1M}^{\delta}, \quad k^3 m_{x1}^{\delta} = (m_{x1M}^{\delta})_1 + M^2 (m_{x1M}^{\delta})_2, \quad (15.58)$$

where

$$m_{x1M}^{\delta} = \frac{b_M}{l_M} m_{xM}^{\delta}, \quad (m_{x1M}^{\delta})_1 = \frac{b_M}{l_M} (m_{xM}^{\delta})_1, \quad (m_{x1M}^{\delta})_2 = \frac{b_M}{l_M} (m_{xM}^{\delta})_2.$$

Page 394.

It is analogous, for an angular rate of rotation Ω_x as characteristic linear dimension is accepted not the chord, but the half of spread/scope $l/2$ or respectively $l_M/2$. In this case the kinematic parameters, which determine the motion of wing in the compressed medium, are equal to

$$\omega_{x1} = \omega_x \frac{l}{2b}, \quad \dot{\omega}_{x1} = \dot{\omega}_x \left(\frac{l}{2b} \right)^2, \quad (15.59)$$

and
the parameters, which assign the motion of the converted wing in the incompressible medium, they are determined by the following relationship/ratios:

$$\omega_{x1M} = \omega_{xM} \frac{l_M}{2b_M}, \quad \dot{\omega}_{x1M} = \dot{\omega}_{xM} \left(\frac{l_M}{2b_M} \right)^2. \quad (15.60)$$

Hence easily we find

$$\left. \begin{aligned} km_{x1}^{\omega_{x1}} &= m_{x1M}^{\omega_{x1}}, & k^2 m_{x1}^{\omega_{x1}} &= (m_{x1M}^{\omega_{x1}})_1 + M^2 (m_{x1M}^{\omega_{x1}})_2, \\ \text{where} \quad m_{x1M}^{\omega_{x1}} &= \frac{2b_M^2}{l_M^2} m_{xM}^{\omega_{x1}}, & (m_{x1M}^{\omega_{x1}})_1 &= \frac{4b_M^3}{l_M^3} (m_{xM}^{\omega_{x1}})_1, \\ (m_{x1M}^{\omega_{x1}})_2 &= \frac{4b_M^3}{l_M^3} (m_{xM}^{\omega_{x1}})_2. \end{aligned} \right\} \quad (15.61)$$

Analogously are derive/concluded formulas for the recalculation of the coefficients aerodynamic derivative sections ζ_{hh-1} and ζ_{Mhh-1}/k initial and converted wings. Substituting in (10.42) the appropriate values from (15.48) and taking into account (15.38), we obtain

$$\left. \begin{aligned}
 kc'_{y0} &= c'_{y0M}, & km'_{z0} &= m'_{z0M}, \\
 kc'^{q_i}_y &= c'^{q_i}_{yM}, & k^3c'^{q_i}_y &= c'^{q_i}_{y1M} + M^2c'^{q_i}_{y2M}, \\
 km'^{q_i}_z &= m'^{q_i}_{zM}, & k^3m'^{q_i}_z &= m'^{q_i}_{z1M} + M^2m'^{q_i}_{z2M}, \\
 & & i &= 1, 3, 4; \\
 k^2c'^{q_i}_y &= c'^{q_i}_{yM}, & k^4c'^{q_i}_y &= c'^{q_i}_{y1M} + M^2c'^{q_i}_{y2M}, \\
 k^2m'^{q_i}_z &= m'^{q_i}_{zM}, & k^4m'^{q_i}_z &= m'^{q_i}_{z1M} + M^2m'^{q_i}_{z2M}, \\
 & & i &= 2.
 \end{aligned} \right\} \quad (15.62)$$

Page 395.

The coefficients aerodynamic derivative sections of the converted wing are determined from the formulas

$$c'_{y0M} = 2 \frac{b_M}{b_{Mkk-1}} \sum_{\mu=1}^n \Gamma_{0M\mu k-1}, \quad (15.63)$$

$$m'_{z0M} = 2 \left(\frac{b_M}{b_{Mkk-1}} \right)^2 \sum_{\mu=1}^n \Gamma_{0M\mu k-1} \xi_{M\mu k-1}^{\mu k},$$

$$c'_{yM} = 2 \frac{b_M}{b_{Mkk-1}} \sum_{\mu=1}^n \Gamma_{M\mu k-1}^{q_i},$$

$$m'_{zM} = 2 \left(\frac{b_M}{b_{Mkk-1}} \right)^2 \sum_{\mu=1}^n \Gamma_{M\mu k-1}^{q_i} \xi_{M\mu k-1}^{\mu k},$$

$$i = 1, 2, 3, 4;$$

$$c'_{y1M} = 2 \frac{b_M}{b_{Mkk-1}} \sum_{\mu=1}^n \Gamma_{M\mu k-1}^{q_i},$$

$$c'_{y2M} = 2 \frac{b_M}{b_{Mkk-1}} \left[\sum_{\mu=1}^n \Delta \Gamma_{M\mu k-1}^{q_i} - m'_{zM} \right],$$

$$m'_{z1M} = 2 \left(\frac{b_M}{b_{Mkk-1}} \right)^2 \sum_{\mu=1}^n \Gamma_{M\mu k-1}^{q_i} \xi_{M\mu k-1}^{\mu k},$$

$$m'_{z2M} = 2 \left(\frac{b_M}{b_{Mkk-1}} \right)^2 \sum_{\mu=1}^n \left[\Delta \Gamma_{M\mu k-1}^{q_i} \xi_{M\mu k-1}^{\mu k} - \Gamma_{M\mu k-1}^{q_i} (\xi_{M\mu k-1}^{\mu k})^2 \right], \quad (15.63)$$

$$i = 1, 2, 3;$$

$$c'_{y1M} = 2 \frac{b_M}{b_{Mkk-1}} \sum_{\mu=1}^n (\Gamma_{M\mu k-1}^{\delta} + \Delta_1 \Gamma_{M\mu k-1}^{\delta}),$$

$$c'_{y2M} = 2 \frac{b_M}{b_{Mkk-1}} \sum_{\mu=1}^n (\Delta_2 \Gamma_{M\mu k-1}^{\delta} - \Delta_1 \Gamma_{M\mu k-1}^{\delta} - \Gamma_{M\mu k-1}^{\delta} \xi_{M\mu k-1}^{\mu k}),$$

$$m'_{z1M} = 2 \left(\frac{b_M}{b_{Mkk-1}} \right)^2 \sum_{\mu=1}^n (\Gamma_{M\mu k-1}^{\delta} + \Delta_1 \Gamma_{M\mu k-1}^{\delta}) \xi_{M\mu k-1}^{\mu k},$$

$$m'_{z2M} = 2 \left(\frac{b_M}{b_{Mkk-1}} \right)^2 \sum_{\mu=1}^n (\Delta_2 \Gamma_{M\mu k-1}^{\delta} - \Delta_1 \Gamma_{M\mu k-1}^{\delta} - \Gamma_{M\mu k-1}^{\delta} \xi_{M\mu k-1}^{\mu k}) \xi_{M\mu k-1}^{\mu k}.$$

Page 396

Chapter XVI.

THE VELOCITY FIELD OF UNSTEADY DISCRETE VORTEX IN A COMPRESSED MEDIUM.

§1. Velocity potential, induced by oblique transient vortex in the subsonic compressible flow.

Page 396.

During the study of the arbitrary motion of wing at subsonic speeds, just as in the case of the incompressible medium ($M = 0$), as special feature/peculiarity is utilized oblique transient vortex. Let us find its velocity field in the compressed medium.

Let us introduce motionless rectangular coordinate system $Oxyz$, by orienting by its in such a way that axis Ox would be directed posigrade unperturbed flow U_0 (Fig. 16.1). Let us place in plane Oxz the motionless (connected) eddy/vortex AB , after combining its middle with the origin of coordinates. The width of eddy/vortex (measured

along axis Oz) let us designate l_0 , and the angle between AB and axis Oz - through χ (positive reference direction χ we consider direction from one Oz to Ox). Let us consider that the vorticity is constant along the length, but it is changed in the course of time. Let us designate vorticity by Γ_+ , at the time by t . Let us assume that the eddy/vortex appears at torque/moment $t = 0$. Under these conditions we have

$$\Gamma_+ = \Gamma_+(t) \text{ при } t \geq 0, \quad \Gamma_+ \equiv 0 \text{ при } t < 0. \quad (16.1)$$

Key: (1) with

The emergence of bound vortex and change in its intensity/strength produces the appearance of a system of free vortices. Let us assume that at torque/moment $t = 0$ appeared bound vortex Λ_{+1} . On the strength of the theorem about the invariability of circulation in time and the theorem about the constancy of vorticity over its length the formation/education of bound vortex can be visualized as follows.

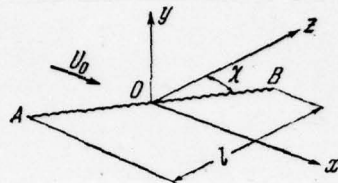


Fig. 16.1. Adopted system of coordinates for a horseshoe vortex.

Page 397.

With $t < 0$ on AB is arranged/located two superimposed to each other of eddy/vortex with intensity/strength Λ_{+1} and $-\Lambda_{+1}$. Since vorticity are differing by absolute value and are opposite on sign, the eddy/vortices of each other neutralize. At torque/moment $t = 0$ of second eddy/vortex is separate/liberated from the first and is carried by flow (Fig. 16.2). In this case, according to Helmholtz' theorem, between the end/leads of that taken away by the flow of free vortex DC and of bound vortex AB appear elongated along flow free vortices AD and BC the same intensity/strength Λ_{+1} . Thus appearing at torque/moment $t = 0$ bound vortex AB with intensity/strength Λ_{+1} is part of the locked, expanding in the course of time eddy/vortex ABCD

with intensity/strength Λ_{+1} . The subsequent changes in the intensity/strength of bound vortex produce the appearance of newly closed expanded eddy/vortices $ABB'A'$, $ABB''A''$ (Fig. 16.3). During a continuous change in the intensity/strength of bound vortex appears the continuous system of the locked eddy/vortices.

The examined vortex system, which consists of the finite number of locked being expanded eddy/vortices or of their continuous totality, is called subsequently simply unsteady oblique eddy/vortex. Let us find velocity potential, induced by this eddy/vortex.

It is known that the velocity potential, induced by the locked vortex line with intensity/strength Λ_{+1} , coincides with velocity potential, induced by the layer of the dipoles, which are arranged/located into parts of the plane, surrounded by eddy/vortex, and having the density of distribution of torque/moments, equal to $\sigma_1 = -\Lambda_{+1}$. Thus, during finding velocity potential, induced like the wind, depicted on Fig. 16.2, it is possible to replace with the layer of the dipoles, arranged/located inside ABCD with the uniform density of distribution of torque/moments $\sigma_1 = -\Lambda_{+1}$.

with intensity/strength Λ_{+1} . The subsequent changes in the intensity/strength of bound vortex produce the appearance of newly closed expanded eddy/vortices $ABB'A'$, $ABB'A$ (Fig. 16.3). During a continuous change in the intensity/strength of bound vortex appears the continuous system of the locked eddy/vortices.

The examined vortex system, which consists of the finite number of locked being expanded eddy/vortices or of their continuous totality, is called subsequently simply unsteady oblique eddy/vortex. Let us find velocity potential, induced by this eddy/vortex.

It is known that the velocity potential, induced by the locked vortex line with intensity/strength Λ_{+1} , coincides with velocity potential, induced by the layer of the dipoles, which are arranged/located into parts of the plane, surrounded by eddy/vortex, and having the density of distribution of torque/moments, equal to $\sigma_1 = -\Lambda_{+1}$. Thus, during finding velocity potential, induced like the wind, depicted on Fig. 16.2, it is possible to replace with the layer of the dipoles, arranged/located inside ABCD with the uniform density of distribution of torque/moments $\sigma_1 = -\Lambda_{+1}$.

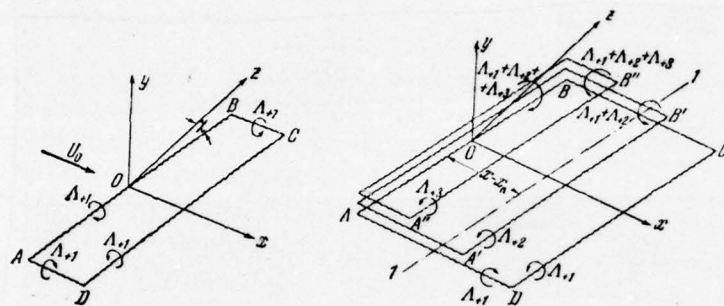


Fig. 16.2. Oblique horseshoe vortex at torque/moment $t > 0$.

Fig. 16.3. Oblique horseshoe vortex with the changing in time intensity/strength.

Page 398.

During the determination of velocity potential, induced by the transient vortex, depicted on Fig. 16.3, vortex/eddy system it is necessary to replace with the layer of the dipoles, which have in $A'B'CD$ the density of distribution of torque/moments, equal to $\sigma_1 = -\Lambda_{+1,1}$

in A "B" B'A' equal to $\sigma_2 = -(\Lambda_{+1} + \Lambda_{+2})$, in ABB "A" $\sigma_3 = -(\Lambda_{+1} + \Lambda_{+2} + \Lambda_{+3})$. Free vortices DC, A'B', A "B" are carried by flow with a velocity of U_0 . At the same velocity are moved areas A'B'CD, A "B" B'A' it is expanded area ABB'A'. By taking into account this, it is possible to present the emergence of the layer of dipoles as follows. On the straight line AB continuously appear the dipoles. They are free and immediately are carried by flow with a velocity of U_0 . As a result appears the being extracted along flow layer of dipoles. The density of this layer on the straight line AB is equal to the undertaken with opposite sign intensity/strength of bound vortex at the given instant. At a distance $x - x_n$ (measured according to flow) the density of distribution of dipole moments at the given instant t is equal to the undertaken with opposite sign vorticity at torque/moment $[t - (x - x_n)/U_0]$ (see Fig. 16.4). If the intensity/strength of bound vortex is changed continuously, then the density of distribution of dipole moments on AB will be also changed continuously and on certain straight line l_1 , parallel AB (see Fig. 16.3), at the given torque/moment t it will be equal to the intensity/strength of bound vortex at the moment of time $[t - (x - x_n)/U_0]$.

Let us examine the vortex/eddy system of oblique transient vortex, in which the intensity/strength of bound vortex is changed continuously and with $t < 0$ is equal to zero, but with $t \geq 0$, is equal to $\Gamma_+(t)$. Up to torque/moment t the vortex/eddy system of

transient vortex will engage parallelogram ABCD (Fig. 16.4). Let us replace transient vortex with the equivalent system of dipoles. In accordance with this system presented is the layer of dipoles, arranged/located inside ABCD and having at torque/moment t at the fixed/recorded point P with coordinates $x, 0, z$ the density of distribution of torque/moments, equal (see Fig. 16.4)

$$\left. \begin{aligned} \sigma(x, 0, z, t) &= -\Gamma_+ \left(t - \frac{x-x_n}{U_0} \right) && \text{при } t - \frac{x-x_n}{U_0} \geq 0, \\ \sigma(x, 0, z, t) &= 0 && \text{при } t - \frac{x-x_n}{U_0} < 0, \end{aligned} \right\} \quad (16.2)$$

$x_n = z \operatorname{tg} \chi.$

KEY: (1) with

It is known that velocity potential, induced by dipole, it is possible to obtain, by differentiating velocity potential, induced by source. Therefore let us examine the layer of sources. For this let us introduce parallelogram $A_1B_1C_1D_1$, equivalent to ABCD, but displaced up to distance y along axis Oy (Fig. 16.5).

Page 399.

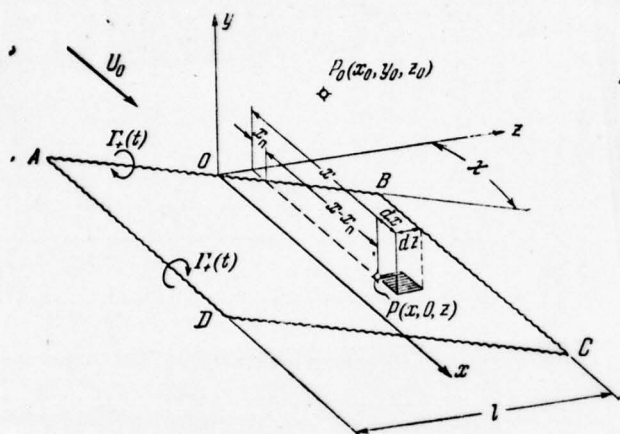


Fig. 16.4.

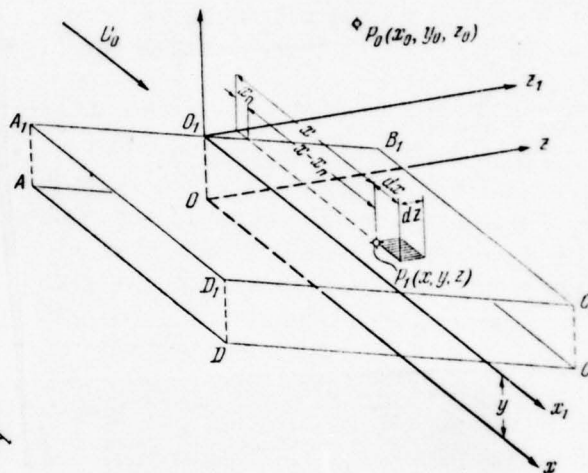


Fig. 16.5.

Fig. 16.4. Replacement of horseshoe vortex by the layer of dipoles. σ

$$(\sigma, t) = -\Gamma_s \left(t - \frac{x - x_0}{U_0} \right).$$

Fig. 16.5. To the derivation of formula for the induced velocities of

oblique horseshoe vortex in the compressed medium.

$$g(P_1, t) = g\left(t - \frac{x - x_n}{U_0}\right).$$

Page 400.

Let us fill it with sources according to the same law, as parallelogram ABCD was filled by dipoles, i.e., we will consider that on $A_1 B_1 C_1 D_1$ at the given torque/moment t at point P_1 with coordinates x, y, z the source strength was equal to

$$\left. \begin{aligned} g(x, y, z, t) &= g\left(t - \frac{x - x_n}{U_0}\right) & \begin{matrix} \textcircled{1} \\ \text{on } P_1 \end{matrix} & t - \frac{x - x_n}{U_0} \geq 0, \\ g(x, y, z, t) &= 0 & \begin{matrix} \textcircled{1} \\ \text{on } P_1 \end{matrix} & t - \frac{x - x_n}{U_0} < 0. \end{aligned} \right\} \quad (16.3)$$

KEY: (1) with

Let us designate by $\Delta\psi(x_0, y_0, z_0, x, y, z, t)$ the velocity potential, induced at torque/moment t in point P_0 with coordinates x_0, y_0, z_0 by the sources, arranged/located on surface element $dx dz$ (near point P_1) utilizing results [1.15], we obtain

$$\left. \begin{aligned}
 \Delta\psi &= -\frac{1}{4\pi} \frac{g \left[t - \frac{x-x_n}{U_0} + \frac{M(x_0-x)}{ak^2} - \frac{R_1}{ak^2} \right]}{R_1} dx dz, \\
 R_1 &= \sqrt{(x_0-x)^2 + k^2[(y_0-y)^2 + (z_0-z)^2]}, \\
 k &= \sqrt{1-M^2}, \quad M = \frac{U_0}{a}; \\
 g &\equiv 0 \quad \text{при} \quad t - \frac{x-x_n}{U_0} + \frac{M(x_0-x)}{ak^2} - \frac{R_1}{ak^2} < 0,
 \end{aligned} \right\} \quad (16.4)$$

KEY: (U) with

where a - the speed of sound.

Velocity potential, induced by all sources, arrange/located on $A_1B_1C_1D_1$, we find, integrating (16.4):

$$\psi = -\frac{1}{4\pi} \int_{-l_0/2}^{l_0/2} dz \int_{x_n}^{x_n+U_0 t} \frac{g \left[t - \frac{x-x_n}{U_0} + \frac{M(x_0-x)}{ak^2} - \frac{R_1}{ak^2} \right]}{R_1} dx. \quad (16.5)$$

In order to obtain velocity potential $\psi(x_0, y_0, z_0, x, 0, z, t)$, induced in point $P_0(x_0, y_0, z_0)$ at torque/moment t by the layer of the dipoles, arrange/located on ABCD, necessary in equation (16.5) to replace g by $\sigma = -\Gamma_+$, to differentiate this expression for y and to find then limit at $y \rightarrow 0$. Making these actions, we obtain

$$\varphi = \frac{1}{4\pi} \lim_{y \rightarrow 0} \frac{\partial}{\partial y} \int_{-l_0/2}^{l_0/2} dz \int_{x_{II}}^{x_{II} + U_0 t} \frac{\Gamma_+ \left[t - \frac{x - x_{II}}{U_0} + \frac{M(x_0 - x)}{ak^2} - \frac{R_1}{ak^2} \right]}{R_1} dx. \quad (16.6)$$

Page 401.

The obtained expression can be substantially simplified. For this let us pass to dimensionless quantities, after placing

$$\left. \begin{aligned} \Gamma_+ &= U_0 b \Gamma, \quad \xi = \frac{x}{b}, \quad \eta = \frac{y}{b}, \quad \zeta = \frac{z}{b}, \\ \xi_0 &= \frac{x_0}{b}, \quad \eta_0 = \frac{y_0}{b}, \quad \zeta_0 = \frac{z_0}{b}, \end{aligned} \right\} \quad (16.7)$$

where b - characteristic linear dimension. Substituting (16.7) in (16.6), we obtain

$$\begin{aligned} \varphi &= \frac{U_0 b}{4\pi} \lim_{\eta \rightarrow 0} \frac{\partial}{\partial \eta} \int_{-l_0/2b}^{l_0/2b} d\zeta \int_{\xi_{II}}^{\xi_{II} + \tau} \frac{\Gamma \left[t - \frac{b}{U_0} (\xi - \xi_{II}) + \frac{bM}{ak^2} (\xi_0 - \xi) - \frac{br_1}{ak^2} \right]}{r_1} d\xi; \\ r_1 &= \sqrt{(\xi_0 - \xi)^2 + k^2 [(\eta_0 - \eta)^2 + (\zeta_0 - \zeta)^2]}, \\ \xi_{II} &= \frac{x_{II}}{b} = \zeta \operatorname{tg} \chi, \quad \tau = \frac{U_0 t}{b}. \end{aligned} \quad (16.8)$$

After introducing the new variable

$$\beta = \xi_0 - \xi, \quad (16.9)$$

after replacement we obtain

$$\varphi = \frac{U_0 b}{4\pi} \lim_{\eta \rightarrow 0} \frac{\partial}{\partial \eta} \int_{-l_0/2b}^{l_0/2b} d\zeta \int_{\beta_1}^{\beta_2} \frac{\Gamma \left[t - \frac{b}{U_0} (\xi_0 - \xi_n) + \frac{b\beta}{U_0 k^2} - \frac{b}{ak^2} r \right]}{r} d\beta, \quad (16.10)$$

where

$$\beta_1^* = \xi_0 - \xi_n - \tau, \quad \beta_2 = \xi_0 - \xi_n, \\ r = \sqrt{\beta^2 + k^2 [(\eta_0 - \eta)^2 + (\xi_0 - \xi)^2]}.$$

During the calculation of potential by this formula one should bear in mind that in accordance with (16.2), (16.7) $\Gamma \equiv 0$ with

$$F = t - \frac{b}{U_0} (\xi_0 - \xi_n) + \frac{b\beta}{U_0 k^2} - \frac{b}{ak^2} r < 0. \quad (16.11)$$

However, virtually last/latter condition to conveniently consider, after changing in an appropriate manner integration limits. Let us designate the minimum and maximum values of the alternating/variable ζ area, filled by dipoles, where is satisfied the condition

$$t - \frac{b}{U_0} (\xi_0 - \xi_n) + \frac{b\beta}{U_0 k^2} - \frac{b}{ak^2} r \geq 0, \quad (16.12)$$

respectively through ζ_1 , ζ_2 , and the limiting values of the alternating/variable β boundary of this area - through β_1 , β_2 .

Now the formula, which determines potential, takes the following form:

$$\varphi = \frac{U_0 b}{4\pi} \lim_{\eta \rightarrow 0} \frac{\partial}{\partial \eta} \int_{\xi_1}^{\xi_2} d\xi \int_{\beta_1}^{\beta_2} \times \\ \times \frac{\Gamma \left[t - \frac{b}{U_0} (\xi_0 - \xi_n) + \frac{b\beta}{U_0 k^2} - \frac{br}{ak^2} \right] d\beta}{r}. \quad (16.13)$$

Values β_1 we find, solving relatively β the following equation:

$$F = t - \frac{b}{U_0} (\xi_0 - \xi_n) + \frac{b\beta}{U_0 k^2} - \frac{br}{ak^2} = 0. \quad (16.14)$$

In this case we obtain two values β_1 :

$$\beta_1 = \xi_0 - \zeta \lg \chi - \tau + M \sqrt{(\xi_0 - \zeta \lg \chi - \tau)^2 + (\eta_0 - \eta)^2 + (\xi_0 - \zeta)^2}, \quad (16.15)$$

$$\beta'_1 = \xi_0 - \zeta \lg \chi - \tau - M \sqrt{(\xi_0 - \zeta \lg \chi - \tau)^2 + (\eta_0 - \eta)^2 + (\xi_0 - \zeta)^2}. \quad (16.16)$$

By direct checking it is possible to establish that when $\beta'_1 < \beta < \beta_1$ $F < 0$. Therefore as the lower limit of internal integral in (16.13) above to take β_1 .

In order to find limits ζ_1 and ζ_2 , let us compute coordinates ζ the points of intersection of curves β_1 and β_2 (Fig. 16.6).

Set/assuming $\beta_1 = \beta_2$ and solving this equation relatively ζ , we find

$$\left. \begin{aligned} \zeta_{10}'' &= \zeta_0 + (\xi_0 - \zeta_0 \operatorname{tg} \chi - \tau) \sin \chi \cos \chi - \\ &\quad - \sqrt{\left(\frac{\tau}{M}\right)^2 - (\xi_0 - \zeta_0 \operatorname{tg} \chi - \tau)^2 \cos^2 \chi - (\eta_0 - \eta)^2 \cos \chi}, \\ \zeta_{20}'' &= \zeta_0 + (\xi_0 - \zeta_0 \operatorname{tg} \chi - \tau) \sin \chi \cos \chi + \\ &\quad + \sqrt{\left(\frac{\tau}{M}\right)^2 - (\xi_0 - \zeta_0 \operatorname{tg} \chi - \tau)^2 \cos^2 \chi - (\eta_0 - \eta)^2 \cos \chi}. \end{aligned} \right\} \quad (16.17)$$

If in the last/latter relationship/ratios radicand is equal to zero either negative, then ζ_{10}'' and ζ_{20}'' are equal or apparent/imaginary. In the first case the curve β_1 passes above β_2 and concerns by the latter at one point, in the second - curve β_1 passes above β_2 and it does not have with the latter of common points. In both cases the velocity potential is equal to zero, $\phi \equiv 0$.

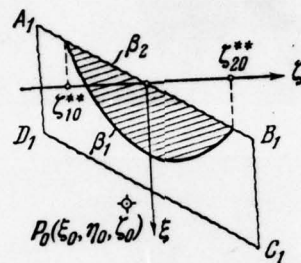


Fig. 16.6. To the determination of integration limits.

Page 403.

At actual values $\zeta_{10}^{**}, \zeta_{20}^{**}$ the integration limits for ζ are determined by the position of points $\zeta_{10}^{**}, \zeta_{20}^{**}$ relative to eddy/vortex and can be equal to $\pm l_0/2b$ or $\zeta_{10}^{**}, \zeta_{20}^{**}$. Taking into account that the integration limits for ζ are either the constants ($\pm l_0/2b, l_0$ - the spread/scope of eddy/vortex), or are equal to $\zeta_{10}^{**}, \zeta_{20}^{**}$, i.e., by such, with which $\beta_1 = \beta_2$, formula (16.13) can be rewritten as follows:

$$\varphi = \frac{U_0 b}{4\pi} \int_{\zeta_1}^{\zeta_2} d\zeta \lim_{\eta \rightarrow 0} \frac{\partial}{\partial \eta} \int_{\beta_1}^{\beta_2} \frac{\Gamma \left[1 - \frac{b}{U_0} (\xi_0 - \xi_n) + \frac{b\beta}{U_0 k^2} - \frac{br}{ak^2} \right] d\beta}{r}. \quad (16.18)$$

In this formula ζ_1, ζ_2 have the following values:

$$\left. \begin{aligned}
 \zeta_1 = \zeta_2 & \stackrel{(1)}{\text{при}} \zeta_{10}^*, \zeta_{20}^* \leq -\frac{l_0}{2b}, \zeta_{10}^*, \zeta_{20}^* \geq \frac{l_0}{2b}; \\
 \zeta_1 = -\frac{l_0}{2b}, \zeta_2 = \zeta_{20}^* & \stackrel{(1)}{\text{при}} \zeta_{10}^* \leq -\frac{l_0}{2b}, -\frac{l_0}{2b} \leq \zeta_{20}^* \leq \frac{l_0}{2b}; \\
 \zeta_1 = -\frac{l_0}{2b}, \zeta_2 = \frac{l_0}{2b} & \stackrel{(1)}{\text{при}} \zeta_{10}^* \leq -\frac{l_0}{2b}, \zeta_{20}^* \geq \frac{l_0}{2b}; \\
 \zeta_1 = \zeta_{10}^*, \zeta_2 = \zeta_{20}^* & \stackrel{(1)}{\text{при}} \zeta_{10}^* \geq -\frac{l_0}{2b}, \zeta_{20}^* \leq \frac{l_0}{2b}; \\
 \zeta_1 = \zeta_{10}^*, \zeta_2 = \frac{l_0}{2b} & \stackrel{(1)}{\text{при}} -\frac{l_0}{2b} \leq \zeta_{10}^* \leq \frac{l_0}{2b}, \zeta_{20}^* \geq \frac{l_0}{2b}.
 \end{aligned} \right\} (16.19)$$

KEY: (1) with

Here

$$\left. \begin{aligned}
 \zeta_{10}^* &= \zeta_0 + (\xi_0 - \zeta_0 \operatorname{tg} \chi - \tau) \sin \chi \cos \chi - \\
 &\quad - \sqrt{\left(\frac{\tau}{M}\right)^2 - (\xi_0 - \zeta_0 \operatorname{tg} \chi - \tau)^2 \cos^2 \chi - \eta_0^2 \cos \chi}, \\
 \zeta_{20}^* &= \zeta_0 + (\xi_0 - \zeta_0 \operatorname{tg} \chi - \tau) \sin \chi \cos \chi + \\
 &\quad + \sqrt{\left(\frac{\tau}{M}\right)^2 - (\xi_0 - \zeta_0 \operatorname{tg} \chi - \tau)^2 \cos^2 \chi - \eta_0^2 \cos \chi}.
 \end{aligned} \right\} (16.20)$$

§2. Velocity potential, induced by the transient vortex whose

intensity/strength is changed abruptly.

Let us examine the case, when the intensity/strength of bound vortex is changed abruptly. Let in torque/moment $t = 0$ intensity/strength of bound vortex instantly reach the value

$$\Gamma_+ = U_0 b \Gamma, \quad (16.21)$$

and then it remains always of constant. In this case up to torque/moment t the transient vortex will be the locked eddy/vortex ABCD (Fig. 16.7) whose intensity/strength in all sections is identical and equal to Γ_+ . In the course of time this eddy/vortex will be increasingly more and more extracted on flow.

Page 404.

Velocity potential, induced like the wind at torque/moment t in point (x_0, y_0, z_0) , let us find from (16.18), by set/assuming $\Gamma = \text{const.}$ After differentiation with respect to η , integration for β and passage to limit we obtain

$$\varphi = \frac{U_0 b \Gamma}{4\pi} \eta_0 \int_{\zeta_1}^{\zeta_2} \left\{ \frac{\xi_0 - \zeta \operatorname{tg} \chi}{[\eta_0^2 + (\zeta_0 - \zeta)^2] V(\xi_0 - \zeta \operatorname{tg} \chi)^2 + k^2 [\eta_0^2 + (\zeta_0 - \zeta)^2]} - \frac{\xi_0 - \zeta \operatorname{tg} \chi - \tau}{[\eta_0^2 + (\zeta_0 - \zeta)^2] V(\xi_0 - \zeta \operatorname{tg} \chi - \tau)^2 + \eta_0^2 + (\zeta_0 - \zeta)^2} \right\} d\zeta, \quad (16.22)$$

where ζ_1, ζ_2 are determined by relationship/ratios (16.19), (16.20).

Integration for ζ [1.91] gives

$$\begin{aligned} \varphi = \frac{U_0 b \Gamma}{4\pi} & \left[\operatorname{arctg} \left(V(\xi_0 - \zeta_0 \operatorname{tg} \chi)^2 + \eta_0^2 \operatorname{tg}^2 \chi [\eta_0^2 \operatorname{tg} \chi - (\xi_0 - \zeta_0 \operatorname{tg} \chi)(\zeta_0 - \zeta)] \right) \times \right. \\ & \times \eta_0^{-1} \{ k^2 [\eta_0^2 \operatorname{tg} \chi - (\xi_0 - \zeta_0 \operatorname{tg} \chi)(\zeta_0 - \zeta)]^2 + \\ & + [(\xi_0 - \zeta_0 \operatorname{tg} \chi)^2 + (k^2 + \operatorname{tg}^2 \chi) \eta_0^2] [(\xi_0 - \zeta \operatorname{tg} \chi) + (\zeta_0 - \zeta) \operatorname{tg} \chi]^2 \}^{-1/2} - \\ & - \operatorname{arctg} \left(V(\xi_0 - \zeta_0 \operatorname{tg} \chi - \tau)^2 + \eta_0^2 \operatorname{tg}^2 \chi [\eta_0^2 \operatorname{tg} \chi - (\xi_0 - \zeta_0 \operatorname{tg} \chi - \tau)(\zeta_0 - \zeta)] \right) \times \\ & \times \eta_0^{-1} \{ [\eta_0^2 \operatorname{tg} \chi - (\xi_0 - \zeta_0 \operatorname{tg} \chi - \tau)(\zeta_0 - \zeta)]^2 + [(\xi_0 - \zeta_0 \operatorname{tg} \chi - \tau)^2 + \\ & + (1 + \operatorname{tg}^2 \chi) \eta_0^2] [(\xi_0 - \zeta_0 \operatorname{tg} \chi - \tau) + (\zeta_0 - \zeta) \operatorname{tg} \chi]^2 \}^{-1/2} \Big]_{\zeta=\zeta_1}^{\zeta=\zeta_2}. \quad (16.23) \end{aligned}$$

The entering this formula values ζ_1 and ζ_2 are located from (16.19), (16.20).

Let us find velocity potential in some special cases. We

determine first potential in the case, when from the torque/moment of the emergence of eddy/vortex pass very long time (medium compressed).

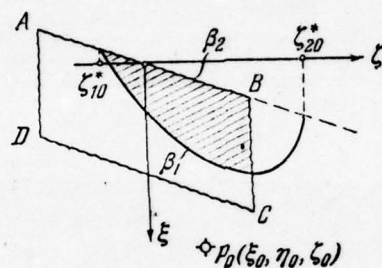


Fig. 16.7. To the determination of integration limits.

Page 405.

In this case of $t \rightarrow -\infty$, and consequently,

$$\frac{at}{b} = \frac{\tau}{M} \rightarrow \infty, \quad \tau = \frac{U_0 t}{b} \rightarrow \infty.$$

Under these conditions from (16.20) it follows that $\zeta_{10}^* \rightarrow -\infty$, $\zeta_{20}^* \rightarrow +\infty$, and it is necessary to count $\zeta_1 = l_0/2b$, $\zeta_2 = l_0/2b$. Substituting these values in (16.23) and set/assuming $\tau \rightarrow -\infty$, we find

$$\begin{aligned} \varphi = \frac{U_0 b \Gamma}{4\pi} & \left[\operatorname{arctg} \left(\sqrt{(\xi_0 - \zeta_0 \operatorname{tg} \chi)^2 + \eta_0^2 \operatorname{tg}^2 \chi} \times \right. \right. \\ & \times [\eta_0^2 \operatorname{tg} \chi - (\xi_0 - \zeta_0 \operatorname{tg} \chi)(\zeta_0 - \zeta)] \eta_0^{-1} \{ k^2 [\eta_0^2 \operatorname{tg} \chi - (\xi_0 - \zeta_0 \operatorname{tg} \chi)(\zeta_0 - \zeta)]^2 + \\ & \quad \left. + [(\xi_0 - \zeta_0 \operatorname{tg} \chi)^2 + (k^2 + \operatorname{tg}^2 \chi) \eta_0^2] \times \right. \\ & \left. \left. \times [(\xi_0 - \zeta_0 \operatorname{tg} \chi) + (\zeta_0 - \zeta) \operatorname{tg} \chi]^2 \right\}^{-1/2} \right] - \operatorname{arctg} \frac{\xi_0 - \zeta}{\eta_0} \Big|_{\zeta = -l_0/2b}^{\zeta = l_0/2b}. \quad (16.24) \end{aligned}$$

Set/assuming in the last/latter formula $k = 1$, we find velocity potential, induced like the wind in the incompressible medium:

$$\begin{aligned} \varphi = \frac{U_0 b \Gamma}{4\pi} & \times \\ & \times \left\{ \operatorname{arctg} \frac{\sqrt{(\xi_0 - \zeta_0 \operatorname{tg} \chi)^2 + \eta_0^2 \operatorname{tg}^2 \chi} [\eta_0^2 \operatorname{tg} \chi - (\xi_0 - \zeta_0 \operatorname{tg} \chi)(\zeta_0 - \zeta)]}{\eta_0 \sqrt{[(\xi_0 - \zeta_0 \operatorname{tg} \chi)^2 + (1 + \operatorname{tg}^2 \chi) \eta_0^2] [(\xi_0 - \zeta_0 \operatorname{tg} \chi) + (\zeta_0 - \zeta) \operatorname{tg} \chi]^2}} - \right. \\ & \left. - \operatorname{arctg} \frac{\xi_0 - \zeta}{\eta_0} \right\} \Big|_{\zeta = -l_0/2b}^{\zeta = l_0/2b}. \quad (16.25) \end{aligned}$$

Let us examine by now case when transient vortex is the system, which consists of the infinite bound vortex, arranged/located on the axis Oz , and parallel to it free vortex, taken away by flow with a velocity of U_0 (medium compressed). As before let us consider that the eddy/vortex appeared at torque/moment $t = 0$. The formula, which determines potential, in this case let us find from (16.19), (16.20),

(16.23), by set/assuming $\chi \rightarrow 0, l_0 \rightarrow -$:

$$\varphi = \frac{U_0 b \Gamma}{4\pi} \left\{ \operatorname{arctg} \frac{(\xi_0 - \tau)(\xi_0 - \xi)}{\eta_0 \sqrt{(\xi_0 - \tau)^2 + (\xi_0 - \xi)^2 + \eta_0^2}} - \right. \\ \left. - \operatorname{arctg} \frac{\xi_0(\xi_0 - \xi)}{\eta_0 \sqrt{\xi_0^2 + k^2 [\eta_0^2 + (\xi_0 - \xi)^2]}} \right\}_{\xi=\xi_1}^{\xi=\xi_2}, \quad (16.26)$$

$$\xi_1 = \xi_0 - \sqrt{\left(\frac{\tau}{M}\right)^2 - (\xi_0 - \tau)^2 - \eta_0^2},$$

$$\xi_2 = \xi_0 + \sqrt{\left(\frac{\tau}{M}\right)^2 - (\xi_0 - \tau)^2 - \eta_0^2}.$$

Page 406.

Substituting limits and carrying out a series of transformations, we obtain

$$\varphi = \frac{U_0 b \Gamma}{2\pi} \operatorname{arctg} \frac{\eta_0 \sqrt{\tau^2 - M^2 [(\xi_0 - \tau)^2 + \eta_0^2]}}{\eta_0^2 + \xi_0(\xi_0 - \tau)}. \quad (16.27)$$

The obtained expression coincides with the formula, derived in [2.24].

§3. Velocity, induced like the wind with an abrupt change in the intensity/strength.

Let us find the velocity W_y , parallel to axis Oy (see Fig. 16.1), induced by transient vortex in plane $y = 0$. Taking into account (16.8), we have

$$W_y = \frac{1}{b} \lim_{\eta_0 \rightarrow 0} \frac{\partial \varphi}{\partial \eta_0}. \quad (16.28)$$

Differentiating (16.23), we obtain

$$W_y = \frac{U_0 \Gamma}{4\pi} w_y, \quad (16.29)$$

where

$$\left. \begin{aligned} w_y &= w_{y1} + w_{y2}, \\ w_{y1} &= - \frac{V[(\xi_0 - \zeta_0 \operatorname{tg} \chi) + (\zeta_0 - \zeta_1) \operatorname{tg} \chi]^2 + k^2 (\zeta_0 - \zeta_1)^2}{(\xi_0 - \zeta_0 \operatorname{tg} \chi) (\zeta_0 - \zeta_1)} + \\ &\quad + \frac{V[(\xi_0 - \zeta_0 \operatorname{tg} \chi) + (\zeta_0 - \zeta_2) \operatorname{tg} \chi]^2 + k^2 (\zeta_0 - \zeta_2)^2}{(\xi_0 - \zeta_0 \operatorname{tg} \chi) (\zeta_0 - \zeta_2)}, \\ w_{y2} &= \frac{V[(\xi_0 - \zeta_0 \operatorname{tg} \chi - \tau) + (\zeta_0 - \zeta_1) \operatorname{tg} \chi]^2 + (\zeta_0 - \zeta_1)^2}{(\xi_0 - \zeta_0 \operatorname{tg} \chi - \tau) (\zeta_0 - \zeta_1)} - \\ &\quad - \frac{V[(\xi_0 - \zeta_0 \operatorname{tg} \chi - \tau) + (\zeta_0 - \zeta_2) \operatorname{tg} \chi]^2 + (\zeta_0 - \zeta_2)^2}{(\xi_0 - \zeta_0 \operatorname{tg} \chi - \tau) (\zeta_0 - \zeta_2)}. \end{aligned} \right\} \quad (16.30)$$

The entering the last/latter relationship/ratios values ζ_1, ζ_2 are determined from (16.19), (16.20) with $\eta_0 = 0$ have the following values:

$$\begin{aligned}
 \zeta_1 = \zeta_2 & \quad \textcircled{2} \text{ при } \zeta_1^*, \zeta_2^* \leq -\frac{l_0}{2b} \quad \textcircled{1} \text{ или } \zeta_1^*, \zeta_2^* \geq \frac{l_0}{2b}; \\
 \zeta_1 = -\frac{l_0}{2b}, \zeta_2 = \zeta_2^* & \quad \textcircled{3} \text{ при } \zeta_1^* \leq -\frac{l_0}{2b}, -\frac{l_0}{2b} \leq \zeta_2^* \leq \frac{l_0}{2b}; \\
 \zeta_1 = -\frac{l_0}{2b}, \zeta_2 = \frac{l_0}{2b} & \quad \textcircled{2} \text{ при } \zeta_1^* \leq -\frac{l_0}{2b}, \zeta_2^* \geq \frac{l_0}{2b}; \\
 \zeta_1 = \zeta_1^*, \zeta_2 = \zeta_2^* & \quad \textcircled{2} \text{ при } \zeta_1^* \geq -\frac{l_0}{2b}, \zeta_2^* \leq \frac{l_0}{2b}.
 \end{aligned}
 \quad (16.31)$$

$$\begin{aligned}
 \zeta_1 = \zeta_1^*, \zeta_2 = \frac{l_0}{2b} & \quad \textcircled{2} \text{ при } -\frac{l_0}{2b} \leq \zeta_1^* \leq \frac{l_0}{2b}, \zeta_2^* \geq \frac{l_0}{2b}, \\
 \zeta_1^* = \zeta_0 + (\xi_0' - \zeta_0 \operatorname{tg} \chi - \tau) \sin \chi \cos \chi - \\
 & - \sqrt{\left(\frac{\tau}{M}\right)^2 - (\xi_0 - \zeta_0 \operatorname{tg} \chi - \tau)^2 \cos^2 \chi \cos \chi}, \\
 \zeta_2^* = \zeta_0 + (\xi_0' - \zeta_0 \operatorname{tg} \chi - \tau) \sin \chi \cos \chi + \\
 & + \sqrt{\left(\frac{\tau}{M}\right)^2 - (\xi_0 - \zeta_0 \operatorname{tg} \chi - \tau)^2 \cos^2 \chi \cos \chi}.
 \end{aligned}
 \quad (16.31)$$

Key:
(1) or

(2) with.

Let us examine again some special cases. Set/assuming in (16.30) and (16.31) $t \rightarrow \infty$, we find the velocity, induced by transient vortex in the compressed medium, when from the torque/moment of the emergence of eddy/vortex pass very long time. Taking into account that with $t \rightarrow \infty$ $r \rightarrow \infty$, $\frac{\tau}{M} \rightarrow \infty$ and $\zeta_1 = l_0/2b$, $\zeta_2 = l_0/2b$, we obtain

$$W_y = \frac{U_0 \Gamma}{4\pi} w_y, \quad \left. \begin{aligned} w_y = & \frac{1}{\zeta_0 - \frac{l_0}{2b}} + \frac{\sqrt{\left(\zeta_0 - \frac{l_0}{2b} \lg \chi\right)^2 + k^2 \left(\zeta_0 - \frac{l_0}{2b}\right)^2}}{(\zeta_0 - \zeta_0 \lg \chi) \left(\zeta_0 - \frac{l_0}{2b}\right)} - \\ & - \frac{1}{\zeta_0 + \frac{l_0}{2b}} - \frac{\sqrt{\left(\zeta_0 + \frac{l_0}{2b} \lg \chi\right)^2 + k^2 \left(\zeta_0 + \frac{l_0}{2b}\right)^2}}{(\zeta_0 - \zeta_0 \lg \chi) \left(\zeta_0 + \frac{l_0}{2b}\right)}. \end{aligned} \right\} \quad (16.32)$$

This same result is obtained, differentiating (16.24) and set/assuming then $\eta_0 \rightarrow 0$.

In the case of the incompressible medium ($k = 1$) we have

$$w_y = \frac{1}{\xi_0 - \frac{l_0}{2b}} + \frac{\sqrt{\left(\xi_0 - \frac{l_0}{2b} \lg \chi\right)^2 + \left(\xi_0 - \frac{l_0}{2b}\right)^2}}{(\xi_0 - \xi_0 \lg \chi) \left(\xi_0 - \frac{l_0}{2b}\right)} -$$

$$- \frac{1}{\xi_0 + \frac{l_0}{2b}} - \frac{\sqrt{\left(\xi_0 + \frac{l_0}{2b} \lg \chi\right)^2 + \left(\xi_0 + \frac{l_0}{2b}\right)^2}}{(\xi_0 - \xi_0 \lg \chi) \left(\xi_0 + \frac{l_0}{2b}\right)}. \quad (16.33)$$

The obtained expression coincides with formula (9.8). During comparison it is necessary to keep in mind that in the present chapter accepted opposite direction of axis Oz in comparison with chapter IX.

Page 408.

Let us find now the vertical velocity, induced by the transient vortex of infinite width, i.e., by the vortex/eddy system, which consists of the infinite bound vortex, arranged/located on the axis Oz, and parallel to it infinite free vortex, taken away by flow. Set/assuming in (16.30) and (16.31) $l_0 \rightarrow -\infty$ we obtain

$$\left. \begin{aligned} W_y &= \frac{U_0 \Gamma}{2\pi} w_y, \\ w_y &= \frac{\sqrt{\tau^2 - M^2 (\xi_0 - \tau)^2}}{\xi_0 (\xi_0 - \tau)}. \end{aligned} \right\} \quad (16.34)$$

The same result is obtained, differentiating (16.27) on η_0 and transfer/converting to $\eta_0 \rightarrow 0$. Formula (16.34) coincides with the expression, obtained in work [2.24].

Page 409.

Chapter XVII.

METHOD OF THE CALCULATION OF AERODYNAMIC WING CHARACTERISTICS WITH
ARBITRARY TIME DEPENDENCES.

§1. Calculation of the intensity/strength of the bound vortexes of
wings with $\eta = 1$.

The method of the calculation of aerodynamic characteristics during the aperiodic motion of lifting surface in the incompressible medium is described in chapter XI. By utilizing the derived in preceding chapter formulas, it is possible analogously to solve the problem of the aperiodic motion of wing at subsonic speed in the compressed medium. For a clarity let us examine first wing with direct/straight edges and the contraction, equal to one.

Let us introduce the rectangular coordinate system $Oxyz$, connected with wing. The origin of coordinates let us place in tip noside of root chord, axis Ox is directed along this chord back/ago, and axis Oz - along the right half wing (Fig. 17.1). Let us designate by U_0 the average speed of the motion of wing, time-independent, but the kinematic parameters, which characterize supplementary motions, let us consider assigned in the form

$$q_i(\tau) = q_i^* \left(\frac{q_i(\tau)}{q_i^*} \right). \quad (17.1)$$

Here q_i are the parameters, introduced according to (2.19), a q_i^* are their maximum values. As already mentioned, the parameters $q_2 = \omega_x$, $q_3 = \omega_z$ are taken in standard axes. Let us accept also, that the lifting surface transforms and at given torque/moment its equation takes the form

$$\eta = f_0(\xi, \zeta) + f_0(\xi, \zeta) \delta(\tau). \quad (17.2)$$

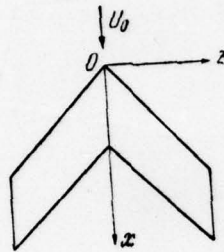


Fig. 17.1. System of the axes.

Page 410.

Under boundary condition (3.56) we will obtain the following terms

$$\left(\frac{\partial \bar{\Phi}_\delta}{\partial \eta}\right)_0 = \frac{\partial f_0(\xi, \zeta)}{\partial \xi}, \quad \left(\frac{\partial \bar{\Phi}_\delta}{\partial \eta}\right)_1 = \delta(\tau), \quad \left(\frac{\partial \bar{\Phi}_\delta}{\partial \eta}\right)_2 = \frac{d\delta}{d\tau}. \quad (17.3)$$

Let us assume still that in its motion the lifting surface encounters gust. Let us introduce fixed coordinate system $O_1x_1y_1z_1$ (Fig. 17.2). The relative velocity of breakaway in fixed coordinate systems is assigned and equal to

$$\frac{W_{y\Delta}}{U_0} = w_{y\Delta}(x_1) = \dot{w}_{y\Delta}(\xi_1). \quad (17.4)$$

Let us consider that at the initial moment $t = 0$ spout of root chord coincides with the beginning of motionless system and it is oriented in such a way that axis Ox_1 coincides with vector U_0 , and axis Oz_1 and Oy_1 - in accordance with axes Oz and Oy . Taking into account communication/connection between the coordinates of movable and motionless systems, we find the appropriate term under boundary condition (3.56)

$$\left(\frac{\partial \bar{\varphi}_\Delta}{\partial \eta} \right) = - w_{y\Delta}^* \left[\frac{w_{y\Delta} (\tau - \xi)}{w_{y\Delta}^*} \right]. \quad (17.5)$$

By following the method, presented in chapter XI, lifting surface and vortex wake let us replace with the system of discrete transient vortices. For this let us break half wing (Fig. 17.3) by the planes, parallel to the plane of symmetry, into N of bands. The numbers of sections let us designate by k (or p) and count conduct from tip of the wing (where we set/assume $k = p = 0$) to root section ($k = N$). By such, with form, k or p will vary within the limits of $k = 0, 1, 2, \dots, N$; $p = 0, 1, 2, \dots, N$.

The planes which separate chords into n of equal parts, let us cut bands on panel.

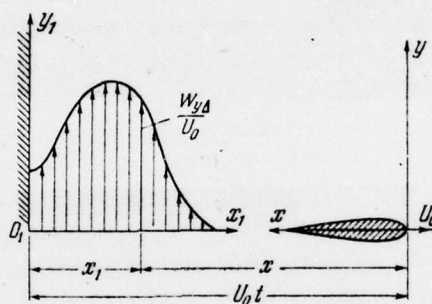


Fig. 17.2. Motionless and moving coordinate system upon the entrance of wing into gust.

Page 411.

On each panel at a distance (measured according to flow), equal to $1/4$ lengths of panel, i.e., at a distance, equal to $b^*/4n$, from the leading edge of panel (b^* - the current chord), let us place the bound vortexes of constant along the length, but the changing in the course of time intensity/strength. To the vortex line, formed by the bound vortexes of one series of panels, let us ascribe number μ . Is obvious, $\mu = 1, 2, \dots, n$.

764

Let us designate x_{0k}, z_{0k} (x_{0p}, z_{0p}) - the coordinates of leading edge in section k (or p) and by $x_{1k}, z_{1k}, x_{1p}, z_{1p}$ and b_k, b_p - the coordinates of trailing edge and chord in cross section. For the appropriate

relative coordinates let us introduce the following designations:

$$\left. \begin{aligned} \xi_{0k} &= \frac{x_{0k}}{b}, & \zeta_{0k} &= \frac{z_{0k}}{b}, \\ \xi_{0p} &= \frac{x_{0p}}{b}, & \zeta_{0p} &= \frac{z_{0p}}{b}; \\ \xi_{1k} &= \frac{x_{1k}}{b}, & \zeta_{1k} &= \frac{z_{1k}}{b}, \\ \xi_{1p} &= \frac{x_{1p}}{b}, & \zeta_{1p} &= \frac{z_{1p}}{b}; \\ \bar{b}_k &= \frac{b_k}{b} = \frac{x_{1k} - x_{0k}}{b}, \\ \bar{b}_p &= \frac{b_p}{b} = \frac{x_{1p} - x_{0p}}{b}. \end{aligned} \right\} (17.6)$$

In this paragraph is examined the case, when contraction $\bar{\eta} = 1$, i.e., $\bar{b}_k = \bar{b}_p = 1$. The slope tangent, the relative coordinates of end/leads and middle of the bound vortex, which lies between sections $k, k - 1$ and belonging to μ -th vortex line, are determined from formulas (10.5), (10.6), (10.8) and for the case in question take the following form:

$$\left. \begin{aligned} \operatorname{tg} \chi_{\mu k-1}^{\mu k} &= \frac{\xi_{\mu k-1} - \xi_{\mu k}}{\zeta_{\mu k-1} - \zeta_{\mu k}}, & \xi_{\mu k} &= \xi_{0k} + \frac{\mu - \frac{3}{4}}{n}, & \zeta_{\mu k} &= \zeta_{0k}, \\ \xi_{\mu k-1}^{\mu k} &= \frac{1}{2}(\xi_{\mu k-1} + \xi_{\mu k}), & \zeta_{\mu k-1}^{\mu k} &= \frac{1}{2}(\zeta_{\mu k-1} + \zeta_{\mu k}). \end{aligned} \right\} (17.7)$$

Let us conduct guide lines in such a way that in each section they would be arranged/located at a distance (measured according to flow), equal to $b'/4n$, from the trailing edges of panels.

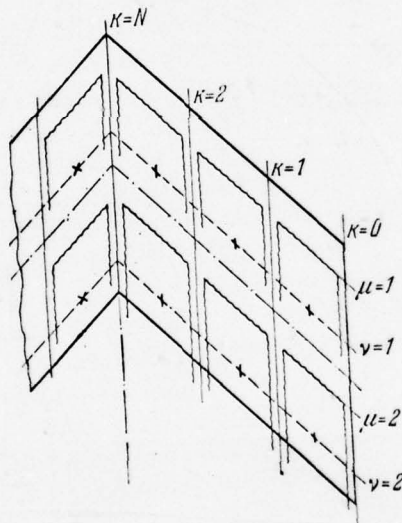


Fig. 17.3. Replacement of wing without contraction by oblique horseshoe vortices.

Page 412.

The number of guide line let us designate ν ($\nu = 1, 2, \dots, n$). As the control points, at which must accurately be fulfilled boundary conditions, let us accept the points, which lie on guide lines on the middle of panel. The relative coordinates of end/leads and middles of guide line ν , arrange/located on band between sections $p - 1$ and p , we find through formulas (10.11). In the case, i.e., with ~~in question~~ $\tilde{n} = 1$ they will be determined by the relationship/ratios

$$\left. \begin{aligned} \xi_{\nu p} &= \xi_{0p} + \frac{\nu - \frac{1}{4}}{n}, & \zeta_{\nu p} &= \zeta_{0p}, \\ \xi_{\nu p-1} &= \frac{1}{2} (\xi_{\nu p-1} + \xi_{\nu p}), & \zeta_{\nu p-1} &= \frac{1}{2} (\zeta_{\nu p-1} + \zeta_{\nu p}). \end{aligned} \right\} \quad (17.8)$$

By following the procedure, accepted in chapter XI, the continuous process of a change in the kinematic parameters and aerodynamic characteristics in time let us replace discrete (see Fig. 11.2). The relative time, which takes place between successive torque/moments of a change in the parameters (space of time), let us designate Δr . As calculated let us accept the torque/moments, which directly precede a change in the corresponding characteristics. The calculated torque/moment let us characterize number r (r - positive integer number). Let us consider that to the initial moment of motion it corresponds to $r = 0$, and final $r = R$. Is obvious the time, which

corresponds to the calculated torque/moment r , equally

$$\tau_r = r \Delta \tau. \quad (17.9)$$

Let us designate the intensity/strength of the bound vortex, lying between sections $k - 1$, k and belonging to μ -th vortex line (with q_i -th the form of motion), by

$$\Gamma_{+\mu kk-1} = U_0 b q_i \Gamma_{q_i \mu kk-1}, \quad (17.10)$$

where $\Gamma_{q_i \mu kk-1}$ - relative intensity/strength. Let us consider that the vorticity is changed abruptly into the torque/moments, the following directly after calculated, and in the interval/gaps between them it remains constant/invariable (see Fig. 11.3). The value of relative intensity/strength at the calculated torque/moment and to change in this intensity/strength at the torque/moments, which precede calculated, let us designate respectively by $\Gamma_{q_i \mu kk-1}^r$, $\Lambda_{q_i \mu kk-1}^r$. Between these values there is the following obvious dependence:

$$\left. \begin{aligned} \Lambda_{q_i \mu kk-1}^0 &= \Gamma_{q_i \mu kk-1}^0 = 0, & \Lambda_{q_i \mu kk-1}^1 &= \Gamma_{q_i \mu kk-1}^1, \\ \Lambda_{q_i \mu kk-1}^r &= \Gamma_{q_i \mu kk-1}^r - \Gamma_{q_i \mu kk-1}^{r-1}, & \Lambda_{+\mu kk-1}^r &= U_0 b \Lambda_{q_i \mu kk-1}^r. \end{aligned} \right\} \quad (17.11)$$

Page 413.

For the taken model one should assume that into the torque/moments, the following directly after calculated, from bound vortexes are separate/liberated parallel by it free vortices and are formed the locked, being extracted along flow eddy/vortices of

constant intensity/strength. To Fig. 17.4 it is shown, in that is developed this eddy/vortex toward the calculated torque/moment r , if it was formed immediately after the calculated torque/moment s . Let us find the vertical velocity in control point on line ∇ between sections $p, p - 1$ in the calculated torque/moment r , induced by the locked eddy/vortex, which arose immediately after torque/moment s as a result of a change in the intensity/strength of the bound vortex, which lies between sections $k, k - 1$ and belonging to μ -th vortex line.

Utilizing the formulas, derived in chapter of XVI, and taking into account communication/connection between coordinates in the systems, connected with eddy/vortex and wing, we obtain

$$W_{yvp-p-1s}^{\mu k k-1r} = \frac{U_0}{4\pi} \Lambda_{q, \mu k k-1}^{s+1} w_{yvp-p-1s}^{\mu k k-1r}, \quad (17.12)$$

where

$$\left. \begin{aligned} w_{yvp-p-1s}^{\mu k k-1r} &= -\frac{a_{1vp-p-1s}^{\mu k k-1r}}{\xi_{\mu k k-1}^{\mu k k-1r} \xi_{1vp-p-1s}^{\mu k k-1r}} + \frac{a_{2vp-p-1s}^{\mu k k-1r}}{\xi_{\mu k k-1}^{\mu k k-1r} \xi_{2vp-p-1s}^{\mu k k-1r}} + \\ &\quad + \frac{a_{1vp-p-1s}^{\mu k k-1r}}{\xi_{\mu k k-1r}^{\mu k k-1r} \xi_{1vp-p-1s}^{\mu k k-1r}} - \frac{a_{2vp-p-1s}^{\mu k k-1r}}{\xi_{\mu k k-1r}^{\mu k k-1r} \xi_{2vp-p-1s}^{\mu k k-1r}}; \\ a_{1vp-p-1s}^{\mu k k-1r} &= \sqrt{\left[\xi_{\mu k k-1}^{\mu k k-1r} + \xi_{1vp-p-1s}^{\mu k k-1r} \operatorname{tg} \chi_{\mu k-1}^{\mu k} \right]^2 + k^2 \left[\xi_{1vp-p-1s}^{\mu k k-1r} \right]^2}, \\ a_{2vp-p-1s}^{\mu k k-1r} &= \sqrt{\left[\xi_{\mu k k-1}^{\mu k k-1r} + \xi_{2vp-p-1s}^{\mu k k-1r} \operatorname{tg} \chi_{\mu k-1}^{\mu k} \right]^2 + k^2 \left[\xi_{2vp-p-1s}^{\mu k k-1r} \right]^2}, \\ a_{1vp-p-1s}^{\mu k k-1r} &= \sqrt{\left[\xi_{\mu k k-1r}^{\mu k k-1r} + \xi_{1vp-p-1s}^{\mu k k-1r} \operatorname{tg} \chi_{\mu k-1}^{\mu k} \right]^2 + \left[\xi_{1vp-p-1s}^{\mu k k-1r} \right]^2}, \\ a_{2vp-p-1s}^{\mu k k-1r} &= \sqrt{\left[\xi_{\mu k k-1r}^{\mu k k-1r} + \xi_{2vp-p-1s}^{\mu k k-1r} \operatorname{tg} \chi_{\mu k-1}^{\mu k} \right]^2 + \left[\xi_{2vp-p-1s}^{\mu k k-1r} \right]^2}. \end{aligned} \right\} \quad (17.13)$$

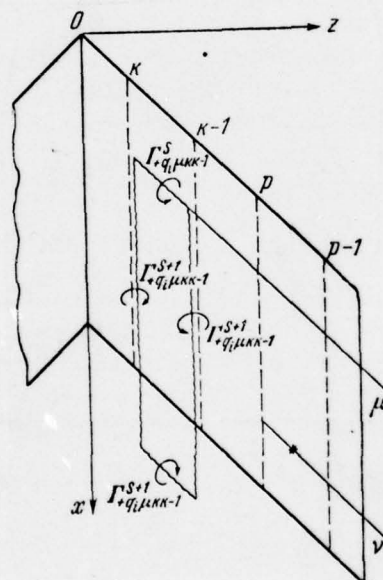


Fig. 17.4. Oblique the eddy/vortex of wing without contraction at the calculated torque/moment r .

Page 414.

Here

$$\left. \begin{aligned} \xi_{vpp-1}^{\mu k k-1} &= (\xi_{vp-1}^{vp} - \xi_{\mu k-1}^{\mu k}) - (\xi_{vp-1}^{vp} - \xi_{\mu k-1}^{\mu k}) \operatorname{tg} \chi_{\mu k-1}^{\mu k}, \\ \xi_{vpp-1s}^{\mu k k-1r} &= (\xi_{vp-1}^{vp} - \xi_{\mu k-1}^{\mu k}) - (\xi_{vp-1}^{vp} - \xi_{\mu k-1}^{\mu k}) \operatorname{tg} \chi_{\mu k-1}^{\mu k} - (\tau_r - \tau_s), \end{aligned} \right\} (17.14)$$

whereupon

$$\left. \begin{aligned} \xi_{1vpp-1s}^{\mu k k-1r} &= \xi_{vp-1}^{vp} - \xi_{\mu k-1}^{\mu k}, \\ \xi_{2vpp-1s}^{\mu k k-1r} &= \xi_{vpp-1s}^{\mu k k-1r} \end{aligned} \right\} \text{при } \left. \begin{aligned} \xi_{1vpp-1s}^{\mu k k-1r} &\geq \xi_{vp-1}^{vp} - \xi_{\mu k-1}^{\mu k}, \\ \xi_{vp-1}^{vp} - \xi_{\mu k-1}^{\mu k} &\leq \xi_{2vpp-1s}^{\mu k k-1r} \leq \xi_{vp-1}^{vp} - \xi_{\mu k-1}^{\mu k}, \end{aligned} \right\} \\ \xi_{1vpp-1s}^{\mu k k-1r} &= \xi_{vp-1}^{vp} - \xi_{\mu k-1}^{\mu k}, \\ \xi_{2vpp-1s}^{\mu k k-1r} &= \xi_{vp-1}^{vp} - \xi_{\mu k-1}^{\mu k} \end{aligned} \right\} \text{при } \left. \begin{aligned} \xi_{1vpp-1s}^{\mu k k-1r} &\geq \xi_{vp-1}^{vp} - \xi_{\mu k-1}^{\mu k}, \\ \xi_{2vpp-1s}^{\mu k k-1r} &\leq \xi_{vp-1}^{vp} - \xi_{\mu k-1}^{\mu k}, \end{aligned} \right\} \\ \xi_{1vpp-1s}^{\mu k k-1r} &= \xi_{1vpp-1s}^{\mu k k-1r}, \\ \xi_{2vpp-1s}^{\mu k k-1r} &= \xi_{2vpp-1s}^{\mu k k-1r} \end{aligned} \right\} \text{при } \left. \begin{aligned} \xi_{vp-1}^{vp} - \xi_{\mu k-1}^{\mu k} &\geq \xi_{1vpp-1s}^{\mu k k-1r} \geq \xi_{vp-1}^{vp} - \xi_{\mu k-1}^{\mu k}, \\ \xi_{vp-1}^{vp} - \xi_{\mu k-1}^{\mu k} &\geq \xi_{2vpp-1s}^{\mu k k-1r} \geq \xi_{vp-1}^{vp} - \xi_{\mu k-1}^{\mu k}, \end{aligned} \right\} \\ \xi_{1vpp-1s}^{\mu k k-1r} &= \xi_{1vpp-1s}^{\mu k k-1r}, \\ \xi_{2vpp-1s}^{\mu k k-1r} &= \xi_{vp-1}^{vp} - \xi_{\mu k-1}^{\mu k} \end{aligned} \right\} \text{при } \left. \begin{aligned} \xi_{vp-1}^{vp} - \xi_{\mu k-1}^{\mu k} &\geq \xi_{1vpp-1s}^{\mu k k-1r} \geq \xi_{vp-1}^{vp} - \xi_{\mu k-1}^{\mu k}, \\ \xi_{2vpp-1s}^{\mu k k-1r} &\leq \xi_{vp-1}^{vp} - \xi_{\mu k-1}^{\mu k}, \end{aligned} \right\} \\ \xi_{1vpp-1s}^{\mu k k-1r} &= \sqrt{\left(\frac{\tau_r - \tau_s}{M}\right)^2 - (\xi_{vpp-1s}^{\mu k k-1r})^2} \cos^2 \chi_{\mu k-1}^{\mu k} \cos \chi_{\mu k-1}^{\mu k} - \\ &\quad - \xi_{vpp-1s}^{\mu k k-1r} \sin \chi_{\mu k-1}^{\mu k} \cos \chi_{\mu k-1}^{\mu k}, \\ \xi_{2vpp-1s}^{\mu k k-1r} &= -\sqrt{\left(\frac{\tau_r - \tau_s}{M}\right)^2 - (\xi_{vpp-1s}^{\mu k k-1r})^2} \cos^2 \chi_{\mu k-1}^{\mu k} \cos \chi_{\mu k-1}^{\mu k} - \\ &\quad - \xi_{vpp-1s}^{\mu k k-1r} \sin \chi_{\mu k-1}^{\mu k} \cos \chi_{\mu k-1}^{\mu k}. \end{aligned} \right\} (17.15)$$

Key: (!) with

Velocity $\omega_{\nu pp-1s}^{\mu kk-1r}$ turns into zero, if

$$\zeta_{\nu p-1}^{\nu p} - \zeta_{\mu k} \leq \zeta_{1\nu pp-1s}^{\mu kk-1r}, \quad \zeta_{\nu p-1}^{\nu p} - \zeta_{\mu k} \leq \zeta_{2\nu pp-1s}^{\mu kk-1r}$$

or

$$\zeta_{\nu p-1}^{\nu p} - \zeta_{\mu k-1} \geq \zeta_{1\nu pp-1s}^{\mu kk-1r}, \quad \zeta_{\nu p-1}^{\nu p} - \zeta_{\mu k-1} \geq \zeta_{2\nu pp-1s}^{\mu kk-1r}$$

and also in the case, when $\zeta_{1\nu pp-1s}^{\mu kk-1r}$, $\zeta_{2\nu pp-1s}^{\mu kk-1r}$ imaginary or $\zeta_{1\nu pp-1s}^{\mu kk-1r}$, $\zeta_{2\nu pp-1s}^{\mu kk-1r}$ simultaneously turn into zero.

During the calculation according to formulas (17.13) appear the complications, when one of the values, entering the denominators, namely $\zeta_{\nu pp-1s}^{\mu kk-1r}$, $\zeta_{1\nu pp-1s}^{\mu kk-1r}$, $\zeta_{2\nu pp-1s}^{\mu kk-1r}$ becomes small or turns into zero. As a result of simple transformation it is not difficult to obtain the expression, suitable for the calculation of the velocity in this case:

$$\begin{aligned}
w_{vpp-1s}^{\mu k k-1r} = & 2(\xi_{vpp-1}^{\mu k k-1} - \xi_{vpp-1s}^{\mu k k-1r}) \left(\frac{1}{A_{vpp-1s}^{\mu k k-1r}} - \frac{1}{D_{vpp-1s}^{\mu k k-1r}} \right) \text{tg } \chi_{\mu k-1}^{\mu k} + \\
& + 2 \frac{(\xi_{vpp-1}^{\mu k k-1})^2 (1 + \text{tg}^2 \chi_{\mu k-1}^{\mu k}) - (\xi_{vpp-1s}^{\mu k k-1r})^2 (k^2 + \text{tg}^2 \chi_{\mu k-1}^{\mu k})}{A_{vpp-1s}^{\mu k k-1r} D_{vpp-1s}^{\mu k k-1r} (\xi_{1vpp-1s}^{\mu k k-1r} D_{vpp-1s}^{\mu k k-1r} + \xi_{2vpp-1s}^{\mu k k-1r} A_{vpp-1s}^{\mu k k-1r})} \times \\
& \times \{ \xi_{vpp-1}^{\mu k k-1} \xi_{vpp-1s}^{\mu k k-1r} [(\xi_{1vpp-1s}^{\mu k k-1r})^2 - (\xi_{2vpp-1s}^{\mu k k-1r})^2] + \\
& + \xi_{1vpp-1s}^{\mu k k-1r} \xi_{2vpp-1s}^{\mu k k-1r} [\xi_{vpp-1}^{\mu k k-1} + \xi_{vpp-1s}^{\mu k k-1r}] [\xi_{1vpp-1s}^{\mu k k-1r} - \xi_{2vpp-1s}^{\mu k k-1r}] \text{tg } \chi_{\mu k-1}^{\mu k} + \\
& + (\xi_{1vpp-1s}^{\mu k k-1r})^2 d_{2vpp-1s}^{\mu k k-1r} a_{2vpp-1s}^{\mu k k-1r} - (\xi_{2vpp-1s}^{\mu k k-1r})^2 d_{1vpp-1s}^{\mu k k-1r} a_{1vpp-1s}^{\mu k k-1r} \}, \quad (17.16)
\end{aligned}$$

where

$$\left. \begin{aligned}
A_{vpp-1s}^{\mu k k-1r} &= \xi_{vpp-1}^{\mu k k-1} a_{1vpp-1s}^{\mu k k-1r} + \xi_{vpp-1s}^{\mu k k-1r} a_{1vpp-1s}^{\mu k k-1r}, \\
D_{vpp-1s}^{\mu k k-1r} &= \xi_{vpp-1}^{\mu k k-1} a_{2vpp-1s}^{\mu k k-1r} + \xi_{vpp-1s}^{\mu k k-1r} a_{2vpp-1s}^{\mu k k-1r}.
\end{aligned} \right\} \quad (17.17)$$

Page 415.

Formula (17.16) one should use instead of relationship/ratios (17.13)

in the cases $\xi_{vpp-1}^{\mu k k-1} \rightarrow 0, \xi_{vpp-1s}^{\mu k k-1r} \rightarrow 0, \xi_{1vpp-1s}^{\mu k k-1r} \rightarrow 0, \xi_{2vpp-1s}^{\mu k k-1r} \rightarrow 0$. By calculating velocity with $M \rightarrow 0$,

in formulas (17.13) it is necessary to set/assume

$$\xi_{1vpp-1s}^{\mu k k-1r} = \xi_{vp-1}^{\mu k k-1r} - \xi_{\mu k}, \quad \xi_{2vpp-1s}^{\mu k k-1r} = \xi_{vp-1}^{\mu k k-1r} - \xi_{\mu k-1}. \quad (17.18)$$

Actually, in this case $(\tau_r - \tau_s)/M \rightarrow \infty$ and according to (17.15) $\xi_{1vpp-1s}^{\mu k k-1r} \rightarrow \infty$, $\xi_{2vpp-1s}^{\mu k k-1r} \rightarrow \infty$ and from (17.15) escape/ensues condition (17.18).

By formulas (17.12) - (17.18) is calculated the velocity for the

case, when eddy/vortex and control point lie/rest on the right half wing. But if the eddy/vortex lie/rests on the left half wing and is the mirror image of examined, but the control point remains on the right half wing, then

$$\sigma W_{yvp-1s}^{\mu k k-lr} = \frac{U_0}{4\pi} \Lambda_{q_i \mu k k-l}^{s+1} \sigma W_{yvp-1s}^{\mu k k-lr}; \quad (17.19)$$

$$\begin{aligned} \sigma W_{yvp-1s}^{\mu k k-lr} = & -\frac{\sigma d_{1vpp-1s}^{\mu k k-lr}}{\sigma \xi_{vpp-1}^{\mu k k-l} \sigma \xi_{1vpp-1s}^{\mu k k-lr}} + \frac{\sigma d_{2vpp-1s}^{\mu k k-lr}}{\sigma \xi_{vpp-1}^{\mu k k-l} \sigma \xi_{2vpp-1s}^{\mu k k-lr}} + \\ & + \frac{\sigma d_{1vpp-1s}^{\mu k k-lr}}{\sigma \xi_{vpp-1s}^{\mu k k-lr} \sigma \xi_{1vpp-1s}^{\mu k k-lr}} - \frac{\sigma d_{2vpp-1s}^{\mu k k-lr}}{\sigma \xi_{vpp-1s}^{\mu k k-lr} \sigma \xi_{2vpp-1s}^{\mu k k-lr}}; \\ \sigma d_{1vpp-1s}^{\mu k k-lr} = & \sqrt{(\sigma \xi_{vpp-1}^{\mu k k-l} - \sigma \xi_{1vpp-1s}^{\mu k k-lr} \operatorname{tg} \chi_{\mu k-1}^{\mu k})^2 + k^2 (\sigma \xi_{1vpp-1s}^{\mu k k-lr})^2}, \\ \sigma d_{2vpp-1s}^{\mu k k-lr} = & \sqrt{(\sigma \xi_{vpp-1}^{\mu k k-l} - \sigma \xi_{2vpp-1s}^{\mu k k-lr} \operatorname{tg} \chi_{\mu k-1}^{\mu k})^2 + k^2 (\sigma \xi_{2vpp-1s}^{\mu k k-lr})^2}, \\ \sigma d_{1vpp-1s}^{\mu k k-lr} = & \sqrt{(\sigma \xi_{vpp-1s}^{\mu k k-lr} - \sigma \xi_{1vpp-1s}^{\mu k k-lr} \operatorname{tg} \chi_{\mu k-1}^{\mu k})^2 + (\sigma \xi_{1vpp-1s}^{\mu k k-lr})^2}, \\ \sigma d_{2vpp-1s}^{\mu k k-lr} = & \sqrt{(\sigma \xi_{vpp-1s}^{\mu k k-lr} - \sigma \xi_{2vpp-1s}^{\mu k k-lr} \operatorname{tg} \chi_{\mu k-1}^{\mu k})^2 + (\sigma \xi_{2vpp-1s}^{\mu k k-lr})^2}. \end{aligned} \quad (17.20)$$

Page 416.

Here

$$\left. \begin{aligned} \sigma \xi_{vpp-1}^{\mu k k-l} &= (\xi_{vpp-1}^{\nu p} - \xi_{\mu k-1}^{\mu k}) + (\xi_{vpp-1}^{\nu p} - \xi_{\mu k-1}^{\mu k}) \operatorname{tg} \chi_{\mu k-1}^{\mu k}, \\ \sigma \xi_{vpp-1s}^{\mu k k-lr} &= \sigma \xi_{vpp-1}^{\mu k k-l} - (\tau_r - \tau_s), \end{aligned} \right\} \quad (17.21)$$

whereupon

$$\begin{aligned}
 & \left. \begin{aligned} \sigma_{\zeta_{1vpp-1s}}^{\mu k k-1r} &= \zeta_{vp-1}^{\nu p} + \zeta_{\mu k-1} \\ \sigma_{\zeta_{2vpp-1s}}^{\mu k k-1r} &= \sigma_{\zeta_{2vpp-1s}}^{\mu k k-1r} \end{aligned} \right\} \begin{aligned} & \text{при } \sigma_{\zeta_{1vpp-1s}}^{\mu k k-1r} \geq \zeta_{vp-1}^{\nu p} + \zeta_{\mu k-1}, \\ & \zeta_{vp-1}^{\nu p} + \zeta_{\mu k} \leq \sigma_{\zeta_{2vpp-1s}}^{\mu k k-1r} \leq \zeta_{vp-1}^{\nu p} + \zeta_{\mu k-1} \end{aligned} \\
 & \left. \begin{aligned} \sigma_{\zeta_{1vpp-1s}}^{\mu k k-1r} &= \zeta_{vp-1}^{\nu p} + \zeta_{\mu k-1} \\ \sigma_{\zeta_{2vpp-1s}}^{\mu k k-1r} &= \zeta_{vp-1}^{\nu p} + \zeta_{\mu k} \end{aligned} \right\} \begin{aligned} & \text{при } \sigma_{\zeta_{1vpp-1s}}^{\mu k k-1r} \geq \zeta_{vp-1}^{\nu p} + \zeta_{\mu k-1}, \\ & \sigma_{\zeta_{2vpp-1s}}^{\mu k k-1r} \leq \zeta_{vp-1}^{\nu p} + \zeta_{\mu k} \end{aligned} \\
 & \left. \begin{aligned} \sigma_{\zeta_{1vpp-1s}}^{\mu k k-1r} &= \sigma_{\zeta_{1vpp-1s}}^{\mu k k-1r} \\ \sigma_{\zeta_{2vpp-1s}}^{\mu k k-1r} &= \sigma_{\zeta_{2vpp-1s}}^{\mu k k-1r} \end{aligned} \right\} \begin{aligned} & \text{при } \zeta_{vp-1}^{\nu p} + \zeta_{\mu k-1} \geq \sigma_{\zeta_{1vpp-1s}}^{\mu k k-1r} \geq \zeta_{vp-1}^{\nu p} + \zeta_{\mu k}, \\ & \zeta_{vp-1}^{\nu p} + \zeta_{\mu k-1} \geq \sigma_{\zeta_{2vpp-1s}}^{\mu k k-1r} \geq \zeta_{vp-1}^{\nu p} + \zeta_{\mu k} \end{aligned} \\
 & \left. \begin{aligned} \sigma_{\zeta_{1vpp-1s}}^{\mu k k-1r} &= \sigma_{\zeta_{1vpp-1s}}^{\mu k k-1r} \\ \sigma_{\zeta_{2vpp-1s}}^{\mu k k-1r} &= \zeta_{vp-1}^{\nu p} + \zeta_{\mu k} \end{aligned} \right\} \begin{aligned} & \text{при } \zeta_{vp-1}^{\nu p} + \zeta_{\mu k-1} \geq \sigma_{\zeta_{1vpp-1s}}^{\mu k k-1r} \geq \zeta_{vp-1}^{\nu p} + \zeta_{\mu k}, \\ & \sigma_{\zeta_{2vpp-1s}}^{\mu k k-1r} \leq \zeta_{vp-1}^{\nu p} + \zeta_{\mu k} \end{aligned} \\
 & \sigma_{\zeta_{1vpp-1s}}^{\mu k k-1r} = \sqrt{\left(\frac{\tau_r - \tau_s}{M}\right)^2 - (\sigma_{\zeta_{vpp-1s}}^{\mu k k-1r})^2} \cos^2 \chi_{\mu k-1}^{\mu k} \cos \chi_{\mu k-1}^{\mu k} + \\
 & \quad + \sigma_{\zeta_{vpp-1s}}^{\mu k k-1r} \sin \chi_{\mu k-1}^{\mu k} \cos \chi_{\mu k-1}^{\mu k}, \\
 & \sigma_{\zeta_{2vpp-1s}}^{\mu k k-1r} = -\sqrt{\left(\frac{\tau_r - \tau_s}{M}\right)^2 - (\sigma_{\zeta_{vpp-1s}}^{\mu k k-1r})^2} \cos^2 \chi_{\mu k-1}^{\mu k} \cos \chi_{\mu k-1}^{\mu k} + \\
 & \quad + \sigma_{\zeta_{vpp-1s}}^{\mu k k-1r} \sin \chi_{\mu k-1}^{\mu k} \cos \chi_{\mu k-1}^{\mu k}. \tag{17.22}
 \end{aligned}$$

KEY: (1) with

Velocity $\sigma_{\zeta_{vpp-1s}}^{\mu k k-1r}$ returns to zero, if

$$\zeta_{vp-1}^{\nu p} + \zeta_{\mu k-1} \leq \sigma_{\zeta_{1vpp-1s}}^{\mu k k-1r}, \quad \zeta_{vp-1}^{\nu p} + \zeta_{\mu k-1} \leq \sigma_{\zeta_{2vpp-1s}}^{\mu k k-1r}$$

or

$$\zeta_{vp-1}^{\nu p} + \zeta_{\mu k} \geq \sigma_{\zeta_{1vpp-1s}}^{\mu k k-1r}, \quad \zeta_{vp-1}^{\nu p} + \zeta_{\mu k} \geq \sigma_{\zeta_{2vpp-1s}}^{\mu k k-1r}$$

and also in the case, when $\sigma_{\zeta_{1vpp-1s}}^{\mu k k-1r}$, $\sigma_{\zeta_{2vpp-1s}}^{\mu k k-1r}$ apparent/imaginary. With $\sigma_{\zeta_{vpp-1s}}^{\mu k k-1r} \rightarrow 0$

or $\sigma_{\zeta_{vpp-1s}}^{\mu k k-1r} \rightarrow 0$ for the calculation of velocity $\sigma_{\zeta_{vpp-1s}}^{\mu k k-1r}$ it is necessary instead of (17.20) to use the following expressions, obtained from (17.20) as a result of the simple transformations:

$$\begin{aligned}
\sigma w_{vpp-1s}^{\mu k k-1r} = & -2(\sigma \xi_{vpp-1}^{\mu k k-1} - \sigma \xi_{vpp-1s}^{\mu k k-1r}) \left(\frac{1}{\sigma A_{vpp-1s}^{\mu k k-1r}} - \frac{1}{\sigma D_{vpp-1s}^{\mu k k-1r}} \right) \operatorname{tg} \chi_{\mu k-1}^{\mu k} + \\
& + 2 \frac{(\sigma \xi_{vpp-1}^{\mu k k-1})^2 (1 + \operatorname{tg}^2 \chi_{\mu k-1}^{\mu k}) - (\sigma \xi_{vpp-1s}^{\mu k k-1r})^2 (k^2 + \operatorname{tg}^2 \chi_{\mu k-1}^{\mu k})}{\sigma A_{vpp-1s}^{\mu k k-1r} \sigma D_{vpp-1s}^{\mu k k-1r} (\sigma \xi_{1vpp-1s}^{\mu k k-1r} \sigma D_{vpp-1s}^{\mu k k-1r} + \sigma \xi_{2vpp-1s}^{\mu k k-1r} \sigma A_{vpp-1s}^{\mu k k-1r})} \times \\
& \times \{ \sigma \xi_{vpp-1}^{\mu k k-1} \sigma \xi_{vpp-1s}^{\mu k k-1r} [(\sigma \xi_{1vpp-1s}^{\mu k k-1r})^2 - (\sigma \xi_{2vpp-1s}^{\mu k k-1r})^2] - \\
& - \sigma \xi_{1vpp-1s}^{\mu k k-1r} \sigma \xi_{2vpp-1s}^{\mu k k-1r} [\sigma \xi_{vpp-1}^{\mu k k-1} + \sigma \xi_{vpp-1s}^{\mu k k-1r}] [\sigma \xi_{1vpp-1s}^{\mu k k-1r} - \sigma \xi_{2vpp-1s}^{\mu k k-1r}] \operatorname{tg} \chi_{\mu k-1}^{\mu k} + \\
& + (\sigma \xi_{1vpp-1s}^{\mu k k-1r})^2 \sigma d_{2vpp-1s}^{\mu k k-1r} \sigma a_{2vpp-1s}^{\mu k k-1r} - (\sigma \xi_{2vpp-1s}^{\mu k k-1r})^2 \sigma d_{1vpp-1s}^{\mu k k-1r} \sigma a_{1vpp-1s}^{\mu k k-1r} \}; \\
& (17.23)
\end{aligned}$$

$$\left. \begin{aligned}
\sigma A_{vpp-1s}^{\mu k k-1r} &= \sigma \xi_{vpp-1}^{\mu k k-1} \sigma d_{1vpp-1s}^{\mu k k-1r} + \sigma \xi_{vpp-1s}^{\mu k k-1r} \sigma a_{1vpp-1s}^{\mu k k-1r}, \\
\sigma D_{vpp-1s}^{\mu k k-1r} &= \sigma \xi_{vpp-1}^{\mu k k-1} \sigma d_{2vpp-1s}^{\mu k k-1r} + \sigma \xi_{vpp-1s}^{\mu k k-1r} \sigma a_{2vpp-1s}^{\mu k k-1r}.
\end{aligned} \right\} \quad (17.24)$$

Page 417.

The obtained relationship/ratios make it possible to calculate the vertical velocity, induced by vortex/eddy system in control points, at any calculated moment of time. Let us require in order that at the calculated torque/moments at control points strictly would be satisfied boundary condition. The calculated torque/moments

let us select in this case in such a way that free vortices, exiting/waste from those which were connected in design data torque/moment, to the following would pass the distance, equal or multiple to distance (measured according to flow) between the adjacent bound vortexes (Fig. 17.5); i.e. let us assume

$$\Delta t = \frac{cb}{U_0 n},$$

and consequently,

$$\Delta \tau = \frac{c}{n}, \quad \tau_r = r \frac{c}{n}, \quad (17.25)$$

where $c = 1, 2, \dots$

According to (3.56) boundary condition (condition of nonoccurrence) at the calculated torque/moment r at the control point, which lies on the guide line between sections $p, p - 1$, will be written as follows:

$$\begin{aligned} \sum_{l=1}^5 \sum_{k=1}^N \sum_{\mu=1}^n \sum_{s=0}^{r-1} \frac{W_{y^{\nu p p-1} s}^{\mu k k-l r} \pm \sigma W_{y^{\nu p p-1} s}^{\mu k k-l r}}{U_0} = \\ = -\alpha(\tau_r) - \omega_x(\tau_r) \xi_{\nu p-1}^{\nu p} - \omega_z(\tau_r) \xi_{\nu p-1}^{\nu p} + \frac{\partial f_\delta(\xi, \zeta)}{\partial \xi} \delta(\tau_r) + \\ + f_\delta(\xi, \zeta) \dot{\delta}(\tau_r) - \frac{W_{y \Delta} \left(r \frac{c}{n} - \xi_{\nu p-1}^{\nu p} \right)}{U_0}, \quad (17.26) \\ p = 1, 2, \dots, N; \quad \nu = 1, 2, \dots, n; \quad r = 1, 2, \dots, R. \end{aligned}$$

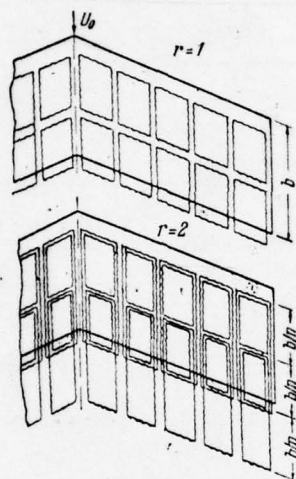


Fig. 17.5. Wing vortex system without contraction at the calculated torque/moments $r = 1$ and $r = 2$.

Page 418.

Here subsequently sign "+" is taken with the symmetric loading of wing, but sign "-" with antisymmetric. By substituting the value of velocity and by introducing the kinematic parameters, we will obtain

$$\frac{1}{4\pi} \sum_{i=1}^5 \sum_{k=1}^N \sum_{\mu=1}^n \sum_{s=0}^{r-1} (\omega_{y\nu pp-1s}^{\mu kk-1r} \pm \sigma \omega_{y\nu pp-1s}^{\mu kk-1}) \Lambda_{q_i \mu kk-1}^{s+1} =$$

$$= \sum_{i=1}^5 (H_{i\nu pp-1}^r + \dot{H}_{i\nu pp-1}^r). \quad (17.27)$$

Taking into account the independence of the kinematic parameters, transfer/converting from s to $s^* = s + 1$ and reject/throwing then prime, from (17.27) we obtain

$$\left. \begin{aligned} \frac{1}{4\pi} \sum_{s=1}^r \sum_{k=1}^N \sum_{\mu=1}^n (\omega_{y\nu pp-1s-1}^{\mu kk-1r} \pm \sigma \omega_{y\nu pp-1s-1}^{\mu kk-1r}) \Lambda_{q_i \mu kk-1}^s &= H_{i\nu pp-1}^r \\ \frac{1}{4\pi} \sum_{s=1}^r \sum_{k=1}^N \sum_{\mu=1}^n (\omega_{y\nu pp-1s-1}^{\mu kk-1r} \pm \sigma \omega_{y\nu pp-1s-1}^{\mu kk-1r}) \Lambda_{q_i \mu kk-1}^s &= \dot{H}_{i\nu pp-1}^r \end{aligned} \right\} \quad (17.28)$$

$$\begin{aligned} i &= 1, 2, \dots, 5; \quad p = 1, 2, \dots, N; \quad \nu = 1, 2, \dots, n; \\ r &= 1, 2, \dots, R. \end{aligned}$$

In systems (17.27) and (17.28) it is marked

$$\left. \begin{aligned} H_{1vpp-1}^r &= -\frac{\alpha(\tau_r)}{\alpha}, \quad H_{2vpp-1}^r = -\xi_{vp-1}^{\nu p} \frac{\omega_x(\tau_r)}{\omega_x}, \\ H_{3vpp-1}^r &= -\xi_{vp-1}^{\nu p} \frac{\omega_z(\tau_r)}{\omega_z}, \\ H_{4vpp-1}^r &= \frac{\partial f_\delta(\xi, \zeta)}{\partial \xi} \bigg|_{\xi=\xi_{vp-1}^{\nu p}} \frac{\delta(\tau_r)}{\delta^*}, \\ &\quad \zeta=\zeta_{vp-1}^{\nu p} \end{aligned} \right\} \quad (17.29)$$

$$\left. \begin{aligned} H_{5vpp-1}^r &= -f_\Delta \left(r \frac{c}{n} - \xi_{vp-1}^{\nu p} \right) \frac{\omega_{y\Delta}(\tau_r)}{\omega_{y\Delta}}; \\ \dot{H}_{1vpp-1}^r &= \dot{H}_{2vpp-1}^r = \dot{H}_{3vpp-1}^r = \dot{H}_{5vpp-1}^r = 0, \\ \dot{H}_{4vpp-1}^r &= \dot{f}_\delta(\xi_{vp-1}^{\nu p}, \zeta_{vp-1}^{\nu p}) \frac{\dot{\delta}(\tau_r)}{\dot{\delta}^*}. \end{aligned} \right\} \quad (17.29)$$

Page 419.

By utilizing communication/connection between vorticity Γ_{q_i} and its change Λ_{q_i} at the calculated torque/moment r (17.11), let us rewrite systems (17.28) as follows:

$$\left. \begin{aligned} &\frac{1}{4\pi} \sum_{k=1}^N \sum_{\mu=1}^n (w_{yvpp-lr-1}^{\mu kk-lr} \pm \sigma w_{yvpp-lr-1}^{\mu kk-lr}) \Gamma_{q_i \mu k k-l}^r = \\ &= H_{lvpp-1}^r + \frac{1}{4\pi} \sum_{k=1}^N \sum_{\mu=1}^n (w_{yvpp-lr-1}^{\mu kk-lr} \pm \sigma w_{yvpp-lr-1}^{\mu kk-lr}) \Gamma_{q_i \mu k k-l}^{r-1} - \\ &\quad - \frac{1}{4\pi} \sum_{s=1}^{r-1} \sum_{k=1}^N \sum_{\mu=1}^n (w_{yvpp-ls-1}^{\mu kk-lr} \pm \sigma w_{yvpp-ls-1}^{\mu kk-lr}) \Lambda_{q_i \mu k k-l}^s, \\ &\frac{1}{4\pi} \sum_{k=1}^N \sum_{\mu=1}^n (w_{yvpp-lr-1}^{\mu kk-lr} \pm \sigma w_{yvpp-lr-1}^{\mu kk-lr}) \Gamma_{q_i \mu k k-l}^r = \\ &= \dot{H}_{lvpp-1}^r + \frac{1}{4\pi} \sum_{k=1}^N \sum_{\mu=1}^n (w_{yvpp-lr-1}^{\mu kk-lr} \pm \sigma w_{yvpp-lr-1}^{\mu kk-lr}) \Gamma_{q_i \mu k k-l}^{r-1} - \\ &\quad - \frac{1}{4\pi} \sum_{s=1}^{r-1} \sum_{k=1}^N \sum_{\mu=1}^n (w_{yvpp-ls-1}^{\mu kk-lr} \pm \sigma w_{yvpp-ls-1}^{\mu kk-lr}) \Lambda_{q_i \mu k k-l}^s, \\ &\Lambda_{q_i \mu k k-l}^s = \Gamma_{q_i \mu k k-l}^s - \Gamma_{q_i \mu k k-l}^{s-1}, \\ &\Lambda_{q_i \mu k k-l}^1 = \Gamma_{q_i \mu k k-l}^1, \quad \Lambda_{q_i \mu k k-l}^0 = 0; \\ &p = 1, 2, \dots, N; \quad v = 1, 2, \dots, n; \quad r = 1, 2, \dots, R; \\ &l = 1, 2, \dots, 5. \end{aligned} \right\} \quad (17.30)$$

Entering in (17.30) values w_y and σw_y are located from relationship/ratios (17.13) - (17.24) and the conditions

$$\tau_r - \tau_s = \frac{c}{n}(r - s). \quad (17.31)$$

The parameters H_p, \dot{H}_i are determined by equalities (17.29).

Page 420.

In the particular case of airfoil/profile (wing of infinite spread/scope) from (17.30) we obtain

$$\left. \begin{aligned} \frac{1}{2\pi} \sum_{\mu=1}^n w_{yvr-1}^{\mu r} \Gamma_{q_i\mu}^r &= \\ &= H_{iv}^r + \frac{1}{2\pi} \sum_{\mu=1}^n w_{yvr-1}^{\mu r} \Gamma_{q_i\mu}^{r-1} - \frac{1}{2\pi} \sum_{s=1}^{r-1} \sum_{\mu=1}^n \Lambda_{q_i\mu}^s w_{yvs-1}^{\mu r}, \\ \frac{1}{2\pi} \sum_{\mu=1}^n w_{yvr-1}^{\mu r} \Gamma_{q_i\mu}^r &= \\ &= \dot{H}_{iv}^r + \frac{1}{2\pi} \sum_{\mu=1}^n w_{yvr-1}^{\mu r} \Gamma_{q_i\mu}^{r-1} - \frac{1}{2\pi} \sum_{s=1}^{r-1} \sum_{\mu=1}^n w_{yvs-1}^{\mu r} \Lambda_{q_i\mu}^s, \\ \Lambda_{q_i\mu}^s &= \Gamma_{q_i\mu}^{rs} - \Gamma_{q_i\mu}^{s-1}, \quad \Lambda_{q_i\mu}^1 = \Gamma_{q_i\mu}^1, \quad \Lambda_{q_i\mu}^0 = \Gamma_{q_i\mu}^0 = 0; \\ i &= 1, 3, 4, 5; \quad v = 1, 2, \dots, n; \quad r = 1, 2, \dots, R. \end{aligned} \right\} \quad (17.32)$$

For the calculation of relative velocity and values H and \dot{H} we will

have the following formulas:

$$\left. \begin{aligned} \omega_{yvr-1}^{\mu r} &= \frac{\sqrt{\left(\frac{c}{n}\right)^2 - M^2 \left(\xi_v - \xi_\mu - \frac{c}{n}\right)^2}}{(\xi_v - \xi_\mu) \left(\xi_v - \xi_\mu - \frac{c}{n}\right)}, \\ \omega_{yvs-1}^{\mu r} &= \frac{\sqrt{\left[\frac{c(r-s+1)}{n}\right]^2 - M^2 \left[\xi_v - \xi_\mu - \frac{c(r-s+1)}{n}\right]^2}}{(\xi_v - \xi_\mu) \left[\xi_v - \xi_\mu - \frac{c(r-s+1)}{n}\right]}, \\ \xi_v &= \frac{\nu - 1/4}{n}, \quad \xi_\mu = \frac{\mu - 3/4}{n}, \end{aligned} \right\} (17.33)$$

and also

$$\left. \begin{aligned} H'_{1v} &= -\frac{\alpha(\tau_r)}{\alpha}, \quad H'_{3v} = -\xi_v \frac{\omega_z(\tau_r)}{\omega_z}, \\ H'_{4v} &= \frac{\partial f_\delta(\xi, \zeta)}{\partial \xi} \Big|_{\substack{\xi=\xi_v \\ \zeta=\zeta_v}} \frac{\delta(\tau_r)}{\delta}, \quad H'_{5v} = -\frac{\omega_{y\Delta} \left(r \frac{c}{n} - \xi_v\right)}{\omega_{y\Delta}}, \\ \dot{H}_{1v} &= \dot{H}_{3v} = \dot{H}_{5v} = 0, \quad \dot{H}_{4v} = f_\delta(\xi_v, \zeta_v) \frac{\dot{\delta}(\tau_r)}{\dot{\delta}}. \end{aligned} \right\} (17.34)$$

If during calculation by formulas (17.33) of velocity $\omega_{yvr-1}^{\mu r}$, $\omega_{yvs-1}^{\mu r}$ they are obtained imaginary then one should consider equal to zero.

Page 421.

§2. Calculation of the intensity/strength of bound vortexes for the wings of arbitrary planform.

By utilizing an idea of the replacement of the continuous processes of a change in the kinematic parameters and aerodynamic characteristics stepped and by simulating wing by the system of discrete transient vortices, it is possible to calculate the aerodynamic characteristics of the aperiodically driving wing not only in the case $\bar{\eta} = 1$, but also with arbitrary planform. In order to solve this problem, it is necessary to construct the vortex/eddy along wing. Let us show as this to make.

Let us examine the lifting surface of arbitrary planform (Fig. 17.6). Let us connect with wing rectangular coordinate system $Oxyz$, after placing its beginning in the spout of root chord and after directing axis Ox along root chord back/ago, but axis Oz - along the right half wing.

Fig. 17.6. Replacement of the wing of complex planform by vortex/eddy system.

Page 422.

Let us assume that the motion of lifting surface, its strain and the incoming gust are determined by relationship/ratios (17.1) - (17.5).

In order to realize the expressed above idea, it is necessary vortex/eddy model to construct so that distances along the flow between the adjacent bound vortexes would be everywhere identical and control points they lie/rested between them halfway. For this let us enter as follows. First let us cut wing into parts by the straight lines, parallel to axis Ox and passing through the points of inflection of leading and trailing edges (see Fig. 17.6). Then each part let us divide into the bands of equal width (to divide wing expediently so that all bands would be approximately identical width). The numbers of sections let us designate by k (or p) and count conduct from the end edge of the right half wing ($k = 0$, $p = 0$). To section before the root we will assign number N , and root ($N + 1$). After this let us establish/install the leading edges of each band. The leading edges of central band we form, after conducting through the spout root chord straight line perpendicular Ox . On

remaining bands leading edges let us count straight lines, carried out through the middles of the cuts of leading wing edge (belonging to this band) in parallel to trailing edge. Then, after drawing through the end/lead of the root chord straight line, perpendicular Ox , let us establish/install the trailing edge of central band. After this by straight lines, parallel to the established/installed leading edge, let us break central band into n of the panels of the equal length b/n . Analogously let us break remaining bands on panel. For this let us cut off by straight lines, parallel mounted on leading edges of bands, sections so that the length of each (measured according to flow) was equal to b/n , i.e., to the length of the panels of central band. If in this case the last/latter panel leaves more than half for the edge of wing (trailing edge), then it must be reject/thrown. But if it comes forward less than half, then wing must be increased to the value of the protruding part of the panel. On each panel at distance $b/4n$ from leading edge let us place bound vortex. The number of eddy/vortex on band let us designate μ and count conduct from leading edge. In accordance with the taken diagram

$$\mu = 1, 2, \dots, n_{k-1}^k,$$

where n_{k-1}^k is equal the rounded to the whole value to value (nb_{kk-1}/b) , b_{kk-1} - wing chord halfway between sections k and $k - 1$. Intensity/strength μ go the bound vortex, which lies between sections $k - 1$, k and corresponding q_i the type of motion, let us designate by

$$\Gamma_{+q_i \mu k k-1} = U_0 b \Gamma_{q_i \mu k k-1} \quad (17.35)$$

Page 423.

Control points let us place on the center lines of bands at distances $\frac{3}{4} \frac{b}{n}$ from the leading edges of panels. The numbers of control points on each band let us designate by ν and count conduct from leading edge. On band p , $p - 1$, obviously, $\nu = 1, 2, \dots, n_{p-1}$.

Further the calculation is conducted just as in the case of wing with $\eta = 1$. Requiring satisfaction of boundary condition at control points at all the calculated torque/moments, we obtain system of equations for a vorticity.

It is not difficult to see that in this case these relationship/ratios will take the following form (with the preservation/retention/maintaining of all adopted previously designations):

$$\begin{aligned}
 & \frac{1}{4\pi} \sum_{k=1}^{N+1} \sum_{\mu=1}^{n_{k-1}^k} (\omega_{\mu\nu p p-1 r-1}^{\mu k k-1 r} \pm \sigma \omega_{\mu\nu p p-1 r-1}^{\mu k k-1 r}) \Gamma_{q, \mu k k-1}^r = \\
 & = H'_{i\nu p p-1} + \frac{1}{4\pi} \sum_{k=1}^{N+1} \sum_{\mu=1}^{n_{k-1}^k} (\omega_{\mu\nu p p-1 r-1}^{\mu k k-1 r} \pm \sigma \omega_{\mu\nu p p-1 r-1}^{\mu k k-1 r}) \Gamma_{q, \mu k k-1}^{r-1} - \\
 & - \frac{1}{4\pi} \sum_{s=1}^{r-1} \sum_{k=1}^{N+1} \sum_{\mu=1}^{n_{k-1}^k} (\omega_{\mu\nu p p-1 s-1}^{\mu k k-1 r} \pm \sigma \omega_{\mu\nu p p-1 s-1}^{\mu k k-1 r}) \Lambda_{q, \mu k k-1}^s
 \end{aligned} \quad (17.36)$$

$$\begin{aligned}
& \frac{1}{4\pi} \sum_{k=1}^{N+1} \sum_{\mu=1}^{n_{k-1}^k} (\omega_{y\nu\rho\rho-1r-1}^{\mu k k-1r} \pm \sigma \omega_{y\nu\rho\rho-1r-1}^{\mu k k-1r}) \Gamma_{q,\mu k k-1}^r = \\
& = H_{1\nu\rho\rho-1}^r + \frac{1}{4\pi} \sum_{k=1}^{N+1} \sum_{\mu=1}^{n_{k-1}^k} (\omega_{y\nu\rho\rho-1r-1}^{\mu k k-1r} \pm \sigma \omega_{y\nu\rho\rho-1r-1}^{\mu k k-1r}) \Gamma_{q,\mu k k-1}^{r-1} - \\
& \quad - \frac{1}{4\pi} \sum_{s=1}^{r-1} \sum_{k=1}^{N+1} \sum_{\mu=1}^{n_{k-1}^k} (\omega_{y\nu\rho\rho-1s-1}^{\mu k k-1r} \pm \sigma \omega_{y\nu\rho\rho-1s-1}^{\mu k k-1r}) \Lambda_{q,\mu k k-1}^s, \\
& \Lambda_{q,\mu k k-1}^s = \Gamma_{q,\mu k k-1}^{rs} - \Gamma_{q,\mu k k-1}^{s-1}, \\
& \Lambda_{q,\mu k k-1}^1 = \Gamma_{q,\mu k k-1}^1, \\
& \Lambda_{q,\mu k k-1}^0 = \Gamma_{q,\mu k k-1}^0 = 0, \\
& (\sigma \omega_{y\nu\rho\rho-1r-1}^{\mu k k-1r})_{k=N+1} = (\sigma \omega_{y\nu\rho\rho-1s}^{\mu k k-1r})_{k=N+1} = 0, \\
& p = 1, 2, \dots, N+1; \\
& \nu = 1, 2, \dots, n_{p-1}^p; \\
& r = 1, 2, \dots, R.
\end{aligned} \tag{17.36}$$

(Cont'd)

Page 424.

Sign "-" is taken with $i = 2$, and also with $i = 4$, when the strains of wing are antisymmetric on its spread/scope.

Entering in (17.36) values ω_ν and $\sigma\omega_\nu$ are calculated from formulas (17.13) - (17.24), in which it is necessary to assume (Fig.

17.7)

$$\begin{aligned}
& \xi_{\mu k-1}^{\mu k} = \xi_{0k-1}^{0k} + \frac{\mu-3/4}{n}, \quad \xi_{0k-1}^k = \frac{1}{2} (\xi_{0k} + \xi_{0k-1}), \quad \xi_{\mu k} = \xi_{0k}, \\
& \xi_{\mu k-1}^{\mu k} = \frac{1}{2} (\xi_{0k} + \xi_{0k-1}), \quad \lg \chi_{\mu k-1}^{\mu k} = \frac{\xi_{*k-1} - \xi_{*k}}{\xi_{*k-1} - \xi_{*k}}, \\
& \xi_{\nu p-1}^{\nu p} = \xi_{0p-1}^{0p} + \frac{\nu-1/4}{n}, \quad \xi_{0p-1}^{0p} = \frac{1}{2} (\xi_{0p} + \xi_{0p-1}), \\
& \xi_{\nu p} = \xi_{0p}, \quad \xi_{\nu p-1}^{\nu p} = \frac{1}{2} (\xi_{0p} + \xi_{0p-1}); \\
& \xi_{0k} = \frac{x_{0k}}{b}, \quad \xi_{0k} = \xi_{*k} = \frac{z_{0k}}{b} = \frac{z_{*k}}{b}, \\
& \xi_{*k} = \frac{x_{*k}}{b}, \quad \xi_{0p} = \frac{x_{0p}}{b}, \quad \xi_{0p} = \frac{z_{0p}}{b}.
\end{aligned} \tag{17.37}$$

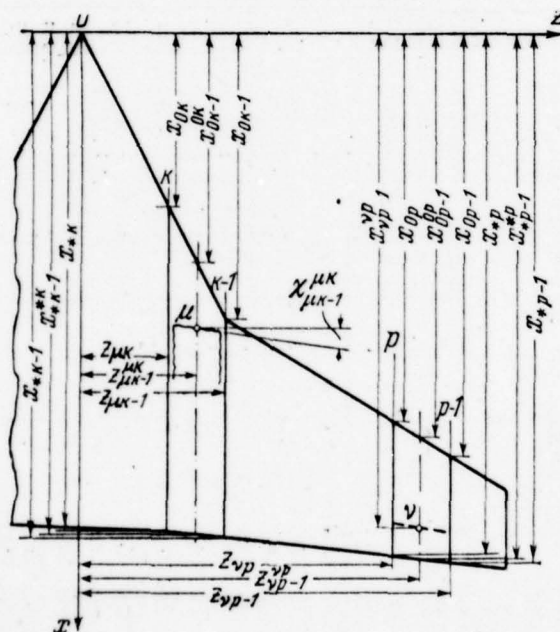


Fig. 17.7. To coordinate determination of bound vortexes and the calculation points of the wing of complex planform.

Page 425.

Here $x_{0k}, z_{0k}, (x_{0p}, z_{0p}), x_{*k}, z_{*k}, (x_{*p}, z_{*p})$ are coordinates of the points of intersection of lines k, p with leading and trailing edges. They are determined by the geometry of wing and by the taken separation, i.e., they are values assigned.

In accordance with explanations to (17.30) during the calculation w_y and σw_y value $\tau_r - \tau_s$ one should determine from (17.31). The limit $n_{k-1}^k (n_{p-1}^p)$ are defined as rounded to the whole value of quantity $n \frac{b_{kk-1}}{b} \left(n \frac{b_{pp-1}}{b} \right)$ (see Fig. 17.7), where

$$\frac{b_{kk-1}}{b} = \xi_{*k-1}^{*k} - \xi_{0k-1}^{0k}, \quad \xi_{*k-1}^{*k} = \frac{1}{2} (\xi_{*k} + \xi_{*k-1}). \quad (17.38)$$

x_{*k} is a point of intersection of line k with trailing edge. In the right sides of equations (17.36) the parameters H'_l, \dot{H}'_l confronting are determined by formulas (17.29).

Analogously can be examined the problem of the effect of flow behind the shock wave, which encounters to wing from any direction. Here will have only to consider the speed of the displacement/movement of its front.

§3. Calculation of the aerodynamic factors of the loads, forces and torque/moments.

For determining loads on wing in the compressed medium we utilize Joukowski's linearized theorem "in small" (3.39), which is valid during isentropic flow for any numbers M .

Let us examine first wing with $\bar{\eta} = 1$. Utilizing (3.39), transfer/converting from vortex/eddy surface to the systems of discrete eddy/vortices (see §6 of chapter X), it is not difficult with the aid of (2.2), (2.7) to obtain the following formulas for determining the coefficients of aerodynamic loadings, of lift and torque/moments at the calculated torque/moment r :

$$\left. \begin{aligned} p'_{q_i}(\xi_{\mu k-1}^{\mu k}, \xi_{\mu k-1}^{\mu k}) &= \frac{\Delta p'_{q_i}(\xi_{\mu k-1}^{\mu k}, \xi_{\mu k-1}^{\mu k})}{\rho_{\infty} \frac{U_0^2}{2} q_i^*} = 2n \Gamma'_{q_i \mu k k-1}, \\ c'_{y q_i} &= \frac{dY'_{q_i}}{\rho_{\infty} \frac{U_0^2}{2} b (z_{\mu k-1} - z_{\mu k}) q_i^*} = 2 \sum_{\mu=1}^n \Gamma'_{q_i \mu k k-1}, \\ c'_{y q_i} &= \frac{Y'_{q_i}}{\rho_{\infty} \frac{U_0^2}{2} S q_i^*} = 4 \frac{b^2}{S} \sum_{k=1}^N \sum_{\mu=1}^n \Gamma'_{q_i \mu k k-1} (\xi_{\mu k-1} - \xi_{\mu k}), \end{aligned} \right\} (17.39)$$

$$\begin{aligned}
 m'_{xq_i} &= \frac{dM'_{xq_i}}{\rho_\infty \frac{U_0^2}{2} b^2 (z_{\mu k-1} - z_{\mu k}) q_i^*} = -2 \sum_{\mu=1}^n \Gamma_{q_i \mu k k-1}^r \xi_{\mu k-1}^{\mu k}, \\
 m'_{xq_i} &= \frac{M'_{xq_i}}{\rho_\infty \frac{U_0^2}{2} S b q_i^*} = -4 \frac{b^2}{S} \sum_{k=1}^N \sum_{\mu=1}^n \Gamma_{q_i \mu k k-1}^r (\xi_{\mu k-1} - \xi_{\mu k}) \xi_{\mu k-1}^{\mu k}, \\
 m'_{zq_i} &= \frac{dM'_{zq_i}}{\rho_\infty \frac{U_0^2}{2} b^2 (z_{\mu k-1} - z_{\mu k}) q_i^*} = 2 \sum_{\mu=1}^n \Gamma_{q_i \mu k k-1}^r \xi_{\mu k-1}^{\mu k}, \\
 m'_{zq_i} &= \frac{M'_{zq_i}}{\rho_\infty \frac{U_0^2}{2} S b q_i^*} = 4 \frac{b^2}{S} \sum_{k=1}^N \sum_{\mu=1}^n \Gamma_{q_i \mu k k-1}^r (\xi_{\mu k-1} - \xi_{\mu k}) \xi_{\mu k-1}^{\mu k},
 \end{aligned}$$

(cond 't)

$$q_1 = \alpha, \quad q_2 = \omega_x, \quad q_3 = \omega_z, \quad q_4 = \delta, \quad \dot{q}_4 = \dot{\delta}, \quad q_5 = \Delta.$$

(17.39)

Page 426.

In the given formulas the entering in them values make following sense:

$\Delta p_{q_i}^r(\xi_{\mu k-1}^{\mu k}, \xi_{\mu k-1}^{\mu k})$ - the load (pressure difference), which acts at point $\xi_{\mu k-1}^{\mu k}, \xi_{\mu k-1}^{\mu k}$ at the calculated torque/moment r with q_i -th the form of motion;

$Y_{q_i}^r$ is the lift, which acts on wing at the calculated torque/moment r with q_i -th the form of motion;

$dY_{q_i}^r$ - the lift, which acts on the strip of wing, which lies between sections $k - 1$ and k , at the calculated torque/moment r with q_i -th the form of motion;

$M_{zq_i}^r$ is the pitching moment, which acts on wing (relative to axis Oz , passing through the spout of root chord) at the calculated torque/moment r with q_i -th the form of motion;

$dM_{zq_i}^r$ - the pitching moment, which acts on the strip of wing, which lies between sections $k - 1, k$ (relative to Oz , the passing through the spout root chord), at torque/moment r with q_i -th the form of motion;

AD-A049 000

FOREIGN TECHNOLOGY DIV WRIGHT-PATTERSON AFB OHIO
A WING IN AN UNSTEADY GAS FLOW. PART 2, (U)
SEP 77 S M BELOTSEKOVSKIY, B K SKRIPACH
FTD-ID(RS)T-1534-77-PT-2

P/0 1/3

UNCLASSIFIED

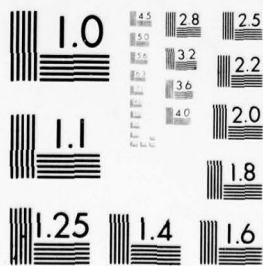
NL

4 OF 6

ADA049000



ADA049000



MICROCOPY RESOLUTION TEST CHART
NATIONAL BUREAU OF STANDARDS-1963-A

M'_{xq_i} is a moment with respect to axis Ox forces, which act at torque/moment r with q_i -th the form of motion;

dM'_{xq_i} is a moment with respect to axis Ox forces, which act at torque/moment r with q_i -th the form of motion to the strip of wing, which lies between sections $k - 1$ and k .

Page 427.

During the calculation according to (17.39), it is necessary to substitute the values $\Gamma'_{q_i \mu k k-1}$, found as a result of the solution of system (17.30), to determine coordinates $\xi_{\mu k-1}^{\mu k}, \zeta_{\mu k-1}^{\mu k}, \zeta_{\mu k}, \zeta_{\mu k-1}$ by (17.7) and to place $b_{kk-1} = b$.

In the case of the wing of arbitrary planform aerodynamic coefficients are located through the following formulas:

$$\begin{aligned}
\left(\frac{p}{q_i}\right)_{\mu k-1}^{\mu k} &= p_{q_i}^r(\xi_{\mu k-1}^{\mu k}, \xi_{\mu k-1}^{\mu k}) = \frac{\Delta p_{q_i}^r(\xi_{\mu k-1}^{\mu k}, \xi_{\mu k-1}^{\mu k})}{\rho_\infty \frac{U_0^2}{2} q_i} = 2n \Gamma_{q_i \mu k k-1}^r, \\
\left(\frac{c_y}{q_i}\right)_{kk-1}^r &= c_{y q_i}^r = \frac{dY_{q_i}^r}{\rho_\infty \frac{U_0^2}{2} b_{kk-1} (z_{\mu k-1} - z_{\mu k}) q_i} = \\
&= 2 \frac{b}{b_{kk-1}} \sum_{\mu=1}^{n_{k-1}^k} \Gamma_{q_i \mu k k-1}^r, \\
\left(\frac{c_y}{q_i}\right)_{kk-1}^r &= c_{y q_i}^r = \frac{Y_{q_i}^r}{\rho_\infty \frac{U_0^2}{2} S q_i} = \\
&= 4 \frac{b^2}{S} \sum_{k=1}^{N+1} \sum_{\mu=1}^{n_{k-1}^k} \Gamma_{q_i \mu k k-1}^r \theta_{k-1}^k (\xi_{\mu k-1}^{\mu k} - \xi_{\mu k}), \\
\left(\frac{m_x}{q_i}\right)_{kk-1}^r &= m_{x q_i}^r = \frac{dM_{x q_i}^r}{\rho_\infty \frac{U_0^2}{2} b_{kk-1} b (z_{\mu k-1} - z_{\mu k}) q_i} = \\
&= -2 \frac{b}{b_{kk-1}} \sum_{\mu=1}^{n_{k-1}^k} \Gamma_{q_i \mu k k-1}^r \xi_{\mu k-1}^{\mu k}, \\
\left(\frac{m_x}{q_i}\right)_{kk-1}^r &= m_{x q_i}^r = \frac{M_{x q_i}^r}{\rho_\infty \frac{U_0^2}{2} b S q_i} = \\
&= -4 \frac{b^2}{S} \sum_{k=1}^N \sum_{\mu=1}^{n_{k-1}^k} \Gamma_{q_i \mu k k-1}^r (\xi_{\mu k-1}^{\mu k} - \xi_{\mu k}) \xi_{\mu k-1}^{\mu k}, \\
\left(\frac{m_z}{q_i}\right)_{kk-1}^r &= m_{z q_i}^r = \frac{dM_{z q_i}^r}{\rho_\infty \frac{U_0^2}{2} b b_{kk-1} (z_{\mu k-1} - z_{\mu k}) q_i} = \\
&= 2 \frac{b}{b_{kk-1}} \sum_{\mu=1}^{n_{k-1}^k} \Gamma_{q_i \mu k k-1}^r \xi_{\mu k-1}^{\mu k}, \\
\left(\frac{m_z}{q_i}\right)_{kk-1}^r &= m_{z q_i}^r = \frac{M_{z q_i}^r}{\rho_\infty \frac{U_0^2}{2} S b q_i} = \\
&= 4 \frac{b^2}{S} \sum_{k=1}^{N+1} \sum_{\mu=1}^{n_{k-1}^k} \Gamma_{q_i \mu k k-1}^r \theta_{k-1}^k \xi_{\mu k-1}^{\mu k} (\xi_{\mu k-1}^{\mu k} - \xi_{\mu k}); \\
\theta_{k-1}^k &= 1 \text{ при } k=1, 2, \dots, N; \quad \theta_{k-1}^k = \frac{1}{2} \text{ при } k=N+1.
\end{aligned}
\tag{17.40}$$

KEY (1) with

Page 428.

During the calculation of aerodynamic characteristics according to these formulas it is necessary to substitute the values $\Gamma_{q, \mu k k-1}^r$ found as a result of the solution of systems (17.36), and the values $\xi_{\mu k-1}^{\mu k}$, $\zeta_{\mu k-1}^{\mu k}$, $\zeta_{\mu k}$, $\zeta_{\mu k-1}$, determined from (17.37), (17.38).

In the case of airfoil/profile aerodynamic coefficients will be equal to

$$\left. \begin{aligned} c_{y q_i}^r &= \frac{dY_{q_i}^r}{\rho_\infty \frac{U_0^2}{2} b q_i^* dz} = 2 \sum_{\mu=1}^n \Gamma_{q_i \mu}^r, \\ m_{z q_i}^r &= \frac{dM_{z q_i}^r}{\rho_\infty \frac{U_0^2}{2} b^2 q_i^* dz} = 2 \sum_{\mu=1}^n \Gamma_{q_i \mu}^r \xi_\mu, \end{aligned} \right\} \quad (17.41)$$

where $\Gamma_{q_i \mu}^r$ it is the solution of system (17.32), $\xi_\mu = \frac{\mu - \frac{3}{4}}{n}$.

DOC = 77171543

PAGE 796

Pages 429-430.

Chapter XVIII.

SOME KNOWN SOLUTIONS.

§1. Infinite-span wing. Coefficients of aerodynamic derivatives.

For the wing (plate) of infinite elongation ($\lambda = \infty$) sufficiently detailed results were obtained during use under the differential equation of continuity and other conditions of elliptical coordinates and representation of solution in the form of series of Mathieu functions [2.35].

Tables 18.1.

M = 0,35

p^*	c_y^a	$c_y^{\dot{a}}$	ω_z c_y^z	$\dot{\omega}_z$ c_y^z	m_z^a	$m_z^{\dot{a}}$	ω_z m_z^z	$\dot{\omega}_z$ m_z^z
0,251	5,190	-3,778	3,887	-3,295	-1,303	0,487	-1,395	0,542
0,501	4,446	-1,126	3,321	-1,292	-1,125	-0,166	-1,261	0,048
0,752	4,082	-0,080	3,040	-0,504	-1,042	-0,424	-1,198	-0,145
1,003	3,902	0,441	2,895	-0,113	-1,007	-0,554	-1,170	-0,241
1,254	3,825	0,740	2,824	0,111	-1,000	-0,630	-1,164	-0,296
1,504	3,816	0,928	2,801	0,248	-1,014	-0,679	-1,171	-0,331
2,006	3,944	1,142	2,850	0,402	-1,093	-0,740	-1,219	-0,370
2,507	4,231	1,254	2,994	0,477	-1,237	-0,777	-1,305	-0,390
3,761	5,611	1,328	3,681	0,517	-1,930	-0,811	-1,690	-0,399
6,519	10,372	0,836	5,640	0,251	-4,732	-0,585	-2,989	-0,263

M = 0,5

p^*	c_y^a	$c_y^{\dot{a}}$	ω_z c_y^z	$\dot{\omega}_z$ c_y^z	m_z^a	$m_z^{\dot{a}}$	ω_z m_z^z	$\dot{\omega}_z$ m_z^z
0,300	5,152	-3,758	3,845	-3,357	-1,306	0,402	-1,430	0,513
0,600	4,373	-0,939	3,239	-1,215	-1,134	-0,279	-1,298	0,000
0,900	4,089	0,048	2,999	-0,471	-1,090	-0,519	-1,262	-0,177
1,200	4,032	0,509	2,918	-0,130	-1,113	-0,632	-1,273	-0,256
1,500	4,111	0,741	2,926	0,046	-1,185	-0,695	-1,314	-0,296
1,800	4,293	0,870	2,992	0,140	-1,302	-0,730	-1,380	-0,315
2,250	4,720	0,947	3,161	0,195	-1,559	-0,749	-1,518	-0,320
3,300	6,094	0,812	3,632	0,143	-2,462	-0,670	-1,930	-0,261
6,000	7,268	0,279	3,337	0,013	-3,337	-0,267	-0,277	-0,094

Table 18.1 (cont.)

M = 0,6

p^*	c_y^a	$c_y^{\dot{a}}$	$c_y^{\omega_z}$	$c_y^{\dot{\omega}_z}$	m_z^a	$m_z^{\dot{a}}$	$m_z^{\omega_z}$	$m_z^{\dot{\omega}_z}$
0,213	5,766	-6,823	4,300	-5,776	-1,464	1,050	-1,635	1,052
0,427	4,823	-2,633	3,567	-2,579	-1,256	0,053	-1,420	0,294
0,640	4,399	-1,052	3,219	-1,371	-1,180	-0,320	-1,339	0,016
0,853	4,218	-0,291	3,047	-0,790	-1,170	-0,499	-1,357	-0,115
1,062	4,173	0,123	2,968	-0,474	-1,205	-0,597	-1,367	-0,182
1,280	4,221	0,361	2,946	-0,292	-1,275	-0,653	-1,404	-0,216
1,600	4,410	0,540	2,978	-0,149	-1,440	-0,689	-1,489	-0,233
1,920	4,688	0,593	3,025	-0,093	-1,631	-0,686	-1,586	-0,224
2,347	5,093	0,553	3,079	-0,081	-2,015	-0,633	-1,661	-0,194
3,413	5,627	0,327	2,896	-0,086	-2,731	-0,413	-1,871	-0,096
6,400	6,588	0,161	3,059	0,029	-3,529	-0,131	-2,010	-0,052

M = 0,7

p^*	c_y^a	$c_y^{\dot{a}}$	$c_y^{\omega_z}$	$c_y^{\dot{\omega}_z}$	m_z^a	$m_z^{\dot{a}}$	$m_z^{\omega_z}$	$m_z^{\dot{\omega}_z}$
0,219	5,956	-8,383	4,422	-7,113	-1,537	1,274	-1,694	1,306
0,437	4,891	-3,198	3,568	-3,121	-1,322	0,077	-1,519	0,394
0,729	4,390	-1,069	3,112	-1,470	-1,278	-0,401	-0,477	0,043
1,093	4,292	-0,196	2,895	-0,773	-1,398	-0,577	-1,520	-0,073
1,311	4,351	0,006	2,823	-0,591	-1,528	-0,597	-1,565	-0,083
1,603	4,465	0,114	2,732	-0,454	-1,733	-0,568	-1,619	-0,067
1,894	4,551	0,138	2,619	-0,367	-1,932	-0,505	-1,645	-0,042
2,331	4,574	0,147	2,426	-0,253	-2,148	-0,400	-1,624	-0,018
3,497	4,757	0,254	2,319	-0,014	-2,438	-0,268	-1,555	-0,046

M = 0,8

p^*	c_y^a	$c_y^{\dot{a}}$	$c_y^{\omega_z}$	$c_y^{\dot{\omega}_z}$	m_z^a	$m_z^{\dot{a}}$	$m_z^{\omega_z}$	$m_z^{\dot{\omega}_z}$
0,225	6,134	-10,748	4,490	-9,160	-1,644	1,587	-1,867	1,722
0,450	4,905	-4,024	3,459	-3,900	-1,446	0,125	-1,698	0,615
0,675	4,451	-1,964	2,993	-2,238	-1,457	-0,273	-1,662	0,327
0,990	4,195	-0,907	2,598	-1,294	-1,598	-0,387	-1,639	0,233
1,170	4,102	-0,624	2,419	-0,991	-1,684	-0,367	-1,602	0,216
1,440	3,981	-0,345	2,211	-0,660	-1,770	-0,315	-1,515	0,181
1,800	3,910	-0,086	2,088	-0,364	-1,822	-0,278	-1,409	0,108
2,160	4,000	0,066	2,108	-0,206	-1,892	-0,272	-1,374	0,044
3,600	4,392	0,154	2,113	-0,029	-2,279	-0,183	-1,417	-0,020

Page 431.

Table 18.1 gives the numerical values of the coefficients of aerodynamic force derivative and moments of wing $\lambda = \infty$ with centering $\bar{x}_T = 0$ and different Mach numbers and Strouhal, obtained by the recalculation of the data [2.35]. These materials are given in chapter of XIX in Fig. by 19.24-19.31 dotted curves.

§2. Infinite-span wing. Instantaneous change in the kinematic parameters.

During an instantaneous stepped variation in the angle of attack α or of angular velocity ω_z , easily are determined the asymptotic values of transient functions with $\tau \rightarrow \infty$. These values are equal to the coefficients of the aerodynamic derivatives of lift and pitching moment in terms of the appropriate kinematic parameter at Strouhal number, which vanishes, i.e., during the steady motion:

$$\left. \begin{aligned} \left[\frac{c_y(M, \tau)}{\alpha^*} \right]_{\tau \rightarrow \infty} &= c_y^a(M, p^*)|_{p^* \rightarrow 0}, \\ \left[\frac{m_z(M, \tau)}{\alpha^*} \right]_{\tau \rightarrow \infty} &= m_z^a(M, p^*)|_{p^* \rightarrow 0}, \\ \left[\frac{c_y(M, \tau)}{\omega_z^*} \right]_{\tau \rightarrow \infty} &= c_y^{\omega_z}(M, p^*)|_{p^* \rightarrow 0}, \\ \left[\frac{m_z(M, \tau)}{\omega_z^*} \right]_{\tau \rightarrow \infty} &= m_z^{\omega_z}(M, p^*)|_{p^* \rightarrow 0} \end{aligned} \right\} \quad (18.1)$$

The initial values of transient functions with $\tau = 0$ can be calculated accurately for the wing of any planform both at subsonic and at supersonic speeds. (About this it is said in detail into §3 chapters IV). The values indicated in the position of the origin of coordinates on the leading edge of rectangular wing are equal to

$$\left. \begin{aligned} \left[\frac{c_y(M, \tau)}{\alpha^*} \right]_{\tau \rightarrow 0} &= \frac{4}{M}, & \left[\frac{m_z(M, \tau)}{\alpha^*} \right]_{\tau \rightarrow 0} &= -\frac{2}{M}, \\ \left[\frac{c_y(M, \tau)}{\omega_z^*} \right]_{\tau \rightarrow 0} &= \frac{2}{M}, & \left[\frac{m_z(M, \tau)}{\omega_z^*} \right]_{\tau \rightarrow 0} &= -\frac{4}{3M}. \end{aligned} \right\} \quad (18.2)$$

In the range of changes of the dimensionless time $0 \leq \tau \leq \frac{M}{1+M}$ in work [2.26] for determining the transient functions of wing $\lambda = \infty$ was used supersonic analogy.

Page 432.

In the remaining range of changes τ the value of transient functions they were calculated approximately.

Table 18.2 (and Fig. 19.8, 19.9 in chapter by the XIX solid lines) give the corrected values of the transient functions of lift force and the pitching moment of the plate of infinite elongation (wing $\lambda = -$) during an instantaneous stepped variation in the angle of attack α for numbers $SM = 0.5$ and 0.8 with centering $\bar{x}_T = 0$, undertaken from work [2.26].

Tables 18.2.

τ	M = 0,5		M = 0,8	
	$\left[\frac{c_y}{a^*} \right]$	$\left[\frac{m_z}{a^*} \right]$	$\left[\frac{c_y}{a^*} \right]$	$\left[\frac{m_z}{a^*} \right]$
0	8,0000	-4,0000	5,0000	-2,5000
0,1	7,2192	-3,5443	4,8801	-2,4086
0,2	6,3993	-2,9602	4,7544	-2,3039
0,3	5,6012	-2,2601	4,6288	-2,1730
0,4	5,0135	-1,6397	4,5031	-1,9640
0,5	4,7596	-1,3894	4,4298	-1,7803
0,6	4,5999	-1,2026	4,4612	-1,7018
0,7	4,4839	-1,0919	4,5345	-1,6546
0,8	4,3823	-1,0176	4,6288	-1,6232
0,9	4,2662	-0,9795	4,7230	-1,6101
1,0	4,2009	-0,9795	4,8277	-1,5996
1,1	4,2154	-1,0031	-	-
1,2	4,3315	-1,0375	-	-
1,3	4,4766	-1,0883	-	-
1,4	4,5999	-1,1627	-	-
1,5	4,6580	-1,1826	5,3095	-1,6023
1,6	4,7813	-1,2098	-	-
1,7	4,8539	-1,2371	-	-
1,8	4,9119	-1,2534	-	-
1,9	4,9700	-1,2679	-	-
2,0	5,0280	-1,2806	5,7179	-1,6206
2,5	5,2529	-1,3187	6,0844	-1,6442
3,0	5,4126	-1,3495	6,3881	-1,6782
3,5	5,5501	-1,3749	6,6185	-1,7148
4,0	5,6665	-1,4003	6,8280	-1,7541
4,5	5,7681	-1,4221	7,0165	-1,7908
5,0	5,8479	-1,4420	7,1945	-1,8143
5,5	5,9204	-1,4602	-	-
6,0	5,9857	-1,4783	7,4772	-1,8876
7,0	6,0946	-1,5091	7,7286	-1,9452
7,5	6,1526	-1,5236	-	-
8,0	6,1961	-1,5418	7,9590	-1,9976
8,5	6,2397	-1,5527	-	-
9,0	6,2832	-1,5672	8,1579	-2,0473
9,5	6,3195	-1,5781	-	-
10	6,3630	-1,5871	8,3569	-2,0892
∞	7,2554	-1,8139	10,4723	-2,6181

Page 433.

Figure 19.2 (in chapter of XIX) gives the distributed chordwise loads for the different moments of dimensionless time τ for these numbers M .

The propagation of formulas, obtained methods of supersonic analogy, in limiting case $M = 1$ gives the following expressions for transient functions [2.26]

$$\left. \begin{aligned} (1) \text{ при } 0 \leq \tau \leq 0,5 \\ \left[\frac{c_y}{\alpha^*} \right] = 4, \quad \left[\frac{m_z}{\alpha^*} \right] = -2 + \tau^2; \\ 0 \text{ при } 0,5 \leq \tau < \infty \\ \left[\frac{c_y}{\alpha^*} \right] = \frac{4}{\pi} \left(2 \sqrt{2\tau - 1} + \arccos \frac{\tau - 1}{\tau} \right), \\ \left[\frac{m_z}{\alpha^*} \right] = -\frac{2}{\pi} \left[\frac{3 + \tau}{2} \sqrt{2\tau - 1} + \left(1 - \frac{\tau^2}{2} \right) \arccos \frac{\tau - 1}{\tau} \right]. \end{aligned} \right\} \quad (18.3)$$

Key: (1). with.

In table 18.3 and in Fig. 19.10, 19.11 following chapters solid lines gave transient functions of lift and pitching moment $[c_y/\omega_z^*]$, $[m_z/\omega_z^*]$ during stepped change in the angular velocity ω_z for a number $M = 0,8$ and $\bar{x}_r = 0$. These data are also borrowed from work [2.26]. The

corresponding load distribution $[\Delta \bar{p}/\omega_z]$ chordwise for the different moments of time τ is given in Fig. 19.3.

Table 18.3.

M = 0,8

τ	$\left[\frac{c_y}{\omega_z} \right]$	$\left[\frac{m_z}{\omega_z} \right]$	τ	$\left[\frac{c_y}{\omega_z} \right]$	$\left[\frac{m_z}{\omega_z} \right]$
0	2,5000	-1,6667	2,5	4,4454	-1,9085
0,1	2,4662	-1,6075	3,0	4,6967	-1,9295
0,2	2,4583	-1,5577	3,5	4,9088	-1,9530
0,3	2,4819	-1,5211	4,0	5,0894	-1,9766
0,4	2,5604	-1,5054	4,5	5,2229	-2,0028
0,5	2,6625	-1,5237	5,0	5,3486	-2,0237
0,6	2,7882	-1,5577	6,0	5,5763	-2,0682
0,7	2,8824	-1,5917	7,0	5,7805	-2,1101
0,8	3,0238	-1,6258	8,0	5,9690	-2,1494
0,9	3,1180	-1,6572	9,0	6,1261	-2,1860
1,0	3,2280	-1,6860	10,0	6,2675	-2,2227
1,5	3,7149	-1,8012	∞	7,8540	-2,6180
2,0	4,1234	-1,8719			

Page 434.

§3. Infinite-span wing. Gradual entrance into step gust.

Work [2.36] gives the results of the calculations of the

transient functions of the plate of infinite elongation upon the gradual entrance into step gust with numbers $M = 0.5$ and 0.8 . Numerical values $[c_y/w_{y\Delta}]$ are given in table 18.4, and the behavior of the transient functions of lift and pitching moment is shown in Fig. by 19.12, 19.13 dotted lines. Load distribution according to airfoil/profile during different τ is given in Fig. 19.4.

For the subsonic flow about the data on the transient functions of pitching moment upon the gradual entrance of wing into gust there is not. However, for the initial period of the entrance into gust with $0 < \tau < \frac{M}{1+M}$ with the aid of the method of supersonic analogy it is possible to show (see [1.19]), that the lift is applied at point on one quarter-chord. In the asymptotic case $\tau \rightarrow \infty$ it, as during steady motion, is also applied at this same point.

Tables 18.4.

M	0,5	0,8	M	0,5	0,8
τ	$\left[\frac{c_y}{w_{y\Delta}} \right]$	$\left[\frac{c_y}{w_{y\Delta}} \right]$	τ	$\left[\frac{c_y}{w_{y\Delta}} \right]$	$\left[\frac{c_y}{w_{y\Delta}} \right]$
0	0	0	1,8	4,4186	—
0,1	0,5877	0,4608	1,9	4,4911	—
0,2	1,1464	0,8901	2,0	4,5637	4,8696
0,3	1,7123	1,3509	2,5	4,8829	5,3723
0,4	2,1839	1,7803	3,0	5,1078	5,7703
0,5	2,5176	2,1887	3,5	5,2748	6,1158
0,6	2,7716	2,4505	4,0	5,4126	6,4510
0,7	2,9965	2,6809	4,5	5,5432	6,7232
0,8	3,1996	2,8908	5,0	5,6520	6,9432
0,9	3,1779	3,0998	5,5	5,7536	—
1,0	3,5407	3,2988	6,0	5,8479	7,3306
1,1	3,6930	—	6,5	5,9132	—
1,2	3,8164	—	7,0	5,9930	7,6448
1,3	3,9542	—	7,5	6,0583	—
1,4	4,0630	—	8,0	6,1308	7,9380
1,5	4,1574	4,2099	9,0	6,2542	8,1684
1,6	4,2517	—	10	6,3630	8,3360
1,7	4,3388	—	∞	7,2554	10,4723

Coefficients of aerodynamic derivatives.

For the airfoil/profile with the oscillating control surface, streamlined with the compressed subsonic flow, work [2.32] gives in the form of tables and curve/graphs the results of the calculations of the lift and pitching moment, which act on entire airfoil/profile, and also hinge moment. The chord of control was 0.1, 0.2 and 0.3 from airfoil chord with control; $M = \sqrt{0.5; 0.6; 0.7; \text{ and } 0.8}$, and Strouhal number (related to the chord of entire airfoil/profile) changed in the range $0 < p^* < 2$. For the calculation, as in the case of oscillating rigid airfoil/profile [2.34], was used the method of solution, connected with expansion in Mathieu functions [2.20].

Without giving the results of the calculations indicated, let us give only transfer equations from the tabulated in [2.32] values ω , k'_c , k''_c , m'_c , m''_c , n'_c and n''_c to the coefficients of aerodynamic derivatives.

Let us present lift and the pitching moment of entire airfoil, and also the hinge moment of control surface relative to fulcrum in the form

$$\left. \begin{aligned} \frac{2Y}{\rho_\infty U_0^2 b} &= c_y^\delta \delta + c_y^{\dot{\delta}} \dot{\delta}, & \frac{2M_z}{\rho_\infty U_0^2 b^2} &= m_z^\delta \delta + m_z^{\dot{\delta}} \dot{\delta}, \\ \frac{2M_{\text{III}}}{\rho_\infty U_0^2 b^2} &= m_{\text{III}}^\delta \delta + m_{\text{III}}^{\dot{\delta}} \dot{\delta}. \end{aligned} \right\} \quad (18.4)$$

Pitching moment M_z is taken relative to axis Oz , passing through the middle of airfoil chord with control $(\bar{x}_T = 0,5)$. In this case the coefficients of aerodynamic derivatives will be connected with the tabulated in [2.32] values by the following relationship/ratios:

$$\left. \begin{aligned} c_y^\delta &= -\pi k'_c, & c_y^\delta &= -\frac{\pi k''_c}{p^*}, \\ m_z^\delta &= \frac{1}{2} \pi m'_c, & m_z^\delta &= \frac{\frac{1}{2} \pi m''_c}{p^*}, & m_w^\delta &= \frac{1}{2} \pi n'_c, & m_w^\delta &= \frac{\frac{1}{2} \pi n''_c}{p^*}, \\ & & p^* &= 2\omega. \end{aligned} \right\} (18.5)$$

Some datum works [2.32] are given in Fig. 19.14, 1915 during the analysis of the results of the calculations by numerical method.

Page 436.

§5. Coefficients aerodynamic derivative of rectangular wings with $M \rightarrow 1$

and $p^* \rightarrow 0$.

As it follows from chapter of VXII, the task of the determination of the coefficients aerodynamic derivative wing characteristics in the compressed medium with $p^* \rightarrow 0$ is reduced to the appropriate task for the converted wing in the incompressible medium.

If the basic forward motion of wing occurs with number $M \rightarrow 1$, the aspect ratio of the converted wing $\lambda_M = k\lambda$ vanishes. In this case for rectangular wings, as shown into §6 chapters of XIII, task within the framework of linear theory can be solved accurately. (Question concerning the applicability of linear theory with numbers M , close to unity, here is not examined).

Let us replace the converted rectangular wing with $\lambda_M \rightarrow 0$ continuous connected vorticity layer $\gamma(x, z)$ and the connected discrete eddy/vortex $\Gamma(z)$. The intensity/strength of discrete eddy/vortex and vorticity layer let us present according to (15.45) in the form

$$\left. \begin{aligned} \Gamma_M &= U_{0M} b_M \left[\Gamma_M^a \alpha + (\Gamma_M^a + M^2 \Delta \Gamma_M^a) \dot{\alpha} + \frac{\Gamma_M^{\omega r}}{k} \omega_x + \right. \\ &\quad \left. + \frac{1}{k} (\Gamma_M^{\omega r} + M^2 \Delta \Gamma_M^{\omega r}) \dot{\omega}_x + \Gamma_M^{\omega z} \omega_z + (\Gamma_M^{\omega z} + M^2 \Delta \Gamma_M^{\omega z}) \dot{\omega}_z \right], \\ \gamma_M &= U_{0M} \left[\gamma_M^a \alpha + (\gamma_M^a + M^2 \Delta \gamma_M^a) \dot{\alpha} + \frac{\gamma_M^{\omega r}}{k} \omega_x + \right. \\ &\quad \left. + \frac{1}{k} (\gamma_M^{\omega r} + M^2 \Delta \gamma_M^{\omega r}) \dot{\omega}_x + \gamma_M^{\omega z} \omega_z + (\gamma_M^{\omega z} + M^2 \Delta \gamma_M^{\omega z}) \dot{\omega}_z \right]. \end{aligned} \right\} (18.6)$$

By following method §7 chapter of XIII, we will obtain with $p^* \rightarrow 0$ system of equations for determining unknown aerodynamic derivative circulations. The beginning of the axes let us place on the middle of the root chord b and retain designations §7. For all unknown values $\Gamma_M^{*q_l}, X_M^{q_l}, \Gamma_M^{*q_t}, X_M^{q_t}$,

except $\Delta\Gamma_M^{*q_l}, \Delta X_M^{q_l}$, we will obtain the equations, which coincide, correspondingly, with systems of equations (13.79), (13.81), (13.83).

For determining $\Delta\Gamma_M^{*q_l}, \Delta X_M^{q_l}$ let us have (axis standard)

$$\left. \begin{aligned} \Delta\Gamma_M^{*a} + \int_{\xi_{CM}}^{1/2} \Delta X_M^a d\xi_M &= 2\xi_M, & \Delta\Gamma_M^{*\omega_x} + \int_{\xi_{OM}}^{1/2} \Delta X_M^{\omega_x} d\xi_M &= \frac{\lambda_M}{2} \xi_M, \\ \Delta\Gamma_M^{*\omega_z} + \int_{\xi_{OM}}^{1/2} \Delta X_M^{\omega_z} d\xi_M &= -2\xi_M^2. \end{aligned} \right\} (18.7)$$

Page 437.

Solution of these supplementary systems of equations gives

$$\left. \begin{aligned} \Delta \Gamma_M^{\omega \dot{\alpha}} &= 1, & \Delta X_M^{\dot{\alpha}} &= -2, & \Delta \Gamma_M^{\omega \dot{\alpha} x} &= \frac{\lambda_M}{4}, \\ \Delta X_M^{\dot{\omega} x} &= -\frac{\lambda_M}{2}, & \Delta \Gamma_M^{\omega \dot{\omega} z} &= -\frac{1}{2}, & \Delta X_M^{\dot{\omega} z} &= 4\xi_M. \end{aligned} \right\} \quad (18.8)$$

By determining according to (13.85) aerodynamic loadings on wing and by introducing the coefficients of aerodynamic derivatives in terms of the formulas, analogous (15.53), we will obtain

$$\left. \begin{aligned} c_{yM}^{\alpha} &= \frac{\pi \lambda_M}{2}, & c_{y1M}^{\dot{\alpha}} &= \frac{\pi \lambda_M}{2}, & c_{y2M}^{\dot{\alpha}} &= -\frac{\pi \lambda_M}{2}; \\ c_{yM}^{\dot{\omega} z} &= \frac{\pi \lambda_M}{4}, & c_{y1M}^{\dot{\omega} z} &= c_{y2M}^{\dot{\omega} z} = 0; \\ m_{zM}^{\alpha} &= \frac{\pi \lambda_M}{4}, & m_{z1M}^{\dot{\alpha}} &= m_{z2M}^{\dot{\alpha}} = 0; \\ m_{zM}^{\dot{\omega} z} &= -\frac{\pi \lambda_M}{8}, & m_{z1M}^{\dot{\omega} z} &= -\frac{\pi \lambda_M}{24}, & m_{z2M}^{\dot{\omega} z} &= \frac{\pi \lambda_M}{24}; \\ m_{xM}^{\dot{\omega} x} &= -\frac{\pi \lambda_M^2}{64}, & (m_{xM}^{\dot{\omega} x})_1 &= -\frac{\pi \lambda_M^2}{64}, & (m_{xM}^{\dot{\omega} x})_2 &= \frac{\pi \lambda_M^2}{64}. \end{aligned} \right\} \quad (18.9)$$

If we the origin of coordinates arrange on leading wing edge, and rolling moment and angular velocity Ω_x to relate, correspondingly, to spread/scope γ and $l/2$, then, by utilizing formulas of recalculation (2.59) and (2.73), let us have

$$\left. \begin{aligned} c_{yM}^a &= \frac{\pi\lambda_M}{2}, & c_{y1M}^a &= \frac{\pi\lambda_M}{2}, & c_{y2M}^a &= -\frac{\pi\lambda_M}{2}; \\ c_{yM}^{\omega_z} &= \frac{\pi\lambda_M}{2}, & c_{y1M}^{\omega_z} &= \frac{\pi\lambda_M}{4}, & c_{y2M}^{\omega_z} &= -\frac{\pi\lambda_M}{4}; \\ m_{zM}^a &= 0, & m_{z1M}^a &= -\frac{\pi\lambda_M}{4}, & m_{z2M}^a &= \frac{\pi\lambda_M}{4}; \\ m_{zM}^{\omega_z} &= -\frac{\pi\lambda_M}{4}, & m_{z1M}^{\omega_z} &= -\frac{\pi\lambda_M}{6}, & m_{z2M}^{\omega_z} &= \frac{\pi\lambda_M}{6}; \\ m_{x1M}^{\omega_{x1}} &= -\frac{\pi\lambda_M}{32}, & (m_{x1M}^{\omega_{x1}})_1 &= -\frac{\pi}{16}, & (m_{x1M}^{\omega_{x1}})_2 &= \frac{\pi}{16}. \end{aligned} \right\} (18.10)$$

Formulas (18.9), (18.10) are obtained under condition $\lambda_M = k\lambda \rightarrow 0$.

Page 438.

In the case, when $M < 1$, they are precise for the rectangular wings of maximally small elongation ($\lambda \rightarrow 0$). By substituting in (15.53) values (18.10), we will obtain for the rectangular wing of any elongation λ with $M \rightarrow 1$

$$\left. \begin{aligned} c_y^a &= \frac{\pi\lambda}{2}, & c_y^{\omega} &= \frac{\pi\lambda}{2}, & c_z^{\omega} &= \frac{\pi\lambda}{2}, & c_y^{\omega z} &= \frac{\pi\lambda}{4}; \\ m_z^a &= 0, & m_z^{\omega} &= -\frac{\pi\lambda}{4}, & m_z^{\omega z} &= -\frac{\pi\lambda}{4}, & m_z^{\omega z} &= -\frac{\pi\lambda}{6}; \\ m_{x1}^{\omega} &= -\frac{\pi\lambda}{32}, & m_{x1}^{\omega z} &= -\frac{\pi}{16}. \end{aligned} \right\} \quad (18.11)$$

These formulas it is possible, obviously, to use, also, with any $M < 1$, but for very small λ .

Page 439.

Chapter XIX.

CALCULATION OF THE UNSTEADY WING CHARACTERISTICS OF ARBITRARY PLANFORM.

§1. Special feature/peculiarities of calculation procedure.

The method of the calculation of aerodynamic wing characteristics at high subsonic speeds is presented in chapter of XV. For harmonic oscillations with very small Strouhal number ($p^* \rightarrow 0$) the solution of problem is reduced to determining the aerodynamic characteristics of the converted wing for each Mach number in the incompressible medium. In this case the difference is in the appearance of supplementary boundary conditions and need for the solution of new systems of equations for circulations $\Delta\Gamma_M^{\dot{\alpha}}, \Delta\Gamma_M^{\dot{\omega}_x}, \Delta\Gamma_M^{\dot{\omega}_z}$ and so forth. With the arbitrary dependences of the kinematic parameters on time the continuous processes are replaced stepped. At the assigned (calculated) moments of time occurs an abrupt circulation control of the bound vortexes, from which converge free vortices [1.85]. Since

disturbance/perturbations in the incompressible medium are spread at the final velocity, is examined entire process of formation and again free vortices, but not only at the defined, assigned torque/moment as in the incompressible medium. Therefore it is necessary the initial wing to replace saw-tooth - for close to initial.

For the case of high subsonic speeds there are no precise solutions for entire range of a change in the dimensionless time τ . However, there are exact solutions at the initial moment $\tau \rightarrow 0$, for which aerodynamic characteristics take the finite values, which depend on number M and valid for any wing planform. The adjustment of procedure and control of numerical calculations are conducted just as for the incompressible medium, with the use of data points $\tau = 0$.

Just as for the incompressible medium, large value at subsonic speeds has chaplygina - Joukowski's hypothesis about the finiteness of velocities on trailing wing edges.

Page 440.

The obtained from numerical calculations values of circulations and loads make it possible to explain question, is provided the execution by the taken vortex/eddy diagram of chaplygina - Joukowski's hypothesis. Aerodynamic characteristics make it possible to trace the

character of load change in time. For wings with fractures on spread/scope and along chord some distributed loads have special feature/peculiarities in point of rupture. Numerical calculations make it possible to establish/install, how taken a calculation procedure considers the being obtained special feature/peculiarities. The question concerning the rational network, accepted during the definition of the aerodynamic derivatives of wing by high subsonic speeds, is solved as for the incompressible medium. It is necessary to only consider some special feature/peculiarities when selecting network for wings, since with an increase of number M the elongation of the converted wing decreases, and sweepback increases.

The control of the obtained from numerical calculation aerodynamic characteristics is realized just as for the incompressible medium, with the aid of known solutions (most frequently for the wing of infinite elongation), with the use of corollaries of reversibility, theorem of momentum, and also by applying a Duhamel integral. Cross check of numerical and experimental data can be carried out by the comparison of the results of the calculation and experiment both for stationary and unsteady aerodynamic characteristics. This makes it possible to check the reliability of the taken diagram of numerical calculation and to rate/estimate the field of the applicability of linear airfoil theory.

§2. Chaplygin-Joukowski's hypothesis. Distributed characteristics.

Numerical calculations, made at high subsonic speeds, make it possible to establish/install, how taken a calculation procedure provides the execution of chaplygina - Joukowski's hypothesis with the arbitrary dependences of the kinematic parameters on time, including harmonic oscillations.

For the wing of very great lengthening ($\lambda = \infty$) was examined an instantaneous change in the kinematic parameters α and ω_z in stepped law. For a α -problem are obtained the numerical values of the distributed chordwise dimensionless pressure difference $[\Delta \bar{p}/\alpha^*]$ with three Mach numbers: $M = 0,4; 0,5; 0,8$ for the different moments of time (Fig. 19.1 and 19.2). In this case for $M = 0,4$ examined large number of eddy/vortices ($n = 32$), by which is simulated the wing, and therefore a small interval/gap between the calculated torque/moments ($\Delta \tau = 0.0313$), which makes it possible to trace character and rearrangement of loads with different, especially small, values τ (see Fig. 19.1).

Page 441.

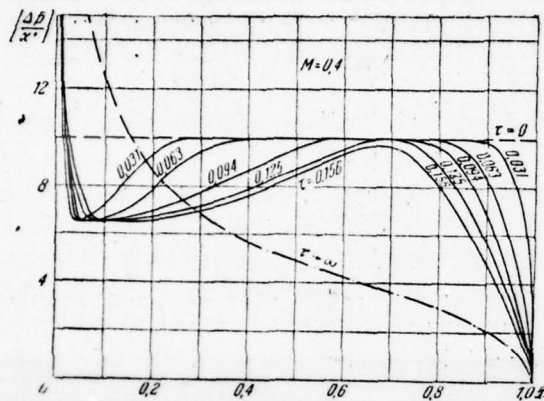


Fig. 19.1. Wing $\lambda = \infty$. Instantaneous change in the kinematic parameters. Dotted curves are a known solution, unbroken curves are a numerical calculation.

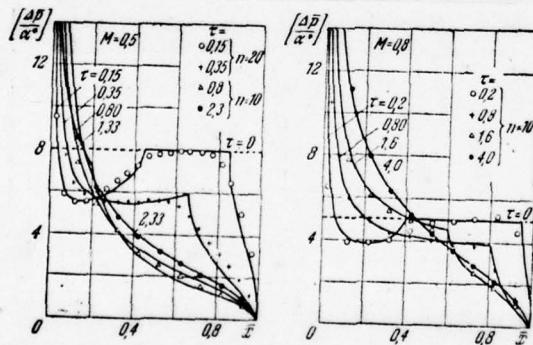


Fig. 19.2. Wing $\lambda = \infty$. Instantaneous change in the kinematic parameters. Curves are a known solution, points are a numerical calculation.

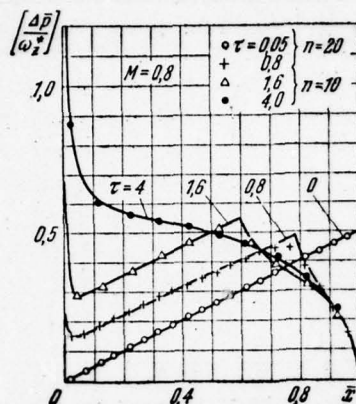


Fig. 19.3. Wing $\lambda = -\bar{x}_p = 0$, Instantaneous change in the kinematic parameters. Curves are a known solution, points are a numerical calculation.

Page 442.

For ω_z -problem Fig. 19.3 gives pressure differences $[\Delta \bar{p}/\omega_z']$ this same wing with $M = 0.8$.

The dependences indicated show following. With $\tau = 0$ occur the exact solutions; flow in this case noncirculating (total circulation is equal to zero). Then disturbance/perturbations at the final velocity are spread from leading and trailing edges in such a way that dimensionless pressure differences on trailing wing edge ($\bar{x} = 1.0$) turn into zero, which indicates the execution of the hypothesis

of Chaylygin-Joukowski. On the leading edge of the wing in question a pressure difference Δp approaches infinite values. In this case on the middle of wing for a while remains the section, which corresponds to exact solution for $r = 0$.

Analogous result is obtained upon the gradual entrance of wing into step gust, only in this case a pressure difference $\sqrt{\frac{[\Delta \bar{p}/w_{y\Delta}^*]}{}}$ turns into zero at the finite values r , when disturbance/perturbations reach trailing wing edge. The degree of the propagation of these disturbance/perturbations depends on Mach number (Fig. 19.4).

Let us note that the results of numerical calculations virtually coincide with the known solutions of the problems in question, by data in work [2.26], already with small n .

Changes in the loads in the wingspan at high subsonic speeds have qualitatively the same special feature/peculiarities as in the incompressible medium. So, if is examined the wing of complex planform, which has fracture on leading edge, then the circulation of the vortex lines, by which it is simulated wing, they have discontinuity/interruptions in the appropriate sections $z = \text{const}$, whereupon total circulation is changed on spread/scope continuously.

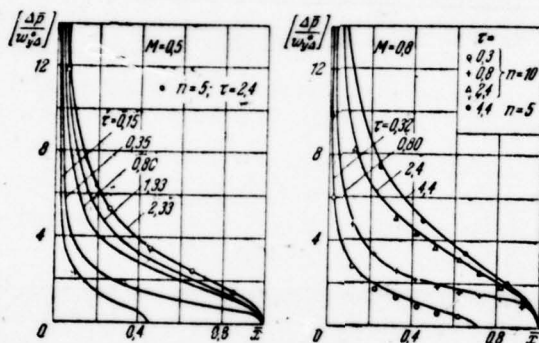


Fig. 19.4. Wing $\lambda = \infty$. Gradual entrance into step gust. Curves are a known solution. Points are a numerical calculation.

Page 443.

19.7
Figure 19.5-19.6 depicts the results of the numerical calculations of the wing with fracture, depicted on Fig. 14.15. The calculation is made for the number of eddy/vortices on of the semirange of wing $N = 11$ and on its chord $n = 5$. Just as in the incompressible medium, at high subsonic speed ($M=0.8$) and $p^* \rightarrow 0$ are observed the

discontinuity/interruptions of circulations in the point of rupture of wing on some vortex lines, especially essential for the cords, which are arranged/located nearer to leading wing edge ($\mu = 1$. $\mu = 2$).

§3. Comparison of numerical calculations with known solutions.

The obtained from numerical calculations aerodynamic characteristics are compared with known solutions. This makes it possible with larger reliability to select the rational diagram of numerical calculation.

Let us conduct the comparison indicated for the distributed and total wing characteristics of infinite lengthening ($\lambda = \infty$) with an instantaneous change in the angle of attack α and the upon gradual entrance into step gust for centering $\tilde{x}_T = 0$.

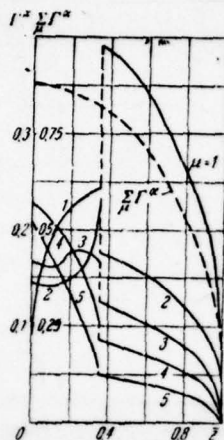


Fig. 19.5. Circulation control r^α in the spread/scope of the wing of complex planform ($M=0.8$).

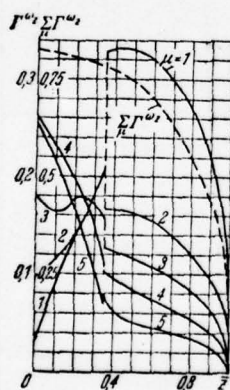


Fig. 19.6. Circulation control r^{ω_z} in the spread/scope of the wing of complex planform ($M=0.8, \bar{x}_p=0$).

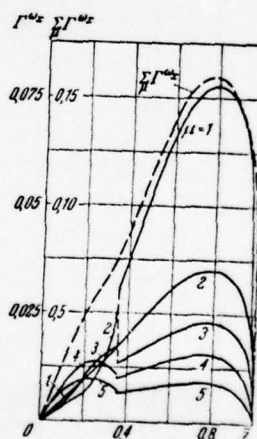


Fig. 19.7

Fig. 19.7. Circulation control r^{ω_x} in the spread/scope of the wing of

complex planform ($M = 0.8$).

Page 444.

Figure 19.1-19.4 depicts the comparison of the data of the known solution, given in work [2.36], and the results of the numerical calculation of the distributed chordwise dimensionless pressure differences $\sqrt{\frac{[\Delta \bar{p}/\alpha^*], [\Delta \bar{p}/\omega_z^*], [\Delta \bar{p}/\omega_{y\Delta}^*]}{}}$ while in Fig. 19.8, 19.9 - the total coefficients of transient functions $[c_y/\alpha^*]$ and $[m_z/\alpha^*]$ this wing. Known solutions in the latter case are undertaken from works [1.19] and [2.26]; here are plotted/applied point for the limiting case $r = 0$, for which there is exact solution. Comparison is carried out also for the total transient functions $[c_y/\omega_z^*]$ and $[m_z/\omega_z^*]$, for which known solutions are also undertaken of above works (Fig. 19.10 and 19.11) indicated. In these figures are given the limiting cases for $r = 0$ and $r \rightarrow \infty$. Upon the gradual entrance of infinite plate into stepped gust Fig. 19.12, 19.13 give the comparison of numerical calculation with known solutions [1.19] and [2.36] and by limiting cases $r = 0$ and $r \rightarrow \infty$.

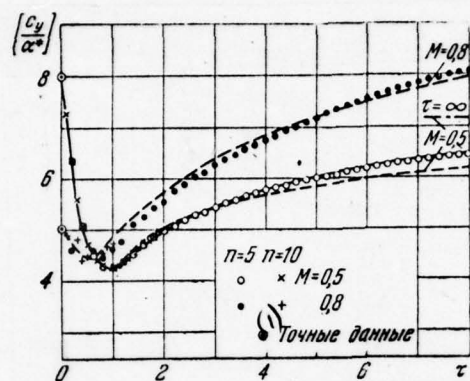


Fig. 19.8.

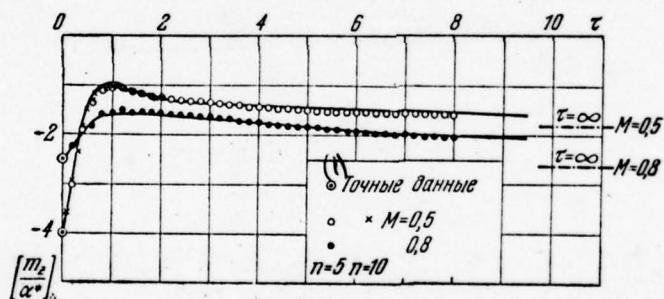


Fig. 19.9.

Fig. 19.8. Wing $\lambda = \infty$. Comparison of numerical calculations (point) with known solutions (curves).

Key: (1). Precise data.

Fig. 19.9. Wing $\lambda = \infty$, $\bar{x}_T = 0$. Comparison of numerical calculations (point) with known solutions (curves).

Key: (1). Precise data.

Page 445.

In all given curve/graphs it is possible to note the completely satisfactory coincidence of numerical data with the results of known solutions. Transient functions during increase r approach limiting values - to the corresponding derivative without points with $p^* \rightarrow 0$.

Thus, in an example of the wing of infinite lengthening establish/install is the completely acceptable coincidence of the data of numerical calculation with known solutions, including limiting cases $r = 0$ and $r = \infty$. To the first case corresponds exact solution, and to the second - numerical, but obtained

independently from the solution of problem for harmonic oscillations.

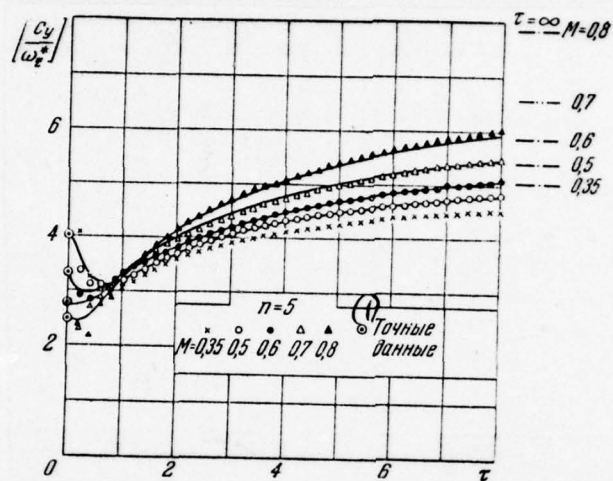


Fig. 19.10.

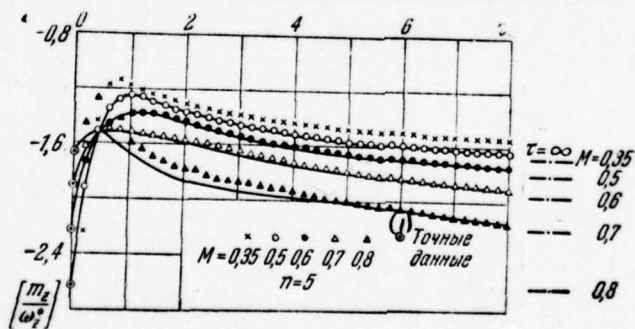


Fig. 19.11.

Fig. 19.10. Wing $\lambda = \infty$, $x_T = 0$. Comparison of numerical calculations (point) with known solutions (curves).

Key: (1). Precise data.

Fig. 19.11. Wing $\lambda = \infty$, $x_T = 0$. Comparison of numerical calculations (point) with known solutions (curves).

Key: (1). Precise data.

Page 446.

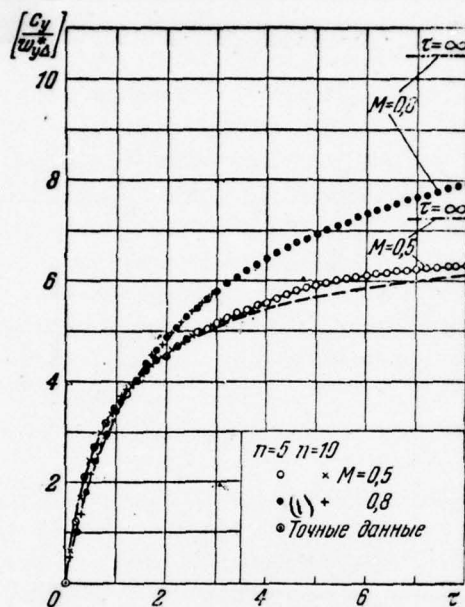


Fig. 19.12.

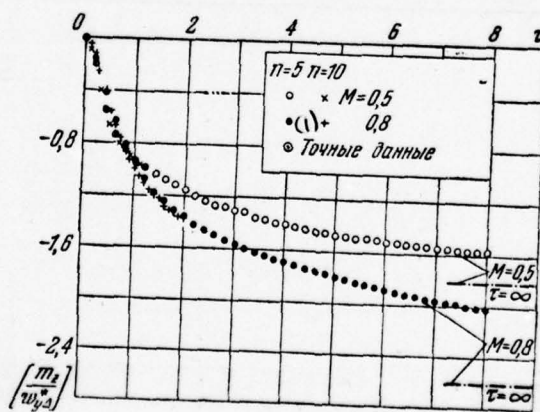


Fig. 19.13.

Fig. 19.12. Wing $\lambda = -$. Comparison of numerical calculations (point) with known solutions (curves).

Key: (1). Precise data.

Fig. 19.13. Wing $\lambda = \infty$, $\beta_1 = 0$. Comparison of numerical calculations (point) with known solutions (dot-dash line).

Key: (1). Precise data.

Page 447.

For an infinite-span wing with control $\bar{b}_p = 0,20$) numerical calculations are compared with known solutions [2.32]. In Fig. 19.14 and 19.15 given this comparisons for derivatives $c_y^{\delta p}$, $m_z^{\delta p}$ with numbers $M < 1$ in terms of the calculations of V. I. Bushuev, based on the use of a Duhamel integral.

§4. Investigation of the practical convergence of solution with an increase in the number of bound vortexes.

The convergence of numerical solution is checked with the aid of the investigation of the effect of the number of the bound vortexes, by which is simulated the wing. Much study according to the procedure of the calculation were carried out by M. I. Nisht, V. Ya. Gordinskiy, and G. I. Turchannikov. The distributed and total aerodynamic coefficients of the transient functions of the wing of infinite lengthening are obtained with the number of eddy/vortices $n = 5$ and 10 (Figs. 19.1-19.4, 19.8-19.13), also, for $n = 5-60$ (Figs. 19.16, 19.17). Given data show that at subsonic speeds already with $n = 5-10$ is observed the practical convergence on n , especially at large values r . The greatest scatter of the calculation points is observed in the range of low values r ; therefore here desirable to take the relatively larger number of eddy/vortices.

The effect of the total number of eddy/vortices, by which is simulated the wing, to the results of the calculations of the transient functions of wings of finite aspect ratio is shown in an example of the transfer function of lift with an instantaneous change in the angle of attack $[c_y/\alpha^*]$ and the upon gradual entrance into step gust $\wedge \left[\frac{c_y}{w_{y\Delta}} \right]$ the rectangular (Fig. 19.18) and triangular (Fig. 19.19) wings of lengthening $\lambda = 2.5$. The calculations were carried out by G. I. Turchannikov for numbers $\overset{M=0.1}{\wedge}$ and $M=0.8$ during the simulation of wings by the total number of eddy/vortices $nN = 30, 55$ and 120 .

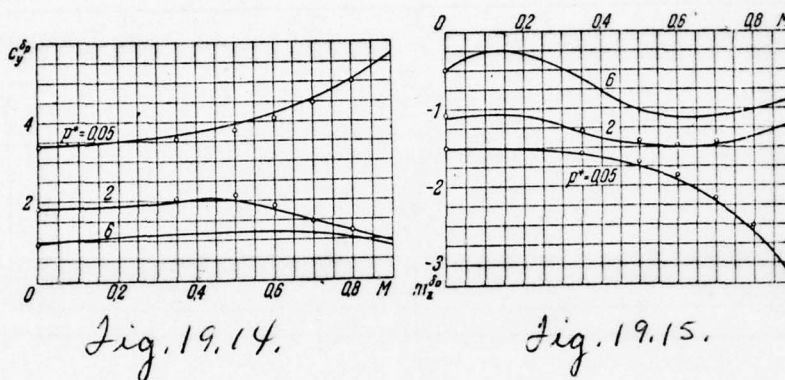


Fig. 19.14. Wing $\lambda = -$ with control $(\bar{b}_p = 0.2)$. Comparison of numerical calculations (curves) with known solutions (point).

Fig. 19.15. Wing $\lambda = -$ with control $(\bar{b}_p = 0.2)$. Comparison of numerical calculations (curves) with known solutions (point).

Page 448.

Given the figures indicated materials show that the simulation of the wings of the final lengthening by the vortex/eddy grid, which consists of the total number of eddy/vortices of order $nN \approx 60$, gives during the numerical calculations of transient functions sufficiently

satisfactory results.

Is investigated also the effect of the calculated interval/gap Δr for an infinite plate $\lambda = \infty$ with number $\sqrt{M = 0.6}$. An increase Δr with the constant/invariable number of eddy/vortices ($n = \text{const}$) makes the convergence of numerical solution somewhat worse, especially in the initial period of time (low value τ); however, during increase τ this convergence noticeably is improved (Fig. 19.20).

The effect of the number of eddy/vortices for a wing with flap here is not examined, since this effect at high subsonic speeds is analogous with the effect, obtained for the incompressible medium (chapter of XIV).

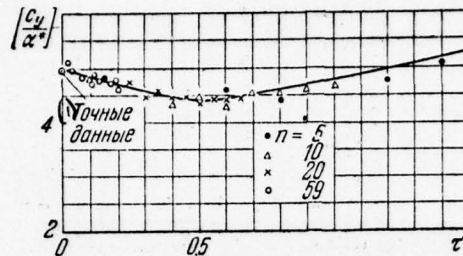


Fig. 19.16. Wing $\lambda = \infty$, $M = 0.8$. The effect of the number of eddy/vortices on coefficient $[C_y / \alpha^2]$ (curve is a known solution, points are a numerical calculation).

Key: (1). Precise data.

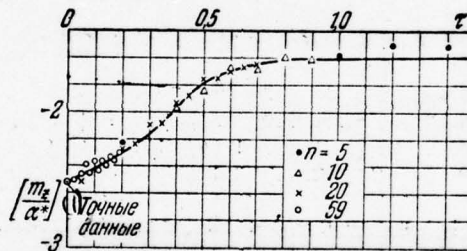


Fig. 19.17. Wing $\lambda = \infty$, $M = 0.8$, $\bar{x}_T = 0$. The effect of the number of eddy/vortices on coefficient $[m_z / \alpha^2]$ (curve is a known solution, points are a numerical calculation).

Key: (1). Precise data.

Page 449.

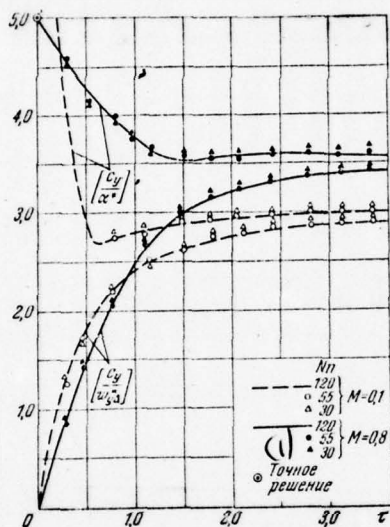


Fig. 19.18.

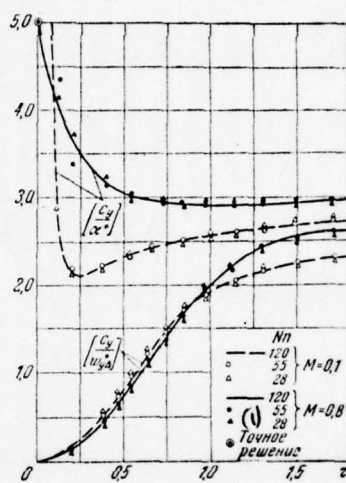


Fig. 19.19.

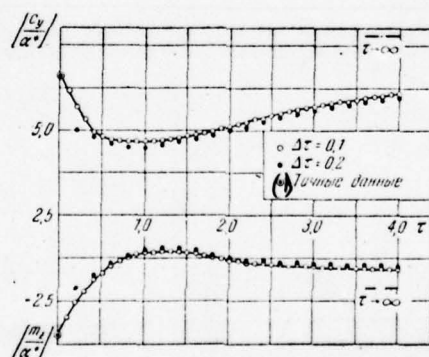


Fig. 19.20.

Fig. 19.18. Rectangular wing $\lambda = 2.5$. Effect of the number of eddy/vortices on transient functions $[c_y/a^*]$ and $[c_y/w_{y\Delta}]$.

Key: (1). Exact solution.

Fig. 19.19. Delta wing $\lambda = 2.5$. Effect of the number of eddy/vortices on transient functions $[c_y/a^*]$ and $[c_y/w_{y\Delta}]$.

Key: (1). Exact solution.

Fig. 19.20. Effect of the calculated time interval $\Delta\tau$ for the transient functions of wing $\lambda = \infty$, $M = 0.6$, $n = 10$. Curves are a known solution, points are a numerical calculation.

Key: (1). Precise data.

Page 450.

§5. Checking of numerical calculations with the aid of reciprocity theorem.

It is known that all consequences of reciprocity theorem are precise for arbitrary Strouhal numbers and Makh with harmonic time dependences. When the kinematic parameters by arbitrary form are changed on τ , the corresponding equalities are accurate with any τ . The control of the obtained from numerical calculation data can be conducted, by utilizing the relationship/ratios, which escape/ensue from reciprocity theorem (chapter VII).

For subsonic speed, which corresponds to number $\sqrt{M=0,6}$ are examined the transient functions of straight line and reverse/inverse delta wings $\lambda = 2.5$ (Fig. 19.21). From the given curve/graphs it is evident that in the numerical calculations indicated for these wings with satisfactory accuracy are fulfilled the relationship/ratios of reciprocity theorem

$$\left[\frac{c_{y+}}{a^*} \right] = \left[\frac{c_{y-}}{a^*} \right], \quad \left[\frac{c_{y+}}{\omega_z} \right] = \left[\frac{m_{z-}}{a^*} \right].$$

An analogous method of control it is expedient to utilize also for the coefficients of aerodynamic derivatives.

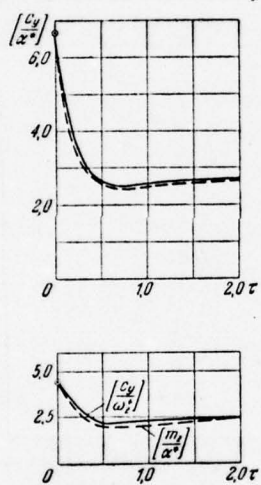


Fig. 19.21.

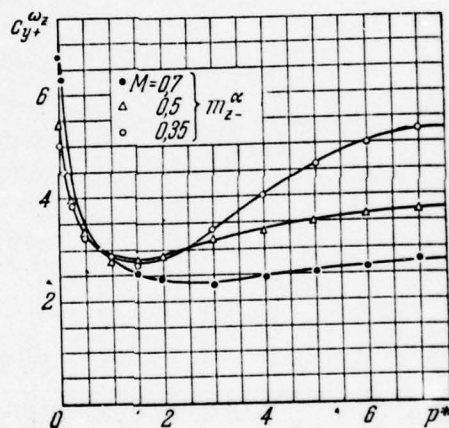


Fig. 19.22.

Fig. 19.21. Transient functions of straight line (unbroken curve) and reverse/inverse (dotted line) delta wings, $\lambda = 2.5$, $M = 0.6$, $\bar{x}_T = 0.5$, \odot - precise data.

Fig. 19.22. Coefficients aerodynamic derivative direct/straight and reverse/inverse wings $\lambda = \infty$, $\bar{x}_T = 0.5$.

Page 451.

For an infinite-span wing were calculated the coefficients $c_{y+}^{\omega z}, c_{y+}^{\dot{\omega} z}, m_{z-}^a, m_{z-}^{\dot{a}}$ and by the corresponding form were compared with each other (Fig. 19.22 and 19.23) over a wide range of Strouhal numbers with different Mach numbers $(M = 0,35; 0.50; 0.70)$. By solid lines on the curve/graphs indicated the corrected values of coefficients $c_{y+}^{\omega z}$ and $c_{y+}^{\dot{\omega} z}$ straight wing, but by points - derivatives m_{z-}^a and $m_{z-}^{\dot{a}}$ reverse/inverse wing. All data correspond to centering $\bar{x}_T = 0,50$. Let us note that in this case the direct/straight and reverse/inverse wings are actually one and the same the wing-plate of infinite span.

According to reciprocity theorem

$$c_{y+}^{\omega z} = m_{z-}^a, \quad c_{y+}^{\dot{\omega} z} = m_{z-}^{\dot{a}}.$$

These equalities are made well, as shown in Fig. 19.22, 19.23. Thus, reciprocity theorem can serve as good means of the control of numerical data, also, at high subsonic speeds.

§6. Checking of numerical calculations with the aid of the theorem of momentum and Duhamel integral.

The use of a Duhamel integral, as is known, makes it possible to carry out a passage to any assigned law of motion or gust. Specifically, by knowing transient functions, it is possible to find the coefficients of aerodynamic derivatives in the large range of Strouhal numbers.

Figure 19.24-19.31 depicts the results of the known solution of the problem of the harmonic oscillations of airfoil/profile ($\lambda = \infty$) at high subsonic speeds [2.35] - dotted curves.

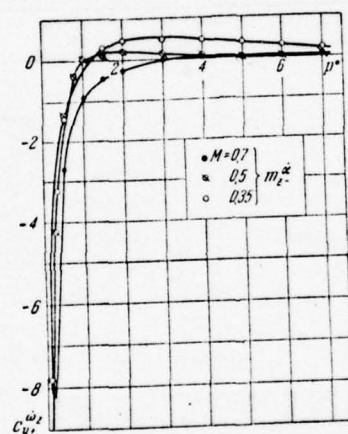


Fig. 19.23. Coefficients of the aerodynamic derivatives of straight line and reverse/inverse wings $\lambda = \infty$, $\bar{x}_T = 0.5$.

Page 452.

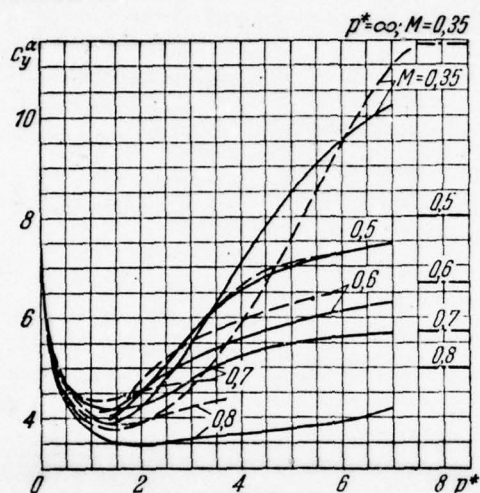


Fig. 19.24. Comparison of numerical calculations according to Duhamel integral (unbroken curves) with known solution (dotted line) for a wing $\lambda = \infty$.

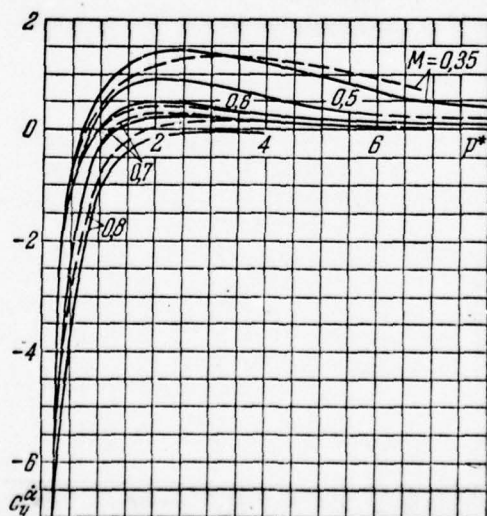


Fig. 19.25. Comparison of numerical calculations according to Duhamel integral (unbroken curves) with known solution (dotted line) for a wing $\lambda = \infty$.

Page 453.

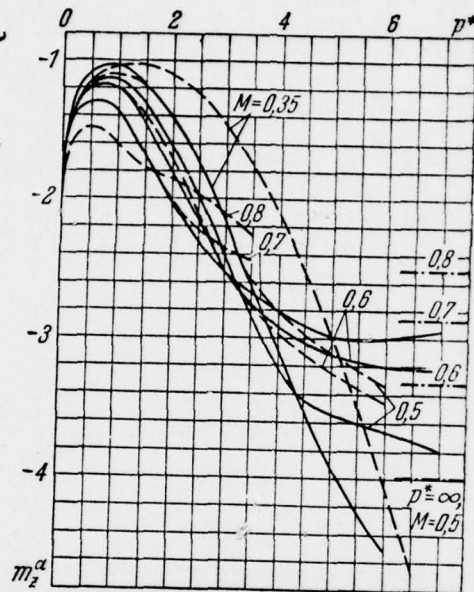


Fig. 19.26. Comparison of numerical calculations according to Duhamel integral (unbroken curves) with known solution (dotted line) for a wing $\lambda = \infty, \bar{x}_T = 0$.

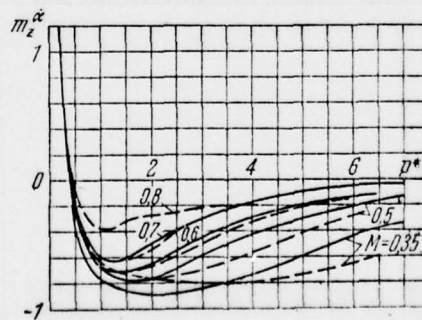


Fig. 19.27. Comparison of numerical calculations according to Duhamel integral (unbroken curves) with known solution (dotted line) for a wing $\lambda = \infty, \bar{x}_T = 0$.

Page 454.

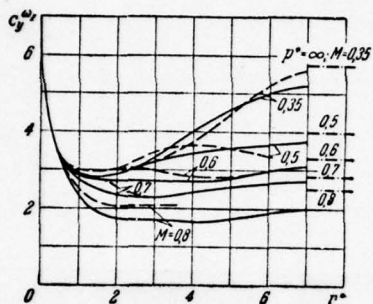


Fig. 19.28

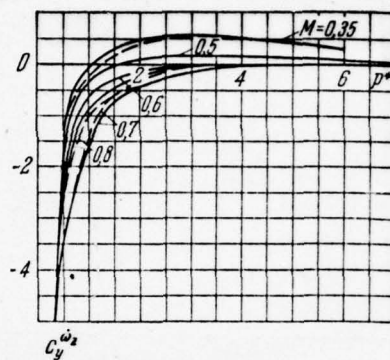


Fig. 19.29.

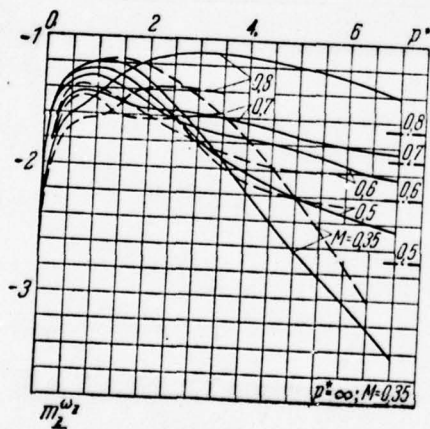


Fig. 19.30.

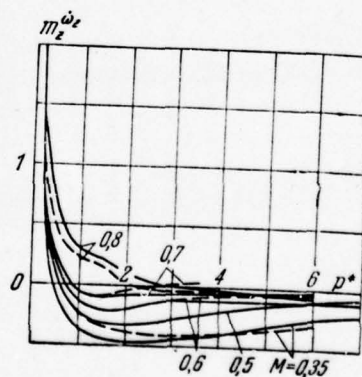


Fig. 19.31.

Fig. 19.28. Comparison of numerical calculations according to Duhamel integral (unbroken curves) with known solution (dotted line) for a wing $\lambda = \infty$, $\bar{x}_T = 0$.

Fig. 19.29. Comparison of numerical calculations according to Duhamel integral (unbroken curves) with known solution (dotted line) for a wing $\lambda = \infty$, $\bar{x}_T = 0$.

Fig. 19.30. Comparison of numerical calculations according to Duhamel integral (unbroken curves) with known solution (dotted line) for a wing $\lambda = \infty$, $\bar{x}_T = 0$.

Fig. 19.31. Comparison of numerical calculations according to Duhamel integral (unbroken curves) with known solution (dotted line) for a wing $\lambda = \infty$, $\bar{x}_T = 0$.

Page 455.

These data are acquired by numerical method with the aid of the recalculation of the corresponding transient functions and use of a Duhamel integral - unbroken curves. Dot-dash line shows limiting case of $p^* \rightarrow \infty$, for which the aim is the corresponding derivatives $c_y^a, c_z^a, m_z^a, m_x^a$, $c_y^{\omega z}, c_z^{\omega z}, m_z^{\omega z}, m_x^{\omega z}$. In this case are examined the numbers $M = 0,35; 0,50; 0,60; 0,70; 0,80$

with centering $\bar{x}_T = 0$. Conformity of data, obtained numerically, to the results [2.35] satisfactory.

The accuracy of numerical calculations for the coefficients of aerodynamic derivatives with points c^{q_i} can be checked also with the aid of the theorem of momentum, which establish/installs communication/connection between the transient function $\bigwedge [c(\tau)/q_i^*]$ and the derivative indicated with point with very small Strouhal number $c^{q_i}(0)$. Thus, for instance, for a lift coefficient this relationship/ratio takes the form

$$\int_0^\infty \left\{ \left[\frac{c_y(\tau)}{q_i} \right] - \left[\frac{c_y(\infty)}{q_i} \right] \right\} d\tau = c_y^{q_i}(0).$$

Theorem of momentum makes it possible also to control the behavior of transient function in all range τ in question. If one considers that are known the exact solutions for limiting cases $\tau = 0$ and $\tau = \infty$, then by these very to a certain extent it can be checked entire dependence $\bigwedge [c(\tau)/q_i^*]$ including extreme points $\tau = 0$ and $\tau = \infty$.

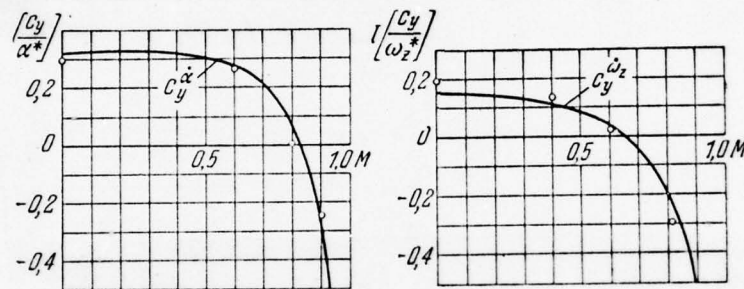


Fig. 19.32. Comparison of the coefficients of aerodynamic derivatives with $p^* \rightarrow 0$ (curves) with the momentum/impulse/pulse of transient functions (point) for a rectangular wing $\lambda = 2.5$, $\bar{x}_T = 0$.

Page 456.

Figure 19.32 depicts the numerical values of the coefficients of aerodynamic derivatives c_y^{α} and $c_y^{\omega_z}$ in the function of Mach number ($M=0-1.0$), obtained for a rectangular wing ($\lambda = 2.5$) by the calculation of aerodynamic derivatives with $p^* \rightarrow 0$ (curves), also, in terms of theorem of momentum with the aid of transient functions $[c_y/\alpha^*]$ and $[c_y/\omega_z^*]$

(point).

As we see, the conformity of two different methods of the numerical calculation of derivatives c_y^a and $c_y^{\omega_z}$ at subsonic speeds completely satisfactory.

§7. Comparison of theoretical and experimental data.

The comparison of experimental and calculated data makes it possible to carry out a cross check of each results and to produce the estimation of the field of the applicability of linear theory.

The experimental determination of aerodynamic derivatives is represented by difficult technical task. These difficulties are especially serious during the measurements of unsteady characteristics at transonic speed; therefore comparison is given only for the small number of wings. In Fig. 19.33 in the form of an example for a zero mean incidence ($\alpha_0 = 0$) is carried out the comparison of the calculated and experimental values of derivatives c_y^a and m_z^a for a delta wing with lengthening $\lambda = 4$ ($\bar{x}_T = 0.37$). Experimental and calculated data on the combination of derivatives the determining the longitudinal attenuation of wings different $m_z^{\omega_z} + m_z^a$,

planforms, with different centering \bar{x}_T and numbers M are given in Fig. 19.34-19.37.

Are here examined the results of the experiments, made by G. A. Kolesnikov for a rectangular wing ($\lambda = 2.5$) (Fig. 19.34), a delta wing ($\lambda = 4.0$ $\sqrt{\bar{x}_T = 0.43}$) (Fig. 19.35), the delta wing ($\lambda = 2.31$) (Fig. 19.36) and of sweptback wing ($\lambda = 3$, $\chi_0 = 60^\circ$, $\eta = 2.5$) (Fig. 19.37). The comparison of the experiments, carried out by Yu. A. Prudnikov and V. S. Bykov, with the calculation for the coefficient of roll damping ($m_{x1}^{\omega, r1}$) is made for rectangular and delta wings (Fig. 19.38). In this case are examined the wings of different lengthening in the parameters of similarity $k\lambda$.

All the given materials testify to the sufficiently satisfactory conformity of theory with experiment.

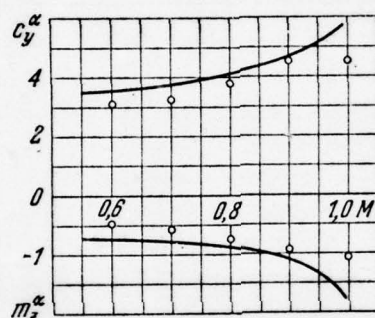


Fig. 19.33. Comparison of the calculation (curves) with experiment (point) for a delta wing $\lambda = 4$ ($\bar{x}_T = 0.37$).

Page 457.

The greatest disagreement of experimental and calculated data with low angles of attack and the amplitudes of oscillations is observed with numbers $\sqrt{M \geq 0.85 \div 0.95.}$ This disagreement can be first of all connected with the advent of on wing at the high subsonic speeds of regions with supersonic zones and the formation of local shocks.

In conclusion is presented the comparison of the results of numerical calculation (curves) with experiment (point) for an airfoil/profile with control $(b_p = 0,25)$ with constant Mach number $(M = 0,5)$. The calculation was performed by V. I. Bushuev employing above procedure presented.

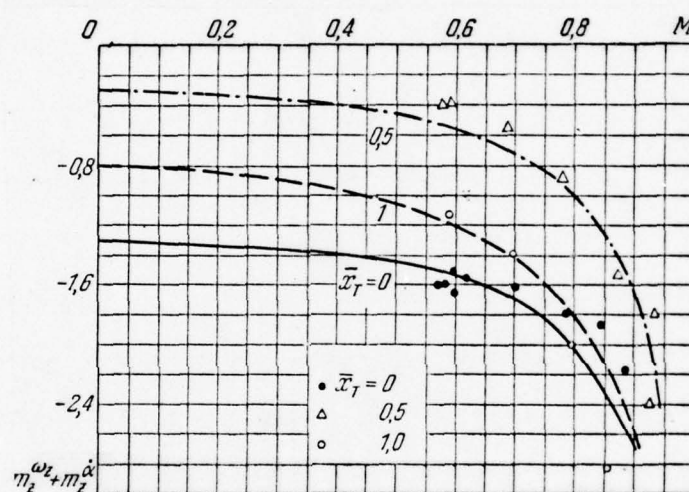


Fig. 19.34

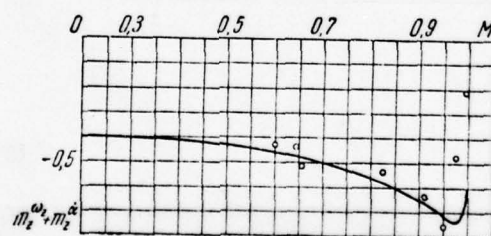


Fig. 19.35

Fig. 19.34. Comparison of the calculation (curves) with experiment (point) for a rectangular wing $\lambda = 2.5$.

Fig. 19.35. The comparison of the calculation (is curve) with experiment (point) for a delta wing $\lambda = 4$ ($\bar{x}_T = 0,43$).

Page 458.

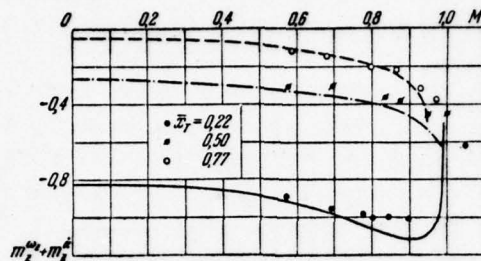


Fig. 19.36.

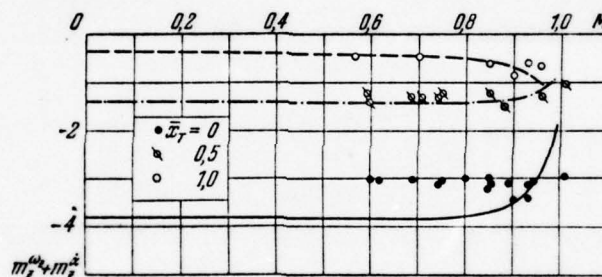


Fig. 19.37.

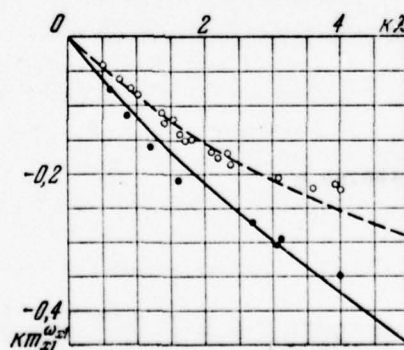


Fig. 19.38.

Fig. 19.36. Comparison of the calculation (curves) with experiment (point) for a delta wing $\lambda = 2.31$.

Fig. 19.37. Comparison of the calculation (curves) with experiment (point) for a sweptback wing $\lambda = 3$, $\chi_s = 60^\circ$, $\eta = 2.5$.

Fig. 19.38. Comparison of the calculation (curves) with experiment (point) for rectangular (unbroken curve) and triangular (dotted line) wings.

Page 459.

Figure 19.39 depicts to the dependence of the total coefficients of aerodynamic derivatives $\dot{c}_y^{\delta_p}$ and $\dot{c}_y^{\delta_p}$ of Strouhal number, while Fig. 19.40 shows the laws of a change aerodynamic derivative loads p^{δ_p} and p^{δ_p} chordwise of wing ($\xi = x/b$) for Strouhal number $p^* = 0.96$. The experimental data, borrowed from work [2.54], are obtained by the method of the measurement of instantaneous pressures during the oscillation of control relative to the axis, passing through its leading edge/nose. Experiments were conducted on airfoil/profile NACA 65A006 by the small amplitudes of the oscillation of control (in the case $\delta_p^* = 1,71^\circ$).

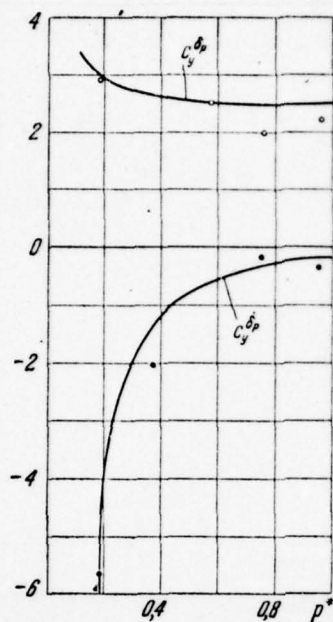


Fig. 19.39. Comparison of numerical calculation (curves) with experiment (point). Wing $\lambda = \infty$, $\bar{b}_p = 0.25$, $M = 0.5$.

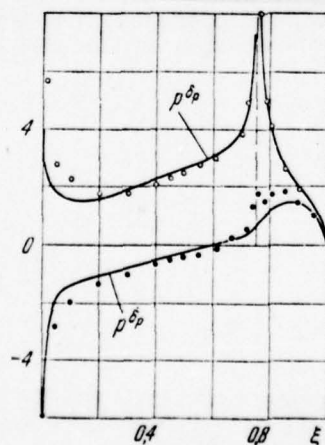


Fig. 19.40. Comparison of numerical calculation (curves) with experiment (point). Wing $\lambda = \infty$, $\bar{b}_p = 0.25$, $M = 0.5$; $p^* = 0.96$.

Page 460.

PART IV

SUPERSONIC SPEEDS ($M > 1$)

INTRODUCTION.

To task of the aerodynamic investigation of lifting surfaces during unsteady motion at supersonic speeds devoted large number of works ([1.15], [1.18], [1.21], [1.23], [1.25], [1.26], [1.38], [1.49], [1.50], [1.59], [1.63]). Sufficiently complete survey/coverage of the existing literature is in monographs [1.9], [1.15], [1.19], [1.26], and also in the article [2.53]. Therefore let us point out here only the state of question, let us note the most essential results in this region, and also briefly let us describe the ideas of those methods, which are set forth further in the present monograph.

The questions of unsteady motions at transonic speed are presented in works [2.46], [2.50], [2.53], there is given

bibliography.

The common/general/total ideas of approach to the solution to the supersonic linear tasks were given by Prandtl [1.10], [2.8] and by Ackeret [2.3], [2.4], which investigated infinite-span wing during steady motion. To the harmonic oscillations of this wing is dedicated the work of Borbeli [2.13]. The following space in the solution of common/general/total problem were Busemann's studies [2.14], the concerning flow of conical flow about the slender bodies, and also M. I. Gurevich' works [1.43], [1.44], in which were examined swept and delta wings in conical flow.

The large role in setting and solution of the problem of the flow around of the wing of the final spread/scope at supersonic speeds it played the scientific seminar led by L. I. Sedov, especially into period 1942-1950.

some of the first works in our country, dedicated to the studies of the unsteady motion of wing at supersonic speeds, were Ye. A. Krasil'shchikovoy's works. At first it solved the task of the harmonic oscillations of wing with supersonic edges without end effect, and then with end effect. The results of the investigations of Ye. A. Krasil'shchikovoy were generalized by it in monograph [1.15].

From the foreign analyses of the analogous content one should note Ward's work [2.19].

Page 461.

On the basis of the results [1.15] with M. K. Fursov [1.63] were obtained the exact solutions for the rigid and deforming wings with supersonic edges. The coefficients of aerodynamic derivatives are determined in this case for very small Strouhal numbers ($p^* \rightarrow 0$).

A number of the authors in us in the country and abroad obtained solutions for the wings of simple planform with different Strouhal numbers. Specifically, Ribner, Mal'vestuto, etc. [2.18], [2.21], [2.22], [2.50] found exact solution for a delta wing with subsonic leading edges with $p^* \rightarrow 0$. For the wings of complex planform with subsonic, supersonic, and also mixed leading and trailing edges was developed numerical method [1.84] of the calculation of aerodynamic characteristics. The method indicated can be used with the harmonic dependences of the kinematic parameters from time. It will be described in this part of the monograph.

In recent years increased the number of investigations,

dedicated to the solutions of the problems, connected with the effect of the vertical gust of air and the aperiodic motions of wing. From the works, which relate to the motion of wing with arbitrary time dependences, one should note the transactions of Miles [1.26], of Ye. A. Krasil'shchikova [1.81], A. I. Golubinskiy [1.65], [1.68], N. F. Vorobyev [1.59]. For infinite-span wings were obtained the exact solutions by the method of supersonic analogy [1.65], [2.23], [2.36] and by the method of pulsed sources [2.17]. Problem for delta wings with supersonic edges is solved in works [1.26], [2.26]. In articles [2.26], [2.36] are given the solutions of problem for a rectangular wing, while in work [1.26] given approximate solution is also for a delta wing of very small lengthening. For the wings of arbitrary planform with the mixed or subsonic and supersonic leading and trailing edges are developed the numerical calculation methods, presented in works [1.84], [1.86].

The idea of the numerical calculation methods both with aperiodic and harmonic time dependences is reduced to the following. The wing and the regions of effect are divide/marked off into unit cells by the lines, parallel to Mach lines which emerge from the apex/vertex of wing. In this case real wing approximately is replaced by wing with saw-tooth sonic edges. The derivative of velocity potential along the axis Oy (downwash) is accepted in each of the cells constant. After determining from the boundary conditions of the

value of taper (but if it is necessary, then also potential) for each cell of wing and regions of effect, we find aerodynamic loadings on wing. They are given below descriptions of the numerical methods indicated.

Page 462.

Is examined at first the task of the harmonic oscillations of wing, and then - a change in the kinematic parameters of motion along stepped law and the gradual entrance of wing into step gust.

For wings with supersonic edges are given also the exact solutions for the coefficients aerodynamic derivative and transient functions, whereupon for the latter are utilized the obtained in chapter IV exact solutions at the initial moment ($\tau \rightarrow 0$). Numerical data are compared with exact solutions, for example for a plate and the wings of the final lengthening with supersonic edges. The results of systematic investigations show the correctness of the proposed numerical methods and sufficient accuracy obtained with their aid of these with comparatively small quantities above unit cells indicated.

For control and testing the accuracy of the calculations of the coefficients of aerodynamic derivatives are utilized the known

consequences of reciprocity theorem. The numerical values of transient functions are monitored with $\tau \rightarrow 0$ by path comparison with exact solutions; with $\tau \rightarrow \infty$ by comparison with the results of the calculation of the coefficients of aerodynamic derivatives without points with $p^* \rightarrow 0$, and also with the aid of the theorem about momentum/impulse/pulses, and, furthermore, are utilized the consequences of reciprocity theorem for arbitrary time dependences. as one of the methods of testing linear theory serves the conducted in monograph comparison of experimental and calculated data, which makes it possible also to establish/install the field of application of this theory.

Page 463.

Chapter XX.

NUMERICAL METHOD OF THE CALCULATION OF AERODYNAMIC WING
CHARACTERISTICS WITH HARMONIC TIME DEPENDENCES.

§1. Velocity potential of source with harmonic time dependences.

As the basis of the solutions of linear unsteady problems at supersonic speeds let us take the velocity potential of pulsed source. As is known, at any source strength the potential of its disturbed speeds will satisfy wave equation (3.30) and to conditions at infinity.

Let us derive expression for a velocity potential in the case, when wing completes unsteady motion along harmonic laws or it is subject to the influence of harmonic gust. In this case the kinematic parameters of the motion in accordance with §2 of chapter of V without limitation generality can be written in the form

$$q_j(t) = q_j^* e^{i\rho t}. \quad (20.1)$$

In this paragraph $i = \sqrt{-1}$, $j = 1, 2, \dots, 5$. From (3.56) it follows that the boundary conditions on wing in this case also will change for harmonic laws and the derivatives of the unknown potential in terms of coordinates (downwashes) can be represented in the form

$$\left[\frac{\partial \varphi}{\partial y}(x, z, t) \right]_{y=0} = \left[\frac{\partial \varphi}{\partial y}(x, z) \right]_{y=0} e^{ip t}. \quad (20.2)$$

The potential of the disturbed speeds is connected with tapers by formula (4.11). After determining according to (4.14), (4.12) times t_1 and t_2 , let us have

$$t_1 = t - \frac{(x_1 - x) M}{a k^2} - \frac{r}{a k^2}, \quad t_2 = t - \frac{(x_1 - x) M}{a k^2} + \frac{r}{a k^2}. \quad (20.3)$$

Page 464.

By substituting these expressions in (4.11), let us find that during a change in the boundary conditions on wing for the harmonic laws

$$\begin{aligned} \varphi(x_1, y_1, z_1, t) = & -\frac{1}{2\pi} \operatorname{Re} e^{ip t} \iint_{\sigma^*(x_1, y_1, z_1)} \left[\frac{\partial \varphi}{\partial y}(x, z) \right]_{y=0} \times \\ & \times e^{-ip \frac{(x_1 - x) M}{a k^2}} \frac{\left(e^{-ip \frac{r}{a k^2}} + e^{ip \frac{r}{a k^2}} \right)}{r} dx dz. \end{aligned} \quad (20.4)$$

Taking into account that

$$e^{-ip \frac{r}{a k^2}} + e^{ip \frac{r}{a k^2}} = 2 \cos \frac{p}{a k^2} r, \quad (20.5)$$

and by introducing the designations

$$\rho^* = \frac{\rho b}{U_0}, \quad \omega = \rho^* \frac{M^2}{k^2} \quad (20.6)$$

(b - characteristic linear dimension), we will obtain the resultant expression for a velocity potential during the harmonic oscillations of the wing:

$$\begin{aligned} \varphi(x_1, y_1, z_1, t) = \\ = -\frac{1}{\pi} \operatorname{Re} q_j^* e^{i\rho t} \int_{\sigma^*} \int \left[\frac{\partial \varphi}{\partial y}(x, z) \right]_{y=0} \frac{e^{-i\omega \frac{x_1-x}{b}} \cos\left(\frac{\omega}{bM} r\right)}{r} dx dz, \quad (20.7) \\ r = \sqrt{(x-x_1)^2 - k^2 y_1^2 - k^2 (z-z_1)^2}. \end{aligned}$$

Is expressed the potential of the disturbed speeds through the coefficients of the aerodynamic derivatives of potential in terms of (3.65). By taking into account the harmonic character of a change in the kinematic parameters in time, let us write (3.65) in the form

$$\varphi(x, y, z, t) = U_0 b \operatorname{Re} e^{i\rho t} \sum_{j=1}^5 q_j^* [\varphi^{qj}(x, y, z) + i\rho^* \varphi^{dj}(x, y, z)]. \quad (20.8)$$

by finding hence expressions for the derivatives of potential in

terms of y and by substituting them in (20.7), we will obtain for determining the coefficients of the aerodynamic derivatives of potential the following relationship/ratios:

$$\left. \begin{aligned} \varphi^{qj}(x_1, y_1, z_1) &= -\frac{1}{\pi} \int_{\sigma} \left\{ \left[\frac{\partial \varphi^{qj}}{\partial y}(x, y, z) \right]_{y=0} \cos \frac{\omega(x_1 - x)}{b} + \right. \\ &\quad \left. + \frac{k^2}{M^2} \omega \left[\frac{\partial \varphi^{qj}}{\partial y}(x, y, z) \right]_{y=0} \sin \frac{\omega(x_1 - x)}{b} \right\} \cos \frac{\omega r}{bM} \frac{dx dz}{r}, \\ \varphi^{qj}(x_1, y_1, z_1) &= -\frac{1}{\pi} \int_{\sigma} \left\{ \left[\frac{\partial \varphi^{qj}}{\partial y}(x, y, z) \right]_{y=0} \cos \frac{\omega(x_1 - x)}{b} - \right. \\ &\quad \left. - \frac{M^2}{k^2} \frac{1}{\omega} \left[\frac{\partial \varphi^{qj}}{\partial y}(x, y, z) \right]_{y=0} \sin \frac{\omega(x_1 - x)}{b} \right\} \cos \frac{\omega r}{bM} \frac{dx dz}{r}, \\ r &= \sqrt{(x - x_1)^2 - k^2 y_1^2 - k^2 (z - z_1)^2}. \end{aligned} \right\} \quad (20.9)$$

Page 465.

§2. Basic positions of the numerical calculation method.

Let us examine the arbitrary in plan/layout wing, which along

with forward motion at supersonic speed U_0 , completes the harmonics of oscillation and undergoes the effect of harmonic gust. The speeds of the supplementary motion of wing we consider small as compared with the speed of the basic motion and let us characterize their dimensionless kinematic parameters q_i (2.19) and by their first time derivatives \dot{q}_i (2.20).

Let us introduce the connected with wing system of coordinates (Fig. 20.1), in which axis Ox is directed from the spout of root wing chord to its tail. The kinematic parameters, which characterize the motion of wing as solid body, we take in standard system of coordinates.

As shown in chapter III, the potential of the disturbed speeds must, taking into account a change in the direction of axis Ox , satisfy wave equation (3.30), boundary conditions on wing (3.56) and to conditions (3.61) on vortex sheet. In the case of harmonic motions of wing in question let us introduce according to (3.65) the coefficients of the aerodynamic derivatives of potential. For determining them let us have equations (5.12), boundary conditions (5.13) on wing and conditions ^(3.68) ~~(3.86)~~ on vortex sheet. Furthermore, outside wing and vortex sheet velocity potential and, consequently, also its coefficients of aerodynamic derivatives must be equal to zero.

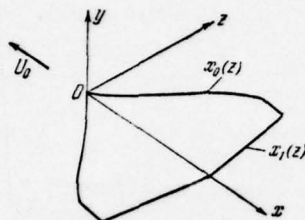


Fig. 20.1. Adopted system of coordinates.

Page 466.

Notation of condition on trailing edge in the form (3.86) frees from the need for searching for the value of jump $\partial\varphi/\partial x$ during passage from wing to vortex sheet for supersonic trailing edges and automatically satisfies Chaplygin - Joukowski's condition (continuity of potential φ during passage from trailing wing edge to vortex sheet) with subsonic trailing edges. Furthermore, this form is more convenient during numerical calculations.

Let us search for the solution to wave equation (3.30) in the

form (20.7). Let us consider that for determining aerodynamic loadings sufficient to calculate the potential on wing surface, for which in (20.7) - (20.9) one should place $y = 0$.

Let us introduce the dimensionless coordinates

$$\xi = \frac{x}{b}, \quad \eta = \frac{y}{b}, \quad \zeta = \frac{z}{b} \quad (20.10)$$

(b - root wing chord).

After presenting potential through the dimensionless coefficients of aerodynamic derivatives (5.11):

$$\varphi(x, y, z, t) = U_0 b \left\{ \varphi_0(\xi, \eta, \zeta) + \sum_{i=1}^5 [\varphi^{q_i}(\xi, \eta, \zeta) q_i + \varphi^{q_i}(\xi, \eta, \zeta) \dot{q}_i] \right\},$$

let us write (20.9) in the form

$$\left. \begin{aligned} \varphi_0(\xi_1, 0, \zeta_1) &= -\frac{1}{\pi} \int_0^{\omega} \left[\frac{\partial \varphi_0}{\partial \eta} \right]_{\eta=0} \frac{d\xi d\zeta}{V(\xi_1 - \xi)^2 - k^2(\zeta_1 - \zeta)^2}, \\ \varphi^{q_i}(\xi_1, 0, \zeta_1) &= -\frac{1}{\pi} \int_0^{\omega} \left\{ \left[\frac{\partial \varphi^{q_i}}{\partial \eta} \right]_{\eta=0} \cos \omega(\xi_1 - \xi) + \right. \\ &\quad \left. + \frac{k_2}{M^2} \omega \left[\frac{\partial \varphi^{q_i}}{\partial \eta} \right]_{\eta=0} \sin \omega(\xi_1 - \xi) \right\} \cos \frac{\omega \rho}{M} \frac{d\xi d\zeta}{\rho}, \\ \varphi^{q_i}(\xi_1, 0, \zeta_1) &= -\frac{1}{\pi} \int_0^{\omega} \left\{ \left[\frac{\partial \varphi^{q_i}}{\partial \eta} \right]_{\eta=0} \cos \omega(\xi_1 - \xi) - \right. \\ &\quad \left. - \frac{M^2}{k^2} \frac{1}{\omega} \left[\frac{\partial \varphi^{q_i}}{\partial \eta} \right]_{\eta=0} \sin \omega(\xi_1 - \xi) \right\} \cos \frac{\omega \rho}{M} \frac{d\xi d\zeta}{\rho}, \\ \rho &= V(\xi_1 - \xi)^2 - k^2(\zeta_1 - \zeta)^2. \end{aligned} \right\} \quad (20.11)$$

These formulas make it possible to solve the task of the determination of potential at the points of wing surface, if in an entire field of effect σ are known values $[\partial\varphi^{q_i}/\partial\eta]_{\eta=0}$ and $[\partial\varphi^{q_i}/\partial\eta]_{\eta=0}$, which subsequently let us call tapers.

Page 467.

However, the direct use of formulas (20.11) for numerical

calculations is impeded by the facts that with

$$\xi_1 - \xi = \pm k(\zeta_1 - \zeta)$$

the integrand has a special feature/peculiarity of order $1/\sqrt{\rho}$.

Therefore we convert them to convenient for numerical calculations form.

First let us transform the system of the coordinates

$$\xi_M = \frac{\xi}{k}, \quad \zeta_M = \zeta, \quad \eta_M = \eta. \quad (20.12)$$

Wing in the converted coordinate system for the cases, when lines Mach from the apex/vertex of wing correspond to lines a, b and c in Fig. 20.2, it is shown in Fig. 20.3, 20.4, 20.5. Equations (20.11) in the converted coordinate system take the form

$$\left. \begin{aligned} \varphi_0(\xi_{1M}, 0, \zeta_{1M}) &= -\frac{1}{\pi} \int \int_{\sigma_M} \left[\frac{\partial \varphi_0}{\partial \eta_M} \right]_{\eta_M=0} \frac{d\xi_M d\zeta_M}{\rho_M}, \\ \varphi^{q_i}(\xi_{1M}, 0, \zeta_{1M}) &= -\frac{1}{\pi} \int \int_{\sigma_M} \left\{ \left[\frac{\partial \varphi^{q_i}}{\partial \eta_M} \right]_{\eta_M=0} \cos \bar{\omega}(\xi_{1M} - \xi_M) + \right. \\ &\quad \left. + p \left[\frac{\partial \varphi^{q_i}}{\partial \eta_M} \right]_{\eta_M=0} \sin \bar{\omega}(\xi_{1M} - \xi_M) \right\} \cos \frac{\bar{\omega} \rho_M}{M} \frac{d\xi_M d\zeta_M}{\rho_M}, \\ \varphi^{q_i}(\xi_{1M}, 0, \zeta_{1M}) &= -\frac{1}{\pi} \int \int_{\sigma_M} \left\{ \left[\frac{\partial \varphi^{q_i}}{\partial \eta_M} \right]_{\eta_M=0} \cos \bar{\omega}(\xi_{1M} - \xi_M) - \right. \\ &\quad \left. - \frac{1}{p} \left[\frac{\partial \varphi^{q_i}}{\partial \eta_M} \right]_{\eta_M=0} \sin \bar{\omega}(\xi_{1M} - \xi_M) \right\} \cos \frac{\bar{\omega} \rho_M}{M} \frac{d\xi_M d\zeta_M}{\rho_M}, \\ \rho_M &= \sqrt{(\xi_{1M} - \xi_M)^2 + (\zeta_{1M} - \zeta_M)^2}. \end{aligned} \right\} \quad (20.13)$$

Here

$$\bar{\omega} = k\omega. \quad (20.14)$$

For simplification in the solution to the obtained equations during nonsteady motion let us introduce the following replacement:

$$\left. \begin{aligned} \varphi^{q_i}(\xi_M, 0, \zeta_M) &= F^{q_i} \cos \bar{\omega} \xi_M + p^* F^{q_i} \sin \bar{\omega} \xi_M, \\ \varphi^{q_i}(\xi_M, 0, \zeta_M) &= F^{q_i} \cos \bar{\omega} \xi_M - \frac{1}{p^*} F^{q_i} \sin \bar{\omega} \xi_M. \end{aligned} \right\} \quad (20.15)$$

Page 468.

Functions F^{q_i} and F^{q_i} , just as φ^{q_i} , φ^{q_i} , satisfy wave equation (3.30), of what it is not difficult to be convinced by direct substitution. Finding from (20.15) the derivatives of potentials and substituting them in equations (20.13), we obtain integral equations for the introduced functions:

$$\left. \begin{aligned} F^{q_i}(\xi_{1M}, 0, \zeta_{1M}) &= -\frac{1}{\pi} \iint_{\sigma_M} \left[\frac{\partial F^{q_i}}{\partial \eta_M} \right]_{\eta_M=0} \cos \frac{\bar{\omega} \rho_M}{M} \frac{d\xi_M d\zeta_M}{\rho_M}, \\ F^{q_i}(\xi_{1M}, 0, \zeta_{1M}) &= -\frac{1}{\pi} \iint_{\sigma_M} \left[\frac{\partial F^{q_i}}{\partial \eta_M} \right]_{\eta_M=0} \cos \frac{\bar{\omega} \rho_M}{M} \frac{d\xi_M d\zeta_M}{\rho_M}. \end{aligned} \right\} \quad (20.16)$$

Let us introduce characteristic coordinates $\beta O x$ (see Fig. 20.3), after selecting their beginning in order to have the only positive values of variables. These coordinates are connected with the converted system by the relationship/ratios

$$\beta = (\xi_M - \xi_{00M}) - \zeta_M, \quad \kappa = (\xi_M - \xi_{00M}) + \zeta_M. \quad (20.17)$$

Value ξ_{00M} the displacement of the beginning of the characteristic system for the wing, planform for which is assigned in the form (1.10), is determined from the relationship/ratio

$$\xi_{00M} = \min [\xi_{0M}(\zeta_M) - \zeta_M], \quad (20.18)$$

where $\xi_{0M}(\zeta_M)$ - the equation of leading edge in the converted coordinate system, ζ_M - moving coordinate.

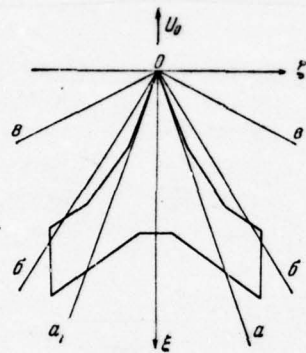


Fig. 20.2.

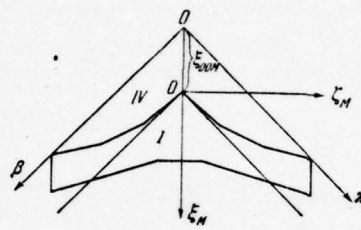


Fig. 20.3.

Fig. 20.2. The wing of complex planform in the adopted system of coordinates; a , b , c are lines Maxa at the different speeds of motion.

Fig. 20.3. Wing with supersonic leading and trailing edges in the converted and characteristic coordinate systems.

Page 469.

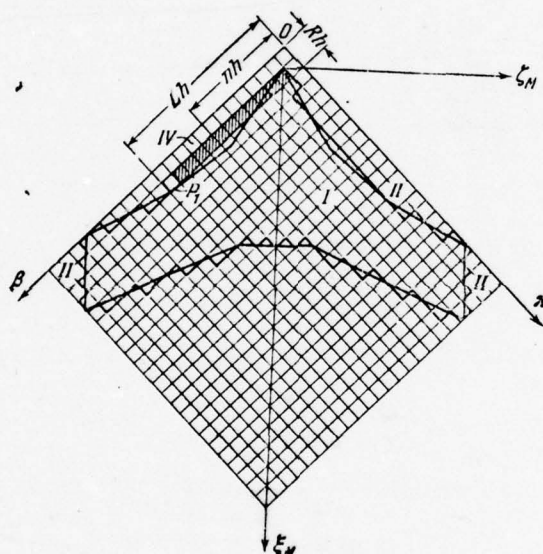


Fig. 20.4. Wing with that which was mixed front/leading and supersonic rear by edges. To the determination of tapers in the field of end effect.

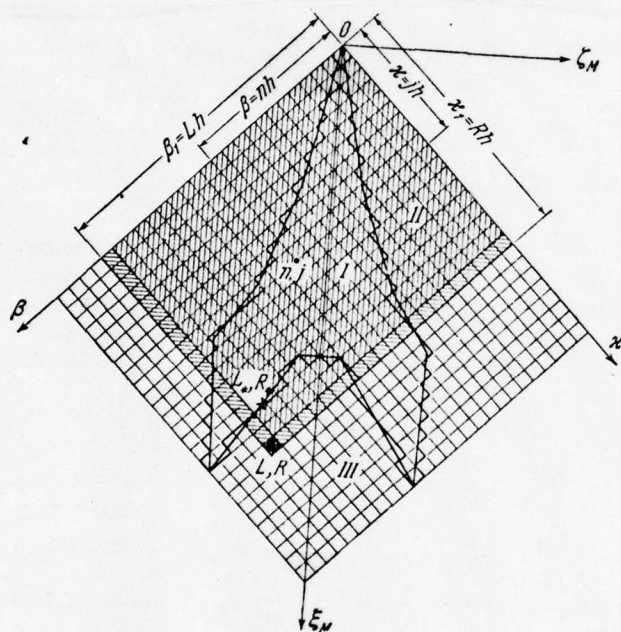


Fig. 20.5. Wing with subsonic front/leading and that which was mixed rear by edges. To the determination of tapers on vortex sheet.

Page 470.

For the wing, leading edge of which is formed by the cuts direct (20.18) it is possible to write in the form

$$\xi_{00M} = \min \left[\sum_{e=1}^m (\zeta_{Me} - \zeta_{Me-1}) \operatorname{tg} \chi_{0Me-1} - \zeta_{Mm} \right], \quad (20.19)$$

$$m = 1, 2, \dots, N_e.$$

Here ξ is the current number of the fracture of leading edge, counting from the root section, in which we set/assume $e = 0$; χ_{0Me-1} the sweep angle of leading edge in the converted coordinate system between $(\xi - 1)$ - and ξ - breaks, N'_e - the total quantity of fractures on one half of wing. If the amount of displacement ξ_{00M} , determined by (20.18), (20.19), turns out to be positive, it one should accept equal to zero.

In the characteristic coordinate system the first equation of system (20.13) and equations (20.16) are written in the form

$$\left. \begin{aligned}
 \varphi_0(\beta_1, 0, \kappa_1) &= -\frac{1}{2\pi} \int_0^{\beta_1} \int_0^{\kappa_1} \left[\frac{\partial \varphi_0}{\partial \eta_M} \right]_{\eta_M=0} \frac{d\beta d\kappa}{V(\beta_1 - \beta)(\kappa_1 - \kappa)}, \\
 F^{q_i}(\beta_1, 0, \kappa_1) &= -\frac{1}{2\pi} \int_0^{\beta_1} \int_0^{\kappa_1} B_i \frac{\cos \frac{\tilde{\omega}}{M} V(\beta_1 - \beta)(\kappa_1 - \kappa)}{V(\beta_1 - \beta)(\kappa_1 - \kappa)} d\beta d\kappa, \\
 F^{q_i}(\beta_1, 0, \kappa_1) &= -\frac{1}{2\pi} \int_0^{\beta_1} \int_0^{\kappa_1} E_i \frac{\cos \frac{\tilde{\omega}}{M} V(\beta_1 - \beta)(\kappa_1 - \kappa)}{V(\beta_1 - \beta)(\kappa_1 - \kappa)} d\beta d\kappa,
 \end{aligned} \right\} \quad (20.20)$$

where markedly

$$B_i = \left[\frac{\partial F^{q_i}}{\partial \eta_M} \right]_{\eta_M=0}, \quad E_i = \left[\frac{\partial F^{q_i}}{\partial \eta_M} \right]_{\eta_M=0}. \quad (20.21)$$

For the elimination of special feature/peculiarities in the formulas written above let us assume

$$\mu = \sqrt{\beta_1 - \beta}, \quad v = \sqrt{\kappa_1 - \kappa}. \quad (20.22)$$

After this (20.20) they take the form

$$\left. \begin{aligned}
 \varphi_0(\beta_1, 0, \kappa_1) &= -\frac{2}{\pi} \int_0^{\sqrt{\beta_1}} \int_0^{\sqrt{\kappa_1}} \left[\frac{\partial \varphi_0(\beta_1 - \mu^2, \kappa_1 - v^2)}{\partial \eta_M} \right]_{\eta_M=0} d\mu dv, \\
 F^{q_i}(\beta_1, 0, \kappa_1) &= -\frac{2}{\pi} \int_0^{\sqrt{\beta_1}} \int_0^{\sqrt{\kappa_1}} B_i(\beta_1 - \mu^2, \kappa_1 - v^2) \cos\left(\frac{\tilde{\omega}}{M} \mu v\right) d\mu dv, \\
 F^{q_i}(\beta_1, 0, \kappa_1) &= -\frac{2}{\pi} \int_0^{\sqrt{\beta_1}} \int_0^{\sqrt{\kappa_1}} E_i(\beta_1 - \mu^2, \kappa_1 - v^2) \cos\left(\frac{\tilde{\omega}}{M} \mu v\right) d\mu dv.
 \end{aligned} \right\} \quad (20.23)$$

Page 471.

Integrals in the form (20.23) no longer have special feature/peculiarities (more precise saying, they have the same special feature/peculiarities, as function B_i, E_i), and to them is used the law of mean.

Let us break range of integration σ_M into cells. For this let us divide the spread/scope of wing l into $2N$ parts and through dividing points let us conduct straight lines, parallel to the axes of coordinates β, x (see Fig. 20.4). Division we continue until we fill entire field σ_M . The projection of the cut between points $n, n + 1$ ($j, j + 1$) on the axis of coordinates let us designate h . The

coordinates of the fixed/recorded points, at which searches for the potential (or functions F^{q_i}, F^{d_i}) or taper, let us designate by L and R, the coordinates of the current points, according to which is carried out integration over n, j let us write them as follows:

$$\beta_i = Lh, \quad \alpha_i = Rh, \quad \beta = nh, \quad \alpha = jh. \quad (20.24)$$

As is easy to establish/install, the dimensionless value h is equal to

$$h = \frac{l}{2Nb}. \quad (20.25)$$

We define of fields, in particular leading (L_0, R_0) and trailing (L_*, R_*) wing edges. Counting functions $B_i(\beta_i - \mu^2, \alpha_i - \nu^2), E_i(\beta_i - \mu^2, \alpha_i - \nu^2)$ in each of the squares by variables (these functions subsequently let us also call for a brevity tapers), present (20.23) through the sums of integrals in terms of the cells:

$$\left. \begin{aligned} F^{q_i}(\beta_i, 0, \alpha_i) &= \\ &= -\frac{2}{\pi} \sum_{n=0}^{L-1} \sum_{j=0}^{R-1} \int_{V_{nh}}^{V_{(n+1)h}} \int_{V_{jh}}^{V_{(j+1)h}} B_i \cos\left(\frac{\tilde{\omega}}{M} \mu \nu\right) d\mu d\nu, \\ F^{d_i}(\beta_i, 0, \alpha_i) &= \\ &= -\frac{2}{\pi} \sum_{n=0}^{L-1} \sum_{j=0}^{R-1} \int_{V_{nh}}^{V_{(n+1)h}} \int_{V_{jh}}^{V_{(j+1)h}} E_i \cos\left(\frac{\tilde{\omega}}{M} \mu \nu\right) d\mu d\nu. \end{aligned} \right\} \quad (20.26)$$

Let us change range of integration Σ (projection of wing on plane $\eta=0$), Σ_1 (vortex sheet) and Σ_2 (disturbed region outside Σ and Σ_1) so that they would consist of the whole cells. In this case let us consider that the cell belongs to the appropriate region, if its middle lie/rests on it. Figures 20.4, 20.5, show that the real wing will be replaced in this case by wing with the jagged edges.

Page 472.

It is clear that the to larger number of cells is divided the region

σ_M

the less this wing will differ from the real. Since small changes of the wing planform lead to small changes in its aerodynamic characteristics, the latter for a real wing and a wing with the jagged edges will be close, but with an increase in the number of separations N to infinity they will coincide.

Velocity potential for a wing with the jagged edges they will determine accurately by formulas (20.26).

Let us determine velocity potentials approximately, for which accept tapers B_i, E_i in each of the cells as constants and equal to their values in the middle of cell. Then instead of precise relationship/ratios (20.26) we obtain those which were approximated:

$$\left. \begin{aligned} F^{q_i}(Lh, Rh) &= -\frac{2h}{\pi} \sum_{n=1}^L \sum_{j=1}^R B_{inj} P_{LnRj}, \\ F^{q_i}(Lh, Rh) &= -\frac{2h}{\pi} \sum_{n=1}^L \sum_{j=1}^R E_{inj} P_{LnRj}. \end{aligned} \right\} \quad (20.27)$$

where the value of tapers are equal to

$$\left. \begin{aligned} B_{inj} &= B_i \left[\left(n - \frac{1}{2} \right) h, \left(j - \frac{1}{2} \right) h \right] \cos \left[\frac{\bar{\omega} h}{M} \sqrt{\left(L - n - \frac{1}{2} \right) \left(R - j - \frac{1}{2} \right)} \right], \\ E_{inj} &= E_i \left[\left(n - \frac{1}{2} \right) h, \left(j - \frac{1}{2} \right) h \right] \cos \left[\frac{\bar{\omega} h}{M} \sqrt{\left(L - n - \frac{1}{2} \right) \left(R - j - \frac{1}{2} \right)} \right]. \end{aligned} \right\} \quad (20.28)$$

The function of effect P_{LnRl} is determined by the formula

$$P_{LnRl} = (\sqrt{L-n+1} - \sqrt{L-n})(\sqrt{R-j+1} - \sqrt{R-j}) = \frac{1}{(\sqrt{L-n+1} + \sqrt{L-n})(\sqrt{R-j+1} + \sqrt{R-j})}. \quad (20.29)$$

As shown in chapter VI, one of the basic calculated cases is the harmonic oscillation of wing with Strouhal number, which vanishes. Since $\bar{\omega}$ in this case also tends to zero, formulas (20.15) with $p^* \rightarrow 0$ take the form

$$\varphi^{q_l} = F^{q_l}, \quad \varphi^{q_i} = F^{q_i} - \frac{M^2}{k} \xi_M F^{q_l}, \quad (20.30)$$

while the value of tapers, determined by relationship/ratios (20.28), in this case they will be

$$\left. \begin{aligned} B_{lnl} &= B_l \left[\left(n - \frac{1}{2} \right) h, \left(j - \frac{1}{2} \right) h \right], \\ E_{lnl} &= E_l \left[\left(n - \frac{1}{2} \right) h, \left(j - \frac{1}{2} \right) h \right]. \end{aligned} \right\} \quad (20.31)$$

Page 473.

If are known tapers B_{inj}, E_{inj} in an entire region of integration, then formula (20.27), (20.29) and (20.30) makes it possible to determine the aerodynamic derivatives of velocity potential in any point (cell) of wing.

§3. Tapers on wing.

As shown in the preceding/previous paragraph, for determining potentials on wing it is necessary to know the values of tapers in an entire region of integration σ . Let us show, as are determined the tapers in the different parts of this region. Let us begin from the case, when leading wing edge supersonic or arbitrary, and rear - supersonic. Lines Maxa for these cases are noted by indices a and b in Fig. 20.2, and wings itself in the converted characteristic coordinate system - respectively in Fig. 20.2, 20.3.

In order that all coordinates of region σ would be positive, the beginning of characteristic system of coordinates is displaced to value ξ_{00M} , determined by formula (20.19). The area σ , by which occurs the integration during the determination of velocity potential, in this case will consist of regions I, II, and IV (see Fig. 20.3, 20.4). Let us examine, how are determined tapers in each of these regions. Subsequently will be examined only the case $p^* \rightarrow 0$. The affiliation/accessory of the tapers of one region or the other let us note by the appropriate superscript. For example, when is determined the taper in region II, it will have indices $B_{inf}^{(2)}$, $E_{inf}^{(2)}$

and so forth.

Let us begin from region IV, which is limited by the axes of characteristic system of coordinates, by leading wing edge (see Fig. 20.3) and by the characteristics, which emerge from the apex/vertex of wing (see Fig. 20.4). Since the motion of wing occurs at supersonic speed, obviously, the medium in this region is not agitated; therefore all tapers in it will be equal to zero:

$$B_{inl}^{(4)} = E_{inl}^{(4)} \equiv 0. \quad (20.32)$$

Region I lie/rests wholly on wing, and the tapers on it are determined by boundary conditions (5.13). Taking into account that with $p^* \rightarrow 0$ are fulfilled relationship/ratics (20.31), from (5.13) we get

$$\left. \begin{aligned} B_{1nl}^{(1)} &= -1, & B_{2nl}^{(1)} &= \frac{h}{2}(n-j), \\ B_{3nl}^{(1)} &= -\frac{kh}{2}(n+j-1) - k\xi_{00M}, \\ B_{4nl}^{(1)} &= \frac{1}{k} \frac{\partial j_\delta [(n-1/2)h, (j-1/2)h]}{\partial \xi_M}. \end{aligned} \right\} \quad (20.33)$$

Page 474.

On rigid wing according to (5.13) value $\left[\frac{\partial \Phi^{q_l}}{\partial \eta} \right]_{\eta=0} = 0$.
utilizing (20.30), (20.27) and (20.33), we will obtain

Hence, by

$$\left. \begin{aligned} E_{1nj}^{(1)} &= -\frac{M^2}{k} \left[\frac{h}{2} (n+j-1) + \xi_{00M} \right], \\ E_{2nj}^{(1)} &= \frac{M^2}{k} \left[\frac{h}{2} (n+j-1) + \xi_{00M} \right] \frac{h(n-j)}{2}, \\ E_{3nj}^{(1)} &= -M^2 \left[\frac{h}{2} (n+j-1) + \xi_{00M} \right]^2. \end{aligned} \right\} \quad (20.34)$$

For the deforming wing from (5.13) we have with $p^* \rightarrow 0$

$$\left[\frac{\partial \varphi^\delta}{\partial \eta} \right]_{\eta=0} = f_\delta,$$

therefore in this case

$$E_{4nj}^{(1)} = f_\delta \left[\left(n - \frac{1}{2} \right) h, \left(j - \frac{1}{2} \right) h \right] + B_{4nj}^{(1)} \frac{M^2}{k} \left[\frac{h}{2} (n+j-1) + \xi_{00M} \right]. \quad (20.35)$$

The task of the determination of the aerodynamic derivatives of the wing, which affects harmonic gust, with $p^* \rightarrow 0$ is not examined, since they are connected in this case with the aerodynamic derivatives of rigid wing by relationship/ratios (5.55), (5.56).

§4. Tapers in the region of end effect.

Let us find the expressions, which determine tapers in the disturbed region, limited front/leading and lateral wing edges and by

the surface, envelope characteristic cones with apex/vertexes at the points of wing contour. The section of the region indicated by plane Oxy in Fig. 20.4 and 20.5 is noted by mark II. Outside the surface of characteristic cones the medium rests, and velocity potential there retains the constant value, which it is accepted equal to zero. Therefore on interference wave velocity potential also will be equal to zero:

$$\varphi(x, y, z, t) = 0. \quad (20.36)$$

The velocity potential everywhere outside the flat/plane region, occupied with wing and vortex/eddy after it, is function continuous and as it follows from (3.73), odd relative to coordinate y .

Page 475.

Consequently everywhere in plane Oxz , besides the wing and vortex wake after it, is made the condition

$$\varphi(x, 0, z, t) = 0, \quad (20.37)$$

which it escape/ensues from (3.73).

Let us pass to characteristic coordinates on (20.17), and velocity potential let us present in the form (20.11) through the coefficients of its aerodynamic derivatives. By utilizing replacement

(20.15), we will obtain from (20.20) with $p^* \rightarrow 0$ condition in region II:

$$\left. \begin{aligned} F^{q_i} &= -\frac{1}{2\pi} \int_0^{\beta_1} \int_0^{x_1} B_i \frac{d\beta dx}{V(\beta_1 - \beta)(x_1 - x)} = 0, \\ F^{q_i} &= -\frac{1}{2\pi} \int_0^{\beta_1} \int_0^{x_1} E_i \frac{d\beta dx}{V(\beta_1 - \beta)(x_1 - x)} = 0. \end{aligned} \right\} \quad (20.38)$$

Let us write these integrals as follows:

$$\left. \begin{aligned} \int_0^{x_1} \frac{dx}{V_{x_1-x}} \int_0^{\beta_1} B_i \frac{d\beta}{V_{\beta_1-\beta}} &= 0, \quad \int_0^{x_1} \frac{dx}{V_{x_1-x}} \int_0^{\beta_1} E_i \frac{d\beta}{V_{\beta_1-\beta}} = 0 \\ \text{or} \quad \int_0^{\beta_1} \frac{d\beta}{V_{\beta_1-\beta}} \int_0^{x_1} B_i \frac{dx}{V_{x_1-x}} &= 0, \quad \int_0^{\beta_1} \frac{d\beta}{V_{\beta_1-\beta}} \int_0^{x_1} E_i \frac{dx}{V_{x_1-x}} = 0. \end{aligned} \right\} \quad (20.39)$$

These equalities are the equations of Abel with the right sides, identically equal to zero. Consequently, internal integrals with $x = x_1$ (first two equalities) and with $\beta = \beta_1$ (last/latter two equalities) are equal to zero. Hence we obtain the following equations for determining tapers in region II:

$$\left. \begin{aligned} \int_{\kappa_1-h}^{\kappa_1} B_l^{(2)} \frac{d\kappa}{\sqrt{\kappa_1-\kappa}} &= - \int_0^{\kappa_1-h} B_l \frac{d\kappa}{\sqrt{\kappa_1-\kappa}}, \\ \int_{\beta_1-h}^{\beta_1} B_l^{(2)} \frac{d\beta}{\sqrt{\beta_1-\beta}} &= - \int_0^{\beta_1-h} B_l \frac{d\beta}{\sqrt{\beta_1-\beta}}. \end{aligned} \right\} \quad (20.40)$$

Accurately the same equations let us have for determining tapers E_i .

Page 476.

By applying substitution (20.22), by considering tapers in cells constants and by transfer/converting from integrals to sums, we will obtain for determining taper at point (cell) with coordinates $\beta_1 = Lh$, $\kappa_1 = Rh$ the following relationship/ratios: for the points, which lie to the left of axis ξ_M ,

$$\left. \begin{aligned} B_l^{(2)}(Lh, Rh) &= - \sum_{n=1}^{L-1} B_l \left[\left(n - \frac{1}{2}\right)h, \left(j - \frac{1}{2}\right)h \right] P_{Ln}, \\ E_l^{(2)}(Lh, Rh) &= - \sum_{n=1}^{L-1} E_l \left[\left(n - \frac{1}{2}\right)h, \left(j - \frac{1}{2}\right)h \right] P_{Ln}, \\ P_{Ln} &= \frac{1}{\sqrt{L-n+1} + \sqrt{L-n}}; \end{aligned} \right\} \quad (20.41)$$

for the cells, which lie to the right of axis ξ_M ,

$$\left. \begin{aligned} B_l^{(2)}(Lh, Rh) &= - \sum_{j=1}^{R-1} B_l \left[\left(n - \frac{1}{2} \right) h, \left(j - \frac{1}{2} \right) h \right] P_{Rl}, \\ E_l^{(2)}(Lh, Rh) &= - \sum_{j=1}^{R-1} E_l \left[\left(n - \frac{1}{2} \right) h, \left(j - \frac{1}{2} \right) h \right] P_{Rl}, \\ P_{Rl} &= \frac{1}{\sqrt{R-j+1} + \sqrt{R-j}}. \end{aligned} \right\} \quad (20.42)$$

In such a way as to calculate taper at the points of region II, necessary to sum up tapers according to band $n = \text{const}$ ($j = \text{const}$), on which is located this point. The calculation is performed consecutively, beginning from the cell, which lies at the apex/vertex

of wing. Cell in the apex/vertex of wing always we consider belonging to wing, therefore, taper in it is known according to (20.33) - (20.35). The inaccuracy, introduced by the assumption that the taper in this cell is constant and equal to its value in middle, decreases with the removal/distance of the calculated cells from the apex/vertex of wing. Furthermore, by increasing the number of separations, it is possible this inaccuracy to make as small as desired.

§5. Tapers on vortex sheet.

Let us pass to the case of the determination of tapers on vortex sheet (line Maxa from the apex/vertex of wing is noted by index c in Fig. 20.2). The corresponding wing in the converted and characteristic coordinate systems is shown in Fig. 20.5, and the region of vortex sheet on it is noted by mark III.

For determining tapers on vortex sheet during a change in the kinematic parameters in harmonic laws we will use condition (3.68) a in the case of $p^* \rightarrow 0$ we utilize (3.69).

AD-A049 000

FOREIGN TECHNOLOGY DIV WRIGHT-PATTERSON AFB OHIO
A WING IN AN UNSTEADY GAS FLOW. PART 2, (U)
SEP 77 S M BELOTSEKOVSKIY, B K SKRIPACH
FTD-ID(RS)T-1534-77-PT-2

F76 1/3

UNCLASSIFIED

NL

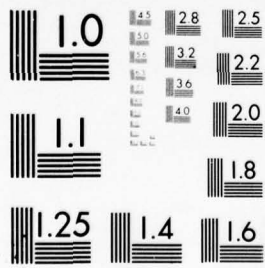
5 OF 6
ADAD49000



5 OF

6

ADAO49000



MICROCOPY RESOLUTION TEST CHART
NATIONAL BUREAU OF STANDARDS-1963-A

The last/latter condition in the converted system of coordinates

$O_{\xi_M \zeta_M}$ takes the form

$$\left. \begin{aligned} \varphi^{q_i}(\xi_M, 0, \zeta_M^*) &= \varphi^{q_i}(\xi_M^*, 0, \zeta_M^*), \\ \varphi^{q_i}(\xi_M, 0, \zeta_M^*) &= \varphi^{q_i}(\xi_M^*, 0, \zeta_M^*) - k(\xi_M - \xi_M^*) \varphi^{q_i}(\xi_M^*, 0, \zeta_M^*). \end{aligned} \right\} \quad (20.43)$$

Here through ξ_M^*, ζ_M^* are designated the coordinates of trailing wing edge. Let us present in right sides (20.43) the derivatives of $\overline{\partial \beta x}$ potential in the form (20.30) and pass to characteristic coordinates on (20.17). Then conditions (20.43) are written as follows:

$$\left. \begin{aligned} \varphi^{q_i}(\beta_1, 0, \kappa_1) &= F^{q_i}\left(\frac{\beta^* + \kappa^*}{2}, \frac{\kappa^* - \beta^*}{2}\right), \\ \varphi^{q_i}(\beta_1, 0, \kappa_1) &= F^{q_i}\left(\frac{\beta^* + \kappa^*}{2}, \frac{\kappa^* - \beta^*}{2}\right) - \\ &\quad - \frac{M^2}{2k}(\beta_1 + \kappa_1) F^{q_i}\left(\frac{\beta^* + \kappa^*}{2}, \frac{\kappa^* - \beta^*}{2}\right) + \\ &\quad + \frac{(\beta_1 + \kappa_1) - (\beta^* + \kappa^*)}{2k} F^{q_i}\left(\frac{\beta^* + \kappa^*}{2}, \frac{\kappa^* - \beta^*}{2}\right). \end{aligned} \right\} \quad (20.44)$$

Since conditions (20.43) are satisfied for the points of the vortex sheet whose coordinate $\zeta_{1M} = \zeta_M^*$, conditions (20.44) must be made for the points, characteristic coordinates of which are connected by the relationship/ratios

$$\kappa_1 - \beta_1 = \kappa^* - \beta^*, \quad \beta_1 > \beta^*, \quad \kappa_1 > \kappa^*. \quad (20.45)$$

Here and throughout through β^*, κ^* are designated the characteristic coordinates of trailing wing edge. They easily are determined for the assigned in Cartesian coordinates equation of trailing edge for (20.17).

For these points of vortex sheet from (20.20) and (20.30) with $p^* \rightarrow 0$ let us have

$$\left. \begin{aligned} \varphi^{q_i}(\beta_1, 0, \kappa_1) &= -\frac{1}{2\pi} \int_0^{\kappa_1} \int_0^{\beta_1} B_t \frac{d\beta d\kappa}{V(\beta_1 - \beta)(\kappa_1 - \kappa)}, \\ \varphi^{d_i}(\beta_1, 0, \kappa_1) &= -\frac{1}{2\pi} \int_0^{\kappa_1} \int_0^{\beta_1} E_t \frac{d\beta d\kappa}{V(\beta_1 - \beta)(\kappa_1 - \kappa)} + \\ &+ \frac{M^2}{4\pi k} (\beta_1 + \kappa_1) \int_0^{\kappa_1} \int_0^{\beta_1} B_t \frac{d\beta d\kappa}{V(\beta_1 - \beta)(\kappa_1 - \kappa)}. \end{aligned} \right\} (20.46)$$

Page 478.

By comparing (20.44) and (20.46), we will obtain the following integral equations for determining tapers on the vortex sheet:

$$\left. \begin{aligned}
 -\frac{1}{2\pi} \int_0^{x_1} \int_0^{\beta_1} B_i \frac{d\beta dx}{V(\beta_1 - \beta)(x_1 - x)} &= F^{q_i} \left(\frac{\beta^* + x^*}{2}, \frac{x^* - \beta^*}{2} \right), \\
 -\frac{1}{2\pi} \int_0^{x_1} \int_0^{\beta_1} E_i \frac{d\beta dx}{V(\beta_1 - \beta)(x_1 - x)} &= F^{q_i} \left(\frac{\beta^* + x^*}{2}, \frac{x^* - \beta^*}{2} \right) + \\
 &+ \frac{(\beta_1 + x_1) - (\beta^* + x^*)}{2k} F^{q_i} \left(\frac{\beta^* + x^*}{2}, \frac{x^* - \beta^*}{2} \right).
 \end{aligned} \right\} (20.47)$$

Both equations (20.47) are solved one and the same method. Let us examine it in an example of the solution to the first equation. Let us isolate near point with coordinates β_1, x_1 a small cell with the value of sides h along both axes of characteristic coordinates. Let us present the integral, which stands on the left side of equations (20.47), in the form of the sum of four integrals:

$$\begin{aligned}
 \int_0^{x_1} \int_0^{\beta_1} B_i \frac{d\beta dx}{V(\beta_1 - \beta)(x_1 - x)} &= \int_0^{x_1-h} \frac{dx}{V_{x_1-x}} \int_0^{\beta_1-h} B_i \frac{d\beta}{V_{\beta_1-\beta}} + \\
 &+ \int_{x_1-h}^{x_1} \frac{dx}{V_{x_1-x}} \int_0^{\beta_1-h} B_i \frac{d\beta}{V_{\beta_1-\beta}} + \int_0^{x_1-h} \frac{dx}{V_{x_1-x}} \int_{\beta_1-h}^{\beta_1} B_i \frac{d\beta}{V_{\beta_1-\beta}} + \\
 &+ \int_{x_1-h}^{x_1} \frac{dx}{V_{x_1-x}} \int_{\beta_1-h}^{\beta_1} B_i \frac{d\beta}{V_{\beta_1-\beta}}. \quad (20.48)
 \end{aligned}$$

During the calculation of integrals let us use method described above. Let us divide entire range of integration to cells with side h and tapers in each of the cells let us accept constants. The coordinates of cells let us characterize integers n, j, L, R according to (20.24), (20.25). For the purpose of the elimination of special feature/peculiarities in integrands let us pass on (20.22) to variables μ and ν .

$$\mu^2 = (L - n)h = sh, \quad \nu^2 = (R - j)h = rh. \quad (20.49)$$

Page 479.

For the first of the given integrals we will obtain

$$\begin{aligned}
& \int_0^{\alpha_1-h} \frac{d\alpha}{\sqrt{\alpha_1-\alpha}} \int_0^{\beta_1-h} B_i(\beta, \alpha) \frac{d\beta}{\sqrt{\beta_1-\beta}} = \\
& = \int_{\sqrt{Rh}}^{\sqrt{h}} 2 d\nu \int_{\sqrt{Lh}}^{\sqrt{h}} B_i(\beta_1-\mu^2, \alpha_1-\nu^2) 2 d\mu = \\
& = 4 \sum_{r=1}^{R-1} \int_{\sqrt{(r+1)h}}^{\sqrt{rh}} d\nu \sum_{s=1}^{L-1} \int_{\sqrt{(s+1)h}}^{\sqrt{sh}} B_i[(L-s)h, (R-r)h] d\mu = \\
& = 4h \sum_{r=1}^{R-1} \sum_{s=1}^{L-1} B_i[(L-s)h, (R-r)h] (\sqrt{s+1}-\sqrt{s})(\sqrt{r+1}-\sqrt{r}) = \\
& = 4h \sum_{j=1}^{R-1} \sum_{n=1}^{L-1} B_i(nh, jh) P_{LnRj}.
\end{aligned}$$

Here P_{LnRj} - the function of effect - is determined by formula (20.29). Analogously let us have

$$\begin{aligned}
& \int_{\alpha_1-h}^{\alpha_1} \frac{d\alpha}{\sqrt{\alpha_1-\alpha}} \int_0^{\beta_1-h} B_i(\beta, \alpha) \frac{d\beta}{\sqrt{\beta_1-\beta}} = 4h \sum_{n=1}^{L-1} B_i(nh, Rh) P_{LnRR}, \\
& \int_0^{\alpha_1-h} \frac{d\alpha}{\sqrt{\alpha_1-\alpha}} \int_{\beta_1-h}^{\beta_1} B_i(\beta, \alpha) \frac{d\beta}{\sqrt{\beta_1-\beta}} = 4h \sum_{j=1}^{R-1} B_i(Lh, jh) P_{LLRj},
\end{aligned}$$

where

$$\begin{aligned}
 P_{LnRR} &= (\sqrt{L-n+1} - \sqrt{L-n}) = \\
 &= (\sqrt{L-n+1} - \sqrt{L-n}) (\sqrt{R-R+1} - \sqrt{R-R}), \\
 P_{LLRI} &= (\sqrt{R-j+1} - \sqrt{R-j}) = \\
 &= (\sqrt{L-L+1} - \sqrt{L-L}) (\sqrt{R-j+1} - \sqrt{R-j}).
 \end{aligned}$$

For the last/latter integral of right side (20.48) in terms of is
shone brightly

$$\int_{x_1-h}^{x_1} \frac{dx}{\sqrt{x_1-x}} \int_{\beta_1-h}^{\beta_1} B_i(\beta, x) \frac{d\beta}{\sqrt{\beta_1-\beta}} = 4hB_i(Lh, Rh).$$

Page 480.

By summarizing all the obtained expressions, we will obtain the
following relationship/ratios for determining tapers at point (cell)
L, R, arranged/located in range vortex sheet:

$$\left. \begin{aligned}
 B_i^{(3)}(Lh, Rh) &= -\frac{\pi}{2h} F^{qi}(L, h, R, h) - \sum_{n=1}^L \sum_{j=1}^R B_i(nh, jh) P_{LnRj}, \\
 E_i^{(3)}(Lh, Rh) &= -\frac{\pi}{2h} \left[F^{qi}(L, h, R, h) + \right. \\
 &\quad \left. + \frac{h(L+R-L_*-R_*)}{2k} F^{qi}(L, h, R, h) \right] - \sum_{n=1}^L \sum_{j=1}^R E_i(nh, jh) P_{LnRj}.
 \end{aligned} \right\} \quad (20.50)$$

In formulas (20.50) the symbol $\sum \sum'$ indicates summation over all cells, included in the reverse/inverse cone Maxa, which emerges from point Lh, Rh , eliminating cell itself L, R , in which is determined the taper (see Fig. 20.4). Through L, h, R, h are designated the coordinates of the cells, which belong to trailing wing edge. The latter according to (20.45) will be connected with the coordinates of cell L, R by the relationship/ratios

$$R - L = R_* - L_*, \quad L > L_*, \quad R > R_*. \quad (20.51)$$

Tapers on vortex sheet are calculated consecutively, beginning with cell after trailing edge with smallest number R (for the right half of wing) or L (for the left half). For this we determine the value of functions $F^{qi}(L_*, R_*)$, $F^{qi}(L_*, R_*)$ in the appropriate cell on the trailing wing edge whose coordinates we find from (20.51). Further we compute the sum of the products of tapers and the

function of effect in an entire range, limited by the characteristics, which emerge from the beginning of coordinates and point L, R except cell itself Lh, Rh, and, after using (20.50), we find the unknown tapers in cell Lh, Rh. It is logical, tapers in all remaining cells of the range indicated must be determined previously from the relationship/ratios of the preceding/previous paragraphs. After this I pass along band $L = \text{const}$ ($R = \text{const}$) to the following cell with coordinates Lh, $(R + 1) h$ or, correspondingly, $(L + 1) h$, Rh and, repeating entire process of calculations, we determine tapers in it. Consecutively transfer/converting from one cell to another, we find tapers in an entire range of vortex sheet. Recall that for the calculation of aerodynamic loadings on wing there is no need to search for tapers in entire range III, and sufficient to find them only for part, which affects wing.

§6. Determination of distributed loads on wing.

After by the methods, described in the preceding/previous paragraphs of this chapter, are found the tapers in an entire range of effect, not difficult by formulas (5.11), (20.15) (20.23) to determine velocity potential in all points (cells), which belong to wing.

Page 481.

Let us note that the integrals, in which enter the tapers on wing, can be undertaken accurately, and on ranges II and III, that lie outside wing, obtain the approximate values of integrals, since tapers in the cells of these ranges were assumed to be constants. It is obvious, that the lesser part of the entire range of effect they will to occupy the indicated ranges, the more accurately will be determined potentials on wing. It is also obvious that the potentials will be calculated with the facts by larger accuracy, the lesser will be the size/dimensions of cells, and in principle they can be determined with any predetermined accuracy. In this chapter for the illustration of the application/use of a numerical calculation method during the determination of the value of potentials on wing, as earlier, the calculation of the corresponding integrals in terms of an entire range of effect let us produce numerically, by replacing them by sums. Thus, velocity potential we represent through the aerodynamic derived in the form (5.11), and values of the latter at the points of wing with coordinates L_h, R_h at $p^* \rightarrow 0$ we find, utilizing formulas (20.27), (20.30).

After the made observations let us pass to the determination of

the distributed loads (pressure difference on the upper and lower surfaces) of wing. As is known, loads can be found on the known value of velocity potential with the aid of the Cauchy-Lagrange integral (3.17). Let us present the dimensionless aerodynamic loading through the coefficients of aerodynamic derivatives in the form (2.24), namely:

$$\frac{2\Delta p}{\rho_{\infty} U_0^2} = \Delta \bar{p} = \sum_{i=1}^4 (p^{q_i} q_i + p^{\dot{q}_i} \dot{q}_i), \quad (20.52)$$

where the kinematic parameters q_i, \dot{q}_i are determined by relationship/ratios (2.19), (2.20). Using, taking into account a change in the direction of axis Ox , of relationship/ratio (3.21) and the representation of the aerodynamic derivatives of potential in the form (20.30), let us have for aerodynamic derivatives the loads

$$\left. \begin{aligned} p^{q_i}(\xi, \zeta) &= \frac{4}{k} \frac{\partial F^{q_i}(\xi_M, \zeta_M)}{\partial \xi_M}, \\ p^{\dot{q}_i}(\xi, \zeta) &= \frac{4}{k^3} \left\{ -k F^{q_i}(\xi_M, \zeta_M) + M^2 \left[\frac{k^2}{M^2} \frac{\partial F^{q_i}(\xi_M, \zeta_M)}{\partial \xi_M} - \right. \right. \\ &\quad \left. \left. - k \xi_M \frac{\partial F^{q_i}(\xi_M, \zeta_M)}{\partial \xi_M} \right] \right\}. \end{aligned} \right\} \quad (20.53)$$

Consequently, for determining load at each point of wing it is

necessary to know the particular derivatives F^{qi}, F^{qi} in terms of coordinate ξ_M . It is known that in the numerical calculation methods the determination derivative presents sizable difficulties. Therefore let us examine two paths of the numerical differentiation: by the method of differences and by the method of analytical approximation.

Method of differences. We consider that wing in accordance with higher numerical method presented broken by cells and in all cells of the value of functions F^{qi}, F^{qi} are determined. Further, approximately let us assume that the derived functions indicated on coordinate ξ_M are equal to

$$\frac{\partial F^{qi}(\xi_M, \zeta_M)}{\partial \xi_M} \approx \frac{F^{qi}(\xi_M + \Delta \xi_M, \zeta_M) - F^{qi}(\xi_M, \zeta_M)}{\Delta \xi_M}.$$

Let us pass to characteristic coordinates (20.17) and to designations (20.24). If $\zeta_M = \text{const}$, during passage from the cell in question to adjacent value $\Delta \xi_M$ is

$$\Delta \xi_M = \frac{(L+1)h + (R+1)h}{2} - \frac{Lh + Rh}{2} = h. \quad (20.54)$$

Then we obtain, for example,

$$\frac{\partial F^{qi}(\xi_M, \zeta_M)}{\partial \xi_M} = \frac{1}{h} [F^{qi}(L+1, R+1) - F^{qi}(L, R)]. \quad (20.55)$$

Aerodynamic derivative of load will be in this case determined from the formulas

$$\left. \begin{aligned}
 p^{q_i}(\xi, \zeta) &= \frac{4}{kh} \{F^{q_i}(L+1, R+1) - F^{q_i}(L, R)\}, \\
 p^{q_i}(\xi, \zeta) &= \frac{4}{k^3} \left\{ -k F^{q_i}(L, R) \right\} + \\
 &+ \frac{4M^2}{k^3} \left\{ \frac{k^2}{M^2} \frac{1}{h} [F^{q_i}(L+1, R+1) - F^{q_i}(L, R)] - \right. \\
 &\quad \left. - \frac{k(L+R)}{2} [F^{q_i}(L+1, R+1) - F^{q_i}(L, R)] \right\}.
 \end{aligned} \right\} (20.56)$$

The conformity of coordinates ξ , ζ , and Lh , Rh easily is establish/installated with the aid of (20.12), (20.17), (20.24); dimensionless quantity h we determine from (20.25).

Page 483.

It must be noted that the loads with use of the method of differences are determined from (20.56) insufficiently accurately. For an increase in the accuracy it is desirable that the values of potentials or functions F^{q_i} , F^{q_i} would be determined in the larger number of cells, than a quantity of cells, in which are located the loads. In this case the interval $\Delta\xi_M$, in which is determined the derivative, can be into the multiple of times more the value of cell, for example mh . Then derivative we define as relation

$$\frac{\partial F^{q_i}(\xi_M, \zeta_M)}{\partial \xi_M} = \frac{1}{mh} [F^{q_i}(L+m, R+m) - F^{q_i}(L, R)]. \quad (20.57)$$

Respectively will change in this case formulas (20.56).

The advantage of the method of differences lies in the fact that in this case it is not necessary to previously be given the form of the dependence $p^{q_i}(\xi)$, which for different wings and the different mode/conditions of flow (numbers M) has different character. Deficiency/lack it consists in the fact that for obtaining loads in a sufficient quantity of points the calculation of tapers must be given in the considerably larger number of cells, than a quantity of cells, in which are determined the first. This fact substantially increases time of the calculations.

Method of analytical approximation. Aerodynamic derivative loads will be, obviously, determined more accurately, if derivatives $\left(\frac{\partial F^{q_i}}{\partial \xi_M}, \frac{\partial F^{q_i}}{\partial \xi_M} \right)$ are be located of analytical dependences. It is clear that for this it is necessary to preliminarily find from the results of numerical calculations analytical dependences for functions themselves. The complexity of this method consists in the fact that a change in the velocity potential in coordinate ξ_M has different character for different wings (see below Fig. 24.1). So, for the root section, which is special (apex/vertex of wing is point of inflection), of wings both with subsonic and supersonic leading edges the derivative

$\partial\varphi/\partial\xi = \text{const}$ for all ξ . For a section with subsonic leading edges the load and, consequently, also derivatives $\partial\varphi/\partial\xi$ with approach to leading edge approach infinity. Analogously with supersonic trailing edge derivative $\partial\varphi/\partial\xi$ with approach to it has finite quantity. But if trailing edge in this section is subsonic, then as already noted above, $\partial\varphi/\partial\xi$ with approach to it will vanish. In the general case during the flow around of the wing of arbitrary planform in its sections there can be different combination of the character of the flow about the leading and trailing edges. Common/general/total for all them will be that that on leading edge ($\xi = \xi_0$) $\phi = 0$, i.e., the analytical dependence must not contain absolute term.

Page 484.

let us consider also that on subsonic leading edge load and, consequently, also derivative potential they have a special feature/peculiarity of the type $1/\sqrt{x}$. Let us introduce the dimensionless coordinate \bar{x} for each section throughout the formula

$$\bar{x} = \frac{x - x_0}{b'} = \frac{\xi_M - \xi_{0M}}{\xi_M^* - \xi_{0M}^*}. \quad (20.58)$$

Here b' is a chord of section, ξ_{0M}, ξ_M^* - the dimensionless coordinates of the leading and trailing edges of the converted wing. Let us present function F^q, F^q in the form

$$\left. \begin{aligned} F^{q_l}(\bar{x}) &= d_1 \bar{x}^{\frac{1}{2}} + d_2 \bar{x} + \dots + d_{2\gamma-1} \bar{x}^{\frac{2\gamma-1}{2}} + d_{2\gamma} \bar{x}^\gamma, \\ F^{q_l}(\bar{x}) &= e_1 \bar{x}^{\frac{1}{2}} + e_2 \bar{x} + \dots + e_{2\gamma-1} \bar{x}^{\frac{2\gamma-1}{2}} + e_{2\gamma} \bar{x}^\gamma, \\ \gamma &= 1, 2, \dots, m. \end{aligned} \right\} \quad (20.59)$$

Derivatives F^{q_l}, F^{q_l} in terms of ξ_M will be

$$\left. \begin{aligned} \frac{\partial F^{q_l}}{\partial \xi_M} &= \frac{b'}{b} \frac{\partial F^{q_l}(\bar{x})}{\partial \bar{x}} = \\ &= \frac{b'}{b} \left(\frac{d_1}{2\sqrt{\bar{x}}} + d_2 + \dots + \frac{2\gamma-1}{2} d_{2\gamma-1} \bar{x}^{\frac{2\gamma-3}{2}} + \gamma d_{2\gamma} \bar{x}^{\gamma-1} \right), \\ \frac{\partial F^{q_l}}{\partial \xi_M} &= \frac{b'}{b} \left(\frac{e_1}{2\sqrt{\bar{x}}} + e_2 + \dots + \frac{2\gamma-1}{2} e_{2\gamma-1} \bar{x}^{\frac{2\gamma-3}{2}} + \gamma e_{2\gamma} \bar{x}^{\gamma-1} \right). \end{aligned} \right\} \quad (20.60)$$

Task consists in that in order to fit coefficients $d_{2\gamma-1}, d_{2\gamma}, e_{2\gamma-1}, e_{2\gamma}$ in such a way as to approximate in the best way by dependence (20.59) the obtained by numerical method values F^{q_l}, F^{q_l} . Further, under error e_{LR} let us understand the difference between these values in the middles of cells, calculated by formulas (20.59) and numerical method. Let us use for an approximation the method of least squares, i.e., the optimum values of coefficients let us count those, with which the sum of the squares of all errors turns out to be smallest:

$$\sum e_{LR}^2 = \min. \quad (20.61)$$

Page 485.

As a result we will obtain the systems of equations for determining the coefficients of series (20.59), which in designations (20.24) will take the form

$$\begin{aligned}
 & \sum_{\gamma=1}^m \sum_{L_0 R_0}^{L_* R_*} d_{2\gamma-1} \left[\frac{(L+R)-(L_0+R_0)}{(L_*+R_*)-(L_0+R_0)} \right]^{\frac{2\gamma-1+n}{2}} + \\
 & + \sum_{\gamma=1}^m \sum_{L_0 R_0}^{L_* R_*} d_{2\gamma} \left[\frac{(L+R)-(L_0+R_0)}{(L_*+R_*)-(L_0+R_0)} \right]^{\frac{2\gamma+n}{2}} - \\
 & - \sum_{L_0 R_0}^{L_* R_*} F^{q_i}(L, R) \left[\frac{(L+R)-(L_0+R_0)}{(L_*+R_*)-(L_0+R_0)} \right]^{\frac{n}{2}} = 0, \\
 & \sum_{\gamma=1}^m \sum_{L_0 R_0}^{L_* R_*} e_{2\gamma-1} \left[\frac{(L+R)-(L_0+R_0)}{(L_*+R_*)-(L_0+R_0)} \right]^{\frac{2\gamma-1+n}{2}} + \\
 & + \sum_{\gamma=1}^m \sum_{L_0 R_0}^{L_* R_*} e_{2\gamma} \left[\frac{(L+R)-(L_0+R_0)}{(L_*+R_*)-(L_0+R_0)} \right]^{\frac{2\gamma+n}{2}} - \\
 & - \sum_{L_0 R_0}^{L_* R_*} F^{q_i}(L, R) \left[\frac{(L+R)-(L_0+R_0)}{(L_*+R_*)-(L_0+R_0)} \right]^{\frac{n}{2}} = 0; \\
 & n = 1, 2, \dots, 2m-1, 2m; \\
 & L_0 \leq L \leq L_*, R_0 \leq R \leq R_*, R-L = R_0-L_0 = R_*-L_*
 \end{aligned} \tag{20.62}$$

Here through L_0, R_0 and L_*, R_* are designated the numbers of the cells, which correspond to leading and trailing wing edges in the

section in question. After solving system from $2n - 1$ or $2n$ equations (20.62), we find unknown coefficients d_{2n-1} , d_{2n} , e_{2n-1} , e_{2n} . Since for each case (different section, number M wings) it cannot be previously determined which polynomial gives the best result, quantity of terms in (20.59) and respectively the number of equations in systems (20.62) we increase consecutively. Each time we compute the sum of the squares of errors. If additive term increases this error, then we are stopped on the number of terms without it, i.e., we select this polynomial, for which

$$\sum e_{LR}^2 = \min.$$

After this it is not difficult by formulas (20.59), (20.60) to determine in any point of the section of the value of functions F^q_i , F^q_i and their derivatives and, utilizing (20.53), to find the coefficients of the aerodynamic derivatives of load.

The results of some calculations of load during the use both of the method of differences and approximation method are given below (see Fig. 24.1-24.3).

Page 486.

§7. Calculation of total aerodynamic wing characteristics.

After are determined the load factors on wing, it is possible to find from formulas (2.25) the coefficients aerodynamic derivative total characteristics of entire wing and its sections.

However, the calculation of loads sufficiently is laborious, and numerical differentiation of velocity potential lowers the accuracy of the calculations. At the same time in many instances basic interest are of the only total wing characteristics. By taking into account this, we will obtain for the total characteristics such formulas in order that in them would not enter derivative of velocity potential.

Let us present the coefficients aerodynamic derivative total characteristics in the form, analogous (15.53), namely:

$$\left. \begin{aligned} kc_y^{q_i} &= c_{yM}^{q_i}, & k^3 c_y^{q_i} &= c_{y1M}^{q_i} + M^2 c_{y2M}^{q_i}, \\ km_z^{q_i} &= m_{zM}^{q_i}, & k^3 m_z^{q_i} &= m_{z1M}^{q_i} + M^2 m_{z2M}^{q_i}, \\ i &= 1, 3, 4 \quad (q_1 = \alpha, q_3 = \omega_z, q_4 = \delta); \\ k^2 m_x^{\omega_x} &= m_{xM}^{\omega_x}, & k^4 m_x^{\omega_x} &= (m_{xM}^{\omega_x})_1 + M^2 (m_{xM}^{\omega_x})_2. \end{aligned} \right\} \quad (20.63)$$

Page 487.

By substituting (20.53) in (2.25), let us have

$$\begin{aligned}
 c_{yM}^{q_i} &= \frac{4b^2 k \lambda}{l^2} \int_{-l/2b}^{l/2b} \int_{\xi_{0M}}^{\xi_M} \frac{\partial F^{q_i}(\xi_M, \zeta_M)}{\partial \xi_M} d\xi_M d\zeta_M, \\
 c_{y1M}^{q_i} &= -\frac{4b^2 k^2 \lambda}{l^2} \int_{-l/2b}^{l/2b} \int_{\xi_{0M}}^{\xi_M} F^{q_i}(\xi_M, \zeta_M) d\xi_M d\zeta_M, \\
 c_{y2M}^{q_i} &= \frac{4b^2 k^2 \lambda}{l^2} \left[\frac{k}{M^2} \int_{-l/2b}^{l/2b} \int_{\xi_{0M}}^{\xi_M} \frac{\partial F^{q_i}(\xi_M, \zeta_M)}{\partial \xi_M} d\xi_M d\zeta_M - \right. \\
 &\quad \left. - \int_{-l/2b}^{l/2b} \int_{\xi_{1M}}^{\xi_M} \frac{\partial F^{q_i}(\xi_M, \zeta_M)}{\partial \xi_M} \xi_M d\xi_M d\zeta_M \right],
 \end{aligned} \tag{20.64}$$

$$\begin{aligned}
m_{z\dot{M}}^{q_i} &= -\frac{4b^2k^2\lambda}{l^2} \int_{-l/2b}^{l/2b} \int_{\xi_{0M}}^{\xi_M} \frac{\partial F^{q_i}(\xi_M, \zeta_M)}{\partial \xi_M} \xi_M d\xi_M d\zeta_M, \\
m_{z\dot{M}}^{q_i} &= \frac{4b^2k^3\lambda}{l^2} \int_{-l/2b}^{l/2b} \int_{\xi_{0M}}^{\xi_M} F^{q_i}(\xi_M, \zeta_M) \xi_M d\xi_M d\zeta_M, \\
m_{z\dot{M}}^{q_i} &= -\frac{4b^2k^3\lambda}{l^2} \left[\frac{k}{M^2} \int_{-l/2b}^{l/2b} \int_{\xi_{0M}}^{\xi_M} \frac{\partial F^{q_i}(\xi_M, \zeta_M)}{\partial \xi_M} \xi_M d\xi_M d\zeta_M - \right. \\
&\quad \left. - \int_{-l/2b}^{l/2b} \int_{\xi_{0M}}^{\xi_M} \frac{\partial F^{q_i}(\xi_M, \zeta_M)}{\partial \xi_M} \xi_M^2 d\xi_M d\zeta_M \right], \\
i &= 1, 3, 4; \\
m_{x\dot{M}}^{\omega_x} &= -\frac{4b^2k^2\lambda}{l^2} \int_{-l/2b}^{l/2b} \int_{\xi_{0M}}^{\xi_M} \frac{\partial F^{\omega_x}(\xi_M, \zeta_M)}{\partial \xi_M} \xi_M d\xi_M d\zeta_M, \\
(m_{x\dot{M}}^{\omega_x})_1 &= \frac{4b^2k^3\lambda}{l^2} \int_{-l/2b}^{l/2b} \int_{\xi_{0M}}^{\xi_M} F^{\omega_x}(\xi_M, \zeta_M) \xi_M d\xi_M d\zeta_M, \\
(m_{x\dot{M}}^{\omega_x})_2 &= -\frac{4b^2k^3\lambda}{l^2} \left[\frac{k}{M^2} \int_{-l/2b}^{l/2b} \int_{\xi_{0M}}^{\xi_M} \frac{\partial F^{\omega_x}(\xi_M, \zeta_M)}{\partial \xi_M} \xi_M d\xi_M d\zeta_M - \right. \\
&\quad \left. - \int_{-l/2b}^{l/2b} \int_{\xi_{0M}}^{\xi_M} \frac{\partial F^{\omega_x}(\xi_M, \zeta_M)}{\partial \xi_M} \xi_M^2 d\xi_M d\zeta_M \right].
\end{aligned}
\tag{20.64}$$

Let us note that on leading wing edge the velocity potential is equal to zero, and consequently,

$$F^{q_l}(\xi_{0M}, \zeta_M) = F^{q_l}(\xi_M^*, \zeta_M) = 0.$$

Page 488.

Therefore

$$\begin{aligned} \int_{\xi_{0M}}^{\xi_M^*} \frac{\partial F^{q_l}(\xi_M, \zeta_M)}{\partial \xi_M} d\xi_M &= F^{q_l}(\xi_M^*, \zeta_M), \\ \int_{\xi_{0M}}^{\xi_M^*} \frac{\partial F^{q_l}(\xi_M, \zeta_M)}{\partial \xi_M} \xi_M d\xi_M &= \xi_M^* F^{q_l}(\xi_M^*, \zeta_M) - \int_{\xi_{0M}}^{\xi_M^*} F^{q_l}(\xi_M, \zeta_M) d\xi_M, \\ \int_{\xi_{0M}}^{\xi_M^*} \frac{\partial F^{q_l}(\xi_M, \zeta_M)}{\partial \xi_M} \zeta_M d\xi_M &= \zeta_M F^{q_l}(\xi_M^*, \zeta_M), \\ \int_{\xi_{0M}}^{\xi_M^*} \frac{\partial F^{q_l}(\xi_M, \zeta_M)}{\partial \xi_M} \zeta_M \xi_M d\xi_M &= \\ &= \zeta_M \xi_M^* F^{q_l}(\xi_M^*, \zeta_M) - \int_{\xi_{0M}}^{\xi_M^*} F^{q_l}(\xi_M, \zeta_M) \zeta_M d\xi_M, \\ \int_{\xi_{0M}}^{\xi_M^*} \frac{\partial F^{q_l}(\xi_M, \zeta_M)}{\partial \xi_M} \xi_M^2 d\xi_M &= \\ &= (\xi_M^*)^2 F^{q_l}(\xi_M^*, \zeta_M) - 2 \int_{\xi_{0M}}^{\xi_M^*} \xi_M F^{q_l}(\xi_M, \zeta_M) d\xi_M. \end{aligned} \quad (20.65)$$

And it is analogous for coefficients with points.

Let us pass in (20.64) to characteristic coordinates (20.24).

Page 489.

Considering in each of the cells potential to constants and by replacing integrals by sums, we will obtain taking into account (20.65) for the coefficients of the aerodynamic derivatives of the lift

$$\left. \begin{aligned} c_{\nu M}^{q_i} &= \frac{4b^2 k \lambda}{l^2} h \sum_{L_*} F^{q_i}(L_*, R_*), \\ c_{\nu 1M}^{q_i} &= - \frac{4b^2 k^2 \lambda}{l^2} h^2 \sum_S \sum F^{q_i}(L, R) \end{aligned} \right\} \quad (20.66)$$

$$\left. \begin{aligned} c_{\nu 2M}^{q_i} &= \frac{4b^2 k^2 \lambda}{l^2} h \left\{ \frac{k}{M^2} \sum_{L_*} F^{q_i}(L_*, R_*) - \right. \\ &\quad - \sum_{L_*} \left[(L_* + R_*) \frac{h}{2} + \xi_{00M} \right] F^{q_i}(L_*, R_*) + \\ &\quad \left. + h \sum_S \sum F^{q_i}(L, R) \right\}, \\ &\quad i = 1, 3, 4; \end{aligned} \right\} \quad (20.66)$$

for the coefficients of the aerodynamic derivatives of the pitching moment

$$\left. \begin{aligned}
 m_{z\dot{M}}^{q_i} &= -\frac{4b^2k^3\lambda}{l^2} h \left\{ \sum_{L_*} \left[(L_* + R_*) \frac{h}{2} + \xi_{O0M} \right] F^{q_i}(L_*, R_*) - \right. \\
 &\quad \left. - h \sum_S \sum F^{q_i}(L, R) \right\}, \\
 m_{z\dot{M}}^{q_i} &= \frac{4b^2k^3\lambda}{l^2} h^2 \sum_S \sum \left[(L + R) \frac{h}{2} + \xi_{O0M} \right] F^{q_i}(L, R), \\
 m_{z\dot{M}}^{q_i} &= -\frac{4b^2k^3\lambda}{l^2} h \left\{ \frac{k}{M^2} \sum_{L_*} \left[(L_* + R_*) \frac{h}{2} + \xi_{O0M} \right] F^{q_i}(L_*, R_*) - \right. \\
 &\quad - \frac{kh}{M^2} \sum_S \sum F^{q_i}(L, R) - \sum_{L_*} \left[(L_* + R_*) \frac{h}{2} + \xi_{O0M} \right]^2 F^{q_i}(L_*, R_*) + \\
 &\quad \left. + 2h \sum_S \sum \left[(L + R) \frac{h}{2} + \xi_{O0M} \right] F^{q_i}(L, R) \right\}, \\
 &\quad i = 1, 3, 4;
 \end{aligned} \right\} \quad (20.67)$$

for the coefficients of the aerodynamic derivatives of the rolling moment

$$\left. \begin{aligned}
 m_{xM}^{\omega_x} &= -\frac{4b^2k^2\lambda}{l^2} h \sum_{L_*} \left[(R_* - L_*) \frac{h}{2} \right] F^{\omega_x}(L_*, R_*), \\
 (m_{xM}^{\omega_x})_1 &= \frac{4b^2k^3\lambda}{l^2} h^2 \sum_S \sum \left[(R - L) \frac{h}{2} \right] F^{\omega_x}(L, R), \\
 (m_{xM}^{\omega_x})_2 &= -\frac{4b^2k^3\lambda}{l^2} h \left\{ \frac{k}{M^2} \sum_{L_*} \left[(R_* - L_*) \frac{h}{2} \right] F^{\omega_x}(L_*, R_*) - \right. \\
 &\quad - \sum_{L_*} \left[(R_* - L_*) \frac{h}{2} \right] \left[(L_* + R_*) \frac{h}{2} + \xi_{OOM} \right] F^{\omega_x}(L_*, R_*) + \\
 &\quad \left. + h \sum_S \sum \left[(R - L) \frac{h}{2} \right] F^{\omega_x}(L, R) \right\}.
 \end{aligned} \right\} \quad (20.68)$$

Page 490.

Here sign \sum_{L_*} indicates summing on cells, that belongs to trailing wing edge, and $\sum_S \sum$ - summing on all cells, that lie on wing; the dimensionless quantity h is determined from (20.25).

If for significant dimension for a rolling moment is undertaken the spread/scope of wing l , and for $\omega_x - l/2$, then let us have

$$\left. \begin{aligned} km_{x1}^{\omega_{x1}} &= m_{x1M}^{\omega_{x1}}, \\ k^2 m_{x1}^{\omega_{x1}} &= (m_{x1M}^{\omega_{x1}})_1 + M^2 (m_{x1M}^{\omega_{x1}})_2, \end{aligned} \right\} \quad (20.69)$$

where

$$\left. \begin{aligned} m_{x1M}^{\omega_{x1}} &= -8k\lambda \left(\frac{b}{l}\right)^4 h \sum_{L_*} \left[(R_* - L_*) \frac{h}{2}\right] F^{\omega_x}(L_*, R_*), \\ (m_{x1M}^{\omega_{x1}})_1 &= 16k\lambda \left(\frac{b}{l}\right)^5 h^2 \sum_S \sum \left[(R - L) \frac{h}{2}\right] F^{\omega_x}(L, R), \\ (m_{x1M}^{\omega_{x1}})_2 &= -16k\lambda \left(\frac{b}{l}\right)^5 h \left\{ \frac{k}{M^2} \sum_{L_*} \left[(R_* - L_*) \frac{h}{2}\right] F^{\omega_x}(L_*, R_*) - \right. \\ &\quad - \sum_{L_*} \left[(R_* - L_*) \frac{h}{2}\right] \left[(L_* + R_*) \frac{h}{2} + \xi_{00M}\right] F^{\omega_x}(L_*, R_*) + \\ &\quad \left. + h \sum_S \sum \left[(R - L) \frac{h}{2}\right] F^{\omega_x}(L, R) \right\}. \end{aligned} \right\} \quad (20.70)$$

Let us note that during the calculation of all total characteristics, including for sections, is taken the standard system of the axes of Fig. 1.1 with there the rule of signs indicated, but geometric values

and loads correspond to the axes of Fig. 20.1, i.e., everywhere

$\bar{x}_T = 0$.

^ If the beginning of standard system of coordinates is arranged in the spout of the mean aerodynamic chord whose value b_a is accepted as characteristic linear dimension, the appropriate coefficients of aerodynamic derivatives we will obtain, by recounting the values, determined from (20.66) - (20.70) by formulas (2.59).

Page 491.

For the aerodynamic characteristics of sections $\zeta = \text{const}$ ($R-L = \text{const}$) by transforms, analogous given, we obtain for the coefficients of the aerodynamic derivatives of section lift

$$\left. \begin{aligned} c'_{yM}{}^{q_i} &= 4 \frac{b}{b'} k F^{q_i}(L_*, R_*), \\ c'_{y1M}{}^{q_i} &= -4 \frac{b}{b'} k^2 h \sum_{L, R} F^{q_i}(L, R), \\ c'_{y2M}{}^{q_i} &= 4 \frac{b}{b'} k^2 \left\{ \frac{k}{M^2} F^{q_i}(L_*, R_*) - \right. \\ &\quad \left. - \left[(L_* + R_*) \frac{h}{2} + \xi_{O0M} \right] F^{q_i}(L_*, R_*) + h \sum_{L, R} F^{q_i}(L, R) \right\}, \\ &\quad i = 1, 3, 4; \end{aligned} \right\} (20.71)$$

for the coefficients of the aerodynamic derivatives of the pitching moment of the section

$$\left. \begin{aligned}
 m'_{zM}{}^{q_i} &= \tau 4 \left(\frac{b}{b'} \right)^2 k^2 \left\{ \left[(L_* + R_*) \frac{h}{2} + \xi_{O0M} \right] \times \right. \\
 &\quad \left. \times F^{q_i}(L_*, R_*) - h \sum_{L, R} F^{q_i}(L, R) \right\}, \\
 m'_{z1M}{}^{q_i} &= 4 \left(\frac{b}{b'} \right)^2 k^3 h \sum_{L, R} \left[(L + R) \frac{h}{2} + \xi_{O0M} \right] F^{q_i}(L, R), \\
 m'_{z2M}{}^{q_i} &= -4 \left(\frac{b}{b'} \right)^2 k^3 \left\{ \frac{k}{M^2} \left[(L_* + R_*) \frac{h}{2} + \xi_{O0M} \right] F^{q_i}(L_*, R_*) - \right. \\
 &\quad \left. - \frac{kh}{M^2} \sum_{L, R} F^{q_i}(L, R) - \left[(L_* + R_*) \frac{h}{2} + \xi_{O0M} \right]^2 F^{q_i}(L_*, R_*) + \right. \\
 &\quad \left. + 2h \sum_{L, R} \left[(L + R) \frac{h}{2} + \xi_{O0M} \right] F^{q_i}(L, R) \right\}, \\
 &\quad i = 1, 3, 4;
 \end{aligned} \right\} \quad (20.72)$$

for the coefficients of the aerodynamic derivatives of the rolling moment of the section

$$\left. \begin{aligned}
 m_{xM}^{\omega x} &= -4 \left(\frac{b}{b'} \right)^2 k^2 \left[(R_* - L_*) \frac{h}{2} \right] F^{\omega x}(L_*, R_*), \\
 (m_{xM}^{\omega x})_1 &= 4 \left(\frac{b}{b'} \right)^2 k^3 h \sum_{L, R} \left[(R - L) \frac{h}{2} \right] F^{\omega x}(L, R), \\
 (m_{xM}^{\omega x})_2 &= -4 \left(\frac{b}{b'} \right)^2 k^3 \left\{ \frac{k}{M^2} \left[(R_* - L_*) \frac{h}{2} \right] F^{\omega x}(L_*, R_*) - \right. \\
 &\quad \left. - \left[(R_* - L_*) \frac{h}{2} \right] \left[(L_* + R_*) \frac{h}{2} + \xi_{OCM} \right] F^{\omega x}(L_*, R_*) + \right. \\
 &\quad \left. + h \sum_{L, R} \left[(R - L) \frac{h}{2} \right] F^{\omega x}(L, R) \right\}.
 \end{aligned} \right\} \quad (20.73)$$

Page 492.

In this case the sign $\sum_{L, R}$ indicates summation over cells, that lies at this section from leading edge to the rear, i.e., on the fact, for which is satisfied the condition

$$L_0 \leq L \leq L_*, \quad R_0 \leq R \leq R_*, \quad R - L = R_0 - L_0 = R_* - L_*.$$

The characteristics of sections are determined from the obtained values with the aid of (20.63).

Page 493.

Chapter XXI.

NUMERICAL METHOD OF THE CALCULATION OF AERODYNAMIC WING CHARACTERISTICS WITH ARBITRARY TIME DEPENDENCES.

§1. Basic condition/positions of the numerical calculation method.

For determining aerodynamic wing characteristics with the arbitrary dependences of the kinematic parameters of motion from time let us develop the numerical method, to a certain degree analogous described in the preceding/previous chapter for harmonic dependences.

We consider that fine/thin the wing-plate of arbitrary planform moves with the constant supersonic forward velocity U_0 and zero angle of attack. From the moment of time $t = 0$ kinematic parameters of motion $q_i(t)$ (2.19) begin to change according to arbitrary from time law, and upon the gradual entrance into the arbitrary gust $q_s(t)$

it changes only into parts of the wing, which entered the gust. It is obvious that for the solution of problem it is necessary in each torque/moment t to find the potential of the absolute disturbed velocities $\Phi(x, y, z, t)$. This potential must satisfy wave equation (3.30), boundary conditions (3.56) on wing, conditions (3.61) on vortex sheet and conditions (3.62) in wing plane, but outside its and vortex sheet. Furthermore, on subsonic trailing edges must be fulfilled Chaplygina - Joukowski's hypothesis. The latter will be provided, if, as shown in §7 of chapter III, there will be satisfied condition (3.72), i.e., velocity potential will be continuous during the passage through subsonic trailing edges.

Let us introduce dimensionless velocity potentials as functions of the characteristic coordinates:

$$\left. \begin{aligned} \Phi_i(\beta, \kappa, \tau) &= U_0 b \varphi_i(\beta, \kappa, \tau), \\ \tau &= \frac{iU_0}{b}, \end{aligned} \right\} \quad (21.1).$$

whereupon number $i = 1, 2, 3, 4, 5$ are selected by the same as of the kinematic parameter q_i [see (2.19)].

Page 494.

For determining the unknown values of potential we will use integral relationship/ratio (4.11), which in characteristic coordinates and designations (21.1) takes the form

$$\left. \begin{aligned} \varphi_l(\beta_1, \kappa_1, \tau) = & -\frac{1}{4\pi} \int_{S_1} \int \left[\frac{\partial \varphi_l}{\partial \eta}(\beta, \kappa, \tau_1) \right]_{\eta=0} \frac{d\beta d\kappa}{\rho_M} - \\ & -\frac{1}{4\pi} \int_{S_2} \int \left[\frac{\partial \varphi_l}{\partial \eta}(\beta, \kappa, \tau_2) \right]_{\eta=0} \frac{d\beta d\kappa}{\rho_M}, \end{aligned} \right\} (21.2)$$

$$\rho_M = V(\beta_1 - \beta)(\kappa_1 - \kappa).$$

The values of times τ_1 and τ_2 we will obtain from (4.12), (4.15):

$$\left. \begin{aligned} \tau_1 = \tau - \frac{M^2}{k} \left[\frac{\beta_1 - \beta + \kappa_1 - \kappa}{2} - \frac{\rho_M}{M} \right] - ck \left(\frac{\beta + \kappa}{2} + \xi_{OUM} \right), \\ \tau_2 = \tau - \frac{M^2}{k} \left[\frac{\beta_1 - \beta + \kappa_1 - \kappa}{2} + \frac{\rho_M}{M} \right] - ck \left(\frac{\beta + \kappa}{2} + \xi_{OUM} \right). \end{aligned} \right\} (21.3)$$

Factor $c = 0$ during an instantaneous change in the kinematic parameters, $c = 1$ at the gradual entrance into gust.

Drawing a line, parallel to characteristic axes, we will generalize the wing and the area of effect on identical cells with the side, equal by h whose value is determined by formula (20.25). Range of integration will consist of the integer of cells. Cell we consider belonging to wing, if its geometric center is located within wing contour or on it. Real wing, thus, is replaced by wing with

saw-tooth edges (Fig. 21.1). It is obvious, that the greater will be undertaken the number N , that less such wing will to differ from the real. We consider that small changes of the wing planform lead to small changes in its aerodynamic characteristics and that they for a real wing and a wing with saw-tooth edges will be close, but with an increase in number N a difference in the analogous/similar characteristics will vanish.

By following the taken procedure, the continuous process of a change in the kinematic parameters and aerodynamic characteristics in time let us replace discrete (see Fig. 11.2). The relative time, which takes place between the consecutive torque/moments of a change in the parameters (space of time), let us designate $\Delta\tau$. As calculated let us accept the torque/moments, which directly precede a change in the corresponding characteristics. Let us consider that the kinematic parameters are changed abruptly at the calculated torque/moments, and in the spaces between them they remain constant/invariable. The time, which corresponds to the calculated torque/moment, is equal

$$\tau_r = r \Delta\tau, \quad (21.4)$$

where r is positive integer number; $r = 0$ corresponds $\tau = 0$. We consider also that outside wing the taper at the fixed/recorded moment of time is constant within the limits of cell.

Page 495.

By numerical method it is possible to solve problems at any laws of a change in the kinematic parameters in time. However, without disrupting generality, in this chapter is presented the solution only of basic problems, i.e., such, when the kinematic parameters change in time according to single stepped law or wing gradually enters in step gust. Aerodynamic characteristics for arbitrary dependences are obtained by the imposition of obtained solutions with the aid of Duhamel integral (see Chapter VI). Thus, we consider that the kinematic parameters change according to the law

$$\frac{q_i(\tau)}{q_i} = \begin{cases} 0 & \text{when } \tau < 0, \\ 1 & \text{when } 0 \leq \tau < \infty. \end{cases} \quad (21.5)$$

Wing is assigned by table $L = \beta/h$, $R = x/h$, arrange/located on wing contour, whereupon let L_0 , R_0 (see Fig. 21.1) indicates the affiliation/accessory of cells with duct $C'D'DC$, i.e., leading wing edge, and L_1 , R_1 - to duct $C'Q'QC$, i.e., to trailing edge, L_2 , R_2 - to duct $LDC'Q'$, L_3 , R_3 - to duct $DQ'Q'$.

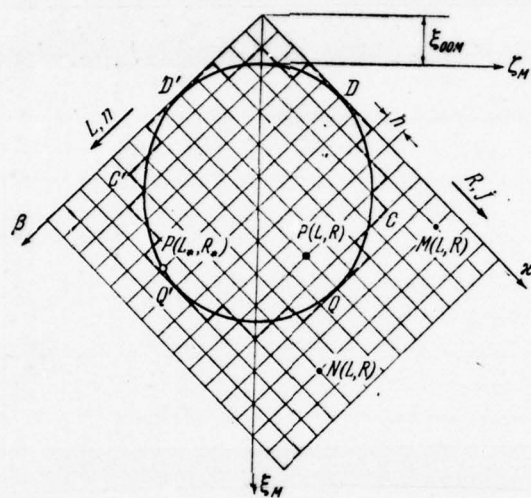


Fig. 21.1. To the numerical calculation method with arbitrary time dependences.

The calculation of expressions (21.2) is conducted by means of the addition of integrals in terms of the cells, which entered the range of integration:

$$\begin{aligned}
 \varphi_i(Lh, Rh, \tau) &= -\frac{1}{4\pi} \sum_{n=1}^L \sum_{j=1}^K J_{iLR}^{n/j}(\tau_1) - \frac{1}{4\pi} \sum_{n=1}^L \sum_{j=1}^K J_{iLR}^{n/j}(\tau_2), \\
 J_{iLR}^{n/j}(\tau) &= \int_{nh}^{(n+1)h} \int_{jh}^{(j+1)h} \left[\frac{\partial \varphi_i}{\partial \eta}(\beta, \kappa, \tau) \right]_{\eta=0} \frac{d\beta d\kappa}{\rho_M}, \\
 \tau_1 &= \tau - \frac{M^2 h}{k} \left[\frac{L-n+R-j}{2} - \frac{\sqrt{(L-n)(R-j)}}{M} \right] - \\
 &\quad - ck \left(\frac{n+j}{2} h + \xi_{00M} \right), \\
 \tau_2 &= \tau - \frac{M^2 h}{k} \left[\frac{L-n+R-j}{2} + \frac{\sqrt{(L-n)(R-j)}}{M} \right] - \\
 &\quad - ck \left(\frac{n+j}{2} h + \xi_{00M} \right), \\
 \rho_M &= h \sqrt{(L-n)(R-j)}.
 \end{aligned} \tag{21.6}$$

§2. Determination of the potentials of the disturbed velocities in the absence of end effect and effect of vortex sheet.

For any point of the wing plane of the value of tapers they are determined by boundary conditions (3.56). Therefore for the points, the area of integration of which does not exceed the limits of wing, value of integrals J_{iLR}^n they are calculated accurately in each cell and (2.16) directly it gives solution for a velocity potential. This is related, for example, to wings with supersonic leading and trailing edges. Figure 21.2 shows to range of integration during the determination of velocity potential for an arbitrary point $P(\beta_1, \kappa_1)$

delta wing with supersonic edges. In this case the tapers outside wing are equal to zero and range of integration S_1 and S_2 are common only for wing surface.

Let us substitute boundary condition (3.56) in (2.16); we consider that the kinematic parameters are changed according to the law (2.15). By taking into account the only range of integration, limited by wing contour, for the basic problems we will obtain:

For the α -problem

$$\left[\frac{\varphi(\tau)}{\alpha^*} \right] = \frac{1}{4\pi} \sum_{n=1}^L \sum_{j=R_1}^{R'_2} J_{iLR}^n(\tau_1) + \frac{1}{4\pi} \sum_{n=1}^L \sum_{j=R_1}^{R'_2} J_{iLR}^n(\tau_2). \quad (21.7)$$

For the Δ -problem, in which $\mathfrak{f}_{\Delta} = 1$,

$$\left[\frac{\varphi(\tau)}{\omega_{y\Delta}} \right] = \frac{1}{4\pi} \sum_{n=1}^L \sum_{j=R_1}^{R'_2} J_{5LR}^{n/j}(\tau_1) + \frac{1}{4\pi} \sum_{n=1}^L \sum_{j=R_1}^{R'_2} J_{5LR}^{n/j}(\tau_2),$$

$$J_{5LR}^{n/j}(\tau) = J_{1LR}^{n/j}(\tau) \quad (21.8)$$

In this case in integrals $J_{5LR}^{n/j}$ in the cells of wing, which did not enter the gust, the derivative $[\partial\varphi/\partial\eta]_{\eta=0}$ will according to (2.16) automatically turn zero.

For ω_x the problems

$$\left[\frac{\varphi(\tau)}{\omega_x} \right] = \frac{1}{8\pi} \sum_{n=1}^L \sum_{j=R_1}^{R'_2} [J_{3LR}^{n/j}(\tau_1) - J_{2LR}^{n/j}(\tau_1)] +$$

$$+ \frac{1}{8\pi} \sum_{n=1}^L \sum_{j=R_1}^{R'_2} [J_{3LR}^{n/j}(\tau_2) - J_{2LR}^{n/j}(\tau_2)]. \quad (21.9)$$

For ω_z the problems

$$\left[\frac{\varphi(\tau)}{\omega_z} \right] = \frac{k}{8\pi} \left\{ \sum_{n=1}^L \sum_{j=R_1}^{R'_2} [J_{2LR}^{n/j}(\tau_1) + J_{3LR}^{n/j}(\tau_1) + 2\mathfrak{E}_{00M} J_{1LR}^{n/j}(\tau_1)] + \right.$$

$$\left. + \sum_{n=1}^L \sum_{j=R_1}^{R'_2} [J_{2LR}^{n/j}(\tau_2) + J_{3LR}^{n/j}(\tau_2) + 2\mathfrak{E}_{00M} J_{1LR}^{n/j}(\tau_2)] \right\}. \quad (21.10)$$

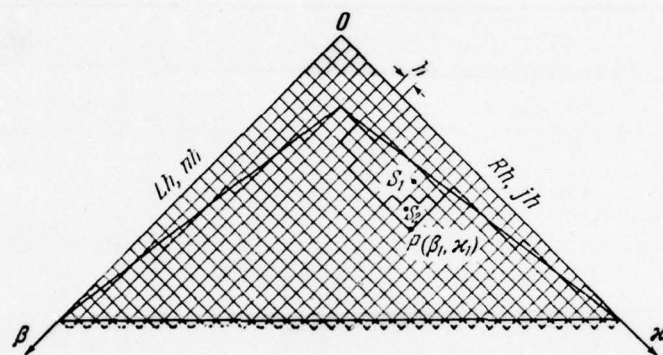


Fig. 21.2. Ranges of integration for a wing without end effect.

[Page 498] Here $R'_2 = R$, if $R < R_2$, and $R'_2 = R_2$, if $R \geq R_2$; $\beta_1 = Lh$, $x_1 = Rh$, and also

$$\left. \begin{aligned} J_{1LR}^n(\tau) &= \int_{nh}^{(n+1)h} \int_{jh}^{(j+1)h} \frac{1(\tau) d\beta dx}{V(\beta_1 - \beta)(x_1 - x)}, \\ J_{2LR}^n(\tau) &= \int_{nh}^{(n+1)h} \int_{jh}^{(j+1)h} \frac{1(\tau) \beta d\beta dx}{V(\beta_1 - \beta)(x_1 - x)}, \\ J_{3LR}^n(\tau) &= \int_{nh}^{(n+1)h} \int_{jh}^{(j+1)h} \frac{1(\tau) x d\beta dx}{V(\beta_1 - \beta)(x_1 - x)}. \end{aligned} \right\} \quad (21.11)$$

Here subsequent dependences $1(\tau_1)$, $1(\tau_2)$ they mean that the corresponding functions are calculated for cell n_j only in such a case, when $\tau_1 \geq 0$ ($\tau_2 \geq 0$). Otherwise we take, that these expressions are equal to zero, since disturbance/perturbation up to torque/moment τ will not have time to reach from point n_j into point LR.

Let us compute integrals (21.11) and simultaneously examine the possibility of the composition of the tables of the values of these integrals for each cell. Let us take in the fixed/recorded torque/moment two arbitrary points M_1 and M_3 (Fig. 21.3) and compute integrals (21.11) in terms of the equidistant of these points cells a and b :

$$J_{1LR}^{na/a}(\tau) = \int_{\beta_2}^{\beta_2+h} \int_{\kappa_2}^{\kappa_2+h} \frac{1(\tau) d\beta d\kappa}{V(\beta_1 - \beta)(\kappa_1 - \kappa)},$$

$$J_{1LR}^{nb/b}(\tau) = \int_{\beta_1}^{\beta_1+h} \int_{\kappa_1}^{\kappa_1+h} \frac{1(\tau) d\beta d\kappa}{V(\beta_3 - \beta)(\kappa_3 - \kappa)},$$

$$J_{2LR}^{na/a}(\tau) = \int_{\beta_2}^{\beta_2+h} \int_{\kappa_2}^{\kappa_2+h} \frac{1(\tau) \beta d\beta d\kappa}{V(\beta_1 - \beta)(\kappa_1 - \kappa)},$$

$$J_{2LR}^{nb/b}(\tau) = \int_{\beta_1}^{\beta_1+h} \int_{\kappa_1}^{\kappa_1+h} \frac{1(\tau) \beta d\beta d\kappa}{V(\beta_3 - \beta)(\kappa_3 - \kappa)},$$

$$J_{3LR}^{na/a}(\tau) = \int_{\beta_2}^{\beta_2+h} \int_{\kappa_2}^{\kappa_2+h} \frac{1(\tau) \kappa d\beta d\kappa}{V(\beta_1 - \beta)(\kappa_1 - \kappa)},$$

$$J_{3LR}^{nb/b}(\tau) = \int_{\beta_1}^{\beta_1+h} \int_{\kappa_1}^{\kappa_1+h} \frac{1(\tau) d\beta d\kappa}{V(\beta_3 - \beta)(\kappa_3 - \kappa)}.$$

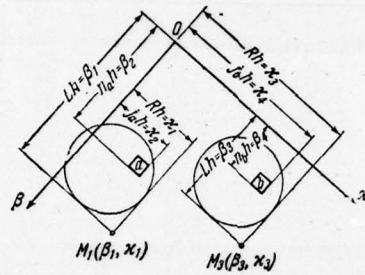


Fig. 21.3. To the calculation of integrals.

Page 499.

Let us assume

$$\sqrt{\beta_1 - \beta} = v_1, \quad \sqrt{\beta_2 - \beta} = v_2, \quad \sqrt{\alpha_1 - \alpha} = \mu_1, \quad \sqrt{\alpha_2 - \alpha} = \mu_2.$$

Then

$$J_{1LR}^{na^l a}(\tau) = 4 \int_{\sqrt{\beta_1 - \beta_2}}^{\sqrt{\beta_1 - \beta_2 - h}} \int_{\sqrt{\alpha_1 - \alpha_2}}^{\sqrt{\alpha_1 - \alpha_2 - h}} l(\tau) dv d\mu,$$

$$J_{1LR}^{nb^l b}(\tau) = 4 \int_{\sqrt{\beta_3 - \beta_4}}^{\sqrt{\beta_3 - \beta_4 - h}} \int_{\sqrt{\alpha_3 - \alpha_4}}^{\sqrt{\alpha_3 - \alpha_4 - h}} l(\tau) dv d\mu,$$

$$J_{2LR}^{na^l a}(\tau) = 4 \int_{\sqrt{\beta_1 - \beta_2}}^{\sqrt{\beta_1 - \beta_2 - h}} \int_{\sqrt{\alpha_1 - \alpha_2}}^{\sqrt{\alpha_1 - \alpha_2 - h}} l(\tau)(\beta_1 - v_1^2) dv d\mu,$$

$$J_{2LR}^{nb^l b}(\tau) = 4 \int_{\sqrt{\beta_3 - \beta_4}}^{\sqrt{\beta_3 - \beta_4 - h}} \int_{\sqrt{\alpha_3 - \alpha_4}}^{\sqrt{\alpha_3 - \alpha_4 - h}} l(\tau)(\beta_3 - v_3^2) dv d\mu,$$

$$J_{3LR}^{na^l a}(\tau) = 4 \int_{\sqrt{\beta_1 - \beta_2}}^{\sqrt{\beta_1 - \beta_2 - h}} \int_{\sqrt{\alpha_1 - \alpha_2}}^{\sqrt{\alpha_1 - \alpha_2 - h}} l(\tau)(\alpha_1 - \mu_1^2) dv d\mu,$$

$$J_{3LR}^{nb^l b}(\tau) = 4 \int_{\sqrt{\beta_3 - \beta_4}}^{\sqrt{\beta_3 - \beta_4 - h}} \int_{\sqrt{\alpha_3 - \alpha_4}}^{\sqrt{\alpha_3 - \alpha_4 - h}} l(\tau)(\alpha_3 - \mu_3^2) dv d\mu.$$

Page 500.

Since $\beta_1 - \beta_2 = \beta_3 = \beta_4$ and $\kappa_1 - \kappa_2 = \kappa_3 - \kappa_4$, then

$$\begin{aligned}
 J_{1LR}^{a|a}(\tau) &= J_{1LR}^{b|b}(\tau) = \\
 &= 1(\tau) 4h [(\sqrt{L-n+1} - \sqrt{L-n})(\sqrt{R-j+1} - \sqrt{R-j})], \\
 J_{2LR}^{a|a}(\tau) &= 1(\tau) 4L_1' h^2 \times \\
 &\quad \times [(\sqrt{L-n+1} - \sqrt{L-n})(\sqrt{R-j+1} - \sqrt{R-j})] - \\
 &\quad - 1(\tau) \frac{4h^2}{3} [(\sqrt{L-n+1})^3 - \sqrt{(L-n)^3}] \times \\
 &\quad \times (\sqrt{R-j+1} - \sqrt{R-j}), \\
 J_{2LR}^{b|b}(\tau) &= 1(\tau) 4L_2 h^2 [(\sqrt{L-n+1} - \sqrt{L-n}) \times \\
 &\quad \times (\sqrt{R-j+1} - \sqrt{R-j})] - 1(\tau) \frac{4h^2}{3} \times \\
 &\quad \times [(\sqrt{L-n+1})^3 - \sqrt{(L-n)^3}](\sqrt{R-j+1} - \sqrt{R-j}), \\
 J_{3LR}^{a|a}(\tau) &= 1(\tau) 4R_1' h^2 [(\sqrt{L-n+1} - \sqrt{L-n}) \times \\
 &\quad \times (\sqrt{R-j+1} - \sqrt{R-j})] - 1(\tau) \frac{4h^2}{3} \times \\
 &\quad \times [(\sqrt{L-n+1} - \sqrt{L-n})(\sqrt{R-j+1})^3 - \sqrt{(R-j)^3}], \\
 J_{3LR}^{b|b}(\tau) &= 1(\tau) 4R_3 h^2 [(\sqrt{L-n+1} - \sqrt{L-n}) \times \\
 &\quad \times (\sqrt{R-j+1} - \sqrt{R-j})] - 1(\tau) \frac{4h^2}{3} \times \\
 &\quad \times [(\sqrt{L-n+1} - \sqrt{L-n})(\sqrt{R-j+1})^3 - \sqrt{(R-j)^3}].
 \end{aligned} \tag{21.12}$$

Here L'_1 and L_3 is a quantity of cells from the origin of coordinates to the point being investigated along axis β ; R'_1 and R_3 - the same along axis α . Formulas (21.12) do not depend on number M , but the expressions, in brackets, are the functions of the number of cells to the point being investigated and can be tabulated or represented in the form of standard subroutines ETSVM [digital computer]. After supplying (21.12) in (21.7) - (21.10), we will obtain relationship/ratios for the potentials of the basic problems in the form, convenient for the calculations.

For the α -problem

$$\begin{aligned} \left[\frac{\Phi(\tau)}{a^*} \right] &= \frac{h}{2\pi} \sum_{n=1}^L \sum_{j=R_1}^{R'_2} (\sqrt{L-n+1} - \sqrt{L-n}) (\sqrt{R-j+1} - \sqrt{R-j}) \times \\ &\times l(\tau_1) - \frac{h}{2\pi} \sum_{n=1}^L \sum_{j=R_1}^{R'_2} (\sqrt{L-n+1} - \sqrt{L-n}) (\sqrt{R-j+1} - \sqrt{R-j}) l(\tau_2). \end{aligned} \quad (21.13)$$

Page 501.

For the Δ -problem

$$\begin{aligned}
 \left[\frac{\Phi(\tau)}{\omega_{\mu\Delta}} \right] &= \frac{h}{2\pi} \sum_{n=1}^L \sum_{j=R_1}^{R'_2} (\sqrt{L-n+1} - \sqrt{L-n}) (\sqrt{R-j+1} - \sqrt{R-j}) \times \\
 &\times 1(\tau_1) - \frac{h}{2\pi} \sum_{n=1}^L \sum_{j=R_1}^{R'_2} (\sqrt{L-n+1} - \sqrt{L-n}) (\sqrt{R-j+1} - \sqrt{R-j}) 1(\tau_2).
 \end{aligned}
 \tag{21.14}$$

For ω_x the problems

$$\begin{aligned}
 \left[\frac{\Phi(\tau)}{\omega_x} \right] &= \frac{h^2}{4\pi} \sum_{n=1}^L \sum_{j=R_1}^{R'_2} (\sqrt{L-n+1} - \sqrt{L-n}) (\sqrt{R-j+1} - \sqrt{R-j}) \times \\
 &\times \left\{ R-L - \frac{1}{3} [2(R-j-L+n) + \sqrt{R-j} \sqrt{R-j+1} - \right. \\
 &- \sqrt{L-n} \sqrt{L-n+1}] \Big\} 1(\tau_1) + \frac{h^2}{4\pi} \sum_{n=1}^L \sum_{j=R_1}^{R'_2} (\sqrt{L-n+1} - \sqrt{L-n}) \times \\
 &\times (\sqrt{R-j+1} - \sqrt{R-j}) \times \left\{ R-L - \frac{1}{3} [2(R-j-L+n) + \right. \\
 &+ \sqrt{R-j} \sqrt{R-j+1} - \sqrt{L-n} \sqrt{L-n+1}] \Big\} 1(\tau_2).
 \end{aligned}
 \tag{21.15}$$

For ω_z the problems

$$\begin{aligned}
\left[\frac{\Phi(\tau)}{\omega_z} \right] = & \frac{kh^2}{4\pi} \sum_{n=1}^L \sum_{j=R_1}^{R'_2} (\sqrt{L-n+1} - \sqrt{L-n})(\sqrt{R-j+1} - \sqrt{R-j}) \times \\
& \times \left\{ L+R - \frac{1}{3} \left[2(L-n+R-j+1) + \sqrt{L-n} \sqrt{L-n+1} + \right. \right. \\
& \quad \left. \left. + \sqrt{R-j} \sqrt{R-j+1} + \frac{2\xi_{00M}}{h} \right] \right\} I(\tau_1) + \\
& + \frac{kh^2}{4\pi} \sum_{n=1}^L \sum_{j=R_1}^{R'_2} (\sqrt{L-n+1} - \sqrt{L-n})(\sqrt{R-j+1} - \sqrt{R-j}) \times \\
& \times \left\{ L+R - \frac{1}{3} \left[2(L-n+R-j+1) + \sqrt{L-n} \sqrt{L-n+1} + \right. \right. \\
& \quad \left. \left. + \sqrt{R-j} \sqrt{R-j+1} + \frac{2\xi_{00M}}{h} \right] \right\} I(\tau_2). \quad (21.16)
\end{aligned}$$

Page 502.

Let us examine, as are calculated the transient functions with deformations of wing. Since the rough form of strain on coordinates can be represented as superposition of power laws, let us present function $f_0(\xi_0)$, entering under boundary condition (3.56), in the form

$$\begin{aligned}
 f_{\delta}(\xi_0) &= a_0 + a_1 \xi_0 + \dots + a_m \xi_0^m = \sum_0^m a_m \xi_0^m = \\
 &= \sum_0^m \frac{a_m k^m}{2^m} (\beta + \kappa + 2\xi_{00M})^m. \quad (21.17)
 \end{aligned}$$

Then

$$\begin{aligned}
 \frac{\partial f_{\delta}}{\partial \xi_0} &= a_1 + 2a_2 \xi_0 + \dots + m a_m \xi_0^{m-1} = \sum_0^m m a_m \xi_0^{m-1} = \\
 &= \sum_0^m \frac{m a_m k^{m-1}}{2^{m-1}} (\beta + \kappa + 2\xi_{00M})^{m-1}. \quad (21.18)
 \end{aligned}$$

We consider that $\delta(\tau)$ changes according to the law (21.5). After substituting (21.17) in (21.6), we will obtain

$$\left. \begin{aligned}
 \left[\frac{\varphi(\tau)}{\delta} \right] &= -\frac{1}{4\pi} \sum_{n=1}^L \sum_{j=R_1}^{R_2'} \sum_0^m \frac{a_m k^m}{2^m} J_{1\delta LR}^{n/}(\tau_1) - \\
 &\quad - \frac{1}{4\pi} \sum_{n=1}^L \sum_{j=R_1}^{R_2'} \sum_0^m \frac{a_m k^m}{2^m} J_{1\delta LR}^{n/}(\tau_2), \\
 J_{1\delta LR}^{n/}(\tau) &= \int_{nh}^{(n+1)h} \int_{jh}^{(j+1)h} 1(\tau) \frac{(\beta + \kappa + 2\xi_{00M})^m}{V(\beta_1 - \beta)(\kappa_1 - \kappa)} d\beta d\kappa.
 \end{aligned} \right\} \quad (21.19)$$

The last/latter integral at the assigned number M can be found, by expanding integrand on Newton's binomial expression. Let us note that from the solution of this problem it is possible to obtain the solution of the basic problems for a rigid (undeformable) wing. So, set/assuming $m = 0$, $a_0 = 1$, we will obtain $\delta^* = -\alpha_*$ and, therefore, we come to α -problem. With $m = 1$, $a_0 = 0$, $a_1 = 1$, $\delta^* = -\omega_z^*$, i.e. we will obtain solution ω_z of problem. Finally, by replacing series (21.18) by (21.17) and δ^* on δ , let us arrive at δ -problem.

Page 503.

Let us present now function $f_\delta(\zeta_0)$ in the form of the

series

$$\left. \begin{aligned} f_{\delta}(\xi_0) &= d_0^* + d_1 \xi_0 + \dots + d_m \xi_0^m = \sum_0^m d_m \xi_0^m = \sum_0^m \frac{d_m}{2^m} (\alpha - \beta)^m, \\ \frac{\partial f_{\delta}(\xi_0)}{\partial \xi_0} &= 0. \end{aligned} \right\} \quad (21.20)$$

After substituting (21.20) in (21.6), we will obtain

$$\left. \begin{aligned} \left[\frac{\varphi(\tau)}{\delta^*} \right] &= -\frac{1}{4\pi} \sum_{n=1}^L \sum_{j=R_1}^{R_2'} \sum_0^m \frac{d_m}{2^m} J_{2\delta LR}^{nj}(\tau_1) - \\ &\quad - \frac{1}{4\pi} \sum_{n=1}^L \sum_{j=R_1}^{R_2'} \sum_0^m \frac{d_m}{2^m} J_{2\delta LR}^{nj}(\tau_2), \\ J_{2\delta LR}^{nj}(\tau) &= \int_{nh}^{(n+1)h} \int_{jh}^{(j+1)h} l(\tau) \frac{(\alpha - \beta)^m}{V(\beta_1 - \beta)(\alpha_1 - \alpha)} d\beta d\alpha. \end{aligned} \right\} \quad (21.21)$$

It is analogous with the preceding/previous case with $m = 1$, $d_0 = 0$, $d_1 = 1$ we obtain solution ω_s of problem for a rigid wing, and also we complete passage to δ -problem.

§3. Determination of velocity potential taking into account end effect.

In order to calculate velocity potential in the points of wing, for which the range of integration includes the disturbed range outside wing and vortex sheet, it is necessary to find derivatives $[\partial\varphi/\partial\eta]_{\eta=0}$ in this range. For example, if point P (L, R) (see Fig. 21.1) it includes the disturbed range outside wing, then in this case we deal with the so-called end effect. Let us examine at first the simplest case of the manifestation of end effect, when range of integration, for example, for point M (L, R), arranged/located to the right outside vortex sheet and outside wing, includes only wing surface and range outside wing to the right.

Let us write expression for the velocity potential, which corresponds to the parameter q_i in point M (L, R) for a torque/moment τ :

$$\begin{aligned} \varphi_i(Lh, Rh, \tau) = & -\frac{1}{4\pi} \sum_{n=1}^L \sum_{j=R_1}^{R_2} J_{iLR}^{n/}(\tau_1) - \frac{1}{4\pi} \sum_{n=1}^L \sum_{j=R_1}^{R_2} J_{iLR}^{n/}(\tau_2) - \\ & - \frac{1}{4\pi} \sum_{n=1}^L \sum_{j=R_1+1}^R B_{n/}^i(\tau_1) J_{LR}^{n/} - \frac{1}{4\pi} \sum_{n=1}^L \sum_{j=R_1+1}^R B_{n/}^i(\tau_2) J_{LR}^{n/}. \end{aligned} \quad (21.22)$$

Page 504.

Here

$$B_{n,j}^i(\tau) = \left[\frac{\partial \Phi_i}{\partial \eta} (nh, jh, \tau) \right]_{\eta=0},$$

$$J_{LR}^{n,j} = \int_{nh}^{(n+1)h} \int_{jh}^{(j+1)h} \frac{d\beta d\kappa}{V(\beta_1 - \beta)(\kappa_1 - \kappa)}, \quad \text{in which regard } J_{LR}^{LR} = 4h.$$

Since times τ_1 and τ_2 identically determine the value of taper in cell n, j , limits in sums show only the affiliation/accessory of cells with wing or range outside wing.

Using condition (3.62), we assume that the tapers in all in front of the lying/horizontal cells are known. Then taper at

torque/moment τ in cell Lh , Rh is determined from the expression

$$B_{LR}^l(\tau) = -\frac{1}{16h} \left[\sum_{n=1}^L \sum_{j=R_1}^{R_2} J_{iLR}^{nl}(\tau_1) + \sum_{n=1}^L \sum_{j=R_1}^{R_2} J_{iLR}^{nl}(\tau_2) + \right. \\ \left. + \sum_{n=1}^L \sum_{j=R_2+1}^{R'_1} B_{nI}^l(\tau_1) J_{LR}^{nl} + \sum_{n=1}^L \sum_{j=R_2+1}^{R'_1} B_{nI}^l(\tau_2) J_{LR}^{nl} \right]; \quad (21.23)$$

$$R'_1 = R, \text{ if } n < L; \quad R'_1 = R - 1, \text{ if } n = L.$$

If the range of integration hits the disturbed range outside wing to the left, then in brackets (21.23) they will be added two members:

$$\sum_{n=1}^L \sum_{j=1}^{R_1-1} B_{nI}^l(\tau_1) J_{LR}^{nl} + \sum_{n=1}^L \sum_{j=1}^{R_1-1} B_{nI}^l(\tau_2) J_{LR}^{nl}. \quad (21.24)$$

So as ever during the determination of taper, at least in the first cell outside wing to the right, sum (21.24), entering expression (21.23), turns into zero, then during the determination of tapers outside wing to the left the tapers outside the wing to the right can be considered known. For wings symmetric relative to axis ξ , the tapers outside the wing to the left to determine is not necessary, since they are equal to tapers in the appropriate cells outside wing to the right. Page 505.

If are known tapers everywhere in the range of integration, then

velocity potential, for example, in point Lh , Rh will be determined from the relationship/ratio

$$\begin{aligned} \varphi_i(Lh, Rh, \tau) = & -\frac{1}{4\pi} \sum_{n=1}^L \sum_{j=R_1}^{R_2} J_{iLR}^{nI}(\tau_1) - \frac{1}{4\pi} \sum_{n=1}^L \sum_{j=R_1}^{R_2} J_{iLR}^{nI}(\tau_2) - \\ & - \frac{1}{4\pi} \sum_{n=1}^L \sum_{j=R_2+1}^R B_{nI}^I(\tau_1) J_{LR}^{nI} - \frac{1}{4\pi} \sum_{n=1}^L \sum_{j=R_2+1}^R B_{nI}^I(\tau_2) J_{LR}^{nI} - \\ & - \frac{1}{4\pi} \sum_{n=1}^L \sum_{j=1}^{R_1-1} B_{nI}^I(\tau_1) J_{LR}^{nI} - \frac{1}{4\pi} \sum_{n=1}^L \sum_{j=1}^{R_1-1} B_{nI}^I(\tau_2) J_{LR}^{nI}. \quad (21.25) \end{aligned}$$

The determination of potential on wing taking into account end effect is conducted as follows. Are determined at first the values of unknown tapers outside wing to the right in the first nearest to wing cell for different values τ . The obtained dependence $B_{nI}^I(\tau)$ is used in (21.23) for determining tapers as functions of time in the following cell, etc. After the determination of all tapers outside wing at all calculated torque/moments interesting it is determined from (21.25) velocity potential in all points of wing, at which manifests itself the end effect.

§4. Determination of velocity potential in the range of the effect of

vortex sheet.

If range of integration seizes the range of vortex sheet, as for instance, for a point $P(L_*, R_*)$ (see Fig. 21.1), then for determining the value of velocity potential in it it is necessary to preliminarily find unknown tapers on vortex sheet. For the arbitrary point $N(L, R)$ of vortex sheet at torque/moment τ we can write the potential, which corresponds to the kinematic parameter q_i :

$$\left. \begin{aligned} \varphi_i(Lh, Rh, \tau) = -\frac{1}{4\pi} & \left[\Phi_{LRi}^{nI}(\tau) + \sum_{n=1}^L \sum_{j=R_1+1}^R B_{nI}^I(\tau_1) J_{LR}^{nI} + \right. \\ & \left. + \sum_{n=1}^L \sum_{j=R_1+1}^R B_{nI}^I(\tau_2) J_{LR}^{nI} \right], \\ \Phi_{LRi}^{nI}(\tau) = & \sum_{n=1}^L \sum_{j=R_1}^{R_1} J_{iLR}^{nI}(\tau_1) + \sum_{n=1}^L \sum_{j=R_1}^{R_1} J_{iLR}^{nI}(\tau_2) + \\ & + \sum_{n=1}^L \sum_{j=1}^{R_1-1} B_{nI}^I(\tau_1) J_{LR}^{nI} + \sum_{n=1}^L \sum_{j=1}^{R_1-1} B_{nI}^I(\tau_2) J_{LR}^{nI}. \end{aligned} \right\} \quad (21.26)$$

Page 506.

Two last/latter sums of expression for $\Phi_{LRi}^{nI}(\tau)$ will turn of zero,

if range outside wing does not fall to the left into range of integration.

Utilizing condition (3.72) for a vortex sheet and solving (21.26) relatively $B_{LR}^i(\tau)$, we will obtain

$$B_{LR}^i(\tau) = -\frac{1}{16h} \left[\Phi_{LR}^i(\tau) + \sum_{n=1}^L \sum_{j=R_1+1}^{R_+} B_{nj}^i(\tau_1) J_{LR}^i + \right. \\ \left. + \sum_{n=1}^L \sum_{j=R_1+1}^{R_+} B_{nj}^i(\tau_2) J_{LR}^i \right] - \frac{\pi}{4h} \varphi_i(\beta^*, \kappa^*, \tau^*), \quad (21.27)$$

where

$$R_+ = \begin{cases} R & \text{при } n > L, \\ R-1 & \text{при } n = L, \end{cases}$$

$$\tau^* = \tau - (\xi - \xi_*), \quad \beta^* = n^*h, \quad \kappa^* = hj^*, \quad j^* - n^* = R - L.$$

[при = with]

Here, as earlier by asterisk are noted the coordinates of the point, which belongs to trailing wing edge.

The determination of velocity potentials in the points of wing, which manifests itself the effect of vortex sheet, is conducted as follows. Are determined at first the values of unknown tapers outside wing and vortex sheet at all the calculated torque/moments from the

method, presented in the preceding/previous paragraph. The obtained dependences $B_{nj}(\tau)$ are used in (21.27) for determining the value of tapers as functions of time in the nearest to trailing edge cell of wing. After constructing dependences $B_{nj}(\tau)$ for this cell, I pass to the following and so forth. After are found for the calculated torque/moment the tapers in an entire range of integration. through formulas (21.25) are located the velocity potentials in all points (cells) of wing.

§5. Calculation of aerodynamic loadings, force coefficients and torque/moments.

After determining at the calculated torque/moments τ , the value of potentials on wing, it is not difficult, using the Cauchy-Lagrange integral (3.19), to find for these torque/moments aerodynamic loadings on wing and from formulas (2.5), (2.7) to calculate the force coefficients and torque/moments of the wing sections and wing as a whole.

Page 507.

By transfer/converting in (3.19) to characteristic coordinates

and the designations of this chapter, by determining the derivatives of potential in terms of coordinate ξ and time τ , for example, according to the method of differences, for a load in cell Lh , Rh to torque/moment τ , let us have

$$\left[\frac{\Delta \bar{p}(Lh, Rh, \tau_r)}{q_i} \right] = 2 \left(\frac{1}{kh} \left\{ \left[\frac{\varphi(L+1, R+1, \tau_r)}{q_i} \right] - \left[\frac{\varphi(L-1, R-1, \tau_r)}{q_i} \right] \right\} + \right. \\ \left. + \frac{1}{\Delta \tau} \left\{ \left[\frac{\varphi(L, R, \tau_{r+1})}{q_i} \right] - \left[\frac{\varphi(L, R, \tau_{r-1})}{q_i} \right] \right\} \right). \quad (21.28)$$

Let us note that for an increase in the accuracy of the definition of load can be used the approximations of velocity potential on coordinate ξ and on the time τ , analogous that as this was shown in §6 of chapter XX.

During the calculation of forces and torque/moments let us integrate preliminarily (2.5), (2.7) with respect to ξ in order to exclude from formulas the derivatives of potential in terms of coordinate. As a result for the force coefficients and torque/moments of section $\zeta = \text{const}$ let us have with the rule of the signs of Fig.

1.1

$$\left. \begin{aligned}
 \left[\frac{c'_y(\tau_r)}{q_i} \right] &= 4 \frac{b}{b'} \left\{ \left[\frac{\varphi(\xi_M^*, \zeta_M^*, \tau_r)}{q_i} \right] + \right. \\
 &\quad \left. + k \int_{\xi_{0M}}^{\xi_M^*} \left(\frac{\partial}{\partial \tau} \left[\frac{\varphi(\xi_M, \zeta_M, \tau_r)}{q_i} \right] \right) d\xi_M \right\}, \\
 \left[\frac{m'_x(\tau_r)}{q_i} \right] &= -4 \left(\frac{b}{b'} \right)^2 \left\{ \zeta_M \left[\frac{\varphi(\xi_M^*, \zeta_M^*, \tau_r)}{q_i} \right] + \right. \\
 &\quad \left. + k \zeta_M \int_{\xi_{0M}}^{\xi_M^*} \left(\frac{\partial}{\partial \tau} \left[\frac{\varphi(\xi_M, \zeta_M, \tau_r)}{q_i} \right] \right) d\xi_M \right\}, \\
 \left[\frac{m'_z(\tau_r)}{q_i} \right] &= -4 \left(\frac{b}{b'} \right)^2 \left\{ k \xi_M^* \left[\frac{\varphi(\xi_M^*, \zeta_M^*, \tau_r)}{q_i} \right] - \right. \\
 &\quad - k \int_{\xi_{0M}}^{\xi_M^*} \left[\frac{\varphi(\xi_M, \zeta_M, \tau_r)}{q_i} \right] d\xi_M + \\
 &\quad \left. + k^2 \int_{\xi_{0M}}^{\xi_M^*} \left(\frac{\partial}{\partial \tau} \left[\frac{\varphi(\xi_M, \zeta_M, \tau_r)}{q_i} \right] \right) \xi_M d\xi_M \right\}.
 \end{aligned} \right\} \quad (21.29)$$

Page 508.

Analogously for the force coefficients and torque/moments of entire wing we will obtain

$$\begin{aligned}
 \left[\frac{c_u(\tau_r)}{q_i} \right] &= 4 \frac{b^2}{S} \left\{ \int_{-l/2b}^{l/2b} \left[\frac{\varphi(\xi_M, \zeta_M, \tau_r)}{q_i} \right] d\zeta_M + \right. \\
 &\quad \left. + k \int_{-l/2b}^{l/2b} \int_{\xi_{0M}}^{\xi_M} \left(\frac{\partial}{\partial \tau} \left[\frac{\varphi(\xi_M, \zeta_M, \tau_r)}{q_i} \right] \right) d\xi_M d\zeta_M \right\}, \\
 \left[\frac{m_x(\tau_r)}{q_i} \right] &= -4 \frac{b^2}{S} \left\{ \int_{-l/2b}^{l/2b} \zeta_M \left[\frac{\varphi(\xi_M, \zeta_M, \tau_r)}{q_i} \right] d\zeta_M + \right. \\
 &\quad \left. + k \int_{-l/2b}^{l/2b} \int_{\xi_{0M}}^{\xi_M} \left(\frac{\partial}{\partial \tau} \left[\frac{\varphi(\xi_M, \zeta_M, \tau_r)}{q_i} \right] \right) \zeta_M d\xi_M d\zeta_M \right\}, \\
 \left[\frac{m_z(\tau_r)}{q_i} \right] &= -4 \frac{b^2}{S} \left\{ k \int_{-l/2b}^{l/2b} \left[\frac{\varphi(\xi_M, \zeta_M, \tau_r)}{q_i} \right] \xi_M d\zeta_M - \right. \\
 &\quad - k \int_{-l/2b}^{l/2b} \int_{\xi_{0M}}^{\xi_M} \left[\frac{\varphi(\xi_M, \zeta_M, \tau_r)}{q_i} \right] d\xi_M d\zeta_M + \\
 &\quad \left. + k^2 \int_{-l/2b}^{l/2b} \int_{\xi_{0M}}^{\xi_M} \left(\frac{\partial}{\partial \tau} \left[\frac{\varphi(\xi_M, \zeta_M, \tau_r)}{q_i} \right] \right) \xi_M d\xi_M d\zeta_M \right\}; \\
 &\quad i = 1, 2, 3, 4, 5.
 \end{aligned} \tag{21.30}$$

Recall that here, as earlier, through ξ_{OM}, ζ_{OM} are designated the coordinates of leading wing edge, but through ξ_M, ζ_M rear.

Page 509.

By transfer/converting in relationship/ratios (21.29), (21.30) to characteristic coordinates (20.17), to designations (20.24) and by replacing integrals by sums, we will obtain the following expressions for the calculation of forces and torque/moments:

for wing sections $\xi = \text{const}$, $R - L = \text{const}$

$$\begin{aligned}
 \left[\frac{c'_y(\tau_r)}{q_i} \right] &= 4 \frac{b}{b'} \left\{ \left[\frac{\varphi(L_*, R_*, \tau_r)}{q_i} \right] + \right. \\
 &\quad \left. + \frac{kh}{\Delta\tau} \left(\sum_{L_*, R_*}^{L_*, R_*} \left[\frac{\varphi(L, R, \tau_r)}{q_i} \right] - \sum_{L_*, R_*}^{L_*, R_*} \left[\frac{\varphi(L, R, \tau_{r-1})}{q_i} \right] \right) \right\}, \\
 \left[\frac{m'_x(\tau_r)}{q_i} \right] &= -4 \left(\frac{b}{b'} \right)^2 \left\{ \frac{(R_* - L_*)h}{2} \left[\frac{\varphi(L_*, R_*, \tau_r)}{q_i} \right] + \right. \\
 &\quad \left. + \frac{kh}{\Delta\tau} \left(\sum_{L_*, R_*}^{L_*, R_*} \frac{(R - L)h}{2} \left[\frac{\varphi(L, R, \tau_r)}{q_i} \right] - \right. \right. \\
 &\quad \left. \left. - \sum_{L_*, R_*}^{L_*, R_*} \frac{(R - L)h}{2} \left[\frac{\varphi(L, R, \tau_{r-1})}{q_i} \right] \right) \right\}, \quad (21.31) \\
 \left[\frac{m'_z(\tau_r)}{q_i} \right] &= -4 \left(\frac{b}{b'} \right)^2 \left\{ k \left[(L_* + R_*) \frac{h}{2} + \xi_{OM} \right] \left[\frac{\varphi(L_*, R_*, \tau_r)}{q_i} \right] - \right. \\
 &\quad \left. - kh \sum_{L_*, R_*}^{L_*, R_*} \left[\frac{\varphi(L, R, \tau_r)}{q_i} \right] + \right. \\
 &\quad \left. + \frac{k^2 h}{\Delta\tau} \left(\sum_{L_*, R_*}^{L_*, R_*} \left[(L + R) \frac{h}{2} + \xi_{OM} \right] \left[\frac{\varphi(L, R, \tau_r)}{q_i} \right] - \right. \right. \\
 &\quad \left. \left. - \sum_{L_*, R_*}^{L_*, R_*} \left[(L + R) \frac{h}{2} + \xi_{OM} \right] \left[\frac{\varphi(L, R, \tau_{r-1})}{q_i} \right] \right) \right\}.
 \end{aligned}$$

and
for entire wing

$$\left. \begin{aligned} \left[\frac{c_y(\tau_r)}{q_i} \right] &= 4 \frac{b^2}{S} \left\{ h \sum_{L_*, R_*} \left[\frac{\varphi(L_*, R_*, \tau_r)}{q_i} \right] + \right. \\ &\quad \left. + \frac{kh^2}{\Delta\tau} \left(\sum_S \sum \left[\frac{\varphi(L, R, \tau_r)}{q_i} \right] - \sum_S \sum \left[\frac{\varphi(L, R, \tau_{r-1})}{q_i} \right] \right) \right\}, \\ \left[\frac{m_x(\tau_r)}{q_i} \right] &= -4 \frac{b^2}{S} \left\{ h \sum_{L_*, R_*} \frac{(R_* - L_*) h}{2} \left[\frac{\varphi(L_*, R_*, \tau_r)}{q_i} \right] + \right. \\ &\quad \left. + \frac{kh^2}{\Delta\tau} \left(\sum_S \sum \frac{(R - L) h}{2} \left[\frac{\varphi(L, R, \tau_r)}{q_i} \right] - \right. \right. \\ &\quad \left. \left. - \sum_S \sum \frac{(R - L) h}{2} \left[\frac{\varphi(L, R, \tau_{r-1})}{q_i} \right] \right) \right\}, \end{aligned} \right\} \quad (21.32)$$

$$\left. \begin{aligned} \left[\frac{m_z(\tau_r)}{q_i} \right] &= -4 \frac{b^2}{S} \left\{ kh \sum_{L_*, R_*} \left[\frac{(L_* + R_*) h}{2} + \xi_{OUM} \right] \left[\frac{\varphi(L_*, R_*, \tau_r)}{q_i} \right] - \right. \\ &\quad \left. - kh^2 \sum_S \sum \left[\frac{\varphi(L, R, \tau_r)}{q_i} \right] + \right. \\ &\quad \left. + \frac{k^2 h^2}{\Delta\tau} \left(\sum_S \sum \left[\frac{(L + R) h}{2} + \xi_{OUM} \right] \left[\frac{\varphi(L, R, \tau_r)}{q_i} \right] - \right. \right. \\ &\quad \left. \left. - \sum_S \sum \left[\frac{(L + R) h}{2} + \xi_{OUM} \right] \left[\frac{\varphi(L, R, \tau_{r-1})}{q_i} \right] \right) \right\}. \end{aligned} \right\} \quad (21.32)$$

In the obtained expressions the sign $\sum_{L_0, R_0}^{L_*, R_*}$ indicates summation over cells from the front/leading to trailing edge in section λ . $R_0 - L_0 = R - L = R_* - L_*$.
 sign \sum_{L_*, R_*} - addition on cells, that belongs to trailing wing edge, and \sum_s - summation over all cells, that lie on wing. All the total aerodynamic characteristics are given in standard axes (Fig. 1.1) with beginning in the leading edge/nose of wing ($\bar{x}_T = 0$). For significant dimension is undertaken the root chord b . The values of coordinates and load are taken in the axes of Fig. 20.1.

Recall, that in perfect analogy outlined above can be solved the problem of the effect of flow behind the shock wave, which encounters to wing from any direction. In this case will have to consider the speed of the displacement/movement of its front.

Page 511.

Chapter XXII.

SOME EXACT SOLUTIONS FOR WINGS WITH SUPERSONIC EDGES WITH HARMONIC TIME DEPENDENCES.

§1. Expression for a velocity potential in supersonic edges and the absence of end effect.

When all wing edges supersonic, but its planform sufficiently simple, for example all edges are straight, there is no need to utilize for determining aerodynamic characteristics the numerical method, described in chapter of XX. In this case can be obtained the exact solutions (see [1.15], [1.19], [1.26], [1.63]).

Before how to give the results of the calculations for some wings, let us give the basic formulas, with the aid of which they were obtained. Recall that at harmonic oscillations and the strains of wing the dependence of the kinematic parameters of motion from

time takes form (20.1). The potential of the disturbed velocities is expressed (20.8) through the coefficients of the aerodynamic derivatives of potential, for determining which we have integral equations (20.11). As is known, the derivative of potential on wing surface is connected with the kinematic parameters of motion by boundary conditions (3.56). For the harmonically oscillating and deforming wing these conditions will be written in the form

$$\left. \frac{\partial \Phi}{\partial \eta} \right|_{\eta=0} = \frac{\partial f_0}{\partial \xi} + e^{i p t} \left[-\alpha^* - \omega_x^* \zeta - \omega_z^* \xi + \delta^* \left(\frac{\partial f_0}{\partial \xi} + i p f_0 \right) \right]. \quad (22.1)$$

Here α^* , ω_x^* , ω_z^* , δ^* are amplitude values of the kinematic parameters, $f_0(\xi, \zeta)$ - the equation of the strains on surface of wing, time-independent, $f_\delta(\xi, \zeta)$ are an equation of the additional strains, which depend on time, ξ, η, ζ - the dimensionless coordinates, determined by relationship/ratios (20.10).

Page 512.

For the derivatives of potential in terms of coordinate (tapers) of (20.8), (22.1) let us have (indices make the same sense, as in chapter of XX).

$$\left. \begin{aligned}
 \frac{\partial \Phi_0(\xi, \zeta)}{\partial \xi} &= B_0^{(1)}(\xi, \zeta), & \frac{\partial \Phi^{qi}(\xi, \zeta)}{\partial \xi} &= B_i^{(1)}(\xi, \zeta), \\
 \frac{\partial \Phi^{qi}(\xi, \zeta)}{\partial \xi} &= E_i^{(1)}(\xi, \zeta); \\
 B_0^{(1)} &= \frac{\partial f_0(\xi, \zeta)}{\partial \xi}, & B_1^{(1)} &= -1, & B_2^{(1)} &= -\zeta, & B_3^{(1)} &= -\xi, \\
 B_1^{(1)} &= \frac{\partial f_0(\xi, \zeta)}{\partial \xi}, & E_1^{(1)} &= E_2^{(1)} = E_3^{(1)} = 0, & E_1^{(1)} &= f_0(\xi, \zeta).
 \end{aligned} \right\} \quad (22.2)$$

Let us introduce functions Φ^{qi}, Φ^{qi} , connected with the aerodynamic derivatives of potential by the relationship/ratios

$$\pi \Phi_0 = \Phi_0, \quad \pi \Phi^{qi} = \Phi^{qi}, \quad \pi \frac{M^2 - 1}{M^2} \Phi^{qi} = \Phi^{qi}. \quad (22.3)$$

By substituting (22.2) into the right side of equation (20.11), and (22.3) - into left, we will obtain integral equations for the introduced functions:

$$\left. \begin{aligned}
 \Phi_0(\xi_1, \zeta_1) &= - \int \int_{\sigma(\xi_1, \zeta_1)} B_0^{(1)}(\xi, \zeta) \cos[\omega(\xi_1 - \xi)] \cos\left(\frac{\omega \rho}{M}\right) \frac{d\xi d\zeta}{\rho}, \\
 \Phi^{qi}(\xi_1, \zeta_1) &= - \int \int_{\sigma(\xi_1, \zeta_1)} B_i^{(1)}(\xi, \zeta) \cos[\omega(\xi_1 - \xi)] \cos\left(\frac{\omega \rho}{M}\right) \frac{d\xi d\zeta}{\rho}, \\
 \Phi^{qi}(\xi_1, \zeta_1) &= \frac{1}{\omega} \int \int_{\sigma(\xi_1, \zeta_1)} B_i^{(1)}(\xi, \zeta) \sin[\omega(\xi_1 - \xi)] \cos\left(\frac{\omega \rho}{M}\right) \frac{d\xi d\zeta}{\rho}, \\
 & \quad i = 1, 2, 3; \\
 \Phi^{q*}(\xi_1, \zeta_1) &= - \int \int_{\sigma(\xi_1, \zeta_1)} \left[B_4^{(1)} - \frac{k^2}{M^2} \omega E_4^{(1)} \operatorname{tg} \omega(\xi_1 - \xi) \right] \times \\
 & \quad \times \cos[\omega(\xi_1 - \xi)] \cos\left(\frac{\omega \rho}{M}\right) \frac{d\xi d\zeta}{\rho}, \\
 \Phi^{q*}(\xi_1, \zeta_1) &= \frac{1}{\omega} \int \int_{\sigma(\xi_1, \zeta_1)} \left[B_4^{(1)} - \frac{k^2}{M^2} \omega E_4^{(1)} \operatorname{ctg} \omega(\xi_1 - \xi) \right] \times \\
 & \quad \times \sin[\omega(\xi_1 - \xi)] \cos\left(\frac{\omega \rho}{M}\right) \frac{d\xi d\zeta}{\rho}, \\
 \omega &= \frac{M^2}{k^2} p^*, \quad \rho = \sqrt{(\xi_1 - \xi)^2 - k^2(\zeta_1 - \zeta)^2}, \quad k = \sqrt{M^2 - 1}.
 \end{aligned} \right\} \quad (22.4)$$

These formulas make it possible to calculate velocity potential during the harmonic oscillations of wing for any value of the dimensionless parameter ω , if everywhere in range of integration are known the values of functions B_n , E_n .

Page 513.

Specifically, they give the effective solution of problem for the wing, leading and trailing edges of which supersonic and which has it is absent end effect (Fig. 22.1). Range of integration in formulas (22.4) is part of the wing surface within the reverse/inverse characteristic cone, carried out from the point in question. In Fig. 22.1 this areas is shaded.

The calculation of the potentials of the disturbed velocities and coefficients of aerodynamic derivatives at arbitrary values ω presents sufficiently great difficulties and requires the application/use of digital computers. In the case of small Strouhal numbers (more precise saying, with $\omega \rightarrow 0$) are obtained the exact expressions through elementary functions both for the velocity potentials and for the coefficients of aerodynamic derivatives. In the case $\omega \rightarrow 0$ formula (22.4) they take the form

$$\begin{aligned}
 \Phi_0(\xi_1, \zeta_1) &= - \int \int_{\sigma(\xi_1, \zeta_1)} B_0^{(1)}(\xi, \zeta) \frac{d\xi d\zeta}{\rho}, \\
 \Phi^{q_i}(\xi_1, \zeta_1) &= - \int \int_{\sigma(\xi_1, \zeta_1)} B_i^{(1)}(\xi, \zeta) \frac{d\xi d\zeta}{\rho}, \\
 \Phi^{q_i}(\xi_1, \zeta_1) &= \int \int_{\sigma(\xi_1, \zeta_1)} B_i^{(1)}(\xi, \zeta) [\xi_1 - \xi] \frac{d\xi d\zeta}{\rho}, \\
 &\quad i = 1, 2, 3; \\
 \Phi^{q_4}(\xi_1, \zeta_1) &= - \int \int_{\sigma(\xi_1, \zeta_1)} B_4^{(1)}(\xi, \zeta) \frac{d\xi d\zeta}{\rho}, \\
 \Phi^{q_4}(\xi_1, \zeta_1) &= \int \int_{\sigma(\xi_1, \zeta_1)} \left[B_4^{(1)}(\xi, \zeta) - \frac{k^2}{M^2} E^{(1)} \frac{1}{\xi_1 - \xi} \right] \frac{d\xi d\zeta}{\rho}.
 \end{aligned} \tag{22.5}$$

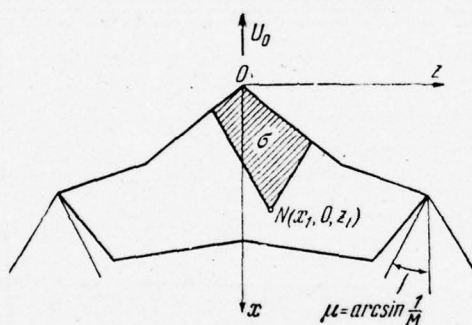


Fig. 22.1. Wing with supersonic edges (there is no end effect).

Page 514.

§2. Solutions for a rigid infinite-span wing.

Let us use formulas (22.2), (22.4) for an infinite-span wing. Let us introduce transformed coordinates ξ_M, ζ_M on (20.12). Then instead of (22.4) we obtain

$$\begin{aligned}
 \Phi^a(\xi_{1M}, \zeta_{1M}) &= \iint_{\sigma(\xi_{1M}, \zeta_{1M})} \cos[k\omega(\xi_{1M} - \xi_M)] \times \\
 &\quad \times \cos\left(\frac{k\omega\rho_M}{M}\right) \frac{d\xi_M d\zeta_M}{\rho_M}, \\
 \Phi^{\dot{a}}(\xi_{1M}, \zeta_{1M}) &= -\frac{1}{\omega} \iint_{\sigma(\xi_{1M}, \zeta_{1M})} \sin[k\omega(\xi_{1M} - \xi_M)] \times \\
 &\quad \times \cos\left(\frac{k\omega\rho_M}{M}\right) \frac{d\xi_M d\zeta_M}{\rho_M}, \\
 \Phi^{\omega_x}(\xi_{1M}, \zeta_{1M}) &= - \int_{\sigma(\xi_{1M}, \zeta_{1M})} \xi_M \cos[k\omega(\xi_{1M} - \xi_M)] \times \\
 &\quad \times \cos\left(\frac{k\omega\rho_M}{M}\right) \frac{d\xi_M d\zeta_M}{\rho_M}, \\
 \Phi^{\omega_x}(\xi_{1M}, \zeta_{1M}) &= \frac{1}{\omega} \iint_{\sigma(\xi_{1M}, \zeta_{1M})} \xi_M \sin[k\omega(\xi_{1M} - \xi_M)] \times \\
 &\quad \times \cos\left(\frac{k\omega\rho_M}{M}\right) \frac{d\xi_M d\zeta_M}{\rho_M}, \\
 \Phi^{\omega_z}(\xi_{1M}, \zeta_{1M}) &= k \iint_{\sigma(\xi_{1M}, \zeta_{1M})} \xi_M \cos[k\omega(\xi_{1M} - \xi_M)] \times \\
 &\quad \times \cos\left(\frac{k\omega\rho_M}{M}\right) \frac{d\xi_M d\zeta_M}{\rho_M}, \\
 \Phi^{\dot{\omega}_z}(\xi_{1M}, \zeta_{1M}) &= -\frac{k}{\omega} \iint_{\sigma(\xi_{1M}, \zeta_{1M})} \xi_M \sin[k\omega(\xi_{1M} - \xi_M)] \times \\
 &\quad \times \cos\left(\frac{k\omega\rho_M}{M}\right) \frac{d\xi_M d\zeta_M}{\rho_M},
 \end{aligned} \tag{22.6}$$

$$\rho_M = \sqrt{(\xi_{1M} - \xi_M)^2 - (\zeta_{1M} - \zeta_M)^2}.$$

Page 515.

In this case the range of integration $\sigma(\xi_{IM}, \zeta_{IM})$ is limited by the line segments NQ, NP, PQ, equations of which they are (Fig. 22.2):

$$\xi_M = 0 \quad \text{for} \quad PQ,$$

$$\zeta_M = \zeta_{IM} + (\xi_{IM} - \xi_M) \quad \text{for} \quad NQ,$$

$$\zeta_M = \zeta_{IM} - (\xi_{IM} - \xi_M) \quad \text{for} \quad NP.$$

After substituting the variables

$$\xi_{IM} - \xi_M = \beta, \quad \zeta_{IM} - \zeta_M = (\xi_{IM} - \xi_M) \cos \theta, \quad (22.7)$$

we will obtain for velocity potentials the following formulas:

$$\begin{aligned}
 \Phi^a(\xi_{1M}, \zeta_{1M}) &= \pi \int_0^{\xi_{1M}} \cos(k\omega\beta) J_0\left[\frac{k\omega}{M}\beta\right] d\beta, \\
 \Phi^{\dot{a}}(\xi_{1M}, \zeta_{1M}) &= -\frac{\pi}{\omega} \int_0^{\xi_{1M}} \sin(k\omega\beta) J_0\left[\frac{k\omega}{M}\beta\right] d\beta, \\
 \Phi^{\omega x}(\xi_{1M}, \zeta_{1M}) &= -\xi_{1M} \Phi^a, \quad \Phi^{\dot{\omega} x}(\xi_{1M}, \zeta_{1M}) = -\zeta_{1M} \Phi^{\dot{a}}, \\
 \Phi^{\omega z}(\xi_{1M}, \zeta_{1M}) &= k \int_0^{\xi_{1M}} (\xi_{1M} - \beta) \cos(k\omega\beta) J_0\left[\frac{k\omega}{M}\beta\right] d\beta, \\
 \Phi^{\dot{\omega} z}(\xi_{1M}, \zeta_{1M}) &= -\frac{k}{\omega} \int_0^{\xi_{1M}} (\xi_{1M} - \beta) \sin(k\omega\beta) J_0\left[\frac{k\omega}{M}\beta\right] d\beta.
 \end{aligned} \tag{22.8}$$

Here

$$J_0\left[\frac{k\omega}{M}\beta\right] = \frac{1}{\pi} \int_0^\pi \cos\left[\frac{k\omega}{M}\beta \sin\theta\right] d\theta$$

is a Bessel function of zero-order, $0 \leq \xi_{1M} \leq 1/k$.

Integration in formulas (22.8) can be carried out numerically, for example according to Simpson's method, with any assigned accuracy.

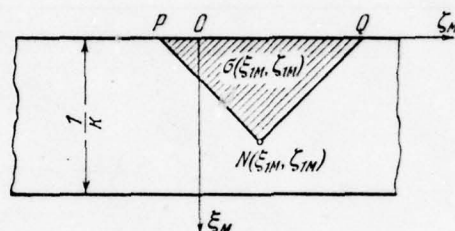


Fig. 22.2. Range of integration on infinite-span wing.

Page 516.

The coefficients of the aerodynamic derivatives of load at the points of wing on the basis of Cauchy-Lagrange's integral (3.21) are determined by the formulas

$$\left. \begin{aligned} p^{q_i} &= \frac{4}{\pi k} \left[\frac{\partial \Phi^{q_i}(\xi_M, \zeta_M)}{\partial \xi_M} - \omega^2 k \frac{M^2 - 1}{M^2} \Phi^{q_i}(\xi_M, \zeta_M) \right], \\ p^{q_i} &= \frac{4}{\pi k} \left[\frac{M^2}{k^2} \frac{\partial \Phi^{q_i}(\xi_M, \zeta_M)}{\partial \xi_M} + k \Phi^{q_i}(\xi_M, \zeta_M) \right]. \end{aligned} \right\} \quad (22.9)$$

The coefficients aerodynamic derivative total characteristics of wing sections let us find, by utilizing formulas (2.8):

$$\left. \begin{aligned}
 c_y^a &= c_y'^a = \frac{4}{\pi} \left[\Phi^a(\xi_M^*) - \omega^2 \frac{k^2}{M^2} \Phi^{\omega z}(\xi_M^*) \right], \\
 c_y^{\dot{a}} &= c_y'^{\dot{a}} = \frac{4}{\pi} \left[\Phi^{\omega z}(\xi_M^*) + \frac{M^2}{k^2} \Phi^{\dot{a}}(\xi_M^*) \right], \\
 c_y^{\omega z} &= c_y'^{\omega z} = \frac{4}{\pi} \left[\Phi^{\omega z}(\xi_M^*) - \omega^2 \frac{k^3}{M^2} \int_0^{1/k} \Phi^{\omega z}(\xi_M) d\xi_M \right], \\
 c_y^{\dot{\omega} z} &= c_y'^{\dot{\omega} z} = \frac{4}{\pi} \left[\frac{M^2}{k^2} \Phi^{\dot{\omega} z}(\xi_M^*) + k \int_0^{1/k} \Phi^{\omega z}(\xi_M) d\xi_M \right], \\
 m_z^a &= m_z'^a = -\frac{4k}{\pi} \left\{ \frac{1}{k} [\Phi^a(\xi_M^*) - \Phi^{\omega z}(\xi_M^*)] - \right. \\
 &\quad \left. - \omega^2 \frac{k^3}{M} \int_0^{1/k} \xi_M \Phi^{\dot{a}}(\xi_M) d\xi_M \right\}, \\
 m_z^{\dot{a}} &= m_z'^{\dot{a}} = -\frac{4k}{\pi} \left\{ \frac{M^2}{k^3} [\Phi^a(\xi_M^*) - \Phi^{\omega z}(\xi_M^*)] + \right. \\
 &\quad \left. + k \int_0^{1/k} \xi_M \Phi^{\dot{a}}(\xi_M) d\xi_M \right\}, \\
 m_z^{\omega z} &= m_z'^{\omega z} = -\frac{4k^2}{\pi} \left[\int_0^{1/k} \xi_M \Phi^a(\xi_M) d\xi_M - \right. \\
 &\quad \left. - \omega^2 \frac{k^2}{M^2} \int_0^{1/k} \xi_M \Phi^{\omega z}(\xi_M) d\xi_M \right], \\
 m_z^{\dot{\omega} z} &= m_z'^{\dot{\omega} z} = -\frac{4k^2}{\pi} \left[\frac{M^2}{k^2} \int_0^{1/k} \xi_M \Phi^{\dot{\omega} z}(\xi_M) d\xi_M + \right. \\
 &\quad \left. + \int_0^{1/k} \xi_M \Phi^{\omega z}(\xi_M) d\xi_M \right],
 \end{aligned} \right\} \quad (22.10)$$

where the values of functions $\Phi^{q_i}(\xi_M^*)$, $\Phi^{q_i}(\xi_M^*)$ they are taken on trailing wing edge, i.e., with $\xi_M^* = 1/k$.

Page 517.

In formulas (22.10) are used escape/ensue from (22.8) the relationship/ratio

$$k\Phi^a = \frac{\partial \Phi^{\omega_z}}{\partial \xi_M}, \quad k\Phi^a = \frac{\partial \Phi^{\omega_z}}{\partial \xi_M}. \quad (22.11)$$

On the basis of the given above expressions of O. N. Sokolov, V. G. Tabachnikov, M. K. Fursov and A. I. Shevchenkos conducted systematic calculations of the distributed and total wing characteristics of infinite lengthening ($\lambda = \infty$) in the range of Mach numbers $M = 1.1 \div 5.0$ and given Strouhal numbers $\omega = 0 - \infty$. The results of the calculations of the aerodynamic derivatives of lift and pitching moment are given in table 22.1, but for numbers M_{\max} $M = 1.4$ and $M = 3$ - in Fig. 22.3-22.6 in the function of given Strouhal number. The points on of the curved figures indicated correspond to the results of the calculations of the coefficients of aerodynamic derivatives with the use of transient functions and Duhamel integral. Let us note that all results correspond to standard system of coordinates with beginning on the wing leading edge. In formulas geometric values and potentials are taken from the calculations in the axes of Fig. 22.1.

In two limiting cases, which are of large practical and theoretical interest, namely $\omega \rightarrow 0$ and $\omega \rightarrow \infty$, the potentials of the disturbed velocities and the coefficients of aerodynamic derivatives are expressed as elementary functions.

Let us examine first the case, when Strouhal number vanishes and, consequently, also $\omega \rightarrow 0$. In this case for determining functions Φ^{qi}, Φ^{qi} we have integral equations (22.5). Transfer/converting to converted coordinates, and then producing the replacement of variables according to (22.7), we obtain

$$\left. \begin{aligned} \Phi^a(\xi_M, \zeta_M) &= \pi \xi_M, & \Phi^{\dot{a}}(\xi_M, \zeta_M) &= -\frac{\pi k}{2} \xi_M^2, \\ \Phi^{\omega z}(\xi_M, \zeta_M) &= \frac{\pi k}{2} \xi_M^2, & \Phi^{\dot{\omega} z}(\xi_M, \zeta_M) &= -\frac{\pi k^2}{6} \xi_M^3. \end{aligned} \right\} \quad (22.12)$$

Hence, utilizing (22.9), (22.10), easily we find with $\omega \rightarrow 0$

$$\left. \begin{aligned} p^a &= \frac{4}{k}, & p^{\dot{a}} &= -\frac{4}{k^3} \xi, & p^{\omega z} &= \frac{4}{k} \xi, & p^{\dot{\omega} z} &= -\frac{2}{k^3} \xi^2; \\ c_y^a &= \frac{4}{k}, & c_y^{\dot{a}} &= -\frac{2}{k^3}, & c_y^{\omega z} &= \frac{2}{k}, & c_y^{\dot{\omega} z} &= -\frac{2}{3k^3}; \\ m_z^a &= -\frac{2}{k}, & m_z^{\dot{a}} &= \frac{4}{3k^3}, & m_z^{\omega z} &= -\frac{4}{3k}, & m_z^{\dot{\omega} z} &= \frac{1}{2k^3}, \end{aligned} \right\} \quad (22.13)$$

where $k = \sqrt{M^2 - 1}$.

Page 518.

Table 22.1.

M = 1,1

ω	c_y^a	\dot{c}_y^a	ω_z	$\dot{\omega}_z$	m_z^a	\dot{m}_z^a	ω_z	$\dot{\omega}_z$
0	8,7286	-20,7824	4,3644	-6,9273	-4,3644	13,8552	-2,9096	5,1955
0,2	8,6569	-20,6160	4,3464	-6,8924	-4,3106	13,7218	-2,8952	5,1721
0,6	8,1102	-19,3293	4,2072	-6,6274	-3,9031	12,6956	-2,7839	4,9538
1,0	7,1520	-16,9845	3,9521	-6,1454	-3,2001	10,8383	-2,5812	4,5494
1,5	5,7226	-13,1822	3,5332	-5,3071	-2,1905	7,8748	-2,2501	3,8603
2,0	4,4662	-9,2626	3,0893	-4,3594	-1,3777	4,9043	-1,9116	3,0827
2,5	3,6803	-5,9839	2,7002	-3,4392	-0,9805	2,5451	-1,6290	2,3453
3,5	3,4339	-2,4933	2,2222	-2,0393	-1,2123	0,4519	-1,3239	1,2799
5,0	3,3771	-1,5499	1,9809	-1,1013	-1,3981	0,4492	-1,2170	0,6529
∞	3,6363	0	1,8181	0	-1,8181	0	-1,2121	0

M = 1,15

ω	c_y^a	\dot{c}_y^a	ω_z	$\dot{\omega}_z$	m_z^a	\dot{m}_z^a	ω_z	$\dot{\omega}_z$
0	7,0436	-10,9204	3,5218	-3,6401	-3,5218	7,2802	-2,3478	2,7301
0,2	6,9906	-10,8340	3,5086	-3,6170	-3,4821	7,2113	-2,3372	2,7246
0,6	6,5862	-10,1668	3,4059	-3,4825	-3,1808	6,6797	-2,2544	2,6107
1,0	5,8745	-8,9468	3,2170	-3,2301	-2,6585	5,7140	-2,1034	2,3980
1,5	4,8034	-6,9542	2,9048	-2,7951	-1,9000	4,1589	-1,8577	2,0347
2,0	3,8476	-4,8762	2,5712	-2,2968	-1,2773	2,5803	-1,6028	1,6250
2,5	3,2358	-3,1085	2,2757	-1,8080	-0,9604	1,3010	-1,3873	1,2322
3,5	3,0407	-1,1635	1,9801	-1,0505	-1,1331	0,1115	-1,1515	0,6532
5,0	3,1085	-0,6570	1,7375	-0,5341	-1,3735	0,1235	-1,0822	0,3063
∞	3,4782	0	1,7391	0	-1,7391	0	-1,1594	0

M = 1,2

ω	c_y^a	\dot{c}_y^a	ω_z	$\dot{\omega}_z$	m_z^a	\dot{m}_z^a	ω_z	$\dot{\omega}_z$
0	6,0302	-6,8525	3,0151	-2,2841	-3,0151	4,5681	-2,0100	1,7132
0,2	5,9885	-6,7991	3,0047	-2,2722	-2,9839	4,5256	-2,0017	1,7056
0,6	5,6701	-6,3852	2,9237	-2,1887	-2,7465	4,1956	-1,9370	1,6358
1,0	5,1075	-5,6263	2,7746	-2,0316	-2,3332	3,5942	-1,8186	1,5049
1,5	4,2544	-4,3791	2,5277	-1,7574	-1,7283	2,6224	-1,6224	1,2802
2,0	3,4830	-3,0647	2,2614	-1,4446	-1,2228	1,6210	-1,4185	1,0226
2,5	2,9794	-1,9300	2,0232	-1,1349	-0,9566	0,7958	-1,2442	0,7730
3,5	2,8167	-0,6446	1,7238	-0,6470	-1,0934	-0,0035	-1,0512	0,3987
5,0	2,9598	-0,3186	1,5963	-0,3088	-1,3664	0,0104	-1,0049	0,1705
∞	3,3333	0	1,6666	0	-1,6666	0	-1,1111	0

Page 519.

Table 22.1 (continuation).

M = 1.3

ω	c_y^a	$c_y^{\dot{a}}$	$c_y^{\omega_z}$	$c_y^{\dot{\omega}_z}$	m_z^a	$m_z^{\dot{a}}$	$m_z^{\omega_z}$	$m_z^{\dot{\omega}_z}$
0	4,8154	-3,4894	2,4077	-1,1631	-2,4077	2,3262	-1,6051	0,8724
0,2	4,7871	-3,4628	2,4006	-1,1568	-2,3865	2,3050	-1,5995	0,8686
0,6	4,5698	-3,2563	2,3455	-1,1152	-2,2245	2,1403	-1,5553	0,8338
1,0	4,1837	-2,8755	2,2434	-1,0366	-1,9405	1,8385	-1,4741	0,7682
1,5	3,5907	-2,2430	2,0735	-0,8976	-1,5188	1,3452	-1,3388	0,6548
2,0	3,0427	-1,5647	1,8878	-0,7383	-1,1564	0,8273	-1,1960	0,5231
2,5	2,6735	-0,9645	1,7190	-0,5781	-0,9551	0,3873	-1,0718	0,3934
3,5	2,5519	-0,2504	1,5030	-0,3184	-1,0492	-0,0686	-0,9315	0,1929
5,0	2,7734	-0,0749	1,4620	-0,1329	-1,3506	-0,0575	-0,9115	0,0667
∞	3,0769	0	1,5384	0	-1,5384	0	-1,0256	0

M = 1.4

ω	c_y^a	$c_y^{\dot{a}}$	$c_y^{\omega_z}$	$c_y^{\dot{\omega}_z}$	m_z^a	$m_z^{\dot{a}}$	$m_z^{\omega_z}$	$m_z^{\dot{\omega}_z}$
0	4,0824	-2,1262	2,0412	-0,7087	-2,0412	1,4175	-1,3608	0,5316
0,2	4,0612	-2,1104	2,0361	-0,7047	-2,0257	1,4048	-1,3567	0,5293
0,6	3,9026	-1,9865	1,9957	-0,6798	-1,9070	1,3061	-1,3243	0,5085
1,0	3,6184	-1,7572	1,9208	-0,6326	-1,6979	1,1243	-1,2647	0,4690
1,5	3,1775	-1,3731	1,7956	-0,5481	-1,3837	0,8248	-1,1646	0,4004
2,0	2,7633	-0,9554	1,6572	-0,4511	-1,1078	0,5051	-1,0578	0,3200
2,5	2,4772	-0,5784	1,5298	-0,3522	-0,9483	0,2271	-0,9637	0,2396
3,5	2,3819	-0,1119	1,3646	-0,1883	-1,0174	-0,0766	-0,8557	0,1123
5,0	2,6322	0,0012	1,3155	-0,0680	-1,3199	-0,0689	-0,8493	0,0299
∞	2,8571	0	1,4300	0	-1,4300	0	-0,9523	0

M = 1.6

ω	c_y^a	$c_y^{\dot{a}}$	$c_y^{\omega_z}$	$c_y^{\dot{\omega}_z}$	m_z^a	$m_z^{\dot{a}}$	$m_z^{\omega_z}$	$m_z^{\dot{\omega}_z}$
0	3,2026	-1,0264	1,6013	-0,3421	-1,6013	0,6842	-1,0675	0,2566
0,2	3,1901	-1,0190	1,5982	-0,3400	-1,5920	0,6783	-1,0651	0,2556
0,6	3,0942	-0,9605	1,5729	-0,3283	-1,5205	0,6318	-1,0456	0,2457
1,0	2,9218	-0,8519	1,5287	-0,3060	-1,3934	0,5456	-1,0095	0,2271
1,5	2,6504	-0,6674	1,4527	-0,2652	-1,1996	0,4021	-0,9483	0,1943
2,0	2,3892	-0,4626	1,3673	-0,2185	-1,0238	0,2448	-0,8820	0,1553
2,5	2,2026	-0,2722	1,2873	-0,1699	-0,9165	0,1033	-0,8225	0,1155
3,5	2,1394	-0,0227	1,1813	-0,0866	-0,9578	-0,0636	-0,7526	0,0502
5,0	2,3859	0,0377	1,1598	-0,0228	-1,2285	-0,0602	-0,7578	0,0060
∞	2,5000	0	1,2500	0	-1,2500	0	-0,8333	0

Page 520.

Table 22.1. (continuation).

M = 2,0

ω	c_y^a	$c_y^{\dot{a}}$	$c_y^{\omega_z}$	$c_y^{\dot{\omega}_z}$	m_z^a	$m_z^{\dot{a}}$	$m_z^{\omega_z}$	$m_z^{\dot{\omega}_z}$
0	2,3094	-0,3849	1,1547	-0,1283	-1,1547	0,2566	-0,7698	0,0962
0,2	2,3037	-0,3822	1,1533	-0,1273	-1,1504	0,2544	-0,7681	0,0958
0,6	2,2592	-0,3609	1,1421	-0,1230	-1,1173	0,2375	-0,7596	0,0923
1,0	2,1787	-0,3210	1,1211	-0,1149	-1,0579	0,2059	-0,7428	0,0854
1,5	2,0498	-0,2523	1,0859	-0,0994	-0,9658	0,1528	-0,7140	0,0733
2,0	1,9223	-0,1740	1,0454	-0,0820	-0,8789	0,0926	-0,6823	0,0586
2,5	1,8277	-0,0987	1,0066	-0,0635	-0,8225	0,0362	-0,6530	0,0433
3,5	1,7951	-0,0068	0,9538	-0,0304	-0,8406	-0,0366	-0,6179	0,0169
5,0	1,9763	0,0329	0,9494	-0,0035	-1,0272	-0,0364	0,6267	-0,0020
∞	2,0000	0	1	0	-1	0	0,6666	0

M = 3,0

ω	c_y^a	$c_y^{\dot{a}}$	$c_y^{\omega_z}$	$c_y^{\dot{\omega}_z}$	m_z^a	$m_z^{\dot{a}}$	$m_z^{\omega_z}$	$m_z^{\dot{\omega}_z}$
0	1,4142	-0,0834	0,7071	-0,0295	-0,7071	0,0589	-0,4714	0,0221
0,2	1,4126	-0,0878	0,7067	-0,0291	-0,7059	0,0584	-0,4711	0,0220
0,6	1,4005	-0,0831	0,7037	-0,0281	-0,6969	-0,0547	-0,4686	0,0212
1,0	1,3783	-0,0741	0,6980	-0,0263	-0,6826	0,0476	-0,4640	0,0222
1,5	1,3423	-0,0584	0,6888	-0,0225	-0,6550	0,0359	-0,4560	0,0169
2,0	1,3056	-0,0401	0,6776	-0,0186	-0,6297	0,0219	-0,4470	0,0135
2,5	1,2774	-0,0219	0,6668	-0,0144	-0,6120	0,0082	-0,4386	0,0099
3,5	1,2676	-0,0054	0,6514	-0,0065	-0,6154	-0,0112	-0,4282	0,0034
5,0	1,3403	0,0125	0,6516	0,0004	-0,6836	-0,0122	-0,4328	-0,0016
∞	1,3333	0	0,6666	0	-0,6666	0	-0,4444	0

M = 5,0

ω	c_y^a	$c_y^{\dot{a}}$	$c_y^{\omega_z}$	$c_y^{\dot{\omega}_z}$	m_z^a	$m_z^{\dot{a}}$	$m_z^{\omega_z}$	$m_z^{\dot{\omega}_z}$
0	0,8165	-0,0170	0,4082	-0,0057	-0,4082	0,0113	-0,2722	0,0043
0,2	0,8162	-0,0169	0,4082	-0,0057	-0,4080	0,0112	-0,2721	0,0043
0,6	0,8137	-0,0160	0,4076	-0,0059	-0,4062	0,0105	-0,2716	0,0041
1,0	0,8090	-0,0143	0,4064	-0,0051	-0,4027	0,0092	-0,2706	0,0038
1,5	0,8014	-0,0113	0,4048	-0,0045	-0,3975	0,0072	-0,2689	0,0033
2,0	0,7936	-0,0077	0,4027	-0,0037	-0,3920	0,0046	-0,2670	0,0026
2,5	0,7874	-0,0041	0,4005	-0,0028	-0,3879	0,0020	-0,2652	0,0019
3,5	0,7853	-0,0015	0,3972	-0,0028	-0,3874	-0,0021	-0,2630	0,0006
5,0	0,8034	0,0029	0,3971	0,0001	-0,4039	-0,0030	-0,2642	-0,0004
∞	0,8000	0	0,4000	0	-0,4000	0	-0,2666	0

Page 521.

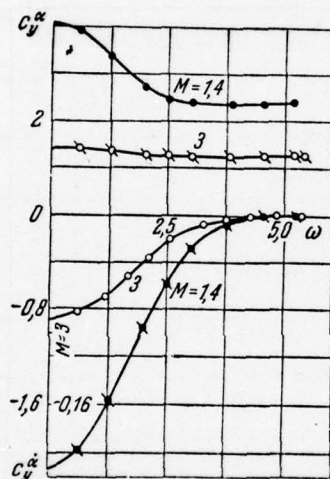


Fig. 22.3

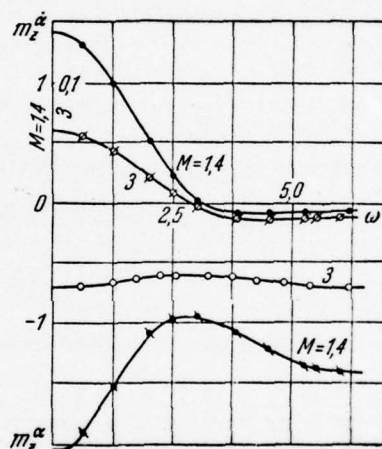


Fig. 22.4

Fig. 22.3. Coefficients of the aerodynamic derivatives $c_y^\alpha, c_y^{\alpha_y}$ of wing $\lambda = \infty$. Exact solutions are curves, the calculation according to Duhamel integral - point.

Fig. 22.4. Coefficients of the aerodynamic derivatives $m_z^\alpha, m_z^{\alpha_y}$ of wing $\lambda = \infty$. exact solutions are curves, the calculation according to

Duhamel integral - point, $\bar{x}_T = 0$.

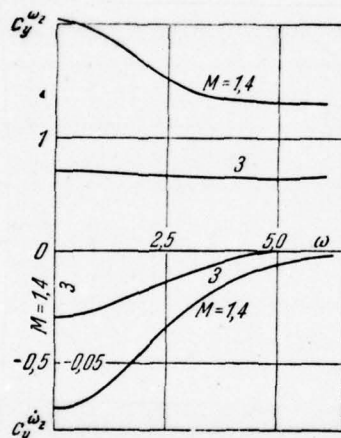


Fig. 22.5

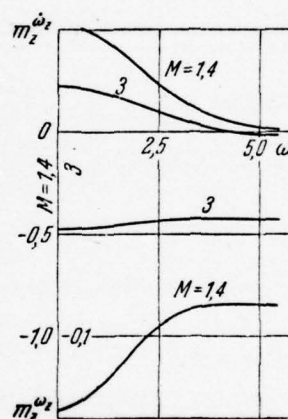


Fig. 22.6

Fig. 22.5. Coefficients of the aerodynamic derivatives $c_y^{\omega_z}$, $c_y^{\dot{\omega}_z}$ of wing $\lambda = 3$, $\bar{x}_T = 0$.

Fig. 22.6. Coefficients of the aerodynamic derivatives $m_z^{\omega_z}$, $m_z^{\dot{\omega}_z}$ of wing $\lambda = 3$, $\bar{x}_T = 0$.

Page 522.

Let us examine now the case $\omega \rightarrow \infty$, for which present the coefficients of the aerodynamic derivatives of load p^{α} , p^{β} as functions directly of coordinate $\xi = x/b$:

$$\left. \begin{aligned} p^{\alpha} &= \frac{4}{k} \left[\cos(\omega\xi) J_0\left(\frac{\omega\xi}{M}\right) + \omega \frac{k^2}{M^2} \int_0^{\xi} \sin(\omega\beta) J_0\left(\frac{\omega\beta}{M}\right) d\beta \right], \\ p^{\beta} &= \frac{4}{k} \left[-\frac{1}{\omega} \frac{M^2}{k^2} \sin(\omega\xi) J_0\left(\frac{\omega\xi}{M}\right) + \int_0^{\xi} \cos(\omega\beta) J_0\left(\frac{\omega\beta}{M}\right) d\beta \right], \\ p^{\omega_z} &= \frac{4}{k} \left\{ \int_0^{\xi} \cos(\omega\beta) J_0\left(\frac{\omega\beta}{M}\right) d\beta + \right. \\ &\quad \left. + \omega \frac{k^2}{M^2} \left[\xi \int_0^{\xi} \sin(\omega\beta) J_0\left(\frac{\omega\beta}{M}\right) d\beta - \int_0^{\xi} \beta \sin(\omega\beta) J_0\left(\frac{\omega\beta}{M}\right) d\beta \right] \right\}, \\ p^{\omega_z} &= \frac{4}{k} \left[-\frac{1}{\omega} \frac{M^2}{k^2} \int_0^{\xi} \sin(\omega\beta) J_0\left(\frac{\omega\beta}{M}\right) d\beta + \right. \\ &\quad \left. + \xi \int_0^{\xi} \cos(\omega\beta) J_0\left(\frac{\omega\beta}{M}\right) d\beta - \int_0^{\xi} \beta \cos(\omega\beta) J_0\left(\frac{\omega\beta}{M}\right) d\beta \right]. \end{aligned} \right\} \quad (22.14)$$

Let us pass to limit in (22.14) with $\omega \rightarrow \infty$. since in this case

$$J_0\left(\frac{\omega\xi}{M}\right) \rightarrow 0 \text{ [1.92]}, \quad |\sin \omega\xi| \leq 1, \quad |\cos \omega\xi| \leq 1,$$

the first two terms in formulas milking p^{α} and p^{β} vanish. It is possible to show that

$$\left. \begin{aligned} \lim_{\omega \rightarrow 0} \int_0^{\xi} \sin(\omega\beta) J_0\left(\frac{\omega\beta}{M}\right) d\beta &= \frac{M}{k}, \\ \lim_{\omega \rightarrow 0} \int_0^{\xi} \cos(\omega\beta) J_0\left(\frac{\omega\beta}{M}\right) d\beta &= 0, \\ \lim_{\omega \rightarrow 0} \omega \int_0^{\xi} \beta \sin(\omega\beta) J_0\left(\frac{\omega\beta}{M}\right) d\beta &= 0, \\ \lim_{\omega \rightarrow 0} \omega \int_0^{\xi} \beta \cos(\omega\beta) J_0\left(\frac{\omega\beta}{M}\right) d\beta &= 0. \end{aligned} \right\} \quad (22.15)$$

[Page 523] By utilizing these relationship/ratios, from (22.14) let us have

$$\left. \begin{aligned} p^a &= \frac{4}{k} \quad \text{при } \xi = 0, \quad p^a = \frac{4}{M} \quad \text{при } \xi \neq 0, \\ p^{\omega z} &= \frac{4}{M} \xi, \quad p^a = p^{\omega z} = 0. \end{aligned} \right\} \quad (22.16)$$

Кстати: (1) with

Thus, with $\omega \rightarrow -$ we obtain for p^a the discontinuous function, and for $p^{\omega z}$ continuous, linear on ξ . Factors of the load p^a and $p^{\omega z}$ vanish.

Integrating load over the wing section of infinite lengthening, let us find the coefficients of the aerodynamic derivatives of lift and pitching moment with $\omega \rightarrow -$ ($p \rightarrow -$):

$$\left. \begin{aligned} c_y^a &= \frac{4}{M}, \quad c_{y^z}^{\omega} = \frac{2}{M}, \quad m_z^a = -\frac{2}{M}, \quad m_z^{\omega} = -\frac{4}{3M}, \\ c_y^a &= c_{y^z}^{\omega} = m_z^a = m_z^{\omega} = 0. \end{aligned} \right\} \quad (22.17)$$

§3. Effect of harmonic gust on infinite-span wing.

Let us examine now the task of determining the aerodynamic wing characteristics of the infinite lengthening, which affects harmonic gust. Let the wing move in the medium whose particles, besides the disturbed speeds from wing, have the supplementary vertical velocity W_{ud} .

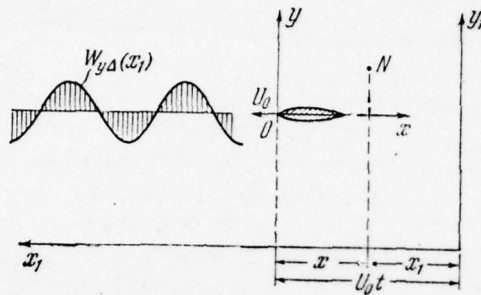


Fig. 22.7. To the effect of harmonic gust on wing.

Page 524.

The profile of these supplementary velocities to moving coordinate system (Fig. 22.7) let us assign to constants on the wingspan by the law

$$\frac{W_{y\Delta}}{U_0} = w_{y\Delta}^* e^{i \frac{2\pi}{l^*} x_1}, \quad (22.18)$$

where l^* - the wavelength of gust, $w_{y\Delta}^* = W_{y\Delta}^*/U_0$ - dimensionless amplitude. In the connected with wing system of coordinates (see Fig. 22.7) speed distribution of signs the form

$$w_{y\Delta}(\xi, t) = e^{-i p^* \xi} \Delta(t). \quad (22.19)$$

Here $\Delta(t) = w_{y\Delta}^* e^{i p t}$ - the kinematic parameter, which characterizes gust, $p = 2\pi U_0/l^*$ - angular frequency, $p^* = p/U_0$ - Strouhal number; as $t = 0$ is accepted the torque/moment of the coincidence of the beginnings

of movable and fixed coordinate systems.

Let us present velocity potential, caused by gust, through the coefficients of the aerodynamic derivatives:

$$\left. \begin{aligned} \varphi_{\Delta}(\xi, \eta, \zeta, t) &= U_0 b [\varphi^{\Delta}(\xi, \eta, \zeta) \Delta(t) + \varphi^{\dot{\Delta}}(\xi, \eta, \zeta) \dot{\Delta}(t)], \\ \dot{\Delta}(t) &= \frac{d\Delta}{dt} \frac{b}{U_0}. \end{aligned} \right\} \quad (22.20)$$

For determining the aerodynamic derivatives of potential we have integral equations (20.11), whereupon from boundary condition (3.56) it follows

$$\left[\frac{\partial \varphi^{\Delta}}{\partial \eta} \right]_{\eta=0} = -\cos(p^* \xi), \quad \left[\frac{\partial \varphi^{\dot{\Delta}}}{\partial \eta} \right]_{\eta=0} = \frac{1}{p^*} \sin(p^* \xi). \quad (22.21)$$

Let us introduce the converted coordinates and dimensionless functions $\varphi^{\Delta}, \varphi^{\dot{\Delta}}$ by formulas (20.12), (22.3). Then instead of equations (20.11) we are have

$$\left. \begin{aligned} \varphi^{\Delta} &= \int_0^{\xi_{1M}} \cos \left[k\omega \left(\xi_{1M} - \frac{\xi_M}{M^2} \right) \right] \int_{\xi_{1M}-\xi_{1M}+\xi_M}^{\xi_{1M}+\xi_{1M}-\xi_M} \cos \left(\frac{k\omega \rho_M}{M} \right) \frac{d\xi_M d\zeta_M}{\rho_M}, \\ \varphi^{\dot{\Delta}} &= -\frac{1}{\omega} \int_0^{\xi_{1M}} \sin \left[k\omega \left(\xi_{1M} - \frac{\xi_M}{M^2} \right) \right] \int_{\xi_{1M}-\xi_{1M}+\xi_M}^{\xi_{1M}+\xi_{1M}-\xi_M} \cos \left(\frac{k\omega \rho_M}{M} \right) \frac{d\xi_M d\zeta_M}{\rho_M}. \end{aligned} \right\} \quad (22.22)$$

By making the replacement of variables for formulas (22.7) and by producing integration, we will obtain

$$\left. \begin{aligned} \varphi^{\Delta} &= \frac{\pi}{k} \int_0^{\xi_1} \cos \left[\omega \left(\frac{k^2}{M^2} \xi_1 + \frac{\beta}{M^2} \right) \right] J_0 \left(\frac{\omega \beta}{M} \right) d\beta, \\ \varphi^{\dot{\Delta}} &= -\frac{\pi}{k\omega} \int_0^{\xi_1} \sin \left[\omega \left(\frac{k^2}{M^2} \xi_1 + \frac{\beta}{M^2} \right) \right] J_0 \left(\frac{\omega \beta}{M} \right) d\beta, \end{aligned} \right\} \quad (22.23)$$

where, as earlier, $J_0\left(\frac{\omega\beta}{M}\right)$ - the function of zero-order Bessel.

Page 525.

Let us present the aerodynamic loading, caused by gust, in the form

$$\Delta\bar{p}(\xi, \zeta, t) = p^\Delta(\xi, \zeta)\Delta(t) + p^\dot{\Delta}(\xi, \zeta)\dot{\Delta}(t). \quad (22.24)$$

Then from the Cauchy integral of - Lagrange (3.21) and of relationship/ratios (22.23), (22.3) we have

$$\left. \begin{aligned} p^\Delta &= \frac{4}{k} \cos(\omega\xi) J_0\left(\frac{\omega\xi}{M}\right), \\ p^\dot{\Delta} &= -\frac{4}{\omega} \frac{M^2}{k^3} \sin(\omega\xi) J_0\left(\frac{\omega\xi}{M}\right). \end{aligned} \right\} \quad (22.25)$$

By integrating by section, we will obtain expressions for the coefficients of the aerodynamic derivatives of lift and pitching moment in standard system of coordinates:

$$\left. \begin{aligned} c_y^\Delta &= \frac{4}{k} \int_0^1 \cos(\omega\xi) J_0\left(\frac{\omega\xi}{M}\right) d\xi, \\ c_y^\dot{\Delta} &= -\frac{4}{\omega} \frac{M^2}{k^3} \int_0^1 \sin(\omega\xi) J_0\left(\frac{\omega\xi}{M}\right) d\xi, \\ m_z^\Delta &= -\frac{4}{k} \int_0^1 \xi \cos(\omega\xi) J_0\left(\frac{\omega\xi}{M}\right) d\xi, \\ m_z^\dot{\Delta} &= \frac{4}{\omega} \frac{M^2}{k^3} \int_0^1 \xi \sin(\omega\xi) J_0\left(\frac{\omega\xi}{M}\right) d\xi. \end{aligned} \right\} \quad (22.26)$$

With $p^* \rightarrow 0$ ($\omega \rightarrow 0$) relationship/ratio they take the form

$$\left. \begin{aligned} p^\Delta &= \frac{4}{k}, & p^\dot{\Delta} &= -\frac{4M^2}{k^3} \xi, & c_y^\Delta &= \frac{4}{k}, \\ c_y^\dot{\Delta} &= -\frac{2M^2}{k^3}, & m^\Delta &= & m_z^\dot{\Delta} &= \frac{4M^2}{3k^3}. \end{aligned} \right\} \quad (22.27)$$

With $\omega \rightarrow \infty$ - all coefficients of aerodynamic derivatives vanish.

Pages 526-527.

Table 22.2.

M = 1,1					M = 1,15				
ω	c_y^{Δ}	$c_y^{\dot{\Delta}}$	m_z^{Δ}	$m_z^{\dot{\Delta}}$	ω	c_y^{Δ}	$c_y^{\dot{\Delta}}$	m_z^{Δ}	$m_z^{\dot{\Delta}}$
0,0	8,7287	-25,1468	-4,3643	16,7646	0,0	7,0436	-14,4422	-3,5218	9,6281
0,25	8,6013	-24,8554	-4,2689	16,5315	0,25	6,9432	-14,2825	-3,4466	9,5004
0,5	8,2314	-24,0013	-3,9927	15,8496	0,5	6,6517	-13,8145	-3,2289	9,1268
1,0	6,9259	-20,8776	-3,0326	13,3721	1,0	5,5168	-12,0963	-2,4671	7,7638
1,5	5,2777	-16,5937	-1,8661	10,0289	1,5	4,2932	-9,7200	-1,5274	5,9068
2,0	3,8042	-12,1601	-0,9067	6,6659	2,0	3,0825	-7,2271	-0,7315	4,0106
2,5	2,8426	-8,4215	-0,4020	3,9733	2,5	2,2590	-5,0842	-0,2832	2,4560
3,0	2,4356	-5,8256	-0,3447	2,2742	3,0	1,8773	-3,5498	-0,1953	1,4369
3,5	2,3826	-4,3466	-0,5292	1,4973	3,5	1,7994	-2,6408	-0,3221	0,9369
4,0	2,4037	-3,6543	-0,7038	1,3122	4,0	1,8098	-2,1946	-0,4671	0,7914
5,0	2,0683	-3,0476	-0,5706	1,3097	5,0	1,5617	-1,8259	-0,3928	0,7854
10	1,0090	-1,0812	-0,1221	0,3973	10	0,5754	-0,6481	+0,0615	0,2367
15	0,5900	-0,6284	+0,0214	0,2399	15	0,2258	-0,3479	0,1628	0,1189
20	0,2682	-0,3844	0,1639	0,1276	20	0,0416	-0,1945	0,2751	0,0486
∞	0	0	0	0	∞	0	0	0	0

M = 1,2					M = 1,3				
ω	c_y^{Δ}	$c_y^{\dot{\Delta}}$	m_z^{Δ}	$m_z^{\dot{\Delta}}$	ω	c_y^{Δ}	$c_y^{\dot{\Delta}}$	m_z^{Δ}	$m_z^{\dot{\Delta}}$
0,0	6,0303	-9,8677	-3,0151	6,5785	0	4,8154	-5,8972	-2,4077	3,9315
0,25	5,9162	-9,7633	-2,9522	6,4950	0,25	4,7509	-5,8395	-2,3593	3,8853
0,5	4,7018	-9,4570	-2,7696	6,2504	0,5	4,5626	-5,6699	-2,2187	3,7499
1,0	4,8299	-8,3289	-2,1272	5,3552	1,0	3,8852	-5,0411	-1,7189	3,2511
1,5	3,7017	-6,7567	-1,3241	4,1253	1,5	2,9910	-4,1546	-1,0794	2,5559
2,0	2,6484	-5,0872	-0,6260	2,8523	2,0	2,1270	-3,1927	-0,4991	1,8194
2,5	1,9058	-3,6261	-0,2097	1,7864	2,5	1,4811	-2,3248	-0,1207	1,1803
3,0	1,5354	-2,5529	-0,0999	1,0640	3,0	1,1206	-1,6591	+0,0184	0,7226
3,5	1,4373	-1,8941	-0,1878	0,6880	3,5	0,9915	-1,2251	-0,0169	0,4610
4,0	1,4371	-1,5562	-0,3121	0,5615	4,0	0,9713	-0,9849	-0,1104	0,3535
5,0	1,2420	-1,2849	-0,2756	0,5489	5,0	0,8390	-0,7925	-0,1214	0,3284
10	0,3086	-0,4477	0,1718	0,1586	10	0,0213	-0,2562	0,2708	0,0802
15	-0,0261	-0,2147	0,2269	0,059	15	-0,1202	-0,0933	0,2291	0,0058
20	-0,1441	-0,1082	0,2691	0,0135	20	-0,0861	-0,0407	0,1220	-0,0078
∞	0	0	0	0	∞	0	0	0	0

M = 1,4					M = 1,5				
ω	c_y^{Δ}	$c_y^{\dot{\Delta}}$	m_z^{Δ}	$m_z^{\dot{\Delta}}$	ω	c_y^{Δ}	$c_y^{\dot{\Delta}}$	m_z^{Δ}	$m_z^{\dot{\Delta}}$
0	4,0825	-4,1675	-2,0412	2,7783	0	3,5777	-3,2199	-1,7889	2,1466
0,25	4,0294	-4,1294	-2,0015	2,7478	0,25	3,5324	-3,1921	-1,7549	2,1244
0,5	3,8745	-4,0171	-1,8857	2,6582	0,5	3,3999	-3,1101	-1,6559	2,0589
1,0	3,3129	-3,5992	-1,4709	2,3262	1,0	2,9169	-2,8035	-1,2988	1,8152
1,5	2,5596	-3,0026	-0,9302	1,8580	1,5	2,2602	-2,3619	-0,8259	1,4682
2,0	1,8112	-2,3444	-0,4223	1,3523	2,0	1,5928	-1,8676	-0,3693	1,0874
2,5	1,2255	-1,7354	-0,0685	0,9006	2,5	1,0511	-1,4005	-0,0346	0,7389
3,0	0,8711	-1,2516	0,0887	0,5626	3,0	0,7029	-1,0185	0,1336	0,4686

M = 1,4

M = 1,5

ω	c_y^{Δ}	$c_y^{\dot{\Delta}}$	m_z^{Δ}	$m_z^{\dot{\Delta}}$	ω	c_y^{Δ}	$c_y^{\dot{\Delta}}$	m_z^{Δ}	$m_z^{\dot{\Delta}}$
3,5	0,7204	-0,9206	0,0883	0,3552	3,5	0,5369	-0,7467	0,1579	0,2935
4,0	0,6823	-0,7256	0,0179	0,2578	4,0	0,4852	-0,5782	0,1059	0,2029
5,0	0,5866	-0,5640	-0,0213	0,2230	5,0	0,4120	-0,4322	0,0486	0,1609
10	-0,0942	-0,1638	0,2799	0,0411	10	-0,1260	-0,1110	0,2176	0,0189
15	-0,1139	-0,0463	0,1617	-0,0100	15	-0,0630	-0,0282	0,0874	-0,0115
20	0,0217	-0,0229	-0,0044	-0,0068	20	0,0623	-0,0188	-0,0452	-0,0021
∞	0	0	0	0	∞	0	0	0	0

M = 2,0

M = 2,5

ω	c_y^{Δ}	$c_y^{\dot{\Delta}}$	m_z^{Δ}	$m_z^{\dot{\Delta}}$	ω	c_y^{Δ}	$c_y^{\dot{\Delta}}$	m_z^{Δ}	$m_z^{\dot{\Delta}}$
0	2,3094	-1,5396	-1,1547	1,0264	0	1,7457	-1,0391	-0,8729	0,6927
0,25	2,2825	-1,5286	-1,1345	1,0176	0,25	1,7262	-1,0324	-0,8582	0,6874
0,5	2,2032	-1,4951	-1,0753	0,9916	0,5	1,6685	-1,0126	-0,8151	0,6716
1,0	1,9091	-1,3730	-0,8571	0,8936	1,0	1,4524	-0,9369	-0,6546	0,6113
1,5	1,4920	-1,1902	-0,5541	0,7495	1,5	0,1396	-0,8228	-0,4263	0,5211
2,0	1,0382	-0,9758	-0,2364	0,5829	2,0	0,7881	-0,6857	-0,1777	0,4141
2,5	0,6293	-0,7594	0,0314	0,4185	2,5	0,4562	-0,5425	0,0446	0,3044
3,0	0,3211	-0,5657	0,2081	0,2766	3,0	0,1892	-0,4085	0,2062	0,2047
3,5	0,1319	-0,4104	0,2853	0,1691	3,5	0,0100	-0,2949	0,2924	0,1237
4,0	0,0449	-0,2986	0,2839	0,0985	4,0	-0,0824	-0,2072	0,3088	0,0654
5,0	0,0181	-0,1819	0,1968	0,0427	5,0	-0,0964	-0,1065	0,2229	-0,0101
10	-0,0161	-0,0265	0,0390	-0,0101	10	0,0387	-0,0141	-0,0262	-0,0080
15	0,0458	-0,0185	-0,0275	0,0032	15	0,0930	-0,0122	0,0102	0,0021
20	-0,0358	-0,0098	0,0457	0,0007	20	0,0117	-0,0047	-0,0076	-0,0009
∞	0	0	0	0	∞	0	0	0	0

M = 3,0

M = 5,0

ω	c_y^{Δ}	$c_y^{\dot{\Delta}}$	m_z^{Δ}	$m_z^{\dot{\Delta}}$	ω	c_y^{Δ}	$c_y^{\dot{\Delta}}$	m_z^{Δ}	$m_z^{\dot{\Delta}}$
0	1,4142	-0,7955	-0,7071	0,5303	0	0,8165	-0,4253	-0,4083	0,2835
0,25	1,3987	-0,7907	-0,6955	0,5265	0,25	0,8078	-0,4229	-0,4018	0,2816
0,5	1,3530	-0,7764	-0,6613	0,5150	0,5	0,7823	-0,4159	-0,3826	0,2761
1,0	1,1807	-0,7215	-0,5332	0,4714	1,0	0,6851	-0,3891	-0,3103	0,2546
1,5	0,9284	-0,6381	-0,3487	0,4054	1,5	0,5405	-0,3476	-0,2011	0,2217
2,0	0,6399	-0,5364	-0,1435	0,3258	2,0	0,3706	-0,2959	-0,0824	0,1811
2,5	0,3605	-0,4282	0,0458	0,2425	2,5	0,2002	-0,2392	0,0349	0,1372
3,0	0,1282	-0,3243	0,1900	0,1646	3,0	0,0516	-0,1827	0,1301	0,0943
3,5	-0,0347	-0,2334	0,2736	0,0988	3,5	-0,0587	-0,1309	0,1910	0,0561
4,0	-0,1234	-0,1607	0,2962	0,0492	4,0	-0,1230	-0,0873	0,2132	0,0254
5,0	-0,1321	-0,0725	0,2172	-0,0020	5,0	-0,1261	-0,0302	0,1592	-0,0102
10	0,0394	-0,0121	-0,0274	-0,0041	10	-0,0017	-0,0108	0,0129	0,0022
15	-0,0205	-0,0070	0,0281	-0,0006	15	-0,0069	-0,0029	0,0096	-0,0010
20	0,0216	-0,0038	-0,0178	-0,0003	20	-0,0151	-0,0025	0,0177	0,0003
∞	0	0	0	0	∞	0	0	0	0

The coefficients of the aerodynamic derivatives of the lift and the pitching moment of the wing of infinite elongation, caused by the action of gust, designed by O. N. Sokolovoy and M. K. Fursov for centering $\bar{x}_T = 0$, $M = 1.1 - 5.0$ and given Strouhal numbers $\omega = 0 - \infty$, are given in table 22.2, and for numbers $M = 1.4$ and 3.0 are given also in Fig. 22.8, 22.9.

As earlier, points showed the values, obtained from transient functions with the aid of Duhamel integral.

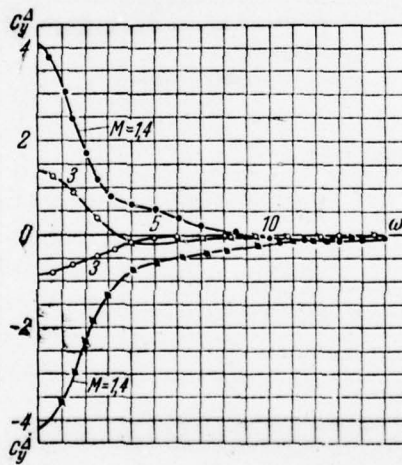


FIG. 22.8.

FIG. 22.9.

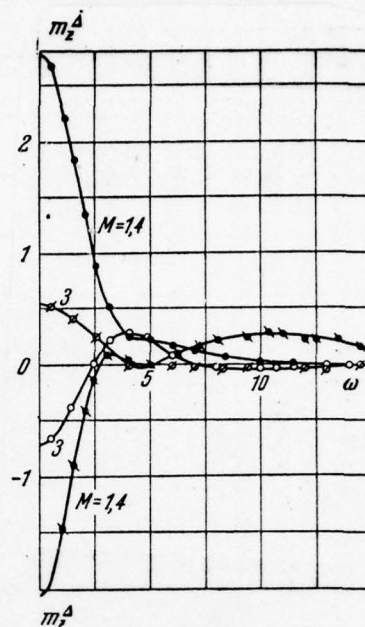


Fig. 22.8. Coefficients of the aerodynamic derivatives $c_y^{\Delta}, c_y^{\Delta}$ of wing $\lambda = \infty$. Exact solutions are curves, the calculation according to Duhamel integral - point.

Fig. 22.9. Coefficients of the aerodynamic derivatives $m_z^{\Delta}, m_z^{\Delta}$ of wing $\lambda = \infty$. Exact solutions are curves, the calculation according to Duhamel integral - point $\bar{x}_T = 0$.

§4. Coefficients aerodynamic derivative wings of the final lengthening in the absence of end effect.

The calculation of the aerodynamic characteristics of arbitrary in plan/layout wing in the absence of end effect one should do as in the preceding/previous paragraphs the methods presented. However, for wings, whose leading edge is normal to flight speed, rear - supersonic and end effect is absent, loads at the points of wing will be equal to loads at the appropriate points of infinite-span wing. Therefore, if are known the coefficients of the aerodynamic derivatives of load for an infinite-span wing, there is no need to solve problem anew.

Page 529.

In order to obtain the coefficients aerodynamic derivative total characteristics of such wings, it suffices to integrate the derived loads, known from the solution of problem for a wing $\lambda = \infty$, in the area (or section) of the wing in question. The absence of end effect superimposes at the given flight speed of limitation on the geometric parameters of wings, since in this case the Mach cone, carried out from the points of inflection of lateral wing edge, must not intersect wing (see Fig. 22.1). For wings with the direct/straight edges of solution they can be obtained from solutions for an infinite-span wing, in particular for the reverse/inverse delta

wings, when

$$\eta = \infty, \quad \lambda \operatorname{tg} \chi_0 = 0, \quad k\lambda \geq 4. \quad (22.28)$$

O. N. Sokolov, M. K. Fursov, V. G. Tabachnikov, A. I. Shevchenkos on the basis of the calculations of loads conducted for an infinite-span wing calculated the coefficients of the aerodynamic derivatives of reverse/inverse delta wing. The results of these calculations in the range of numbers $M = 1.1-5.0$ and of given Strouhal numbers $\omega = 0--$ are given in table 22.3. With $p \rightarrow 0$ ($\omega \rightarrow 0$) the coefficients of the aerodynamic derivatives of load on reverse/inverse delta wing $p^a, p^{\dot{a}}, p^{\omega z}, p^{\dot{\omega} z}$ are determined by expressions (22.13), and the coefficients $p^{\omega x}, p^{\dot{\omega} x}$, which correspond to the rotation of wing around axis Ox , are equal to

$$p^{\omega x} = \bar{z} \frac{\lambda}{4} p^a, \quad p^{\dot{\omega} x} = \bar{z} \frac{\lambda}{4} p^{\dot{a}}, \quad \bar{z} = \frac{2z}{l}. \quad (22.29)$$

The coefficients aerodynamic derivative wing sections and entire wing as a whole with $\omega \rightarrow 0$ are determined by the expressions

$$\left. \begin{aligned} c_y^a &= \frac{4}{k}, \quad c_y^{\dot{a}} = -\frac{2(1-\bar{z})}{k^3}, \quad c_y^{\omega z} = \frac{2(1-\bar{z})}{k}, \\ c_y^{\dot{\omega} z} &= -\frac{2(1-\bar{z})^2}{3k^3}; \quad m_z^a = -\frac{2}{k}, \\ m_z^{\dot{a}} &= \frac{4(1-\bar{z})}{3k^3}, \quad m_z^{\omega z} = -\frac{4(1-\bar{z})}{3k}, \\ m_z^{\dot{\omega} z} &= \frac{(1-\bar{z})^2}{2k^3}, \quad m_z^{\omega x} = \frac{\lambda \bar{z}}{2k}, \quad m_z^{\dot{\omega} x} = \frac{\lambda \bar{z}(1-\bar{z})}{3k^3}; \\ c_y^a &= \frac{4}{k}, \quad c_y^{\dot{a}} = -\frac{4}{3k^3}, \quad c_y^{\omega z} = \frac{4}{3k}, \quad c_y^{\dot{\omega} z} = -\frac{1}{3k^3}; \\ m_z^a &= -\frac{4}{3k}, \quad m_z^{\dot{a}} = \frac{2}{3k^3}, \quad m_z^{\omega z} = -\frac{2}{3k}, \quad m_z^{\dot{\omega} z} = \frac{1}{5k^3}; \\ m_{x1}^{\omega x1} &= -\frac{1}{3k}, \quad m_{x1}^{\dot{\omega} x1} = \frac{4}{15\lambda k^3}. \end{aligned} \right\} \quad (22.30)$$

Pages 530-531.

Table 22.3. Total aerodynamic characteristics of reverse/inverse delta wing.

 $M = 1.1$

ω	c_y^a	$c_y^{\dot{a}}$	$c_y^{\omega_z}$	$c_y^{\dot{\omega}_z}$	m_z^a	$m_z^{\dot{a}}$	$m_z^{\omega_z}$	$m_z^{\dot{\omega}_z}$	$m_{x1}^{\omega_{x1}}$	$\lambda m_{x1}^{\dot{\omega}_{x1}}$
0	8,7286	-13,8550	2,9096	-3,4984	-2,9096	6,9275	-1,4548	2,0875	-0,7274	2,7710
0,2	8,6924	-13,7873	2,9023	-3,4870	-2,8841	6,8734	-1,4481	2,0794	-0,7261	2,7659
0,6	8,4113	-13,2584	2,8451	-3,3975	-2,7175	6,5416	-1,4102	2,0128	-0,7167	2,7153
1,0	7,8967	-12,2682	2,7375	-3,2274	-2,4172	5,8756	-1,3398	1,8957	-0,6985	2,6175
1,5	7,0525	-10,5775	2,5412	-2,9262	-1,9479	4,7870	-1,2202	1,6909	-0,6662	2,4412
2,0	6,1920	-8,6619	2,3388	-2,5659	-1,4825	3,5936	-1,0863	1,4435	-0,6270	2,2219
2,5	5,3851	-6,8272	2,1270	-2,2032	-1,1311	2,5362	-0,9594	1,1966	-0,5852	1,9867
3,5	4,4342	-4,0116	1,7862	-1,5213	-0,8609	1,0368	-0,7749	0,7545	-0,5079	1,5103
5,0	3,9463	-2,1376	1,5119	-0,9196	-0,9212	0,3224	-0,6607	0,4034	-0,4283	0,9802
∞	3,6364	0	1,2121	0	-1,2121	0	-0,6061	0	-0,3030	0

 $M = 1.2$

ω	c_y^a	$c_y^{\dot{a}}$	$c_y^{\omega_z}$	$c_y^{\dot{\omega}_z}$	m_z^a	$m_z^{\dot{a}}$	$m_z^{\omega_z}$	$m_z^{\dot{\omega}_z}$	$m_{x1}^{\omega_{x1}}$	$\lambda m_{x1}^{\dot{\omega}_{x1}}$
0	6,0303	-4,5684	2,0101	-1,1535	-2,0101	2,2842	-1,0050	0,6883	-0,5025	0,9137
0,2	6,0091	-4,5466	2,0058	-1,1498	-1,9948	2,2668	-1,0009	0,6857	-0,5018	0,9121
0,6	5,8455	-4,3767	1,9727	-1,1211	-1,8921	2,1544	-0,9789	0,6653	-0,4963	0,8957
1,0	5,5446	-4,0573	1,9099	-1,0662	-1,7235	1,9450	-0,9378	0,6275	-0,4857	0,8644
1,5	4,0457	-3,5060	1,8009	-0,9685	-1,4405	1,5898	-0,8673	0,5581	-0,4668	0,8073
2,0	4,5110	-2,8725	1,6740	-0,8503	-1,1579	1,1858	-0,7876	0,4774	-0,4436	0,7359
2,5	4,0350	-2,2483	1,5464	-0,7251	-0,9408	0,8196	-0,7106	0,3917	-0,4187	0,6564
3,5	3,4397	-1,2718	1,3373	-0,4974	-0,7643	0,2994	-0,5962	0,2446	-0,3679	0,4981
5,0	3,1815	-0,5968	1,1714	-0,2790	-0,8420	0,0619	-0,5282	0,1190	-0,3232	0,3145
∞	3,3333	0	1,1111	0	-1,1111	0	-0,5555	0	-0,2777	0

 $M = 1.4$

ω	c_y^a	$c_y^{\dot{a}}$	$c_y^{\omega_z}$	$c_y^{\dot{\omega}_z}$	m_z^a	$m_z^{\dot{a}}$	$m_z^{\omega_z}$	$m_z^{\dot{\omega}_z}$	$m_{x1}^{\omega_{x1}}$	$\lambda m_{x1}^{\dot{\omega}_{x1}}$
0	4,0825	-1,4175	1,3608	-0,3575	-1,3608	0,7088	-0,6804	0,2136	-0,3402	0,2835
0,2	4,0720	-1,4110	1,3587	-0,3568	-1,3528	0,7036	-0,6781	0,2128	-0,3399	0,2830
0,6	3,9904	-1,3602	1,3422	-0,3483	-1,3044	0,6698	-0,6671	0,2067	-0,3371	0,2781
1,0	3,8391	-1,2641	1,3107	-0,3316	-1,2160	0,6078	-0,6465	0,1951	-0,3318	0,2687
1,5	3,5847	-1,0959	1,2575	-0,3021	-1,0722	0,4980	-0,6108	0,1742	-0,3226	0,2515
2,0	3,3060	-0,8985	1,1940	-0,2658	-0,9241	0,3739	-0,5696	0,1490	-0,3099	0,2297
2,5	3,0510	-0,6985	1,1236	-0,2264	-0,8028	0,2524	-0,5285	0,1223	-0,2976	0,2050
3,5	2,7227	-0,3697	1,0112	-0,1522	-0,6995	0,0702	-0,4666	0,0738	-0,2729	0,1545
5,0	2,6235	-0,1299	0,9247	-0,0773	-0,7731	0,0174	-0,4323	0,0298	-0,2469	0,0933
∞	2,8572	0	0,9524	0	-0,9524	0	-0,4762	0	-0,2380	0

DOC = 771543

M = 1,6

980-

ω	c_y^a	$c_y^{\dot{a}}$	$c_y^{\omega_z}$	$c_y^{\dot{\omega}_z}$	m_z^a	$m_z^{\dot{a}}$	$m_z^{\omega_z}$	$m_z^{\dot{\omega}_z}$	$m_{x1}^{\omega_{x1}}$	$\lambda m_{x1}^{\dot{\omega}_{x1}}$
0	3,2026	-0,6843	1,0675	-0,1728	-1,0675	0,3415	-0,5338	0,1031	-0,2669	0,1366
0,2	3,1963	-0,6813	1,0663	-0,1723	-1,0623	0,3396	-0,5322	0,1027	-0,2666	0,1366
0,6	3,1471	-0,6573	1,0563	-0,1682	-1,0332	0,3238	-0,5256	0,0999	-0,2650	0,1344
1,0	3,0556	-0,6091	1,0373	-0,1605	-0,9797	0,2932	-0,5131	0,0944	-0,2619	0,1299
1,5	2,9004	-0,5316	1,0038	-0,1464	-0,8916	0,2420	-0,4914	0,0845	-0,2553	0,1217
2,0	2,7278	-0,4360	0,9698	-0,1289	-0,7992	0,1814	-0,4661	0,0723	-0,2489	0,1113
2,5	2,5672	-0,3374	0,9223	-0,1097	-0,7216	0,1212	-0,4407	0,0592	-0,2409	0,0994
3,5	2,3567	-0,1696	0,8514	-0,0734	-0,6530	0,0275	-0,4010	0,0349	-0,2255	0,0745
5,0	2,3138	-0,0426	0,7982	-0,0340	-0,7166	0,0219	-0,3805	0,0128	-0,2092	0,0434
∞	2,5000	0	0,8333	0	-0,8333	0	-0,4167	0	-0,2083	0

M = 2,0

ω	c_y^a	$c_y^{\dot{a}}$	$c_y^{\omega_z}$	$c_y^{\dot{\omega}_z}$	m_z^a	$m_z^{\dot{a}}$	$m_z^{\omega_z}$	$m_z^{\dot{\omega}_z}$	$m_{x1}^{\omega_{x1}}$	$\lambda m_{x1}^{\dot{\omega}_{x1}}$
0	2,3094	-0,2566	0,7698	-0,0648	-0,7698	0,1283	-0,3849	0,0387	-0,1925	0,0513
0,2	2,3085	-0,2555	0,7692	-0,0646	-0,7671	0,1274	-0,3840	0,0385	-0,1923	0,0512
0,6	2,2838	-0,2468	0,7646	-0,0631	-0,7536	0,1216	-0,3811	0,0375	-0,1916	0,0505
1,0	2,2412	-0,2301	0,7559	-0,0605	-0,7286	0,1107	-0,3752	0,0357	-0,1901	0,0488
1,5	2,1692	-0,2005	0,7401	-0,0551	-0,6870	0,0911	-0,3650	0,0318	-0,1876	0,0458
2,0	2,0857	-0,1645	0,7212	-0,0485	-0,6425	0,0685	-0,3529	0,0273	-0,1840	0,0419
2,5	2,0074	-0,1265	0,7013	-0,0413	-0,6040	0,0451	-0,3407	0,0223	-0,1802	0,0375
3,5	1,9025	-0,0593	0,6667	-0,0269	-0,5685	0,0068	-0,3211	0,0128	-0,1727	0,0279
5,0	1,8949	-0,0058	0,6415	-0,0111	-0,6111	0,0150	-0,3119	0,0024	-0,1649	0,0155
∞	2,0000	0	0,6667	0	-0,6667	0	-0,3333	0	-0,1666	0

M = 3,0

ω	c_y^a	$c_y^{\dot{a}}$	$c_y^{\omega_z}$	$c_y^{\dot{\omega}_z}$	m_z^a	$m_z^{\dot{a}}$	$m_z^{\omega_z}$	$m_z^{\dot{\omega}_z}$	$m_{x1}^{\omega_{x1}}$	$\lambda m_{x1}^{\dot{\omega}_{x1}}$
0	1,4142	-0,0589	0,4714	-0,0149	-0,4714	0,0295	-0,2357	0,0089	-0,1179	0,0118
0,2	1,4134	-0,0586	0,4712	-0,0148	-0,4703	0,0292	-0,2353	0,0089	-0,1178	0,0118
0,6	1,4072	-0,0567	0,4700	-0,0144	-0,4666	0,0280	-0,2345	0,0086	-0,1176	0,0116
1,0	1,3955	-0,0530	0,4675	-0,0129	-0,4598	0,0255	-0,2329	0,0082	-0,1172	0,0112
1,5	1,3753	-0,0463	0,4632	-0,0127	-0,4482	0,0211	-0,2300	0,0073	-0,1164	0,0105
2,0	1,3521	-0,0380	0,4580	-0,0112	-0,4362	0,0158	-0,2267	0,0063	-0,1155	0,0097
2,5	1,3296	-0,0290	0,4524	-0,0095	-0,4243	0,0103	-0,2232	0,0052	-0,1131	0,0086
3,5	1,2988	-0,0126	0,4424	-0,0060	-0,4136	0,0007	-0,2175	0,0029	-0,1112	0,0064
5,0	1,3011	0,0015	0,4355	-0,0021	-0,4296	0,0052	-0,2151	0,0004	-0,1101	0,0034
∞	1,3333	0	0,4444	0	-0,4444	0	-0,2222	0	-0,1110	0

M = 5,0

ω	c_y^a	$c_y^{\dot{a}}$	$c_y^{\omega_z}$	$c_y^{\dot{\omega}_z}$	m_z^a	$m_z^{\dot{a}}$	$m_z^{\omega_z}$	$m_z^{\dot{\omega}_z}$	$m_{x1}^{\omega_{x1}}$	$\lambda m_{x1}^{\dot{\omega}_{x1}}$
0	0,8165	-0,0113	0,2722	-0,0029	-0,2722	0,0057	-0,1361	0,0017	-0,0680	0,0023
0,2	0,8163	-0,0113	0,2721	-0,0029	-0,2717	0,0056	-0,1359	0,0017	-0,0680	0,0023
0,6	0,8150	-0,0109	0,2720	-0,0028	-0,2709	0,0054	-0,1357	0,0017	-0,0677	0,0022
1,0	0,8126	-0,0102	0,2713	-0,0027	-0,2695	0,0049	-0,1354	0,0016	-0,0679	0,0022
1,5	0,8084	-0,0089	0,2705	-0,0025	-0,2671	0,0041	-0,1348	0,0014	-0,0677	0,0020
2,0	0,8034	-0,0073	0,2693	-0,0022	-0,2652	0,0031	-0,1341	0,0012	-0,0676	0,0019
2,5	0,7986	-0,0056	0,2682	-0,0018	-0,2620	0,0020	-0,1334	0,0010	-0,0673	0,0017
3,5	0,7920	-0,0023	0,2660	-0,0012	-0,2596	0,0000	-0,1321	0,0003	-0,0669	0,0012
5,0	0,7930	0,0005	0,2646	-0,0004	-0,2635	0,0012	-0,1316	0,0000	-0,0664	0,0006
∞	0,8000	0	0,2667	0	-0,2667	0	-0,1333	0	-0,0667	0

Page 532.

In other limiting case, $\omega \rightarrow \infty$, the coefficients of the aerodynamic derivatives of reverse/inverse delta wing are determined by the formulas

$$\left. \begin{aligned} p^{\omega x} &= \frac{\bar{z}\lambda}{k} \text{ when } \xi = 0, \quad p^{\omega x} = \frac{\bar{z}\lambda}{M} \text{ when } \xi \neq 0, \quad p^{\omega x} = 0; \\ c_y^a &= \frac{4}{M}, \quad c_y^{\omega z} = \frac{2(1-\bar{z})}{M}, \quad m_z^a = -\frac{2}{M}, \\ m_z^{\omega z} &= -\frac{4(1-\bar{z})}{3M}, \quad m_z^{\omega x} = -\frac{\lambda\bar{z}}{2M}; \\ c_y^{\dot{a}} &= c_y^{\dot{\omega}z} = m_z^{\dot{a}} = m_z^{\dot{\omega}z} = m_z^{\dot{\omega}x} = 0; \\ c_y^a &= \frac{4}{M}, \quad c_y^{\omega z} = \frac{4}{3M}, \quad m_z^a = -\frac{4}{3M}, \quad m_z^{\omega z} = -\frac{2}{3M}, \\ m_{x1}^{\omega x1} &= -\frac{1}{3M}; \quad c_y^{\dot{a}} = c_y^{\dot{\omega}z} = m_z^{\dot{a}} = m_z^{\dot{\omega}z} = m_{x1}^{\dot{\omega}x1} = 0. \end{aligned} \right\} (22.31)$$

All relationship/ratios (22.30), (22.31), and also the data of tables 22.3 are given in the standard, connected with wing coordinate system with beginning on the leading edge of root wing chord (centering $\bar{x}_T = 0$). For characteristic linear dimension (besides $m_{x1}^{\omega x1}, m_{x1}^{\dot{\omega}x1}$) is undertaken the value of the root chord b . Moment coefficient m_{x1} are referred to the spread/scope of wing l , and angular velocity ω_{x1} is referred to the semirange of wing $l/2$.

The coefficients aerodynamic derivative direct/straight of delta wings it is easy to obtain by means of calculation of the characteristics of reverse/inverse delta wing on the relationship/ratios, which escape/ensue from reciprocity theorem (see §2 of chapter VII).

Pages 533-534.

Table 22.4. Total aerodynamic characteristics of direct/straight delta wing.

M = 1.1

ω	c_y^α	$c_y^{\dot{\alpha}}$	$c_y^{\omega_z}$	$c_y^{\dot{\omega}_z}$	m_z^α	$m_z^{\dot{\alpha}}$	$m_z^{\omega_z}$	$m_z^{\dot{\omega}_z}$	$m_{x1}^{\omega_{x1}}$	$\lambda m_{x1}^{\dot{\omega}_{x1}}$
0	8,7286	-13,8550	5,9192	-6,9968	-5,8192	10,3913	-4,3644	5,5667	-0,7274	2,7710
0,2	8,9924	-13,7873	5,8033	-6,9138	-5,7901	10,3003	-4,3541	5,5063	-0,7261	2,7659
0,6	8,4113	-13,2584	5,6938	-6,7346	-5,5662	9,8609	-4,2589	5,3321	-0,7167	2,7153
1,0	7,8967	-12,2682	5,4795	-6,3926	-5,1592	9,0408	-4,0818	5,0609	-0,6985	2,6175
1,5	7,1525	-10,5775	5,1046	-5,7905	-4,5113	7,6513	-3,7836	4,5552	-0,6662	2,4412
2,0	6,1920	-8,6619	4,7095	-5,0683	-3,8532	6,0960	-3,4570	3,9459	-0,6270	2,2219
2,5	5,3851	-6,8272	4,2520	-4,2910	-3,2581	4,6240	-3,0864	3,2844	-0,5852	1,9867
3,5	4,4342	-4,0116	3,5733	-2,9748	-2,6480	2,4903	-2,5620	2,2080	-0,5079	1,5105
5,0	3,9463	-2,1376	3,0251	-1,8152	-2,4344	1,2180	-2,1739	1,2990	-0,4283	0,9802
∞	3,5364	0	2,4242	0	-2,4242	0	-1,8182	0	-0,3030	0

M = 1.2

ω	c_y^α	$c_y^{\dot{\alpha}}$	$c_y^{\omega_z}$	$c_y^{\dot{\omega}_z}$	m_z^α	$m_z^{\dot{\alpha}}$	$m_z^{\omega_z}$	$m_z^{\dot{\omega}_z}$	$m_{x1}^{\omega_{x1}}$	$\lambda m_{x1}^{\dot{\omega}_{x1}}$
0	6,0303	-4,5684	4,0202	-2,3070	-4,0202	3,4263	-3,0150	1,8355	-0,5025	0,9137
0,2	6,0091	-4,5466	4,0143	-2,2798	-4,0033	3,3968	-3,0094	1,8157	-0,5018	0,9121
0,6	5,8455	-4,3767	3,9534	-2,2223	-3,8728	3,2556	-2,9596	1,7665	-0,4963	0,8957
1,0	5,5446	-4,0573	3,8211	-2,1123	-3,6317	2,9911	-2,8490	1,6736	-0,4857	0,8644
1,5	5,0457	-3,5060	3,6052	-1,9162	-3,2448	2,5375	-2,6716	1,5058	-0,4668	0,8073
2,0	4,5110	-2,8725	3,3531	-1,6867	-2,8370	2,0222	-2,4667	1,3138	-0,4436	0,7359
2,5	4,0350	-2,2483	3,0942	-1,4287	-2,4886	1,5232	-2,2584	1,0953	-0,4187	0,6564
3,5	3,4397	-1,2718	2,6754	-0,9724	-2,1034	0,7744	-1,9343	0,7196	-0,3679	0,4981
5,0	3,1815	-0,5968	2,3751	-0,5349	-2,0101	0,3178	-1,7325	0,3749	-0,3232	0,3145
∞	3,3333	0	2,2222	0	-2,2222	0	-1,6667	0	-0,2777	0

M = 1.4

ω	c_y^α	$c_y^{\dot{\alpha}}$	$c_y^{\omega_z}$	$c_y^{\dot{\omega}_z}$	m_z^α	$m_z^{\dot{\alpha}}$	$m_z^{\omega_z}$	$m_z^{\dot{\omega}_z}$	$m_{x1}^{\omega_{x1}}$	$\lambda m_{x1}^{\dot{\omega}_{x1}}$
0	4,0825	-1,4175	2,7116	-0,7150	-2,7216	1,0632	-2,0412	0,5696	-0,3402	0,2835
0,2	4,0720	-1,4110	2,7192	-0,7074	-2,7133	1,0542	-2,0386	0,5634	-0,3399	0,2830
0,6	3,9904	-1,3602	2,6800	-0,6904	-2,6482	1,0119	-2,0109	0,5488	-0,3371	0,2781
1,0	3,8391	-1,2641	2,6231	-0,6563	-2,5284	0,9325	-1,9589	0,5198	-0,3318	0,2687
1,5	3,5847	-1,0999	2,5125	-0,5979	-2,3272	0,7978	-1,8658	0,4700	-0,3226	0,2515
2,0	3,3060	-0,8985	2,3819	-0,5246	-2,1120	0,6327	-1,7575	0,4078	-0,3099	0,2297
2,5	3,0510	-0,6985	2,2482	-0,4461	-1,9274	0,4721	-1,6531	0,3420	-0,2976	0,2050
3,5	2,7227	-0,3697	2,0232	-0,2995	-1,7115	0,2175	-1,4786	0,2211	-0,2729	0,1545
5,0	2,6235	-0,1299	1,8474	-0,1473	-1,6988	0,0526	-1,3580	0,0998	-0,2469	0,0933
∞	2,8572	0	1,9048	0	-1,9048	0	-1,4286	0	-0,2381	0

DOC = 771543

M = 1,6

-983-

ω	c_y^a	$c_y^{\dot{a}}$	$c_y^{\omega_z}$	$c_y^{\dot{\omega}_z}$	m_z^a	$m_z^{\dot{a}}$	$m_z^{\omega_z}$	$m_z^{\dot{\omega}_z}$	$m_{x1}^{\omega_{x1}}$	$\lambda m_{x1}^{\dot{\omega}_{x1}}$
0	3,2026	-0,6843	2,1350	-0,3456	-2,1350	0,5123	-1,6014	0,2749	-0,2669	0,1369
0,2	3,1963	-0,6813	2,1340	-0,3417	-2,1300	0,5090	-1,5990	0,2721	-0,2666	0,1366
0,6	3,1471	-0,6573	2,1139	-0,3335	-2,0908	0,4891	-1,5832	0,2652	-0,2650	0,1344
1,0	3,0556	-0,6092	2,0759	-0,3160	-2,0183	0,4488	-1,5517	0,2498	-0,2619	0,1299
1,5	2,9004	-0,5316	2,0088	-0,2896	-1,8966	0,3852	-1,4964	0,2277	-0,2553	0,1217
2,0	2,7278	-0,4360	1,9286	-0,2546	-1,7580	0,3071	-1,4249	0,1980	-0,2489	0,1119
2,5	2,5672	-0,3350	1,8456	-0,2134	-1,6449	0,2253	-1,3640	0,1657	-0,2409	0,0994
3,5	2,3567	-0,1696	1,7037	-0,1421	-1,5053	0,0962	-1,2533	0,1036	-0,2255	0,0745
5,0	2,3138	-0,0426	1,5972	-0,0645	-1,5156	0,0086	-1,1795	0,0443	-0,2092	0,0434
∞	2,5000	0	1,6667	0	-1,6667	0	-1,2500	0	-0,2083	0

M = 2,0

ω	c_y^a	$c_y^{\dot{a}}$	$c_y^{\omega_z}$	$c_y^{\dot{\omega}_z}$	m_z^a	$m_z^{\dot{a}}$	$m_z^{\omega_z}$	$m_z^{\dot{\omega}_z}$	$m_{x1}^{\omega_{x1}}$	$\lambda m_{x1}^{\dot{\omega}_{x1}}$
0	2,3094	-0,2566	1,5396	-0,1296	-1,5396	0,1925	-1,1547	0,1032	-0,1925	0,0513
0,2	2,3065	-0,2555	1,5394	-0,1281	-1,5373	0,1909	-1,1542	0,1020	-0,1923	0,0512
0,6	2,2838	-0,2468	1,5302	-0,1252	-1,5192	0,1837	-1,1467	0,0996	-0,1916	0,0505
1,0	2,2412	-0,2301	1,5126	-0,1194	-1,4853	0,1696	-1,1319	0,0946	-0,1901	0,0488
1,5	2,1692	-0,2005	1,4822	-0,1094	-1,4292	0,1454	-1,1071	0,0861	-0,1876	0,0458
2,0	2,0857	-0,1645	1,4432	-0,0960	-1,3645	0,1160	-1,0749	0,0748	-0,1840	0,0419
2,5	2,0074	-0,1265	1,4034	-0,0814	-1,3061	0,0852	-1,0428	0,0624	-0,1802	0,0375
3,5	1,8949	-0,0058	1,2838	-0,0208	-1,2534	-0,0053	-0,9542	0,0123	-0,1649	0,0155
∞	2,0000	0	1,3333	0	-1,3333	0	-1,0000	0	-0,1666	0

M = 3,0

ω	c_y^a	$c_y^{\dot{a}}$	$c_y^{\omega_z}$	$c_y^{\dot{\omega}_z}$	m_z^a	$m_z^{\dot{a}}$	$m_z^{\omega_z}$	$m_z^{\dot{\omega}_z}$	$m_{x1}^{\omega_{x1}}$	$\lambda m_{x1}^{\dot{\omega}_{x1}}$
0	1,4142	-0,0589	0,9428	-0,0298	-0,9428	0,0443	-0,7071	0,0237	-0,1179	0,0118
0,2	1,4131	-0,0586	0,9431	-0,0294	-0,9422	0,0438	-0,7072	0,0234	-0,1178	0,0118
0,6	1,4072	-0,0567	0,9406	-0,0288	-0,9372	0,0423	-0,7051	0,0229	-0,1176	0,0116
1,0	1,3955	-0,0530	0,9357	-0,0275	-0,9280	0,0391	-0,7011	0,0218	-0,1172	0,0112
1,5	1,3753	-0,0463	0,9271	-0,0252	-0,9121	0,0336	-0,6939	0,0198	-0,1164	0,0105
2,0	1,3521	-0,0382	0,9159	-0,0224	-0,8941	0,0270	-0,6846	0,0172	-0,1155	0,0097
2,5	1,3296	-0,0290	0,9053	-0,0184	-0,8772	0,0195	-0,6761	0,0144	-0,1131	0,0086
3,5	1,2988	-0,0127	0,8852	-0,0119	-0,8574	0,0066	-0,6603	0,0086	-0,1112	0,0064
5,0	1,3011	-0,0015	0,8715	-0,0037	-0,8656	-0,0036	-0,6511	0,0020	-0,1101	0,0034
∞	1,3332	0	0,8889	0	-0,8889	0	-0,6666	0	-0,1110	0

M = 5,0

ω	c_y^a	$c_y^{\dot{a}}$	$c_y^{\omega_z}$	$c_y^{\dot{\omega}_z}$	m_z^a	$m_z^{\dot{a}}$	$m_z^{\omega_z}$	$m_z^{\dot{\omega}_z}$	$m_{x1}^{\omega_{x1}}$	$\lambda m_{x1}^{\dot{\omega}_{x1}}$
0	0,8165	-0,0113	0,5444	-0,0057	-0,5444	0,0085	-0,4083	0,0046	-0,0680	0,0023
0,2	0,8163	-0,0113	0,5446	-0,0057	-0,5442	0,0084	-0,4084	0,0045	-0,0680	0,0023
0,6	0,8150	-0,0109	0,5441	-0,0055	-0,5430	0,0082	-0,4078	0,0044	-0,0680	0,0022
1,0	0,8126	-0,0102	0,5431	-0,0053	-0,5413	0,0075	-0,4072	0,0041	-0,0672	0,0022
1,5	0,8084	-0,0089	0,5413	-0,0049	-0,5379	0,0065	-0,4056	0,0038	-0,0677	0,0020
2,0	0,8034	-0,0073	0,5382	-0,0043	-0,5341	0,0052	-0,4030	0,0033	-0,0676	0,0019
2,5	0,7986	-0,0056	0,5366	-0,0036	-0,5301	0,0037	-0,4018	0,0028	-0,0673	0,0017
3,5	0,7920	-0,0023	0,5324	-0,0023	-0,5260	0,0011	-0,3985	0,0016	-0,0669	0,0012
5,0	0,7930	-0,0005	0,5295	-0,0006	-0,5281	-0,0009	-0,3965	0,0003	-0,0664	0,0006
∞	0,8000	0	0,5333	0	-0,5333	0	-0,4000	0	-0,0667	0

Page 535.

The obtained by this recalculation coefficients aerodynamic derivative direct/straight of delta wings in the range of numbers $M = 1.1-5.0$, $\omega = 0$ are given in table 22.4 and are given in Fig. 22.10-22.14.

Formulas, for the coefficients aerodynamic derivative these wings in the extreme case $\omega \rightarrow 0$ take the form

$$\left. \begin{aligned} c_y^a &= \frac{4}{k}, \quad c_y^{\dot{a}} = -\frac{4}{3k^3}, \quad c_y^{\omega_z} = \frac{8}{3k}, \quad c_y^{\dot{\omega}_z} = -\frac{2}{3k^3}; \\ m_z^a &= -\frac{8}{3k}, \quad m_z^{\dot{a}} = \frac{1}{k^3}, \quad m_z^{\omega_z} = -\frac{2}{k}, \quad m_z^{\dot{\omega}_z} = \frac{8}{15k^3}; \\ m_{x1}^{\omega_{x1}} &= -\frac{1}{43k}, \quad m_{x1}^{\dot{\omega}_{x1}} = \frac{4}{15\lambda k^3}; \\ c_y^{\Delta} &= \frac{4}{k}, \quad c_y^{\dot{\Delta}} = -\frac{4M^2}{k^3}, \quad m_z^{\Delta} = -\frac{8}{3k}, \quad m_z^{\dot{\Delta}} = -\frac{2M^2}{k^3}. \end{aligned} \right\} \quad (22.32)$$

For given Strouhal number $\omega \rightarrow \infty$ the formulas will take the form

$$\left. \begin{aligned} c_y^a &= \frac{4}{M}, \quad c_y^{\omega_z} = \frac{8}{3M}, \quad m_z^a = -\frac{8}{3M}, \\ m_z^{\omega_z} &= -\frac{2}{M}, \quad m_{x1}^{\omega_{x1}} = -\frac{1}{3M}; \\ c_y^{\dot{a}} &= c_y^{\dot{\omega}_z} = m_z^{\dot{a}} = m_z^{\dot{\omega}_z} = m_{x1}^{\dot{\omega}_{x1}} = c_y^{\Delta} = c_y^{\dot{\Delta}} = m_z^{\Delta} = m_z^{\dot{\Delta}} = 0. \end{aligned} \right\} \quad (22.33)$$

As earlier, the data of tables and formula are given in the standard system of the axes with beginning on the spout of root chord ($x_T = 0$).

Let us give also formulas for the coefficients aerodynamic derivative of sweptback wings in the case $\omega \rightarrow \infty$.

Page 536.

AD-A049 000

FOREIGN TECHNOLOGY DIV WRIGHT-PATTERSON AFB OHIO

F/G 1/3

A WING IN AN UNSTEADY GAS FLOW. PART 2, (U)

SEP 77 S M BELOTSEKOVSKIY, B K SKRIPACH

FTD-ID(RS)T-1534-77-PT-2

NL

UNCLASSIFIED

6 OF 6

ADAO49000



END
DATE
FILMED

3-78

DDC

They take the form

$$\left. \begin{aligned} c_y^a &= \frac{4}{M}, \quad c_y^{\omega z} = \frac{1}{M} \left(\frac{\lambda \lg \chi_0}{3} \frac{\eta+2}{\eta} + \frac{4}{3} \frac{1+\eta+\eta^2}{\eta+\eta^2} \right); \\ m_z^a &= -c_y^{\omega z}, \quad m_{x1}^{\omega z} = -\frac{3+\eta}{3M(1+\eta)}, \\ m_z^{\omega z} &= -\frac{2}{3M} \left[\frac{\lambda^2 \lg^2 \chi_0}{16\eta^2} (3+4\eta+\eta^2) + \right. \\ &\quad \left. + \frac{\lambda \lg \chi_0}{4\eta^2} (3+2\eta+\eta^2) + \frac{\eta^2+1}{\eta^2} \right]. \end{aligned} \right\} (22.34)$$

Here λ is lengthening, η is contraction, χ_0 is a sweep angle on leading edge.

Comparing the appropriate formulas for the cases $\omega \rightarrow \infty$ and $\omega \rightarrow 0$, given in the preceding/previous paragraphs, we see that the coefficients of aerodynamic derivatives in terms of kinematic parameters without points with $\omega \rightarrow \infty$ are obtained from their appropriate expressions at $\omega \rightarrow 0$ simple replacement of value $k = \sqrt{M^2 - 1}$ by number M .

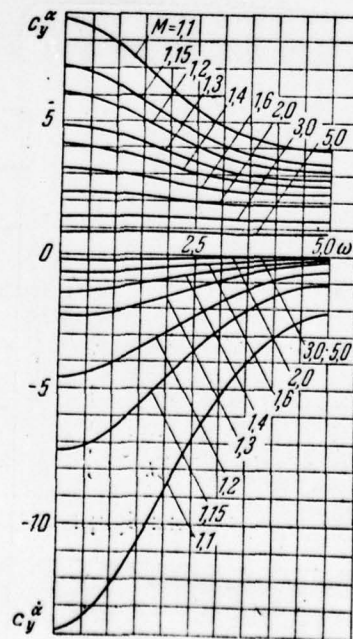


FIG. 22.10.

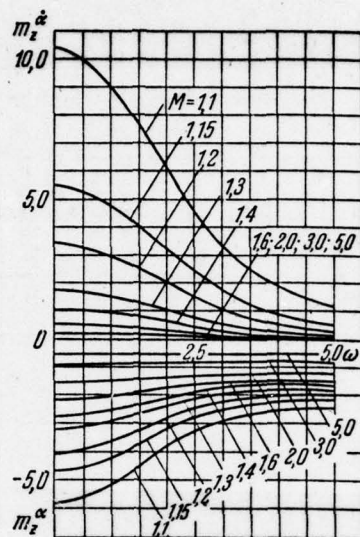


FIG. 22.11

Fig. 22.10. Delta wings with over sonic edges. Coefficients of aerodynamic derivatives c_y^{α} , $c_y^{\dot{\alpha}}$.

Fig. 22.11. Delta wings with supersonic edges. Coefficients of aerodynamic derivatives m_z^{α} , $m_z^{\dot{\alpha}}$, ($\bar{x}_T=0$).

Page 537.

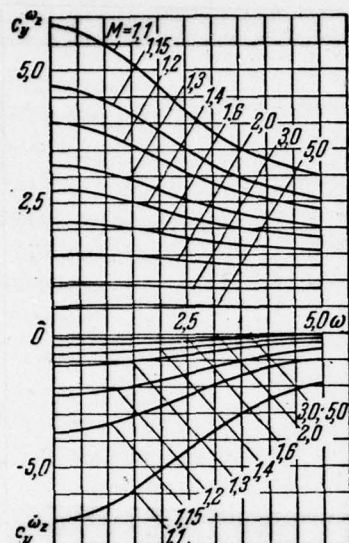


FIG. 22.12.

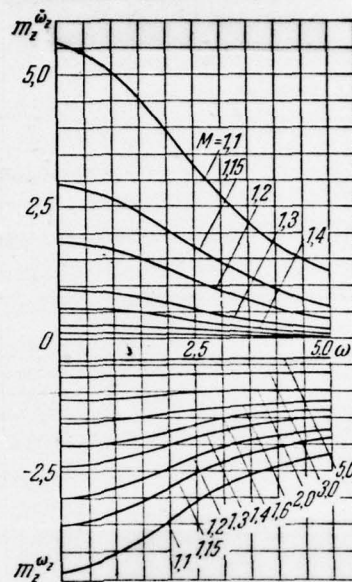


FIG. 22.13

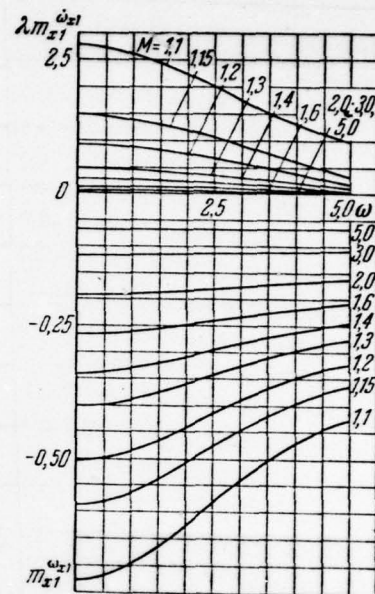


FIG. 22.14.

Fig. 22.12. Delta wings with supersonic edges. Coefficients of aerodynamic derivatives $c_y^{\omega_z}, c_y^{\omega_x}, (\bar{x}_T=0)$.

Fig. 22.13. delta wings with supersonic edges. Coefficients of aerodynamic derivatives $m_z^{\omega_z}, m_z^{\omega_x}, (\bar{x}_T=0)$.

Fig. 22.14. Delta wings with supersonic edges. Coefficients of aerodynamic derivatives $\lambda m_{x1}^{\omega_z}, m_{x1}^{\omega_x}$.

Thus, for a limiting case $\omega \rightarrow \infty$ the coefficients of

aerodynamic derivatives with points (c^{q_i}) turn into zero, and coefficients without points approach the determined limits, by the being functions of number M and of the geometric parameters of wing.

Under the influence on the wing of harmonic gust, all the corresponding coefficients of aerodynamic derivatives (c^A, c^{Δ}) with $\omega \rightarrow \infty$ vanish.

§5. Expressions for the potentials of the disturbed speeds taking into account end effect.

The given in the first paragraph formulas make it possible to calculate the potential of the disturbed speeds only for those points of spaces, whose range of integration σ does not fall outside wing edges, where the derivatives $B_i = \partial \varphi^{q_i} / \partial \eta$ and $E_i = \partial \varphi^{\Delta_i} / \partial \eta$ are assigned. In order to calculate velocity potentials for points, whose range of integration σ falls outside edges, i.e., taking into account end effect, it is necessary from the boundary conditions of the task on plane OΞξ to determine derivative $\partial \varphi / \partial \eta$ in that part of the range of integration, where it is unknown.

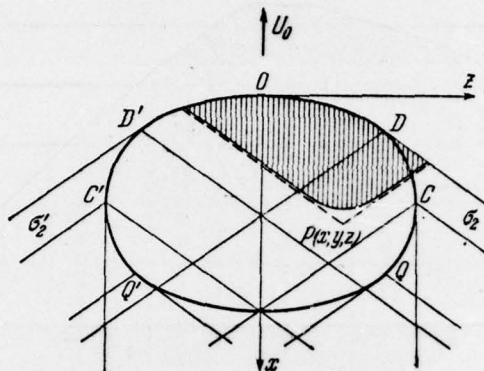


Fig. 22.15. range of integration on the wing of arbitrary planform.

Let us examine the wing of arbitrary planform (Fig. 22.15) and note on its duct some characteristic points D , C on right and D' , C' on left the halves of wing.

The point D on leading wing edge is determined by the facts that to the left from it is satisfied the condition

$$\left| \frac{dx(z)}{dz} \right| \leq \frac{1}{\sqrt{M^2 - 1}}, \quad (22.35)$$

where $x(z)$ - the equation of leading edge. To the right from point D this condition is not observed. It is analogous, the point D' is determined by the facts that to the right from it condition (22.35) is satisfied, but to the left - no. This means that at points D and D' generatrices of characteristic cones concern wing contour. As it follows from condition (22.35), on arc DD' the velocity component, normal to wing contour, will be supersonic; therefore it they call by the supersonic part of leading edge.

Points C, C' correspond to extreme tangent to wing contour, parallel to speed U_0 . The arcs DC, D'C' are the subsonic part of the leading edge, while arc CQ, C'Q' they correspond to the subsonic parts of the trailing wing edge. Arc QQ' will be the supersonic part of the trailing edge.

Let certain point of space P (x, y, z) be arranged within characteristic cone with apex/vertex in point D or D' (see Fig. 22.15). At this point manifests itself the end effect, since for it range of integration σ intersects not only with wing surface, but also with the range σ_2 , which is arranged outside wing within characteristic cone with apex/vertex in point D and outside characteristic cones with apex/vertexes in points D' and C. Let us find integral equations for determining the tapers

$$B_i^{(2)} = \partial \varphi^{q_i} / \partial \eta, \quad E_i^{(2)} = \partial \varphi^{q_i} / \partial \eta$$

in range σ_2 . (Here and throughout as in chapter of XX, the superscripts of B_i, E_i designate the affiliation/accessory of the functions of the corresponding range). Is expressed by formulas (20.11) at the arbitrary point N (x, 0, z) that which was arrange/located in range σ_2 (Fig. 22.16), velocity potentials φ^{q_i} and φ^{q_i} , let us pass to dimensionless coordinates (20.10) and require, in order to according to condition (20.37).

$$\varphi^{q_i}(\xi_i, 0, \zeta_i) = \varphi^{q_i}(\xi_i, 0, \zeta_i) = 0. \quad (22.36)$$

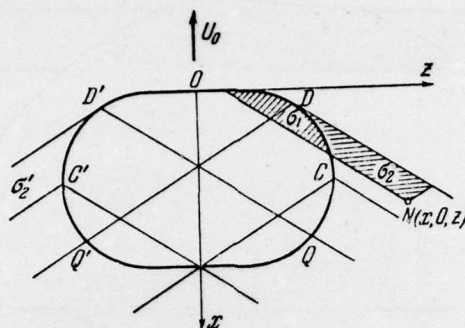


Fig. 22.16. To the determination of tapers in the range of end effect.

Page 540.

Range of integration σ let us break into two parts: σ_1 , that lies on wing, and σ_2 outside it (Fig. 22.16). In range σ_1 the derivatives $\dot{B}_i^{(1)}$, $E_i^{(1)}$ are known and are determined by relationship/ratios (22.2), while in range σ_2 the derivatives $B_i^{(2)}$, $E_i^{(2)}$ are unknown values. In accordance with condition (22.36) it is possible to write

$$\begin{aligned}
& \int_{\sigma_1} \int \left\{ B_l^{(1)}(\xi, 0, \zeta) + \right. \\
& \quad \left. + \omega \frac{k^2}{M^2} E_l^{(1)}(\xi, 0, \zeta) \operatorname{tg} [\omega (\xi_1 - \xi)] \right\} \cos [\omega (\xi_1 - \xi)] \cos \left(\frac{\omega \rho}{M} \right) \frac{d\xi d\zeta}{\rho} = \\
& \quad = - \int_{\sigma_1} \int \left\{ B_l^{(2)}(\xi, 0, \zeta) + \right. \\
& \quad \left. + \omega \frac{k^2}{M^2} E_l^{(2)}(\xi, 0, \zeta) \operatorname{tg} [\omega (\xi_1 - \xi)] \right\} \cos [\omega (\xi_1 - \xi)] \cos \left(\frac{\omega \rho}{M} \right) \frac{d\xi d\zeta}{\rho}, \\
& \int_{\sigma_1} \int \left\{ \omega \frac{k^2}{M^2} E_l^{(1)}(\xi, 0, \zeta) \operatorname{ctg} [\omega (\xi_1 - \xi)] - \right. \\
& \quad \left. - B_l^{(1)}(\xi, 0, \zeta) \right\} \sin [\omega (\xi_1 - \xi)] \cos \left(\frac{\omega \rho}{M} \right) \frac{d\xi d\zeta}{\rho} = \\
& \quad = - \int_{\sigma_1} \int \left\{ \omega \frac{k^2}{M^2} E_l^{(2)}(\xi, 0, \zeta) \operatorname{ctg} [\omega (\xi_1 - \xi)] - \right. \\
& \quad \left. - B_l^{(2)}(\xi, 0, \zeta) \right\} \sin [\omega (\xi_1 - \xi)] \cos \left(\frac{\omega \rho}{M} \right) \frac{d\xi d\zeta}{\rho}, \\
& \rho = \sqrt{(\xi_1 - \xi)^2 - k^2 (\zeta_1 - \zeta)^2}, \quad k = \sqrt{M^2 - 1}; \quad l = 1, 2, 3, 4.
\end{aligned} \tag{22.37}$$

Thus, for determining function $B_l^{(2)}(\xi, 0, \zeta)$, $E_l^{(3)}(\xi, 0, \zeta)$ we have a system of two integral equations. Considerable simplification is obtained in the case of small Strouhal numbers ($p \rightarrow 0$). By passage to the limit $\omega \rightarrow 0$ system (22.37) is converted as follows:

$$\begin{aligned}
& \int_{\sigma_1} \int B_l^{(2)}(\xi, 0, \zeta) \frac{d\xi d\zeta}{\rho} = - \int_{\sigma_1} \int B_l^{(1)}(\xi, 0, \zeta) \frac{d\xi d\zeta}{\rho}, \\
& \int_{\sigma_1} \int \left[\frac{k^2}{M^2} E_l^{(2)}(\xi, 0, \zeta) - (\xi_1 - \xi) B_l^{(2)}(\xi, 0, \zeta) \right] \frac{d\xi d\zeta}{\rho} = \\
& \quad = - \int_{\sigma_1} \int \left[\frac{k^2}{M^2} E_l^{(1)}(\xi, 0, \zeta) - (\xi_1 - \xi) B_l^{(1)}(\xi, 0, \zeta) \right] \frac{d\xi d\zeta}{\rho}.
\end{aligned} \tag{22.38}$$

Let us introduce characteristic coordinates β, x by formulas

(20.12), (20.17). In new coordinates instead of the first equation of system (22.38) we have

$$\int_{\sigma_1} \int B_i^{(2)}(\beta, \kappa) \frac{d\beta d\kappa}{V(\beta_1 - \beta)(\kappa_1 - \kappa)} = - \int_{\sigma_1} \int B_i^{(1)}(\beta, \kappa) \frac{d\beta d\kappa}{V(\beta_1 - \beta)(\kappa_1 - \kappa)}.$$

The solution to this equation is given in [1.15] and equally

$$B_i^{(2)}(\beta_1, \kappa_1) = - \frac{1}{\pi} \frac{1}{V\kappa_1 - \psi(\beta_1)} \int_{\psi_1(\beta_1)}^{\psi(\beta_1)} B_i^{(1)}(\beta_1, \kappa) \frac{V\sqrt{\psi(\beta_1) - \kappa}}{\kappa_1 - \kappa} d\kappa, \quad (22.39)$$

where $\kappa = \psi(\beta_1)$ - the equation of the subsonic part of the leading edge DC, $\kappa = \psi_1(\beta_1)$ - the equation of the supersonic part of the leading edge of arc DD* wing contour in characteristic coordinates.

the second equation of system (22.38) in new coordinates takes the form

$$\int_{\beta_d}^{\beta_1} \frac{d\beta}{V\beta_1 - \beta} \left\{ \frac{k^2}{M^2} \int_{\psi(\beta)}^{\kappa_1} \frac{E_i^{(2)}(\beta, \kappa)}{V\kappa_1 - \kappa} d\kappa + \frac{k^2}{M^2} \int_{\psi_1(\beta)}^{\psi(\beta)} \frac{E_i^{(1)}(\beta, \kappa)}{V\kappa_1 - \kappa} d\kappa - \right. \\ \left. - \int_{\psi_1(\beta)}^{\psi(\beta)} B_i^{(1)}(\beta, \kappa) \frac{\beta_1 - \beta + \kappa_1 - \kappa}{V\kappa_1 - \kappa} d\kappa - \int_{\psi(\beta)}^{\kappa_1} B_i^{(2)}(\beta, \kappa) \frac{\beta_1 - \beta + \kappa_1 - \kappa}{V\kappa_1 - \kappa} d\kappa \right\} = 0.$$

This equation with the right side, identically equal to zero;

therefore with $\beta = \beta_1$ we have

$$\int_{\psi(\beta_1)}^{\kappa_1} \frac{E_i^{(2)}(\beta_1, \kappa)}{V\kappa_1 - \kappa} d\kappa = \frac{M^2}{k^2} \int_{\psi_1(\beta_1)}^{\psi(\beta_1)} B_i^{(1)}(\beta_1, \kappa) V\sqrt{\kappa_1 - \kappa} d\kappa - \\ - \int_{\psi_1(\beta_1)}^{\psi(\beta_1)} E_i^{(1)}(\beta_1, \kappa) \frac{d\kappa}{V\kappa_1 - \kappa} + \frac{M^2}{k^2} \int_{\psi(\beta_1)}^{\kappa_1} B_i^{(2)}(\beta_1, \kappa) V\sqrt{\kappa_1 - \kappa} d\kappa.$$

Page 542.

By substituting the value $B_i^{(2)}(\beta_1, \kappa)$ from (22.39) and by calculating quadratures, let us arrive at the integral equation

$$\int_{\psi(\beta_1)}^{\kappa_1} E_i^{(2)}(\beta_1, \kappa) \frac{d\kappa}{\sqrt{\kappa_1 - \kappa}} = -\frac{M^2}{k^2} \int_{\psi_1(\beta_1)}^{\psi(\beta_1)} \left[B_i^{(1)}(\beta_1, \kappa) \sqrt{\psi(\beta_1) - \kappa} - \frac{B_i^{(1)}(\beta_1, \kappa)}{\sqrt{\kappa_1 - \kappa}} d\kappa \right]$$

solution of which it takes form [1.63]

$$E_i^{(2)}(\beta_1, \kappa_1) = -\frac{1}{\pi} \frac{1}{\sqrt{\kappa_1 - \psi(\beta_1)}} \int_{\psi_1(\beta_1)}^{\psi(\beta_1)} \left[E_i^{(1)}(\beta_1, \kappa) \frac{\sqrt{\psi(\beta_1) - \kappa}}{\kappa_1 - \kappa} - \frac{M^2}{k^2} B_i^{(1)}(\beta_1, \kappa) \sqrt{\psi(\beta_1) - \kappa} \right] d\kappa. \quad (22.40)$$

Expressions for $B_i^{(2)}, E_i^{(2)}$ show that the disturbed speed with approach/approximation to the subsonic parts of the leading edge goes to infinity from without. Let us determine velocity potential according to formulas (20.11) (taking into account $\omega \rightarrow 0$) in the points of the lifting surface $P(\xi_1, 0, \zeta_1)$, for which the range of integration σ intersects with wing surface and with range σ_2 (or σ'_2). Formula for φ^{q_i} with $\omega \rightarrow 0$ in characteristic coordinates takes the form

$$\varphi^{q_i}(\beta_1, \kappa_1) = -\frac{1}{2\pi} \int_{\sigma} \int \left\{ \frac{k^2}{M^2} \left[\frac{\partial \varphi^{q_i}}{\partial \eta} \right]_{\eta=0} - (\beta_1 - \beta + \kappa_1 - \kappa) \times \left[\frac{\partial \varphi^{q_i}}{\partial \eta} \right]_{\eta=0} \right\} \frac{d\beta d\kappa}{\sqrt{(\beta_1 - \beta)(\kappa_1 - \kappa)}}.$$

Range of integration σ in this formula let us break into three parts: S_0, S_1 and S_2 , as shown in Fig. 22.17: then

$$\begin{aligned} \varphi^{(1)}(\beta_1, \kappa_1) = & -\frac{1}{2\pi} \int_{S_0+S_1} \int \left[\frac{k^2}{M^2} E_i^{(1)}(\beta, \kappa) - (\beta_1 - \beta + \kappa_1 - \kappa) B_i^{(1)}(\beta, \kappa) \right] \times \\ & \times \frac{d\beta d\kappa}{V(\beta_1 - \beta)(\kappa_1 - \kappa)} - \frac{1}{2\pi} \int_{S_1} \int \left[\frac{k^2}{M^2} E_i^{(2)}(\beta, \kappa) - \right. \\ & \left. - (\beta_1 - \beta + \kappa_1 - \kappa) B_i^{(2)}(\beta, \kappa) \right] \frac{d\beta d\kappa}{V(\beta_1 - \beta)(\kappa_1 - \kappa)}. \end{aligned}$$

By substituting the value $B_i^{(2)}(\beta, \kappa)$, $E_i^{(2)}(\beta, \kappa)$, we will obtain

$$\begin{aligned} \varphi^{(1)}(\beta_1, \kappa_1) = & -\frac{1}{2\pi} \int_{S_0} \int \left[\frac{k^2}{M^2} E_i^{(1)}(\beta, \kappa) - \right. \\ & \left. - (\beta_1 - \beta + \kappa_1 - \kappa) B_i^{(1)}(\beta, \kappa) \right] \frac{d\beta d\kappa}{V(\beta_1 - \beta)(\kappa_1 - \kappa)}. \end{aligned}$$

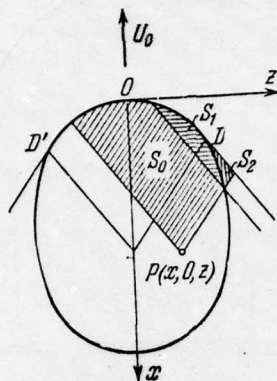


Fig. 22.17. To the calculation of potential on wing taking into account the effect of end effect.

Page 543.

Analogously we find

$$\varphi^q(\beta_1, \kappa_1) = -\frac{1}{2\pi} \int_{S_0} \int B_l^{(1)}(\beta, \kappa) \frac{d\beta d\kappa}{V(\beta_1 - \beta)(\kappa_1 - \kappa)}.$$

Thus, for the calculation of the aerodynamic derivatives of potential in the presence of end effect let us use the formula

$$\left. \begin{aligned} \varphi^{q1}(\xi_1, \zeta_1) &= -\frac{1}{\pi} \int_{S_0} \int B_l^{(1)}(\xi, \zeta) \frac{d\xi d\zeta}{V(\xi_1 - \xi)^2 - k^2(\zeta_1 - \zeta)^2}, \\ \varphi^{q2}(\xi_1, \zeta_1) &= -\frac{1}{\pi} \int_{S_0} \int \left[\frac{k^2}{M^2} E_l^{(1)}(\xi, \zeta) - \right. \\ &\quad \left. - (\xi_1 - \xi) B_l^{(1)}(\xi, \zeta) \right] \frac{d\xi d\zeta}{V(\xi_1 - \xi)^2 - k^2(\zeta_1 - \zeta)^2}. \end{aligned} \right\} (22.41)$$

The functions $B_l^{(1)}, E_l^{(1)}$ are determined from boundary conditions and are

expressed by relationship/ratios (22.2).

In order to calculate velocity potential on wing surface in the points, for which the range of integration σ intersects simultaneously, also, with range σ_2 and with the range of σ_2' , i.e., at points on the surface of the wing, where manifests itself the end effect of both subsonic edges DC and D'C' wing, it suffices to propagate integration in (22.41) to range $S = S^* + S^{**}$, shaded in Fig. 22.18, the integral, distributed on region S^* , in (22.41) one should take with opposite sign.

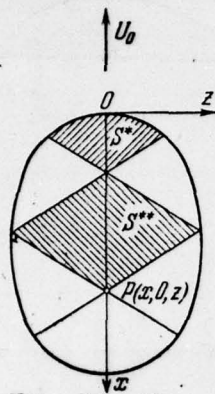


FIG. 22.18.

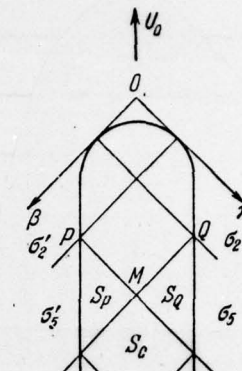


FIG. 22.19

Fig. 22.18. To the calculation of potential on wing taking into account end effect.

Fig. 22.19. Low-aspect-ratio wing. To determination of the wing-tip effect.

Page 544.

In the case of low-aspect-ratio wing (Fig. 22.19) for determining potential in ranges S_p , S_q , S_c it is necessary to determine the values of unknown derivatives $\partial\varphi^{(i)}/\partial\eta$, $\partial\varphi^{(i)}/\partial\eta$ in ranges σ_2 and σ_5 outside wing. These functions are determined from the integral equations, analogous to equations (22.38).

§6. Exact solutions for flat/plane rectangular wings. The limiting case of very small Strouhal numbers.

In the preceding/previous paragraph are given the relationship/ratios, which make it possible to obtain exact solutions taking into account end effect for the wings of the final lengthening. For arbitrary Strouhal number the calculations are obtained very laboriously. Task considerably is simplified with $\omega \rightarrow 0$. For wings with direct/straight edges and the flank edges, parallel to root chord, N. A. Kudryavtseva, M. K. Fursov and V. G. Tabachnikov conducted systematic calculations of the coefficients of aerodynamic derivatives. Some results of these calculations are used into V part of this monograph. In this paragraph let us give only formulas for determining the coefficients aerodynamic derivative of rectangular wings $k\lambda \gg 1$, which take following simple form [1.63]:

$$\left. \begin{aligned} c_y^a &= \frac{4}{k} - \frac{1}{\lambda} \frac{2}{k^2}, & c_y^a &= -\frac{2}{k^3} + \frac{1}{\lambda} \frac{2(M^2+1)}{3k^4}; \\ c_y^{\omega z} &= \frac{2}{k} - \frac{1}{\lambda} \frac{2}{3k^2}, & c_y^{\omega z} &= -\frac{2}{3k^3} + \frac{1}{\lambda} \frac{M^2+1}{6k^4}; \\ m_z^a &= -\frac{2}{k} + \frac{1}{\lambda} \frac{4}{3k^2}, & m_z^a &= \frac{4}{3k^3} - \frac{1}{\lambda} \frac{M^2+1}{2k^4}; \\ m_z^{\omega z} &= -\frac{4}{3k} + \frac{1}{\lambda} \frac{1}{2k^2}, & m_z^{\omega z} &= \frac{1}{2k^3} - \frac{1}{\lambda} \frac{2(M^2+1)}{15k^4}; \\ m_{x1}^{\omega x1} &= -\frac{2}{3k} + \frac{1}{\lambda k^2} - \frac{1}{3\lambda^2 k^3} - \frac{1}{12\lambda^3 k^4}, \\ m_{x1}^{\omega r1} &= \frac{2}{3\lambda k^3} - \frac{2(M^2+1)}{3\lambda^2 k^4} + \frac{2M^2+1}{6\lambda^3 k^5} + \frac{3M^2+1}{30\lambda^4 k^6}. \end{aligned} \right\} (22.42)$$

These formulas correspond to the standard, connected with wing coordinate system with beginning on the leading edge of root wing

chord. As significant dimension (besides $m_{x1}^{\omega_{x1}}, m_{x1}^{\omega_{x1}}$) is accepted root chord. From comparison with expressions (22.13) it follows that the first term in all formulas (22.42) corresponds to the coefficients of the aerodynamic derivatives of infinite-span wing. The second term, and in two last/latter formulas and the following consider the effect of lengthening, i.e., end effect.

UNCLASSIFIED

SECURITY CLASSIFICATION OF THIS PAGE (When Data Entered)

REPORT DOCUMENTATION PAGE		READ INSTRUCTIONS BEFORE COMPLETING FORM
1. REPORT NUMBER FTD-ID(RS)T-1543-77	2. GOVT ACCESSION NO.	3. RECIPIENT'S CATALOG NUMBER
4. TITLE (and Subtitle) A WING IN AN UNSTEADY GAS FLOW		5. TYPE OF REPORT & PERIOD COVERED Translation
		6. PERFORMING ORG. REPORT NUMBER
7. AUTHOR(s) S. M. Belotserkovskiy, B. K. Skripach, and V. G. Tabachnikov		8. CONTRACT OR GRANT NUMBER(s)
9. PERFORMING ORGANIZATION NAME AND ADDRESS Foreign Technology Division Air Force Systems Command U. S. Air Force		10. PROGRAM ELEMENT, PROJECT, TASK AREA & WORK UNIT NUMBERS
11. CONTROLLING OFFICE NAME AND ADDRESS		12. REPORT DATE 1971
		13. NUMBER OF PAGES 1378
14. MONITORING AGENCY NAME & ADDRESS (if different from Controlling Office)		15. SECURITY CLASS. (of this report) UNCLASSIFIED
		15a. DECLASSIFICATION/DOWNGRADING SCHEDULE
16. DISTRIBUTION STATEMENT (of this Report) Approved for public release; distribution unlimited.		
17. DISTRIBUTION STATEMENT (of the abstract entered in Block 20, if different from Report)		
18. SUPPLEMENTARY NOTES		
19. KEY WORDS (Continue on reverse side if necessary and identify by block number)		ACCESSION for NTIS White Section <input checked="" type="checkbox"/> DDC Buff Section <input type="checkbox"/> UNANNOUNCED <input type="checkbox"/> JUSTIFICATION _____
20. ABSTRACT (Continue on reverse side if necessary and identify by block number) 20		BY DISTRIBUTION/AVAILABILITY CODES Dist. AVAIL. and/or SPECIAL A